BEHAVIOUR CHARACTERISTICS OF FACE SHELL MORTARED BLOCK MASONRY UNDER AXIAL COMPRESSION

BY

GEORGES N. CHAHINE,
B.Sc.

BEHAVIOUR CHARACTERISTICS OF FACE SHELL MORTARED BLOCK MASONRY UNDER AXIAL COMPRESSION

BEHAVIOUR CHARACTERISTICS OF FACE SHELL MORTARED BLOCK MASONRY UNDER AXIAL COMPRESSION

By

GEORGES N. CHAHINE, B.Sc.

A Thesis

Submitted to the School of Graduate Studies

in Partial Fulfilment of the Requirements

for the Degree

Master of Engineering

McMaster University

Hamilton, Ontario

1989

MASTER OF ENGINEERING (1989)
(Civil Engineering)

McMASTER UNIVERSITY
Hamilton, Ontario

TITLE: Behaviour Characteristics of Face Shell Mortared Block Masonry under Axial Compression

AUTHOR: Georges Naim Chahine, B.Sc.
(University of New Brunswick)

SUPERVISOR: Dr. R. G. Drysdale

NUMBER OF PAGES: xxii , 423

ABSTRACT

Although face shell mortared blockwork constitutes the main construction practice in North America, its behaviour characteristics are relatively undefined and has traditionally been assumed to behave in a similar manner to brick and solid block masonry. Only recently has it been reported that face shell mortared concrete blockwork failed differently and the failure theories developed for these cases may not be applicable to face shell mortared blockwork. It is the main objective of this investigation to provide a better understanding of behaviour of face shell mortared blockwork and to arrive at the reasonably accurate measure of its strength under axial compression.

A total of 461 concrete block prisms incorporating a broad base of material properties and sources (29 block plants) were tested in axial compression normal to bed joints. In addition over 1400 auxiliary block compression and tension tests and mortar tests were carried out. The experimental investigation included a comprehensive study of the properties of the constituent materials, re-evaluation of current test

methods for measuring the compressive strength of the blockwork, detailed deformation monitoring of the behaviour, parametric study of the variables affecting the strength of face shell mortared blockwork, comparison to other types of concrete masonry construction and quantitative assessment of specified strengths for hollow concrete blockwork.

Regardless of the block size or shape, cracking of the webs is the expected failure pattern in face shell mortared blockwork and failure criteria attributing the dilation of mortar as the cause of failure are not applicable in this case. Since much reserve strength is available after initial observation of web cracking, models which predict cracking should not necessarily be expected to predict ultimate strength. Although the block's compressive strength can be related to blockwork compressive strength, a strong relationship existed with the block tensile strength. While web cracking in face shell mortared blockwork initiates in a mechanism independent of mortar, it cannot be concluded that the ultimate strength is independent of the type or strength of mortar. Employing 2-course prisms for measurement of blockwork compressive strength would result in an unrepresentative failure and overestimated strength. Currently employed relationship for determining the modulus of elasticity of concrete block masonry is clearly an overestimation.

A

mes parents

ACKNOWLEDGEMENTS

The author wishes to express his sincere gratitude to Dr. R. G. Drysdale for his guidance, encouragement and support during the course of this dissertation.

Acknowledgement is due to McMaster University, the Natural Sciences and Engineering Research Council of Canada and the Ontario Concrete Block Association. The author appreciates the contribution of masons' time made available through the Ontario Masonry Contractors Association and the Ontario Masonry Industry Promotion Fund. The Ontario Concrete Block Association, particularly Mr. Mark Patamia, executive director of OCBA, and member companies are gratefully acknowledged for their cooperation and for providing the concrete blocks and related materials.

Gratitude is expressed to Mr. Edward Gazzola and Mr. Mike Wilson for their assistance in the experimental program reported in Chapter 6.

Deep appreciation is due to my parents, specially my sister Nadia and brother in-law Micheal, for their help and encouragement without which this dissertation would have been difficult to complete.

TABLE OF CONTENTS

LIST OF FIGURES

FIGURE		PAGE
	(SERIES PH4-1 AND PH4-5)	134
3.22	TYPICAL FAILURES OF 2 AND 4-COURSE PRISMS WITH FACE SHELL SOFT CAPPING (SERIES PH2-6 AND PH4-6)	136
3.23	LATERAL STRAINS IN WEBS OF FACE SHELL AND FULL SOFT CAPPED 2-COURSE PRISMS (SERIES PH2-6 & PH5)	138
3.24	LATERAL STRAINS AT PLATEN IN SOFT AND HARD FACE SHELL CAPPED 2-COURSE PRISMS (SERIES PH2-6 AND PH2-4)	138
3.25	AXIAL COMPRESSIVE STRAINS AT PLATEN IN SOFT AND HARD FACE SHELL CAPPED 2-COURSE PRISMS (SERIES PH2-6 AND PH2-4)	139
3.26	LATERAL STRAINS IN WEBS OF FACE SHELL AND FULL SOFT CAPPED 4-COURSE PRISMS (SERIES PH4-6 AND PH4-5)	146
3.27	LATERAL STRAINS IN WEBS OF SOFT AND HARD FACE SHELL CAPPED 4-COURSE PRISMS (SERIES PH4-6 AND PH4-4)	146
3.28	LATERAL STRAINS IN WEBS OF STACK AND RUNNING BOND 2-COURSE PRISMS WITH FACE SHELL FIBREBOARD CAPPING (SERIES PH2-7 AND PH2-6)	148
3.29	LOADING ON THE TOP WEB OF A 2-COURSE PRISM WITH FULL BED CAPPING	152
3.30	2-COURSE AND 4-COURSE PRISMS SEPARATED AT THE AT THE MORTAR / UNIT INTERFACE, FULL CAPPING	155
3.31	SPECIMEN COMPRESSIVE STRENGTH VERSUS ASPECT RATIO	160
3.32	LATERAL STRAIN DISTRIBUTION IN A CENTRE WEB OF 4-COURSE FACE SHELL MORTARED PRISM	164
3.33	LATERAL STRAIN DISTRIBUTION IN A CENTRE WEB OF 4-COURSE FACE SHELL MORTARED PRISM	165
3.34	RESPONSE OF ASSEMBLAGE SECANT MODULUS OF ELASTICITY TO INCREASED AXIAL STRESS	167

FIGURE		PAGE

FIGURE		PAGE

FIGURE		PAGE

LIST OF TABLES

TABLE		PAGE

CHAPTER 1

INTRODUCTION

1.1 GENERAL

Plain concrete masonry is a composite material consisting of concrete blocks, mortar and grout. Concrete blocks in use have a wide range of size, shape and coring in addition to the basic variability of materials. The mortar is also subject to variation in strength characteristics, adhesion to the units and properties. Even with all these variables, the traditional approach has been to treat all block masonry as if it will behave in a similar manner under axial compression. In fact, until very recently, permissable compressive stresses in North American codes were based on a single set of data derived for solid or hollow clay or concrete masonry[1,26,67]. Failure theories developed originally for brick masonry[54] were also assumed to be applicable to concrete masonry.

Face shell mortaring of blockwork is the normal construction practice for block masonry in North America. However recent observations[88,104,116] have suggested that face shell mortared blockwork fails in a different mechanism than solid fully mortared blockwork and the "lateral splitting theories"[43,54] taken to explain the failure of fully mortared masonry are not directly applicable to face shell mortared blockwork. This is because the theory implies that the face shells of the wall should develop cracks whereas it is the webs which crack first[104]. Suggestions were also made that the cause of failure in face shell mortared blockwork can be attributed to a mechanism of "deep beam bending"[12,37,88].

Since face shell mortared blockwork appears to behave differently, there is a need to examine the failure pattern, establish the strength characteristics and identify the relevant variables affecting the overall response under axial compression. In addition, comparison of these characteristics to concrete blockwork in general is needed since there is no differentiation currently for specified compressive strengths for hollow blockwork with either face shell or fully mortared bed joints.

Building codes[1,7,26,79] define the compressive strength of masonry by permitting either direct testing of prisms made using site materials or use of previously established tables based on unit strength and type of mortar. However since the values of the tables were also originally based on prism tests, both methods are very much influenced by the way in which prisms are tested.

The compressive strength of block masonry was usually determined by tests of 2 block high stack pattern prisms with full mortar bedding. However as it became understood that full bed joint prisms resulted in conical type of failure, which is unrepresentative of face shell mortared walls and gave higher strength values, use of face shell mortar joints and soft capping were adopted to better simulate the actual behaviour[25]. However this practice itself may have introduced other inconsistencies in behaviour which will affect the test results. The current practices[7,25] regarding testing of prisms differ widely. At best this confused situation makes it very difficult to compare various test results. It likely also means that existing compressive strength provisions are not consistent and current test methods do not provide a uniform basis for assessment of results.

Regarding the alternative approach for obtaining the compressive strength based on a block strength and type of mortar, the current code values were derived from relatively old data mainly obtained from 2 and 3 course high prism tests with sometimes undefined test conditions[67]. Two course prisms have repeatedly been found to yield behaviour unrepresentative of full-scale walls[43,51,97,117]. In order to establish representative compressive strength values, there is a need for new data which incorporates a broad base of materials encompassing manufacturing differences and uses representative specimen configuration which employs reasonably accurate test methods.

1.2 Objectives and Scope

A review of the available literature revealed that there is little information regarding the behaviour characteristics of face shell mortared block masonry under axial compression. Most of the available information was derived from tests on 2 and 3 course high stack pattern prisms with full mortaring or even obtained from solid concrete block and brick masonry. The extensive experimental investigation reported in this dissertation was initiated to help establish the behaviour characteristics and define the compressive capacity of face shell mortared blockwork.

It was decided that the problem could be best approached by fully investigating the properties of the constituent materials, the definition of the compressive strength parameter, the strength characteristics of the assemblage and the compressive capacity for face shell mortared blockwork. Therefore each area of concern presented in this dissertation has its own introduction with reviews of relevant background, details of the experimental study, analysis and interpretations of the results, review of the relevant code provisions, related conclusions and recommendations.

The experimental investigation incorporated a broad base of materials and a sufficient number of test repetitions to provide confidence in the results.

It was decided to first establish the characteristics of the constituent materials under various test conditions. To arrive at a reasonably accurate definition of the compressive strength of block masonry, the various test methods and techniques employed in obtaining this important parameter had to be evaluated and a test procedure developed to be employed throughout the experimental investigation. Also, to explain the failure mechanism for face shell mortared blockwork, a major effort in measuring strain deformations was identified as a necessary part of the program.

It was decided that a parametric study was needed to establish which variables affected the actual failure mechanism and the stress pattern in face shell mortared blockwork under axial compression. Also it was felt that the behaviour characteristics of standard size block face shell mortared masonry should be related to those of other forms of concrete block construction. To provide an effective assessment of the code[26] specified compressive strengths for hollow concrete blockwork, it was decided that the investigation should also incorporate a broad base of material properties encompassing various manufacturing techniques and specimens representative of full-scale walls.

The results from the experimental investigation would be statistically analyzed and empirical relationships describing the relation between the various components of face shell mortared blockwork under axial compression would be drawn. It was decided that conclusions and recommendations should be based on a statistical analysis at a level of confidence of 95 percent.

The applicability of different failure theories for face shell mortared blockwork would be examined. It was also intended to evaluate the potential[32] of predicting the compressive strength of concrete block masonry based on its constituents materials, Various codes and standards[6,7,21,23,24,25,26] provisions related to strength measurements, test procedures, specifications and permissable strength values would be evaluated and corresponding recommendations will be presented.

1.3 ORGANIZATION OF THE THESIS

The materials in this dissertation are organized as follows: Chapter 2 contains an investigation of the properties of the constituent materials (block and mortar). A detailed evaluation of test methods and failure of face shell mortared blockwork under axial compression was reported in Chapter 3. In Chapter 4, a parametric study of the variables affecting the behaviour characteristics of face shell mortared blockwork was presented and Chapter 5 contains a comparison between the standard size face shell mortared blockwork and other forms of construction and loading.

Chapter 6 was organized to provide a quantitative assessment of face shell mortared blockwork based on block from 29 sources. Chapter 7 contains a summary of results and the overall conclusions from this investigation.

1.4 NOTATION

Although each symbol used in this dissertation is described where it first appears, a summary of the symbols is listed below for convenience:

A_n	net cross-section area of the block
A_m	area of mortar in contact with upper and lower units in the prism (effective mortared area)
E_{mb}	secant modulus of elasticity of the block in compression at 0.3 of the ultimate strength
E_m	secant modulus of elasticity of the prism in compression at 0.3 of the ultimate strength
e	eccentricity of loading
f'_m	compressive strength of the block prism based on the mortared area
f'_{me}	compressive strength of the block prism under eccentric loading
f'_{mb}	compressive strength of the block based on net area
f_{tb}	tensile strength of the block
h	height of block or prism

K	ratio of prism modulus of elasticity to compressive strength (stiffness coefficient)
N,S,M	types of mortars as specified in CSA-A179-M76[23]
P_o	axial compression capacity of prism under zero eccentricity
P_e	axial compression capacity of prism under eccentricity e
r	correlation coefficient
t	nominal thickness of block or prism
t_f	thickness of face shell
t_m	equivalent thickness of mortared face shell
σ	applied stress normal to the block bed joint
ϵ	axial compressive strain in the block

CHAPTER 2

PROPERTIES OF THE CONSTITUENT MATERIALS OF CONCRETE BLOCK MASONRY

2.1 INTRODUCTION

The structural properties of concrete masonry cannot be adequately understood unless the properties of concrete blocks and mortar are fully defined.

The block's compressive strength is affected by shape, type of loading and capping material[43]. Due to the absence of a single standard test method, researchers have used various test techniques to obtain the compressive strength of the unit[29,36,40,43,67,77,97,116]. Regardless of the test method it is perhaps more appropriate to consider these tests to be simple standards by which to judge the quality of the unit rather than real measures of the material compressive strength since shape and end conditions have such significant influences.

Vertical cracking through the webs is the major controlling failure mode in hollow load-bearing block masonry under axial compression. The splitting test (similar to the Brazilian Test[82]) is often used to determine the tensile strength. However it is unclear whether the unit or the material is being evaluated because tapering of face shells or existing micro-cracking such as is often seen at the bottom of the web can complicate interpretation.

In recent years the strength of mortar has attracted more attention due to the increase in high-rise load-bearing masonry construction. However current mortar specifications have changed little since they first appeared in ASTM-C270 in the 1930's[30].

In this chapter separate investigations of the block's compressive and tensile strengths and the mortar properties were reported. The influence of the various test methods on the unit compressive strength was examined with the objective of recommending a test technique which most closely or rationally relates to prism tests. Current methods employed for obtaining the unit tensile strength were evaluated with the objective of developing a representative evaluation method. Mortar tests on a broad base of masonry sands and cementitious materials were included, in part, so that mortar specifications could be re-evaluated.

This chapter also contains the documented physical and mechanical properties of the component masonry materials used in other parts of this research program.

2.2 HOLLOW CONCRETE BLOCKS

2.2.1 General

For completeness and to provide a more representative data set, full ranges of tests were performed using 190 mm concrete blocks from two different plants. One plant uses a bubble curing system while the other utilizes an autoclave curing system. In addition, standard 190 mm units from 27 other block manufacturing plants in Ontario were included to provide a comprehensive evaluation for this most commonly used product. Properties of blocks with various sizes, percentage solid and shapes are reported in later chapters in conjunction with prism test results.

2.2.2 Physical Properties

Standard 390 x 190 x 190 mm hollow blocks come in two different shapes:

.A stretcher unit has 2 tapered cores and recesses on both ends (frogged ends).

.A splitter unit has 2 tapered cones, one frogged end, and the other end flat and two webs at the centre to provide two webs for each split half.

For this research program all splitter units were sorted out from the pallets of blocks and only stretcher units were used. Splitter units are randomly incorporated into actual construction as well as providing end blocks and half blocks for running bond. However, use of standard stretcher units represents the normal and the controlling conditions for strength. Figure 2.1 is a drawing of a hollow stretcher concrete unit with pear shaped cores.

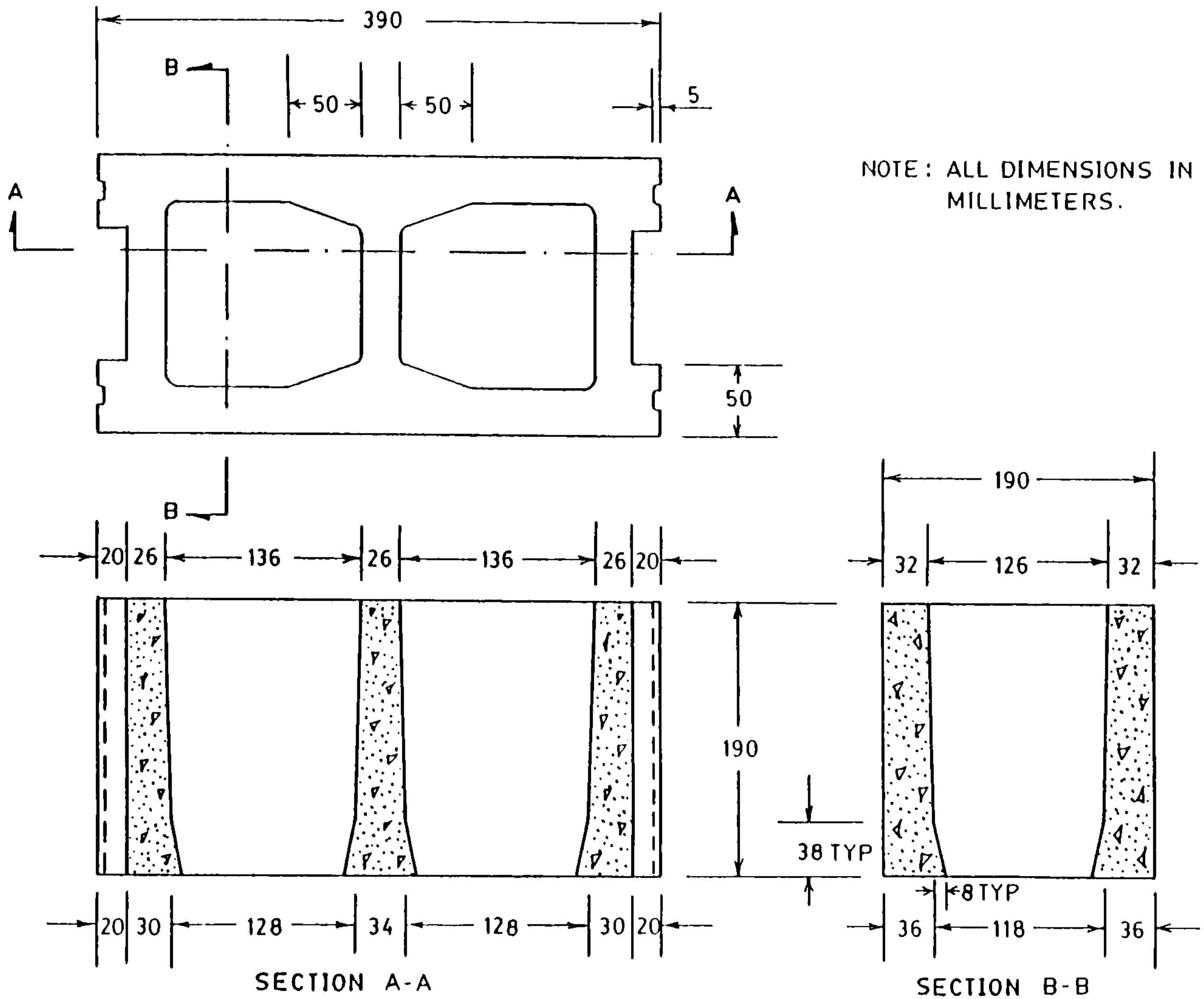

FIGURE 2.1 HOLLOW CONCRETE BLOCK DIMENSIONS (STRETCHER UNIT)

There is a considerable confusion regarding determination of the net area of blocks. In ASTM-C140[3] net area is calculated based on volume and suspended immersed weight of the unit. In CSA-S304[26] the mid-height net area is taken whereas CSA-A165[24] introduced a procedure where net area is determined by subtracting cellulor spaces from the gross area without specifying at what section of the block.

Table 2.1 is a summary of calculated net areas for standard hollow 190 mm blocks performed by the author from nominal dimensions provided by OCBA[85] and from direct measurements. For units with flares, the values are from the average measurements on blocks from 18 different sources. For units without flares, the measurements were made on blocks from 7 different sources. For units with pear shaped cores and flared tops, it was decided to use a net area of 41500 mm^2 quoted by OCBA[85]. This value is greater than the real mid-height area. Use of this area implies that the flares which are provided for handling purposes, also contribute to the compressive strength. This value conforms with the value from volume calculations[116] and corresponds to 56.0% of the gross area. For units with pear shaped cores but without flares a net area of 39860 mm^2 is used which corresponds to the mid-height net area of the block (nominal area, 39892 mm^2). It corresponds to 53.8% of the gross area. Areas calculated from measurements on blocks from 18 different plants showed less than 3.0% coefficient of variation.

TABLE 2.1: NOMINAL AND MEASURED AREAS OF STANDARD HOLLOW UNIT.

DESCRIPTION OF BASIS FOR NET AREA CALCULATION	NET AREA (mm^2) NOMINAL	MEASURED
Minimum	38028	38787
Maximum for blocks with flares	48252	48686
Maximum for blocks without flares	41692	43372
Mid-height	39892	41050

In calculating the block compressive strength, a net area of 41500 mm^2 was used for blocks with flares while a value of 39860 mm^2 was used for blocks without flares.

2.2.3 Compressive Strength Investigation

2.2.3.1 Background

ASTM-C140[3] specifies that a full unit be tested flatwise using Gypsum plaster capping. Some researchers[33,43] have chosen half blocks because the higher aspect ratio tended to reduce the effect of platen restraint. Also tests of half blocks are easier and more economical to perform[116]. The main concern from such an approach is that symmetry in both principal axes is impossible to achieve, and this may very well explain why the half block strengths are slightly less than for full blocks. Tests carried out by Beccia[12] showed that compressive strengths of coupons obtained from hollow blocks were higher than strength obtained according to ASTM-C140[3]. Testing small sized specimens apparently overestimates the strength of the unit[10].

Cross-webs of the blocks are not directly involved in transmitting the loads for masonry constructed with running bond because they do not align vertically. As a result, some researchers have suggested that in determining the unit strength only the face shells should be loaded. As previously reported[116], Redinger et al. recommended that face shell capping be used because the failure modes of units tested resembled those of masonry prisms and walls, namely vertical web cracking. However the type of capping was not specified. Test by Nacos[77] revealed an average of 24 percent increase in strength for full units with face shell capping over those with full capping based on the loaded areas.

Specimens soft capped with various types of board produced a lower indicated strength than hard capped specimens where ratios between 0.85 - 0.90 were found[43,70,97,116]. By using soft capping, researchers anticipated reducing the platen restraint. Maurenbacher[70] reported that the use of fibreboard is simple, cheap and quick, he also reported ratios 0.99 and 0.92 for two series of soft to hard capped units. The requirements of CSA standard CAN3-A369.1[25] are that ASTM-C140 be used to determine the compressive strength of the unit (implying the use of hard capping material) whereas fibreboard is specified for prism compression tests.

The requirements of ASTM-C140[3] are that the thickness of steel bearing plates be at least one third of the distance from the edge of the block to the nearest part of spherical seat. For the standard 190 mm unit and a 225 mm diameter spherical loading seat, the required plate thickness would be 34.8 mm. In this regard, Self[97] reported that 2 in.(51 mm) thick bearing plates experienced bending under small loads. However, from tests with 3 in. (76 mm) and 4 in. (102 mm) thick plates he reported that there was little change and in fact block strength seemed to drop off slightly with increased plate thickness. He concluded that the central portion of the block was strongest and therefore the non-uniform loading caused by plate bending resulted in higher capacities.

Since prism tests in accordance with CSa-A369.1 would require a 104.4 mm thick plate, it seems odd that blocks which reach higher loads can be tested using much thinner plates. Therefore this aspect of test procedure was identified for further study.

2.2.3.2 Outline of Investigation

Past practice has been to develop arbitrary relationships between unit strength and prism strength. However if a better understanding of the real relationship is to be gained, an argument can be made that tests of the units should resemble as closely as possible the conditions of loading of blocks in a prism.

In this chapter, ten different series of block compression test were performed. The influence of capping material was examined using:

1. Hard Capping: A gypsum-cement (Hydrostone) as required by ASTM-C140[3] was used with a thickness less than 3 mm.

2. Soft Capping: A fibreboard material as specified in CSA-A247[22] was used with a board thickness of 11mm (7/16 in).

The influence of full bed capping versus face shell capping on the unit was examined using the two types of capping materials. For face shell capping, a minimum face shell thickness of 32 mm and the equivalent width of effective mortar bedded area of 39.4 mm were both employed. Hollow saw cut, half splitter blocks with full bed hard capping were also tested. In addition, compression tests were carried out on full blocks loaded on the ends of the face shells. Influence of plate thickness was studied in compression tests using 50 mm and 75 mm thick steel bearing plates.

A description of each compression test series, modes of failure, stress-strain relationships and moduli of elasticity were all documented in Appendix A. In addition a statistical assessment of the significance of various differences between the data from the various series was also presented in Appendix A. A summary of the results from the various series of compression tests of individual blocks was listed in Table 2.2. Individual results of different bearing plate thickness tests (Series C13-9 and C13-10) are found in Appendix A.

2.2.3.3 Results and Discussion

Influence of Specimen Size (Series C10-1 and C10-7)

In calculating the difference of strength between loading a full unit flatwise versus half unit, various net areas have been used[40,43,116] and this may very well explain some of the difference between the two tests which led some researchers to conclude that full units produce higher strengths than half units. In this research, the opposite was found where half unit strengths were 8.5% higher than for full units. However based on a statistical assessment at a 5% significance level there was no difference in mean strengths and this also applies for variances. The small observed difference may in part be attributed to the fact that the exact loading area is difficult to determine, especially for half units. With half units, the whole bearing area of the specimen is covered by the testing machine spherical head. While for full units the ends are less confined as a result

TABLE 2.2: COMPRESSIVE STRENGTHS OF CONCRETE BLOCK UNITS.

TEST SERIES	DESCRIPTION OF TEST	ULTIMATE LOAD (KN)	MEAN STRENGTH (MPa)	C.O.V. (%)
C10-1	Full bed Hydrostone capping	996 1121 1095 1055 1032	25.5	4.7
C10-2	Face shell Hydrostone capping (32 mm wide strip)	802 713 781 858 831	31.9	6.9
C10-3	Face shell Hydrostone capping (50 mm wide strip)	999 921 1025	32.0	5.5
C10-4	Full bed fibreboard capping	896 955 936 860 820	21.5	6.2
C10-5	Face shell fibrecapping (32 mm wide strip)	720 599 596 710 669	26.4	9.0
C10-6	Face shell fibrecapping (50 mm wide strip)	734 797 796 776	25.3	3.8
C10-7	Half unit (full Hydrostone capping)	558 642 634 581 606	27.7	5.8
C10-8	End Loading (face shell Hydrostone capping)	350 330 343 307 343	25.9	5.1
C13-9	75 mm bearing plates	TAB. A1.1	22.9	7.7
C13-10	50 mm bearing plates	TAB. A1.1	21.2	5.9

of some bending of the plates even when thick plates are used[97]. Therefore it might be expected that half units would produce somewhat higher strengths since the whole bearing area is under higher platen restraint. The fact that the secant modulus of elasticity, determined at 0.3 of the ultimate stress, from half unit was 26% higher than that determined from full unit tests supports the observation that some difference may exist.

Both specimen sizes had conical type failures. However for the half units shearing action extended to the four sides (See Appendix A). It was not found that compression tests on half units were easier or more economical[116] since cutting of the units was required and also, as a result of the loss of symmetry in the specimen, alignment for loading was more complicated.

Effect of Direction of Loading (Series C10-1, C10-7, C10-8)

The compressive strength of a full unit tested flatwise was the lowest when the influence of direction of loading or size of specimen was examined. However the differences were small and statistically (See Appendix A) there was no difference in strength when full units were tested flatwise, endwise or when half units were used. A similar conclusion was obtained from variances' test. This conclusion should not obscure the fact that geometry of the unit complicates the stress distribution. In Figure A1.5, of Appendix A, the vertical compressive stress-strain data for a full unit tested endwise were shown for two locations. Strains at the cross-web (strain location III in Figure A1.4) were almost twice those at the hollow core. An explanation is that the cross-web section is under eccentric loading. In fact simple calculation shows that for a section with an axial load applied at its centre if a second section was added without changing the location of the load, the maximum compressive strains in the double section are higher than those in the single axially loaded section.

<u>Full Versus Face Shell Hydrostone Capping</u> (Series C10-1, C10-2 and C10-3)

For 32 mm face shell loading, the capacity decreased by 24.8% but the strength based on the loaded area increased by 25%. A 24% increase in strength was reported by Nacos[77]. Face shell loading did significantly change the mode of failure of the unit from that of the typical conical failure to that of spalling of the face shell. Using an effective width of 39.4 mm capping resulted in higher capacity but the same increase in strength, over that of full bed capping. The failure mode in this case can be described as an extensive spalling of the face shells. What is of importance in these test series is that the percent decrease in loading area was larger than the percent decrease of the load capacity of the unit and this in fact resulted in very high compressive strength. Even though the web area is not loaded directly some of the load must be transmitted through the web.

Full Versus Face shell Fibreboard Capping (Series C10-4, C10-5, C10-6)

For face shell loading, a 22.6% increase in the compessive strength of the unit was observed for the minimum face shell capping thickness of 32 mm whereas for the 39.4 mm equivalent mortar bedded area thickness, the increase was 17.4% based on the increased area. For Series C10-5, the failure can be described as shearing of one of the face shells. Some vertical cracking of the face shell was also observed. Increasing the width of the face shell loaded area in Series C10-6, seems to extend the lateral tensile stress into the web and this resulted in significant web cracking. However failure continued to be characterized by shearing of the face shells.

A statistical assessment (See Appendix A) showed that for the same type of block, test method and capping material there is a significant difference in strength between face shell and full bed loading. Since failure load decreased, it is likely that most of the strength difference can be attributed to the web area not included in the strength calculations.

<u>Hydrostone Versus Fibreboard Full Bed Capping</u> (Series C10-1 and C10-4)

Fibreboard capping of full units reduced the compressive strength by 18.6% compared to Hydrostone capping. Similar values were reported by Maurenbrecher[70] and others[43]. Soft capping altered the mode of failure from that of conical failure to failure by either spalling in all sides of the block or by wedge failure which extended well into the web. Further details were shown in Figure A1.7 of Appendix A. The reduced influence of end platen restraint for soft capping is the most obvious explanation for this difference.

<u>Hydrostone Versus Fibreboard Face Shell Capping</u> (Series C10-2 and C10-3 versus C10-5 and C10-6)

Fibreboard capping of the face shells (Series C10-5) also resulted in a 17.4% strength reduction in comparison to hard face shell capping (Series C10-2). Failure continued to be mainly limited to the face shells, however vertical cracking was also observed. For face shell capping the top and bottom zones along the web centreline are relatively free of any axial compressive stresses. Analysis[37] showed there is a tendency for lateral tensile stresses to develop at these locations. With hard face shell capping the larger end platen restraining forces may retard the growth of such tensile stresses and hence resulting in higher strength. It is also possible that the fibreboard material may have induced some tensile stresses at the interface. The observed fine vertical cracking lines in the webs seem to support this suggestion.

Similar behaviour was also observed when the capping strip width was increased to the equivalent mortar bedded thickness of 39.4 mm. Fibreboard capping (Series C10-6) produced a 21.0% strength reduction in comparison to Hydrostone capping. No consistent mode of failure was observed and both vertical cracks in the webs and shearing/conical fracture of face shells were observed.

Effect of Bearing Plates Thickness (Series C13-9 and C13-10)

It should be noted that in these two series concrete blocks from different source than the one used in the other series were employed. The thickness of the steel bearing plates is expected to affect the stress distribution, especially for single unit compression tests where higher loads are required to cause failure[51]. However this influence can only be rationally investigated through use of detailed strain measurements. In this research program a strain gauging arrangement was planned to examine the influence of the plate thickness on concrete prism strength. However for individual blocks, increasing the plate thickness from 50 mm to 75 mm resulted in a small increase of 8.1% in the compressive strength. Eventhough this is a small increase it contradicts the results reported by Self[97] who concluded that the unit compressive strength decreased slightly with increased plate thickness. Further discussion of the influence of plate thickness is deferred to Chapter 3 where this parameter is investigated in regard to two course-high and four course-high prisms.

Influence of Capping on Variability of Results

Fibreboard capping has been reported to produce higher variances of the results[54,70]. From the various series in this research work, the coefficients of variation for hard capping tests were a little less than those for soft capping. For face shell soft capping, the coefficient of variation of 9% was the highest. However based on a statistical assessment at 5% significance level, there was no difference in variances. This different observation may be explained by the fact that fibreboard materials are different from region to region. Also eventhough the use of fibreboard is cheap and quick[70] in block tests at least, its use requires a higher level of testing control than for Hydrostone specially for face shell loading.

2.2.3.4 Conclusions

1. The compressive strength of hollow concrete units, tested flatwise was only 8.5% less than the compressive strength of half units. This observation tends to contradict the results reported by others[40,45,116] where the opposite was observed. However based on a statistical assessment there appears to be no significant difference in strength between the two procedures.

2. The geometry of hollow blocks complicates the stress distribution. Strain measurements, from end-loading of full unit in compression showed that the section of face shell at the hollow core experienced much less strain on the outside face than the section of face shell at the cross-web.

3. The compressive strengths of full units and half units fully hard capped and tested flatwise, and full units hard capped and tested endwise can all be taken to be statistically equal based on the effective loaded area.

4. In comparison to full hard capping, tests with face shell hard capping significantly changed the mode of failure to that of spalling of face shells and resulted in a 25% increase in unit compressive strength. This was true for loading through the minimum thickness of face shell of 32 mm and the equivalent mortar bedded area thickness of 39.4 mm.

5. In comparison to full soft capping face shell soft capping resulted in 22.6% and 17% increase in the unit compressive strength for the minimum and equivalent mortar bedded areas, respectively.

6. Full fibreboard capping resulted in a 19% decrease of the unit compressive strength compred to hard capping. Face shell soft capping reduced the strength, from face shell hard capping, by an average of 24%.

7. Statistically, it appears that there is no difference in variances between test results for hard and soft capping materials. However employing soft capping material in compression tests requires a higher level of testing control than for Hydrostone capping specially for face shell loading. Ideally if face shell soft capping is to be used, the unit should be capped first with Hydrostone. However this procedure would eliminate the argument offered by many that fibreboard capping should be used because it's simple and quick.

8. Increasing the steel bearing plate thickness from 50 mm to 75 mm increased the unit compressive strength by 8%. For uniform strength block, a more uniform distribution of stress should result in an increased failure load.

9. Full bed hard capped single unit compression test appears to offer the most reasonable compressive strength values. In fact the compressive strength was the lowest with

the exception of the value obtained from full bed soft capping compression test. In addition this testing procedure is the simplest and is reasonably accurate; it also ensures a uniform loading surface.

10. Block strengths from tests of full bed hard capped units appear to provide a reasonable measure with relatively low scatter. However, as will be discussed in later chapters, the correlation of any of the above measures of block strength with prism strength is not strong.

2.2.4 Tensile Strength Investigation

2.2.4.1 General

Tensile stresses in masonry, whether they are caused by axial compression or by flexure are important factors in the failure of masonry. Hollow concrete block walls tend to fail by vertical cracking through the webs when loaded in axial compression. Therefore evaluation of the unit as well as the masonry material tensile strength is important to understanding this behaviour.

Masonry researchers have concluded that the "Indirect Tensile Splitting Test" (Brazilian Test) provides a good measure of the tensile strength of block. While such a test is usually carried out by applying the load across the face shells, it should be applied across the webs of the block because it is through the webs of prisms/walls where the cracking occurs as will be shown in later Chapters. In addition there appears to be a confusion whether the splitting tensile strength is a measure of the unit or the material tensile strength. Also there is a need to examine the validity of the Brazilian test in poviding a good measure of concrete masonry tensile strength.

Finally, the block industry is only now becoming aware of the influence of the tensile stresses on the behaviour of block masonry and there is no evidence that the design of the blocks, particularly the web size and locations took this factor into account.

2.2.4.2 Background

The indirect tensile splitting test was first introduced by Fernando Carneiro, a Brazilian[82], to obtain the splitting tensile strength of concrete cylinders. Davies and Bose[17] have shown the theoretical applicability of testing rectilinear units as opposed to cylindrical specimens. Thomas and O'Leary[112] concluded that the indirect tensile test was a desirable measure of bricks' performance in masonry and Holm[55] indicated that tests conforming to ASTM-C496-7 can be employed to determine the tensile strength of 100% solid lightweight concrete masonry.

In an attempt to evaluate the tensile strength of concrete blocks, Hamid[43] looked at four different loading conditions:

1 - axial tension

2 - eccentric tension

3 - flexural tension

4 - splitting test across the face shells.

In the axial tension test a full block was tested. However such a test does not provide the tensile strength of the material since it incorporates stress concentration at the webs. The second and third types of tests, even though they are useful, cannot be taken as a measure of tensile strength of the unit nor of that of the material due to the pronounced effect of the strain gradient. Hamid concluded that the splitting test of a half unit across the face shells is a reliable measure of the direct tensile strength.

Holm[55] reported use of a device called a "Blockbuster" that allows direct measurement of tensile strength; "...Block may be broken in tension simply by inserting the self-aligning rig within the core of a standard block, jacking the ram until failure occurs, and then reading the guage..." However the same author admits that the derivation and the analysis of the stresses developed by the Blockbuster are very complex. This approach was not followed up because stress patterns are not uniform.

When indirect tension tests were carried out on brick masonry in the transverse as well as in the longitudinal direction, significant differences between the results were observed[17]. However in the same investigation, splitting tests were carried out on concrete units with the load being applied only across the face shells. A 20% increase in the tensile splitting strength was reported when the load was applied across the face shells of a half unit, instead of across the webs[36]. Also this research showed that splitting tests carried out on square masonry pieces, cut from the face shells of the unit, yielded similar results to splitting across the face shells of half units. ASTM-C1006-84[6] contains provisions for use of the indirect tensile splitting test as a measure of the splitting tensile strength of masonry. Also it indicates that such tests can be applied in the longitudinal or the transverse direction.

Suggestions have been made to explain why the splitting mode of failure in walls under axial compression tends to occur in the webs of the unit instead of the face shells. The thin web thickness and the possibility that the webs may receive a lesser degree of compaction were identified as possible reasons[55]. Finally the indentation or initial crack which is fairly commonly found in the webs of hollow concrete blocks due to the manufacturing process, was thought to affect its tensile strength and to initiate cracking in the web[34].

2.2.4.3 Outline of Investigation

To minimize the variability of results concrete blocks from the same source and the same mixing batch were used. Furthermore, to give a greater generality to the conclusions in this investigation, "bubble cured" blocks (Company 10) as well as "autoclaved" blocks (Company 21) were investigated.

Some other research work[36,116] has included some of the tests planned for this investigation but none have done all the proposed tests. Two sets of splitting tests were carried out on half stretcher units with the load applied either across the face shells or across the webs. To provide a check on the validity of using half units in splitting tests, splitting tests were done on square specimens saw cut from face shells and webs thus eliminating any geometric influence of thicker sections and intersecting elements. These tests should also provide information to document any difference between the strength of face shells versus webs.

Direct tension tests on square concrete specimens cut from webs and face shells were planned to establish the true tensile strength of the material, not the unit, because the effects of geometry and strain gradient are eliminated. The results from these direct tension tests should also provide an indication of the validity of the Brazilian test as well as provide experience to assess the possibility of using the direct tension test as a standard test. As part of the investigation of difference in strength between the face shell and the web of the units, the effect of the indentation in the bottom of the unit's webs on the tensile strength was determined from direct tension tests of square pieces cut from the webs.

A full description of each tension test series, the individual results, strength values and mode of failure were all documented in Appendix A. In addition a statistical assessment of the data from the various series and the two sources of blocks can also be found in Appendix A. Table 2.3 contains a summary of the results from these tension tests.

2.2.4.4 Results and Discussion

Differences in Tensile Strengths for Face Shells Versus Webs (Series T1, T2, T8 and T9)

Splitting tensile strengths from loading across the face shells of half stretcher units were 25% higher than for loading across the webs for Company 10 and 52% higher for Company 21. On average this amounts to a 38% difference in tensile strength. A similar trend was also observed when splitter units were tested (Series T8 and T9). There are several factors which may contribute to this difference:

TABLE 2.3: RESULTS OF TENSILE STRENGTH INVESTIGASTION

SERIES	COMPANY	10		21	
	TEST DESCRIPTION	MEAN STRENGTH (MPa)	C.O.V. (%)	MEAN STRENGTH (MPa)	C.O.V. (%)
T1	splitting across face shells of half units	1.89	9.1	1.95	5.6
T2	splitting across webs of half units	1.51	11.4	1.28	12.3
T3	splitting square pieces from face shells	2.15	6.2	1.75	4.5
T4	splitting square pieces from webs	1.99	6.5	1.73	8.0
T5	direct tension: square pieces from face shells	1.85	10.3	1.94	12.5
T6	direct tension: square pieces from webs	1.66	10.6	1.74	9.1
T7	direct tension: indentation (webs pieces)	1.56	8.4	1.88	13.8
T8	splitting across face shells: splitter units			1.98	19.0
T9	splitting across webs: splitter units			1.24	16.5
		DIFFERENT BLOCK SOURCE			
ST1	packing: splitting half units across face shells	2.38	5.0		
ST2	no packing: splitting half units across face shells	1.85	4.9		

C.O.V. = coefficient of variation

1. During the manufacturing process, the webs of concrete units tend to be subjected to a lesser degree of compaction than the rest of the unit. In this regard, a direct relationship has been established between the strength of the unit and the degree of compaction, a 5% increase in strength was attributed to a 1% reduction in the "interstitial void content" or porosity[55].

2. The indentation or defect in the bottom of the block's webs has the effect of reducing the actual splitting area of the web and hence makes the calculated splitting tensile stress, based on the whole splitting area, smaller than the actual stress[36]. The zone of local crushing under the direct axial load location was observed to be more extensive when the load was applied across the webs, especially at the indentation.

Since masonry compression failure originates by vertical cracking through the webs of hollow blocks, it seems logical that an improvement is possible if the concrete in this area is made crack free and compacted to the same extent as the face shells.

<u>Influence of Specimen Geometry on Splitting Strength</u> (Series T1 Versus T3 and T2 Versus T4)

The splitting tensile strength of square specimens cut from face shells was 12% higher than the strength of half units loaded across the face shells for Company 10 while an 11% strength reduction was observed for Company 21. A difference in strength of around 6% was reported in another study[116]. For practical purposes it is suggested that the splitting strength of the face shells can be determined by employing specimens with either geometry.

For webs sections, the splitting strengths of square pieces (Series T4) were significantly higher than those from splitting half units across the web (Series T2) for both companies. It is important to note for the square web pieces, the indentations were cut away. Hence, by eliminating the influence of the indentation from the square pieces, it can be concluded that the difference in strength is attributed to the geometry of the specimen and to the indentation in the half units. As a result it is appropriate to distinguish between these two types of tests since splitting of square pieces would give the splitting strength of the concrete material in the web while splitting of half units across the webs is a measure of the splitting strength of the web including to some extent any flaws such as the indentations.

Direct Tensile Strength (Series T5 and T6)

When a specimen is subjected to axial tension, the whole cross-sectional area is under maximum stress and the probability of having a critical combination of weak elements is high. Hence tensile strengths from direct tension tests are expected to be lower than values obtained from other test techniques. Also the beneficial effect of strain gradient is non-existent. Figure 2.2 is a drawing of the direct tension test set-up. Commentary on this specially designed apparatus can be found in Appendix A. The results again showed that the direct tensile strengths of web specimens were indeed lower than those from face shells. Generally, the direct tension test appears to result in tensile strength lower than splitting test. For Company 10, the statistical assessment showed that the axial tensile strength and the splitting tensile strength cannot be taken equal, at the 5% significance level, for both web and face shell specimens.

Worth noting that although the axial tension test was found to be feasible and the variability of the results was quite low, it is a sensitive test and fairly difficult to perform.

Influence of Indentation in Webs (Series T7 Versus T6)

The effect of web indentation was looked at by direct tension testing of square web specimens with indentation.

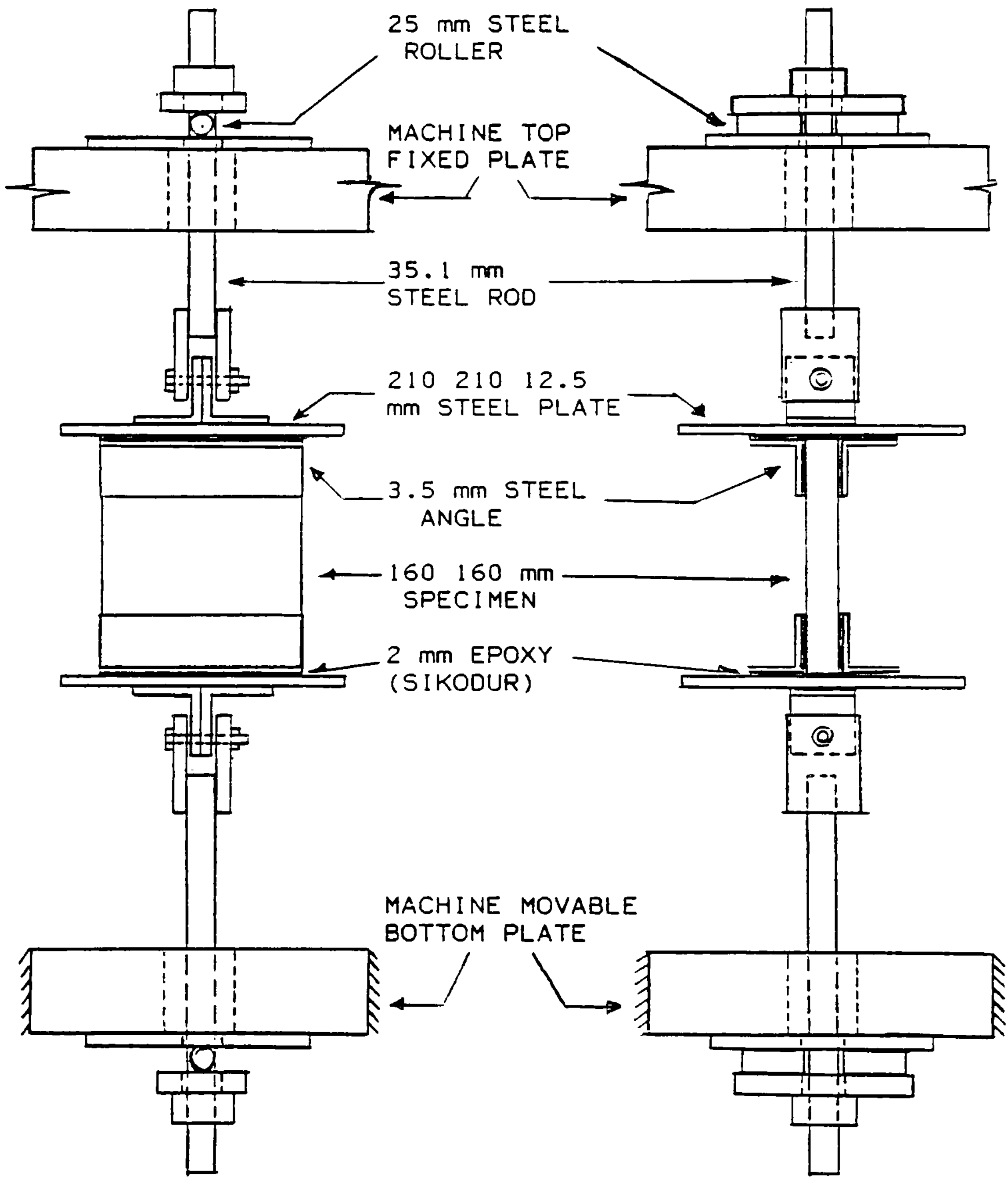

FIGURE 2.2: DIRECT TENSION APPARATUS

.For Company 10 the tensile strength of square specimens with indentation was 6.3% less than that of specimens with no defect. One of the specimens had a very small indentation and if that result is neglected the difference would be 9.5%.

.Surprisingly for Company 21, specimens with indentations showed higher tensile strength than those without the defect. It was observed that for 3 specimens, out of the set of five, the indentation was not very significant (See Appendix A). This may very well have affected the outcome of the results.

There appears to be a small influence of the indentation on the axial tensile strength of web specimens. However this influence was not statistically confirmed at the 5% significane level chosen in this investigation (See Appendix A). The relatively inconsistent degree of indentation as well as the highly sensitive axial tension test may have obscured the importance of the indentation. Nevertheless the observed failure mode in the direct tension test showed that the horizontal cracking line always passed through the indentation.

Tensile Strengths of Face Shells and Webs

The results from almost all series (not including Series T1 and T2) appear to indicate that the tensile strength of the unit's face shell is higher than that of the web. The highest difference obtained was around 11%. When any influence of the indentation was eliminated, differences in strength between the face shell and the web may be due to a lesser degree of compaction in the webs. However, given the fact that tensile strengths are low, differences are difficult to identify and, for the level of significance chosen in this study (See Appendix A), statistically there was no difference between the tensile strength of face shells and webs. Nevertheless different conclusion can be drawn at different significance level.

Influence of Packing Material on Splitting Tensile Strength (Series ST1 and ST2)

In the splitting test, placing the steel rods directly on the bed face of the block (to induce line loading) might create a potential for crushing[17]. As a result, crushing under the line load would be expected to extend into a large area of the specimen. Hence a compressible material is needed between the steel rods and the test specimen to absorb the deformation that would occur if the steel rods were placed directly in contact with the specimen.

Wood strips of 6.5 mm thickness were placed between the steel rods and the specimen in all the splitting test series in this study. Eventhough the thickness of this packing material was not adequate to absorb all the deformations, the splitting tensile strength was enhanced by 28.6%. Although it is difficult to draw conclusions based on a single set of test data, it appears that it is necessary to employ a packing material to reduce the local crushing at the joint load. Further examination is needed regarding the required thickness and type of packing material.

2.2.4.5 Conclusions

1. A significant difference in tensile strength was revealed from splitting half stretcher units across the webs instead of across the face shells.

2. Eventhough a small difference was observed, the splitting strength of half units loaded across the face shells can be taken to be reasonably equal to that from splitting a square piece cut from the face shells.

3. The splitting strengths of half units loaded across the webs were significantly lower than those of square pieces cut from the webs. This was true for both block companies. Splitting of square pieces may be taken as a measure of the tensile strength of the concrete materials in the web while splitting of a half unit across the webs is a measure of the web tensile strength.

4. The direct tension test appear to be a feasible test method but is sensitive to alignment. Specially designed

test apparatus can reduce misalignment greatly.

5. For one block company, the axial tensile strengths were significantly lower than strengths obtained from all other tests.

6. The indentation in the block webs reduced the axial tensile strength by 9% for Company 10. Results from Company 21 did not confirm this observation.

7. From most Series, the tensile strengths of webs were slightly lower than those of face shells. Statistical confirmations depend on the levels of significance.

8. The use of packing material in splitting tests enhanced the tensile strength of the specimen by 28%.

9. The tensile strength from the various tests ranged from 5.0% to 9.5% of the compressive strength of hollow concrete units.

10. No comparison between tensile strengths for different curing conditions was possible because mix design and other factors affect the strength.

2.2.4.6 Recommendations

1. For better correlation with the compressive strength of face shell mortared masonry it is recommended that the tensile strength be determined from splitting tests with the load applied across the webs.

2. Refinement of the direct tension test apparatus is needed before it is to be adopted as a standard test.

3. Research work is needed into the significance of the use of packing in splitting tests. Type of packing material and its required thickness are of concern.

2.3 MORTAR

2.3.1 General

Eventhough mortar constitutes a relatively small proportion of a concrete masonry wall, it is a vital component contributing to strength (compressive and tensile), durability, weather resistance and water-tightness properties of masonry as well as to the effectiveness of the construction process.

Quantitative requirements for mortars have not been well defined in terms which directly relate to their properties. The current "prescription" type method of quality control through assuring that standard proportions of material by volume are met, provides some assurance of reproduction of mortars which are thought to have performed satisfactory in the past. Alternatively the "performance" type of quality control through determination of cube strength provides some indication of adequate presence of cementing material. Except for the experience factor, neither can be claimed to provide an accurate indication of the likely behaviour in terms of the above properties.

The difficulties presented in trying to understand the role of mortar arise from its widely varying properties (fresh and hardened), different types and amount of commentitious materials that can be used and differences in sand properties.

2.3.2 Background

The North America mortar specifications (ASTM-C270[5] and CSA-A179[23]) are very similar and a history of the development of ASTM-C270 was written by Davison[30]. These specifications fall short from offering a real "performance-type" specifications. Instead they are a compromise presenting alternative "prescription-type" (proportion) and "performance-type" (property) specifications[16,30,56].

Under the proportion specifications, only the mix proportion shall be met to produce the desired type of mortar (Types M, S, N, O or K) and only water retentivity test as a quality control test shall be performed[23]. Property specifications differentiate between laboratory prepared mortar and job-prepared mortar in the fresh-mortar state (flow requirement) and in the hardened state (different compressive strengths) in CSA-A179[23]. It was reported[65] that mortar mixed under the proportion specifications yields much higher laboratory cube compressive strength than when mixed to satisfy the property specifications.

Most of the sands currently used to manufacture masonry mortar do not fall within existing grading limits[60] as specified in CSA-A82.56[22]. Masons are generally accustomed to using a fine masonry sand to avoid having to deal with harsh mortar due to high percentage of coarse sand[40]. It appears there is little information on the influence of the sand grading on the mortar properties. ASTM-C270 has limits on Fineness Modulus from 1.65 to 2.5. Gazzola[41] suggested that sands that are somewhat finer than allowed will not adversely affect strengths and are generally preferable for better workmanship. Jessop[60] reported that (within reason) gradation limits per se are of very little significance to mortar mix design. Excellent water retention and desirable bond to masonry units were attributed to fine sand in the mortar[28,106]. However, low prism compressive strength was related to mortar with fine sand[106]. Test data from Belgium[76] showed a small increase in mortar and wall strengths for sand with Fineness Modulus of 0.57 over sand with 1.16 Fineness Modulus. However mortar made of 1.7 Fineness Modulus sand showed a 16% and 7% increase in the strength of mortar and walls, respectively, over those made with the very fine sand with a 0.57 Fineness Modulus. European standards appear to allow a much wider range for sand gradation, especially for fine sand as shown in Table 2.6.

Masonry cement has become the predominant commentitious component of mortar used in most parts of Canada. The use of masonry cement has been associated with better workabiltiy[41,58], higher water retention[28] and enhancing the durability of mortar by enduring freezing and thawing effects[58]. There is practically no information on the influence of masonry cement mortar on the compressive strength of blockwork masonry. Test data have associated the use of masonry cement with low tensile bond values for masonry[28,41]. However, Isberner[58] concluded that masonry cement mortar will develop the necessary compressive, tensile and shear bond strengths if utilized and cured properly. Sneck[106] reported that masonry cement mortar will develop higher bond strength with leaner mortars. The bond strength of 100/800 mortar was about twice that of 100/500 mortar (100/800 = 100 kg of masonry cement and 800 kg of sand).

Air-entraining agents cause the formation of air bubbles which improve the workability and water retention of the plastic mortar and the freeze and thaw durability of hardened mortar. The inclusion of air in masonry does however reduce the compressive strength of mortar. Tests by Fishburn[58] indicated that a 1 percent increase in air content caused about a 2 percent decrease in the compressive strength of Type S Portland Cement-Masonry Cement mortars. High air contents were associated with masonry cement mortar[28]. Limits on air content first appeared in 1962 and a maximum of 24 percent was recommended in 1966. However there appears to be a sharp division of opinion on the issue of limits on air content[30]. Current Canadian specifications[23] don't provide any limits for air content. However ASTM-C270[5] specifies limits for laboratory prepared mortars only under property specification (Maximum air content limit of 22% is specified for masonry cement mortar).

Flow is the most common test method in use throughout the world for assessing the workability of mortar. The workability is of fundamental importance to the mason and as Langan and Jessop[65] defined it"...workability is a complex rheological property embodying such properties as plasticity, consistency, cohesion, adhesion and viscosity". Current code specifications[5,23] for laboratory prepared mortar set flow limits between 110-115%. No limits are set for on-site mortars. Usually mortar is mixed to achieve a certain workability desired by the mason whether in the laboratories or on the job-site. Flow values of fresh mortar mixed in the laboratories are reported to exceed the specification limits[28,36,37,41,116]. Mortar when mixed in the field will have a flow ranging from 130 to 150[16].

The principals of curing for concrete construction have been well documented and practiced but curing of masonry is seldom practiced. Proper curing of mixtures containing Portland Cement is recommended to prolong the hydration process. Application of water or maintenance of moist environments greatly prolongs the hydration period and increases the cementing characteristics of the Portland Cement component. Isberner[58] reported that laboratory tests to determine the hydration period in masonry, relying only on the water initially in the mortar, showed that less than 3 days of hydration are available for the mortar immediately adjacent to the surface mortar joint. Copeland and Saxer[28] concluded, from a study which examined the influence of curing of mortar joints in concrete block pier specimens, that damp curing (daily rewetting for first 4 days) greatly increased tensile bond of high strength, low air content mortars. Hamid[43] reported an 80 percent increase in compressive strength of water-cured mortar, Portland Cement-Lime (Types S and N), over that of air cured mortar. CSA-179M[23] specifies that mortar cubes of laboratory and job mixed mortar shall be placed in moist room at a relative humidity greater than 90 percent for 20-24 hours then in lime-saturated water until tested. There is a need to establish the effect of curing on mortar in atmospheric, water and moist surroundings. In addition there is a lack of information on the effect of curing on mortar made with different compositions, specially masonry cement mortar.

2.3.3 Outline of Investigation

As outlined earlier in Chapter 1, an investigation which incorporates a broad base of material properties was planned. Twenty nine companies from across Ontario supplied hollow concrete units and each company was also asked to supply the common masonry sand from the area which it serves. Sand was sent from only 19 different sources. For the other companies, the local Hamilton masonry sand was used.

The local Hamilton Masonry sand was used even though it has a high percentage of fines passing the 630 microns sieve. It was also decided to use masonry cement. Hence the standard mortar used throughout this research had proportions of Portland-Cement: masonry cement: sand of 1:2:8 by volume which corresponds to 1:1.45:9.58 by weight. This particular composition was designated as Type S2 mortar.

Series BM1 was intended to provide data from a large variety of sand sources in order to evaluate the influence of sand gradation on cube strength, flow and air content. Three 50.8 mm (2 in.) cubes were made from each of the 29 mortar batches comprised of 19 batches corresponding to 19 different types of sand and 10 batches using McMaster masonry sand. Detailed experimental results were listed in Appendix A.

Using 9 different sands and 11 different mortar batches, the influence of curing on the cube strength was investigated under three curing conditions and for two different approaches. Twelve mortar cubes were made from each batch. This study was identified as Series BM2.

Series BM3 was planned to examine the influence of mortar composition, type and strength on properties. For every investigated parameter, two batches were made. The mix proportion and types of mortar used were listed in Table 2.4

Details of the experimental work, individual results and strengths are all found in Appendix A.

TABLE 2.4: MARTAR MIXES

MORTAR TYPE	PROPORTION BY VOLUME (WEIGHT)				
	PORTLAND CEMENT	MASONRY CEMENT	LIME	SAND	WATER
S2*	1.0 (1.0)	2.0 (1.45)	- -	8.0 (9.58)	2
S1	1.0 (1.0)	-	0.5 (0.2)	4.0 (4.81)	
N2	-	1.0 (1.0)	-	3.0 (4.96)	2

* standard mortar used througout the research work, unless noted otherwise

2.3.4 Results and Discussion

2.3.4.1 Series BM1: Effects of Sands on Mortar Properties

A summary for the results from Series BM1 was listed in Table 2.5. Part A of this table is for the results of the mortars made using the different sands while Part B contains the results for the mortar batches made with McMaster masonry sand. The numbering system corresponds to the numbering system for the sources of blocks.

Sand Gradation Limits and Fineness Modulus

Sieve analyses of the 19 different sands revealed that in almost all cases the percentage of sand passing the 0.63 mm sieve size was outside the upper limit of CSA-A82.56[21]. More than two -thirds of these sands did not meet the limits for percent passing at 0.315 mm sieve size. For most sieve sizes, McMaster masonry sand also fell outside the upper limit. These results of the sieve analyses were plotted in Figure 2.3. However, only the sands from Companies 15 and 26 failed to meet the requirement of CSA-A82.56[21] that the percentage of sand retained between any two consecutive seives not exceed 50 percent. Fineness Modulus values ranged from 0.94 to 2.17 with an average of 1.48 and a coefficient of variation of 21%. Details of the sieve analyses are found in Appendix A.

Fineness Modulus of sand appears to have no influence on the compressive strength of mortar cubes, for the range examined here. In fact a linear regression analysis showed

TABLE 2.5: SUMMARY OF SERIES BM1 RESULTS (AIR CURED MORTAR)

SERIES	COMPANY NO.*	SAND F.M.	MORTAR** STRENGTH (MPa)	AGE (days)	FLOW	AIR CONTENT (%)
BM1-A: 19 Types of Sand	1	1.58	7.4	28	120	8.0
	2	1.34	7.7	28	120	7.6
	4	1.35	11.7	54	120	8.5
	5	1.34	12.4	54	120	8.5
	6	0.99	11.3	66	118	9.0
	11	1.08	10.0	72	120	9.0
	12	1.18	9.8	77	116	9.0
	13	0.94	10.0	77	124	7.0
	14	1.37	8.3	83	120	9.5
	15	1.87	10.4	83	121	9.8
	18	1.45	12.9	92	120	8.5
	19	1.67	8.2	94	118	9.0
	20	1.48	6.0	97	118	11.0
	22	1.45	7.5	99	118	9.0
	23	2.17	10.5	100	120	7.5
	24	1.70	8.6	105	120	8.5
	25	1.84	7.7	106	122	11.0
	26	1.67	7.1	106	121	9.0
	28	1.60	10.5	28	124	8.4
BM1-B: McMaster Masonry Sand	3	1.19	12.6	45	119	
	7		10.2	66	116	
	8		16.0	67	120	
	9		13.0	67	120	
	10		11.9	29	125	
	16		12.5	84	120	
	17		11.8	91	121	
	21		11.3	30	121	
	27		12.0	30	120	
	29		13.7	28	118	

* corresponding to source of blocks used with the particular sand
** average of 3 cube compressive strengths
F.M.= Fineness Modulus

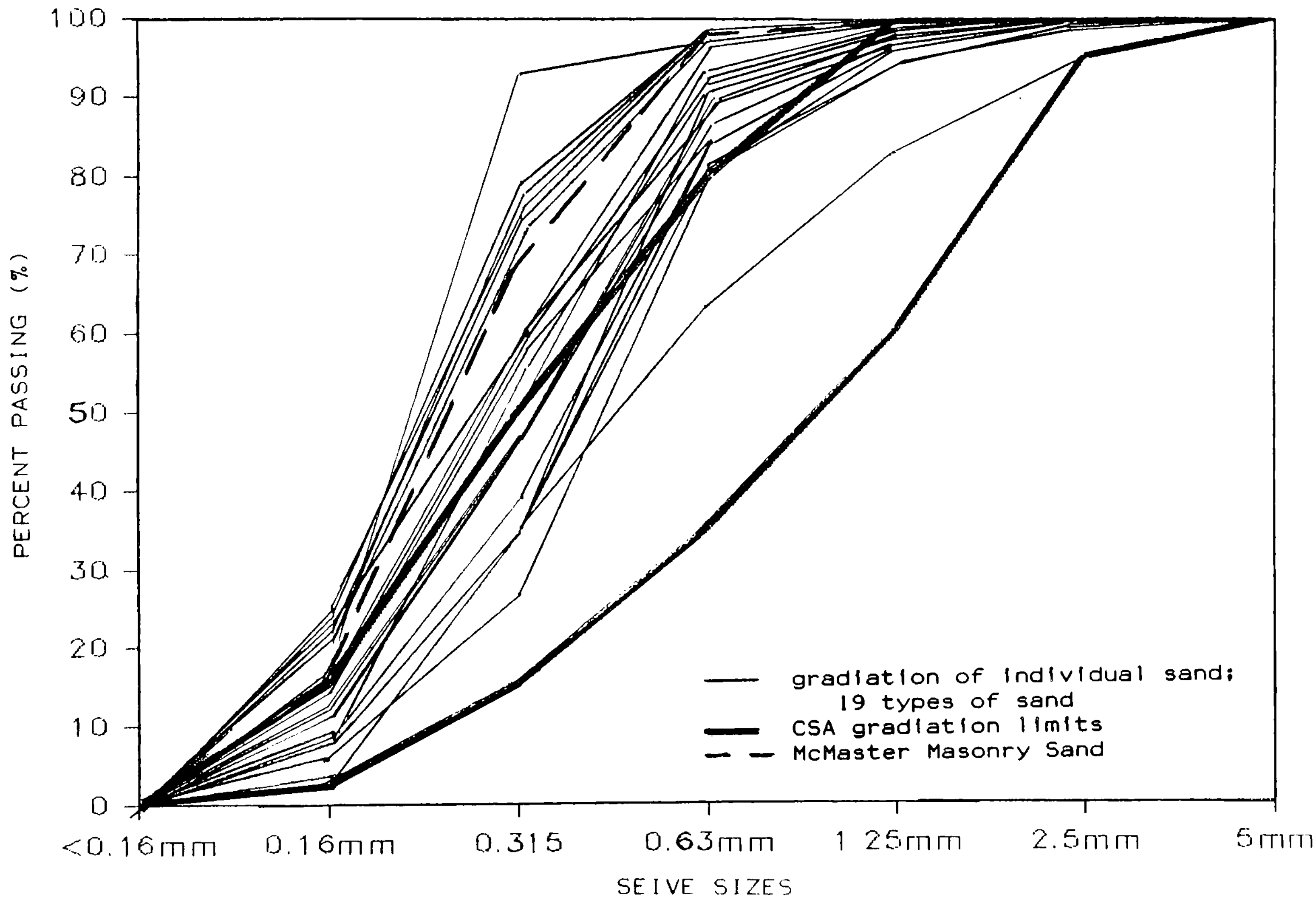

FIGURE 2.3 SEIVE ANALYSES FOR McMASTER MASONRY SAND AND 19 DIFFERENT TYPFS OF SANDS

very little correlation (correlation coefficient r=0.22) suggesting that the compressive strength decreased slightly with increased Fineness Modulus. This finding conforms with previous research results discussed in Section 2.3.2. It is clear from Figure 2.3 that most of the sands currently used in making masonry mortar do not fall within existing grading limits and new limits, designed to wrap around the data would be very broad. Hence a revision to CSA A82.56M-76 is needed so that limits corresponding to actual practice can be applied to sand gradation. Therefore sand gradation limits were drawn based on the sieve analyses of the 19 deferent types of sand. These limits are suggested to replace the current gradation limits set by CSA-A82.56M-1976. The Chahine Practical Masonry Sand Gradation Limits were listed in Table 2.6 and drawn in Figure 2.4

Sieve sizes indicated in CSA-A82.56-M1976 appear to have been rounded off; the actual size are slightly larger, i.e. 0.63 mm versus 0.60 mm, 0.315 mm versus 0.30 mm and 0.16 mm versus 0.15 mm. The sieve sizes used in this investigation were the actual sizes and corresponded to those used for concrete sand as defined by CSA-A23.1-M77, "Concrete Materials."

Flow Limits

Flow limits in CSA-A179[23] of 110 to 115 for laboratory mortar appear to be unsuitable for laying block masonry. Flow

TABLE 2.6: GRADING LIMITS FOR MASONRY MORTAR SAND

SEIVE SIZE	PERCENT PASSING				
	CSA A82.56-M1976	MIN.- MAX. OF VARIOUS SANDS (1)	PROPOSED NEW LIMITS (Chahine)	I.B.N. (2)	JESSOP LIMITS (3)
5 mm	100	99.8-100	95-100	100	95-100
2.5 mm	95-100	94.8-100	90-100	80-100	85-100
1.25 mm	60-100	82.6-100	80-100	60-100	85-100
0.63 mm	35-80	63.0-98.3	55-95	20-98	65-100
0.315 mm	15-50	26.6-92.2	20-85	0-78	15-80
0.16 mm	2-15	3.5-23.9	0-25	0-30	0-35
<0.16 mm	-	0-0.3	0	0-5	-

(1) limits based on 19 different sands from across Ontario.
(2) Institut Belge de Normalisation, Refrence 70.
(3) Jessop, Refrence 60.

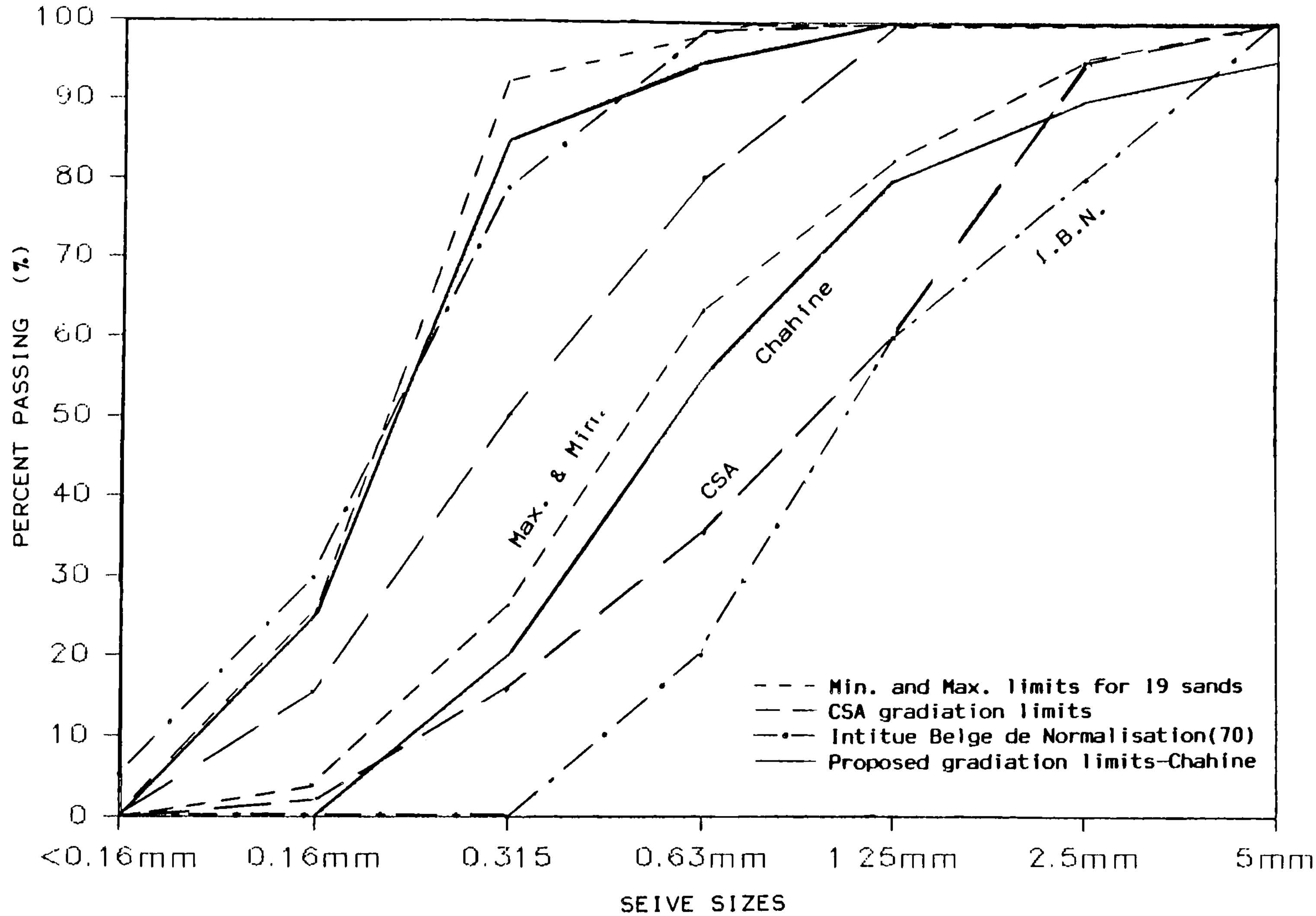

FIGURE 2.4 SAND GRADIATIONS LIMITS

values suitable to the mason ranged from 116 to 124 with an average of 120 and less than 2% coefficient of variation. For the range examined, higher flows did not correlate with lower mortar compressive strengths. The results of Series BM1-B confirm this. Perhaps higher allowable flow limits need to be considered.

Air Content

Air content in fresh mortar ranged from 7.5% to 11% with an average of 8.8% and an 11.6% coefficient of variation. A linear regression analysis did in fact confirm the common belief that high air contents are related to decreases in the compressive strengths of mortar. However, it should be noted that none of the air contents were near the specified 22-24% limit[5].

Influence of Age on the Compressive Strength of Mortar

Results from Series BM1-B indicate the influence of age on the compressive strength of Type S2 mortar since for these 10 batches the same McMaster masonry sand was used and the flow was almost the same. This series included mortar tested at 30, 45, 60 and 90 days. Linear regression analysis showed that, for the dry curing conditions, age beyond 28 days and for the periods examined has no influence on the compressive strength of mortar (See Figure 2.5)

2.3.4.2 Series BM2: Influence of Curing on Strength of Mortar Cubes

Advantages of adequate curing of masonry mortar are clearly observed in the results listed in Table 2.7. Individual results and mortar properties were found in Appendix A. Based on 11 batches of Type S2 mortar, made using 9 different samples of sand, moist curing resulted on average in 27% increase in compressive strength over air cured mortar. The maximum increase was 90%. Moist cured mortar averaged 8% higher compressive strength compared to lime-water cured mortar. The maximum increase was 30%. The compressive strength ratio of air cured to moist cured mortar cubes were shown in Figure 2.6. It is important to indicate that lime-water cured mortar cubes were tested wet as specified by CSA-A179M[23]. This could explain why the lime-water cured mortar had lower strengths than moist cured mortar. If the water cured mortar cubes were allowed to dry for around 20 hours prior to the 28 days testing, the compressive strengths would be expected to be higher than for moist cured cubes.

To illustrate the fact that mortar in an assemblage will be different from mortar placed directly in cube molds, Batch M3 mortar was placed on concrete locks for 2 minutes then used to make cubes. The increase in strength due to

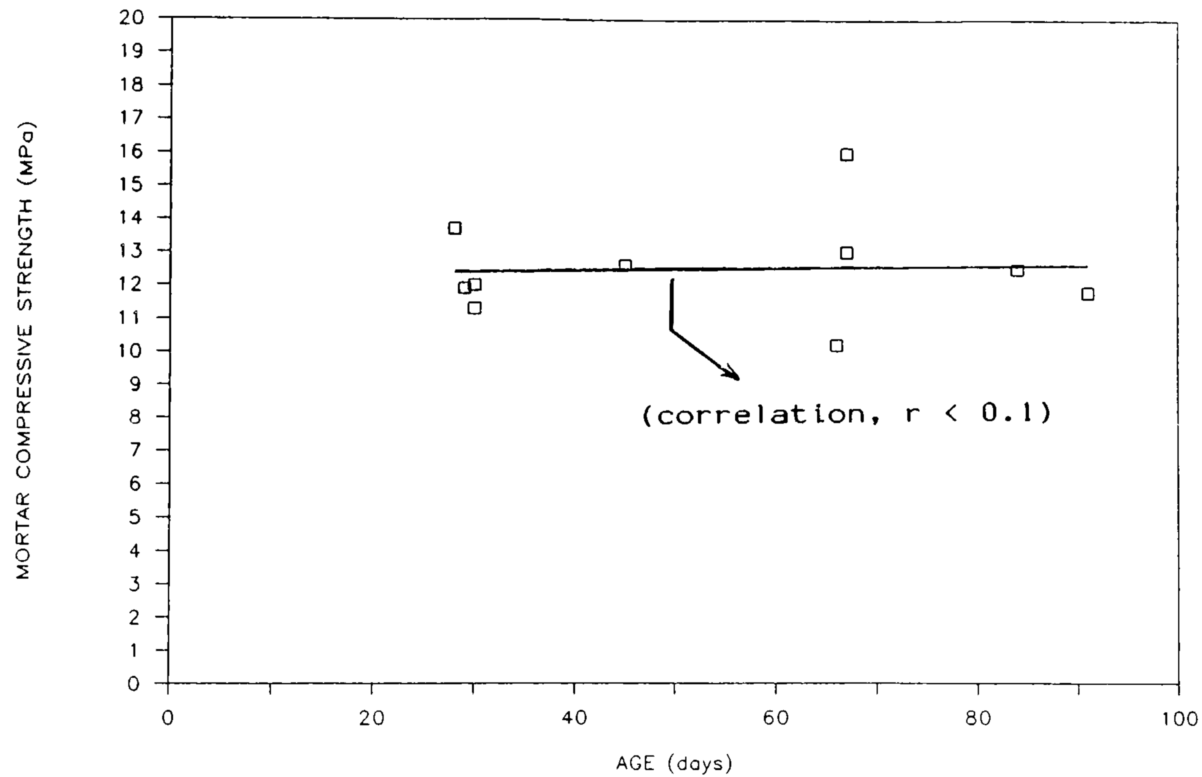

FIGURE 2.5 INLUENCE OF AGE ON COMPRESSIVE STRENGTH OF TYPE S2 MORTAR ,McMASTER MASONRY SAND (SERIES BM1-B)

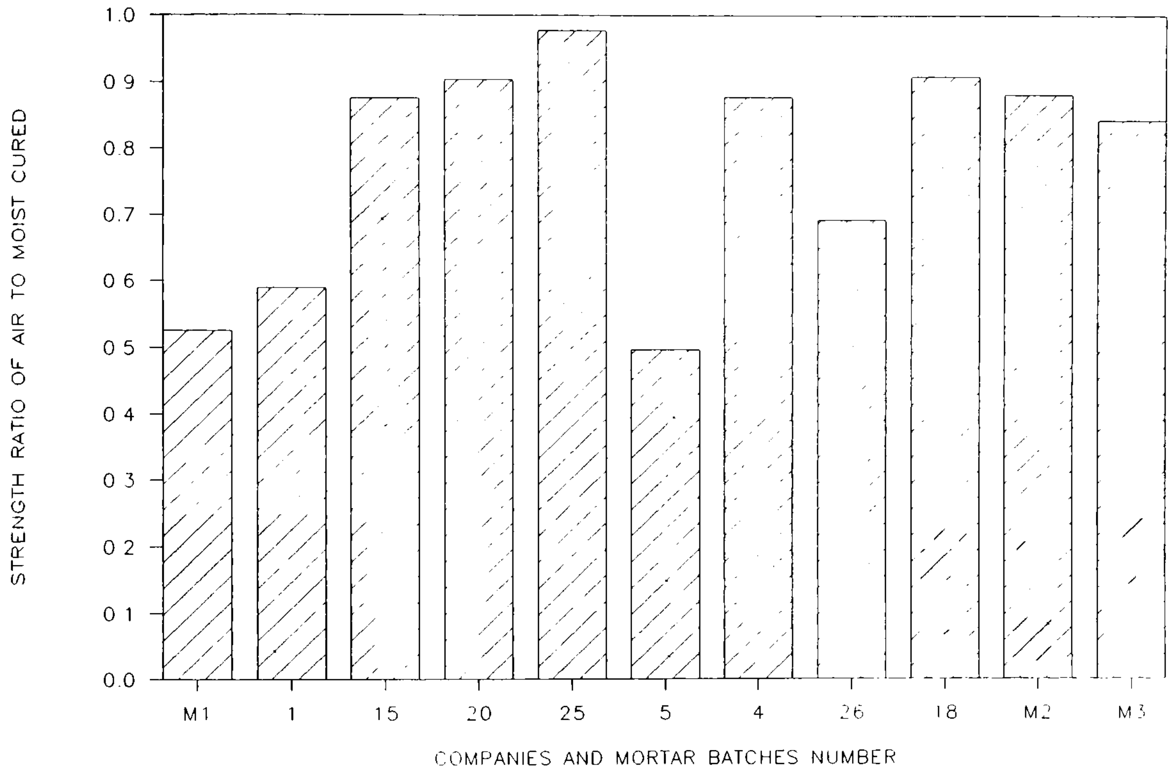

FIGURE 2.6 MORTAR COMPRESSIVE STRENGTH RATIOS FOR AIR CURING VERSUS MOIST CURING (SERIES BM2)

absorbed water can be seen in Table 2.7 where, compared to Batch M2, 14%, 8.5% and 8.7% increases for moist, lime-water and air cured conditions, respectively, were observed. It is important to note that the flow for Batch M3 mortar was a high value of 129. This is an additional evidence that the upper limit set for flow in CSA-A179M[23] is restrictive and a higher upper limit should be considered.

Of particular importance are the results in Table 2.8 for Batch M1 and M2 mortars which both were made using McMaster masonry sand. It is interesting to note that lower flows which correlate with lower water to cement ratio resulted in higher strengths where moist curing ensured sufficient water available to hydration. However for very dry air cured conditions, the high flow (high water content) mortar had higher strength which is likely attributable to this extra amount of water available for hydration. Isberner[58] commented on the influence of water for hydration and it can be seen that when good curing conditions do not exist in construction, use of a high flow mortar may be quite desirable.

2.3.4.3 Series BM3: Study of Mortar with Different Compositions, Types and Strengths

The results from Series BM3 were listed in Table 2.9 along with some of the fresh mortar properties. Mortar was

TABLE 2.7: SERIES BM2, EFFECTS OF CURING ON MORTAR COMPRESSIVE STRENGTH (TYPE S2 MORTAR)

CURING	MOIST		LIME-WATER		AIR	
BATCH NO.	MEAN STRENGTH (MPa)	C.O.V. (%)	MEAN STRENGTH (MPa)	C.O.V. (%)	MEAN STRENGTH (MPa)	C.O.V. (%)
M1	19.4	2.4	15.3	3.1	10.2	2.7
1	16.1	4.4	13.5	2.2	9.5	3.2
15	15.2	2.3	15.6	6.1	13.3	2.6
20	11.4	3.7	10.9	4.4	10.3	5.0
25	13.2	1.7	14.1	1.8	12.9	5.7
5	19.3	3.7	14.0	6.8	9.6	7.0
4	14.7	5.3	14.7	3.1	12.9	8.5
26	15.6	0.9	13.1	8.8	10.8	12.3
18	16.3	0.5	16.2	5.4	14.8	4.8
M2	15.1	3.6	13.8	4.5	13.3	2.2
M1	17.2	2.3	15.0	3.7	14.5	2.3
n	3		6		3	

C.O.V.= coefficient of variation
M= McMaster masonry sand
1 or other number= source of sand (Block Company)
n= number of mortar cubes per batch

TABLE 2.8: EFFECTS OF FLOW AND CURING ON MORTAR COMP. STRENGTH

MORTAR BATCH	INITIAL FLOW	FLOW AFTER SUCTION	WATER RETENTIVITY(%)	MORTAR STRENGTH (MPa)		
				MOIST	WATER	AIR
M1	111.5	96	86.1	19.4	15.3	10.2
M2	129	96	74.4	15.1	13.8	13.3

TABLE 2.9: SERIES BM3, RESULTS OF MORTAR COMPOSITION AND STRENGTH INVESTIGATION

MORTAR TYPE & BATCH NO.	AIR CONTENT (%)	FLOW	FLOW AFTER SUCTION	WATER RETEN-TION(%)	COMPRESSIVE STRENGTH (MPa)	C.O.V. (%)
S2(PC-MC) B1 to B9	12	120			7.8	10.1
N2						
B10		116	86	71	2.1	7.7
B11	13	122			2.0	4.9
B12		117			2.9	6.1
S1(PC-L)						
B12		116			8.2	2.2
B13	3.5	122	76	62	10.1	13.7
B14		118			8.5	20.5
5 MPa*						
B14		117			1.3	2.7
B15	12	116	30	26	1.3	2.0
20 MPa*						
B18	6.5	100	76	76	25.0	8.6
B19		96			24.8	10.1

* specified compressive strength

mixed during the winter and the cubes were air cured until tested at 6 months age. Most of the results tend to be low when compared to the suggested strengths specified in CSA-A179[23]. This is explained by the fact that mortar cubes were placed in a heated room where the very dry atmosphere caused a quick loss of water and the hydration of Portland-Cement was arrested. Eventhough the strength values were relatively low, all mortars in this Series were subjected to the same conditions and that is sufficient for the purpose of cross-comparison.

Mortar Composition

Under the proportion specifications, Portland Cement-Lime mortar (Type S1) resulted in higher compressive strength than Portland Cement-Masonry Cement mortar (Type S2). The three batches of S1 mortar had an average cube compressive strength 14% higher than type S2 mortar. The compressive strength is not the only property affected by the mortar composition. While the mortar flow appeared to be the same for the two different compositions, Portland Cement-Lime mortar has a lower water retentivity (62%) than allowed by CSA[23]. In addition, Type S1 mortar had only 3.5% air content while Type S2 mortar had 12% air content. Eventhough these control tests are not truly descriptive of the actual mortar properties, it may appear that the use of masonry cement slightly sacrifices the compressive strength for better workability.

Type of Mortar

Mortar prepared under the proportion specification (Type N2) yielded higher compressive strength than 5 MPa specified mortar prepared under the property specifications. Eventhough comparable air content and initial flow results were obtained, the water retention values greatly differed. This may be attributed to a combination of differences in composition and mix proportion since the cementitious material in Type N2 mortar constituted solely of Masonry Cement while a mixture of PC-MC was used for the 5 MPa target strength. This aspect was examined in relation to the prism behaviour later on in Chapter 4.

Strength of Mortar

A high strength mortar, with a target strength of 20 MPa, was also included in this series. The results obtained from the two mortar batches showed that high compressive strengths can be achieved with masonry cement, 25 MPa compressive strength was actually obtained. In addition, acceptable fresh mortar properties were maintained with an initial flow of 100 and a very desirable water retentivity of 76%.

It is well known that mortar in masonry joints can have very different properties and be subjected to very different stress conditions than mortar cubes. Therefore, while the above discussion provides some useful insight, the study reported in Chapter 4 where the influence of mortar composition on masonry assemblages was examined may have more direct bearing on this discussion.

2.3.5 Conclusions

The following conclusions have been drawn from this mortar investigation:

1. Masonry sand currently in use across Ontario does not meet the gradation limits specified by CSA-A82.56[21], "Aggregate for Masonry Mortar". Most of the 19 samples of sand examined showed percentage passing of sand falling outside the CSA upper limits and Fineness Moduli ranged between 0.94 and 2.17 with an average value of 1.42. for the range examined. The Fineness Modulus of the sand had little influence on the compressive strength of Type S2 mortar.

2. The upper flow limit of 115, specified in CSA-A179-M76[23], appears to be unsuitable for laboratory mixed mortar used to make concrete block assemblages. Flow values around 120 were found to be suitable.

3. Portland Cement-Masonry Cement (PC-MC) mortar had air contents of up to 12% which were well below the specified

maximum limit of 22%[5].

4. Beyond 28 days, age appears to have no influence on the compressive strength of Type S2 mortar for the time period and curing conditions examined.

5. The compressive strength of PC-MC mortar was greatly affected by the curing methods. Moist curing of mortar cubes enhanced the compressive strength by an average 27% over air curing, based on 11 different mortar batches. Lime-water curing also resulted in an average 18% increase in mortar strength.

6. Flow of mortar and curing method interaction was evident on the strength of Type S2 mortar. Compared to air cured cubes, a 90% increase in strength was attributed to the moist curing of low flow mortar while only 14% increase was achieved in the case of high flow mortar.

7. In comparison to PC-MC mortar, PC-Lime mortar resulted in a little higher compressive strength, below specified limit water retention value and much lower air content percentage.

8. Masonry cement can yield high strength mortar with acceptable flow and water retention properties.

2.3.6 Recommendations.

1. Practical masonry sand gradation limits, "Chahine limits" were drafted. These grading limits are proposed for

revision of CSA-A82.56-M76[21].

2. Correct sieve sizes should be used as defined by CSA-A23.1-M77, "Concrete Materials", since the same sieves are also used for concrete sand.

3. There is a need for evaluating the current specified limits for flow of laboratory mixed masonry mortar[23]. Flow of mortar suitable for use in construction should be used.

4. There is an apparent merit in considering moist curing of masonry assemblages. However the influence of swelling and shrinkage of blocks would have to be considered. Further research work is needed in this area.

CHAPTER 3

EVALUATION OF TEST METHODS AND FAILURE OF FACE SHELL MORTARED CONCRETE BLOCK MASONRY IN AXIAL COMPRESSION

3.1 INTRODUCTION

3.1.1 General

To define compressive strength of masonry, building codes [1,7,26,29] permit either direct testing of prisms made using the job site materials or use of previously established tables based on unit strength and type of mortar. However, since the value of the tables were also originally based on prism tests, both methods are very much influenced by the way in which prisms are tested.

Determination of compressive strength, f'_m, on the basis of a 2-course prism laid in stack pattern is not only allowed but encouraged by adopting height correction factor for various prism geometries[51]. These correction factors enable conversion of the strength of a prism of a particular geometry to that of a standard height to thickness of 2, for which the correction factor is unity. This implies a correlation between the prism with h/t = 2 and full-scale masonry[51].

From a practical point of view, it is understandable that 2 block high prisms have been standard because many commercial test facilities cannot accommodate higher specimens and because larger prisms create additional problems of lifting and transporting without damage. Similarly, it has been convenient to use a stack pattern. As it became understood that full bed joints with a stack pattern and/or fully hard capped ends resulted in a conical type failure not resembling the observed web splitting failure in face shell mortar bedded walls and higher prisms, use of face shell mortar joints and soft capping were adopted to better simulate the actual behaviour[25]. However, this practice itself may have introduced other inconsistencies in behaviour which will affect the test results[68,104].

While the prism test is widely used to establish the ultimate compressive design strength, f'_m, of masonry, current test procedures[1,26,79,107] differ widely and the interpretation of the results is open to question. Items of particular concern include:

1. the code(s) correction factors for prism geometry
2. the influence of capping configuration on prism strength
3. the influence of capping material on prism behaviour

4. the influence of bearing plate thickness
5. the influence of end-loading conditions (boundary conditions).

Different methods have been used to calculate the compressive strength of hollow face shell mortared block masonry. Some investigations[51,77,97] used stacked prisms with face shell mortaring and calculated the ultimate strength based on the minimum face shell area of the block. Others[37,43] used fully mortared joints with minimum net area (or only net area) of the block for stress calculations. Codes also specify different areas for use in ultimate strength calculations [27,26]. Use of the actual loaded mortared area has been suggested recently[67,88]; however it is unclear as to how this area should be determined.

Various failure mechanisms have been proposed for solid masonry[10,32,38,54] with the traditional explanation being centred around the difference in the mechanical properties between the unit and mortar. The vertical tensile "splitting" of masonry has been attributed to the mortar, being softer than the unit, which is confined laterally hence giving rise to lateral tension in the units and triaxial compression in the mortar. Fully mortared hollow masonry has also been assumed to fail in a similar manner. However recent research work[101,102] suggested that these stresses may be too small to be the sole cause of such failures and that stresses which develop at the tip of flaws, used to explain splitting failure of concrete under axial compression, may be equally applicable for solid or full bedded masonry.

Face shell mortared hollow blockwork develops vertical cracking in the webs under axial compression[37,104,105,116]. In this case, the tensile "splitting" theory developed for solid fully mortared masonry does not provide a satisfactory explanation of the cracking of face shell mortared masonry since its application give the expectation that face shells not webs should crack under axial loading. A failure mechanism similar to "deep beam bending" has been suggested[12,37,88] and conceptual analyses have been presented[37,104]. However, eventhough web cracking has been observed in many investigations, no detailed strain (deformation) investigation has been presented to support the suggested failure mechanism.

3.1.2 Background

Since the wallette tests conducted by Richart in 1932[51] an enormous number of compression tests on prisms have been conducted. Hence it was expected that prism configuration (number of courses, stack or running bond) and a test procedure (type of loading, capping material) would have been established to provide a reasonable measure of wall compressive strength. Unfortunately many questions remain unanswered and research literature on concrete masonry is scattered and sometimes not well documented. It seems that current standards and specifications for block masonry have been to some extent derived from traditional methods of masonry construction, behaviour characteristics of brick masonry and from concrete technology.

Effect of Height of Prism

As is the case with concrete, the compressive strength of the test specimen is often confused with the compressive strength in the structure[35]. Therefore it is necessary to interpret the results of concentric compression tests on the 2 block high prisms usually used[1,7,26]. An attempt to provide an answer to why the standard concrete prism height is 2 revealed:

1. The standard brick prism is 5 units high which is roughly equivalent to 2 blocks in height. The fact that more research work has been done on brick masonry and at earlier stages may have influenced specifications on concrete masonry.

2. Concrete masonry as a structural material may be thought to be similar to Portland-Cement concrete. In North America, the compressive strength of concrete is determined from compression tests on concrete cylinder with height to

diameter ratio of 2. Since this ratio is thought to avoid much of the influence of end platen restraint, its adoption for blockwork might be based on this precedent.

3. Correction factors to convert the strength of a prism of particular geometry to that of a prism with a height to thickness, h/t, of 2 have been specified by various national codes[84]. The correction factor for the standard prism is unity. These correction factors are assumed to apply for all types of prisms regardless of the bond-type, percentage solid of the unit and the strength of unit. Foster and Bridgeman investigated the origin of these universal connection factors[51,84,88]. They revealed that "... while different masonry codes may have a different "standard shape", i.e. a different value of h/t for which the correction factor is unity, the ratio of the conversion factors is constant - which suggests a common source..." [51]. The correction factors from various codes, after having been divided by a code factor to produce a value of 0.80 at h/t = 3.0, were listed in Table 3.1. As can be seen, the common source appears to be the exploratory investigation reported[51] to have been carried out by Kerfeld. Eventhough this research involved only one type of brick, one type of mortar and two pier types of varying height[88], it appears that the results have ben accepted as having general validity, not only for brick, but for block masonry also.

4. Many investigators[35,51] have indicated that the use of a 2-course high concrete prism is usually preferred due to the limited clearance of universal testing machines and for handling purposes. It is also the lowest height that still incorporates at least one mortar joint in the specimen.

TABLE 3.1: COMPARISON OF CODE CORRECTION FACTOR
(after FOSTER and BRIDGEMAN in Drysdale et al., Ref. no. 34)

SOURCE	"CODE FACTOR"	h/t= 1.5	2.0	2.5	3.0	4.0	5.0	6.0
Kerfeld	-	-	.67	.75	.80	.89	.96	1.0
New Zealand Standard	1.50	.58	.67	.74	.80	.89	.95	1.0
Australian Standard	1.25	-	.68	.74	.80	.88	.93	.93
Canadian Code: Concrete)	1.50	.57	.67	.74	.80	-	-	-
Canadian Code: Brick	0.93	-	.68	.74	.80	.89	.93	-
Uniform Building Code	1.50	.57	.67	.74	.80	-	-	-
National Bureau of Standards	1.50	.57	.67	.74	.80	-	-	-
Structural Clay Products Institue	0.93	-	.68	.74	.80	.89	.93	-

The compressive strength of prisms, with the same cross-section, decreases as the height of the specimen increases. This is due to the diminishing influence of platen restraint[51,84,88,104]. When a brittle material is loaded free of platen restraint, it expands laterally in a uniform manner and failure occurs by cracking in the vertical direction under the action of lateral tensile stresses induced around flaws in the material[88]. When a shorter specimen is tested, its ends are significantly restrained by the testing machine platens; hence the lateral expansion is inhibited leading to a higher measured compressive strength.

An ideal prism size, to be used for strength determination of block masonry, should meet the following two criteria:

1. The prism failure mode should resemble the failure mode in structural members.

2. The prism compressive strength and elastic properties should correlate well with behaviour in structural members.

Solid and fully mortared hollow concrete walls have been observed to fail by vertical cracking along the wall plane[37,54,72] while face shell mortared walls fail by vertical cracking of the cross webs[37,88,116]. Nacos[77] showed that 2 high stack pattern hollow block prisms failed by shearing along the face shells regardless of whether hard capping was applied to the full area or to the face shells. Similar shearing action observed by others[43,51,97,117] does not resemble failure in walls. Shive[104], however, reported that 2-course prisms with mortared face shells and full fibreboard capping developed vertical web cracking.

In prisms with 3-courses, the failure mode approaches the representative tensile cracking in the central unit[32,51,97]. In 4-course and 5-course prisms the failure mode more closely resembles a wall compression failure[51,117]. Hegemier[51], however, indicated that differentiation of failure modes for grouted prisms is difficult and the failure mode is not a good indicator of platen restraint. He suggested that compressive strength is the most sensitive measure of platen restraint. In the absence of soft capping material, it has a strong influence up to 4 courses. Hegemier also observed that the prism compressive strength was a function of the number of bed joints in the specimen and not the h/t ratio. Boult[14] had found that the variation between results from different batches of prism made it very difficult to make any statement regarding the rate of strength reduction with height. In addition elastic moduli for 2 course were found to be higher than for 4 to 10 courses. He concluded that there is no significant difference in strength between a full storey height column and 3 to 5 block high prisms. However, Fattal and Cattaneo[37] concluded that the initial elastic modulus of concrete masonry wall was reliably predicted from 3-course prism with flat support conditions which consistently showed moduli greater than those obtained from prisms with pinned support conditions. Finally, Wong[117] reported that for hollow and grouted prisms, it is apparent that a 4-course prisms height is desirable to minimize the influence of platen restraint while not having any significant slenderness effect.

Influence of Capping Material

The bed joint planes of concrete units are somewhat uneven and have some degree of roughness. Under compression loading the unevenness of the unit will introduce non-uniform stress distribution and the apparent strength of the specimen is reduced[82]. To overcome the effect of uneven end surfaces of the specimen capping is employed.

An ideal capping material should have strength and elastic properties similar to those of the specimen[82]. Capping material with higher elastic modulus produces lateral restraint leading to an increase in capacity. On the other hand, capping material with lower elastic modulus than those of the specimen causes the specimen to be subjected to tensile stresses arising from lateral strains induced by the capping material's lateral expansion. This leads to a reduction of the specimen strength[43,82]. An alternative approach to capping is to grind the bearing surface of the specimen until plane and smooth to ensure that no artificial enhancement or reduction of strength is introduced. Neville[82] reported that such a method produced satisfactory results but that it was rather expensive.

Capping materials can be identified as either hard or soft. Hard capping using high strength gypsum plaster and Hydrostone is specified in ASTM-C140[3]. Numerous investigations[43,51,70,82,94,97,116] have been conducted to determine its influence on the compressive strength and mode of failure of prisms. The main observation is that, for short specimens with h/t ratios of 2 to 3, hard capping resulted in high strength and the mode of failure was by shearing action. However, information is lacking on the influence of the high strength capping material on strain characteristics of block prisms. Hard capping material was reported to provide an adequate planeness of the specimen bearing surface.

A variety of soft capping materials such as plywood, hardboard, fibreboard, or highly flexible materials such as polysulphide have been used. CAN3-A369.1[25] specifies that fibreboard, conforming to CSA-A247[22], be used in prism testing. Using fibreboard on the specimen surface does not provide uniform stress distribution and capping with hard material first is necessary to achieve plane surface. Self[97] reported a 26% increase in the unit compressive strength of fibreboard cap plus plaster coating over the fibreboard cap only. For 2-course high prisms, fibreboard capping has been observed[70,97] to change the mode of failure and reduce the compressive strength to 92% of similar hard capped prisms. Hegemier[51] indicated that fibreboard capping did not sufficiently relieve platen restraint in grouted prisms and should not be used as a standard capping material for prisms. After examining the use of polysulphide as a soft capping material he judged it to be impractical and commented that its improper use can lead to premature failure.

The above review indicated that there is a lack of information on the influence of capping material on the compressive strength, platen restraint and elastic properties of representative prisms with high aspect ratios.

Effect of Type of Loading: Face Shell versus Full Bed

Face shell mortaring of hollow block masonry is an accepted practice where, even if the mortar is laid over the whole block, lack of vertical alignment of webs means that load cannot be directly transferred by the webs. Use of prisms built in a stack pattern to represent walls built in running board is questionable regardless of whether the bed joint is fully mortared or face shell mortaring is used. Self[97,104] indicated that stack bond prisms with fully mortared bed joints were 50% stronger than running bond prisms

For face shell mortared masonry it is not clear whether the load should be applied on the face shells of the prisms or on the whole bearing surface area. While this concern has tended to be overlooked, Maurenbrecher[69] recently indicated that for face shell mortared masonry, capping should be placed on the face shells only. Otherwise premature failure may occur. This conclusion was based on testing of 2-course prisms with fibreboard capping. Shrive[104] also observed that full capping reduced the strength of face shell mortared specimens by up to 50%. However, examination of these results showed that the conclusions drawn by Shrive are mainly applicable for 2 block high prisms whereas this does not seem to be the case for 3 to 5 block high prisms. In some instance interpretation of the results was affected by variations in mortar strength.

It has been suggested that the reduction in strength of face shell mortared prisms due to the use of full capping can be attributed to bending of the end webs[76,104]. Shrive[104] examined analytically the behaviour of 2 block high prism under full capping. He reported that lateral compressive stresses would exist at the web centreline near the platen. These compressive stresses would decline in magnitude as distance from the end platen increased then became tensile at the bottom of the centerline as a result of the suggested bending action. He also concluded that the strength of face shell mortared face shell capped masonry should be relatively independent of the number of units in a prism.

Face shell capping has been adopted in some standards[25,107] for testing face shell mortared prism. However, ASTM-C140 does not contain any reference to this procedure.

Some difficulties have been encountered in attempting to obtain face shell capping. Shrive[104] reported that it was not possible to test face shell mortared prisms with face shell capping under eccentric loading hence full fibreboard was used. Wong[116] experienced difficulties in achieving face shell Hydrostone (hard) capping. He pointed out that capping tended to flow over the webs. Also, Maurenbrecher[68] noted that further study is needed to verify the effect of full fibreboard capping. Little is known about the effects of full capping versus face shell capping on prisms more than 2 course high.

Influence of Mortar Bedded Area

In determining wall strength, it is important that the same mortared area be employed in calculating stresses for both masonry prisms and walls. In the past, the approach was to use the unit net area regardless of the effective mortar area. This was reflected in the 1978 edition of CAN3-S304[26]. In hollow masonry construction, the effective mortared area on the face shells is considerably less than the net area. The current editions of CAN3-S304-M84 specifies that the "mortar bedded area" should be used for strength calculations. This is defined as the mortared area in a bed joint in full contact with the units above and below. Eventhough the Code definition is clear, determination of the value for this area has been a source of confusion for both designers and researchers. Many have continued to use the net (or minimum) unit area while others used an area based on the minimum thickness of the unit face shells. Neither of these two alternatives is realistic. The former yields a lower strength while the latter overestimates the strength. Wong[116] and Maurenbrecher[67] have reported that the "mortar bedded area", for standard 190 mm hollow masonry in running bond, is around 20% more than the area based on the minimum face shell width.

Influence of Thickness of Loading Plates

ASTM-E447[7] and CAN3-A369.1[25] require that steel bearing plates be used between the spherically seated loading head of the test machine and the prism since the size of the loading head is not sufficient to cover the area of the specimen. However different bearing plate thicknesses are specified. ASTM-E447 specifies that the plate thickness shall be equal to at least one-half of the distance from the edge of the loading head to the most distant corner of the specimen. For a 225 mm diameter loading head and a standard 190 mm block, the loading plate thicknesses as specified in References 7 and 25 should be 52.2 mm and 104.4 mm respectively.

Beccia[12] used 50.8 mm (2 in.) thick bearing plates in his prism test set-up. He reported that the axial strain varied parabolically with the minimum strains at the corners of the prism and the maximum along the centreline. He concluded that this is the actual strain distribution across the prism under axial compression. Wong[116] indicated that the results from Beccia are due to insufficient stiffness in the plates, therefore causing non uniform load transfer. He performed strain measurements on 3 and 4 block high prims using 75 mm thick bearing plates and reported that the plates were suitably stiff and did not reproduce the results reported by Beccia. Strains recorded at the corners and along the centerlines were in fact almost identical at all stress levels up to failure.

The ASTM-E447[7] requirement for minimum plate thickness for block and prism compression tests was reported to be inadequate[45,51] while the CSA-369.1 requirement may be excessive.

Eventhough the current standards[7,25] specify that steel bearing plates should be used, aluminum bearing plates with various thicknesses have been employed[51,69]. Using 75 mm thick aluminum plate[69] may not meet the "hardness" requirement of 620 BRN set by ASTM-E447[7] since the elastic properties of aluminum are much less than steel. Hence adequate transfer of the load is not achieved. Hegemier[51] reported that a 203.2 mm (8 in.) thickness for aluminum plate is considered minimum to provide a uniform strain field. However. if 4 or 5 high prisms are to be tested, the minimum plate size reported by Hegemier is considered impractical since the two plates (top and bottom) would occupy a space of 2 standard 190 mm concrete units. Most suitable universal testing machines cannot accommodate this height requirement. While some research has been conducted to evaluate the influence of bearing plates' thickness on test data, current specifications on plate thickness requirement are in need of evaluation.

Influence of Support (Boundary) Conditions

ASTM-E447[7] and Can3-A369.1[25] contains requirements that the load be transferred to prisms via a spherical loading head with the prism being set flat against the machine bottom plate. This implies that the prism would be bearing against stiff steel plate which would prevent any lateral movement at the bottom of prism in the three orthogonal directions due to high frictional forces. Also, rotation would be restrained and any adjustment for prism crookedness for misalignment must be accommodated by rotation of the loading head and sideways movements of the prism.

While many researchers[43,45,51,84,95] have followed ASTM-E447, others[12,29,69,117] have used line loading. It has been suggested that line loading represents more accurately the loading condition in a masonry wall[12]. Line loading has been achieved by transferring the load to the specimen through hinges at the top and the bottom steel bearing plates (round steel rollers are usually used). The usual use of rollers as hinges permitted rotation at the top and base of the specimen. However, care should be taken in attempting to achieve line loading. If the testing machine has a spherical head, then rollers at the top and base should not be used because such set-up could lead to instability by formation of 3-hinge mechanism.

Fattal and Cattaneo[37] investigated the influence of restraining versus permitting end rotation of prisms and walls under axial compression. Restraining end rotation was achieved by applying the load with flat end conditions while end rotation was made possible by applying the load through rollers (pinned ends) at the top and the base of a specimen. Eventhough the mode of failure was similar for the two different loading conditions, the compressive strengths of prisms and walls tested with flat end conditions were about 5% higher than those tested with pinned-end conditions. Moduli of elasticity from flat end compression tests were also higher than those from pinned-end compression tests. The maximum measured midwall deflections were higher with pinned-end loading conditions. Conversely, tests by Maurenbrecher[71] showed no difference in compressive strengths for prisms tested with flat versus pinned-end conditions.

It is worthwhile mentioning that numerous research reports did not give any indication of whether flat or pinned end conditions were employed. Wong[117] indicated that line loading improved alignment of specimens, thereby reducing accidental eccentricity.

Failure Mechanism of Face Shell Mortared Concrete Masonry

In the past two decades there has been a considerable discussion in the literature related to the failure mechanism of solid masonry. Hilsdorf[54] presented an analytical procedure to predict the compression strength of brick masonry based on a stress analysis approach. His failure criteria has served as the basis for understanding of the masonry failure mechanism[10,11,32,38,53].

In Hilsdorf's failure theory, when the compressive stress being applied to the mortar joints (within the prism) is greater than the uniaxial compressive strength of the mortar, the mortar has to be confined laterally. Hence the lateral compressive stresses imposed upon the mortar are counterbalanced by tensile stresses in the bricks. With increasing external axial load, failure occurs when the lateral tensile strength of the brick is exceeded. Mohr's theory of failure is employed to express the strength of brick under biaxial stresses, and the brickwork compressive strength is determined based on the interaction of the brick and mortar strength properties.

Francis et al[38] proposed an approach to the failure mechanism of brick masonry which was similar to Hilsdorf's[54] approach except that a strain-type analysis was used. Khoo and Hendry[53] presented a failure criterion similar to that of Hilsdorf but it differed in that masonry failure was defined by a limiting maximum lateral tensile strain for the brick. In their theory, Khoo and Hendry used a non-linear stress-strain behaviour of brick and mortar to obtain the failure envelopes of brick and mortar under their appropriate complex states of stresses. Hamid[43] extended the Hilsdorf failure theory to grouted and ungrouted concrete block masonry. Others[10,11] have also proposed some new non-linear theories for brickwork failure, however, these theories continued to evolve around Hilsdorf lateral tension theory.

It is of importance that the assumptions employed in these proposed failure theories be identified. Also some of the concerns are:

1. The lateral stresses in both horizontal principal axes are assumed equal[38,43,54]

2. The lateral and vertical stress distribution are taken as uniform[38,54]. However Atkinson and Noland[10] argued that the assumption of uniform lateral stresses in the mortar and the brick would require a jump discontinuity at boundaries which physically is not possible.

3. An assumption of linear behaviour of the materials is not justified. Above 50% of maximum stress, non-linear behaviour is observed with Poisson's ratio and modulus of elasticity changing rapidly as the load increases[10].

4. None of these theories have included the vertical mortar joint in their analytical models.

5. Even though the tensile strength is included as a parameter in the analytical formulation[43,54], its influence on the masonry assemblage compressive strength is not evident. Independent calculations preformed on the formulas suggested by Hilsdorf[54] and Hamid[43] showed for an increase in the unit tensile strength of 40%, the assemblage compressive strength has only increased 3 to 4%.

6. Observed cracking in assemblages of face shell mortared blocks[37,104,116] is not covered by criteria based on mortar block interaction.

Fattal and Cattaneo[37] examined analytically the behaviour of face shell mortared masonry. A finite element analysis of a hollow concrete unit with load applied on the face shells showed that the stress distribution on the vertical plane of symmentry (centerline of web) "... describes a condition analogous to flexure in deep beams of rectangular cross-section reinforced with vertical flanges at the supports..."[37]. They also reported that a condition of maximum tensile stress occurs at the top of the web in the horizontal direction midway between the two face shells. Beccia[12] suggested "... the mechanism causing vertical splitting of webs appears to be deep beam action induced by platen fixity of the upper and lower units in the three course prisms..."

A conceptual analytical approach for vertical web cracking in face shell mortared masonry was presented by Shrive[104] as depicted in Figure 3.1 where the web and face shell of an axially loaded face shell hollow concrete block were shown in side elevation. Replacing the stress distribution a line EF in Figure 3.1 (d) by a single force P resulted in a clockwise moment which can only be balanced by the stresses on line DE shown in Figure 3.1(f). Having equilibrium and compatibility satisfied, Shrive concluded that this is how the lateral tensile stresses develop near the surface of the web.

Finite element analyses[45,104,105] have confirmed the basis for tensile cracking failure in the webs and led to the conclusion that these tensile stresses develop at the centre of the webs by a mechanism somewhat analogous to deep beam bending.

The review of the literature on the behaviour of face shell mortared blockwork indicated that the failure mechanism has only recently become generally understood but different opinions are offered as to the most applicable model of this mechanism. The exact stress distribution across the height

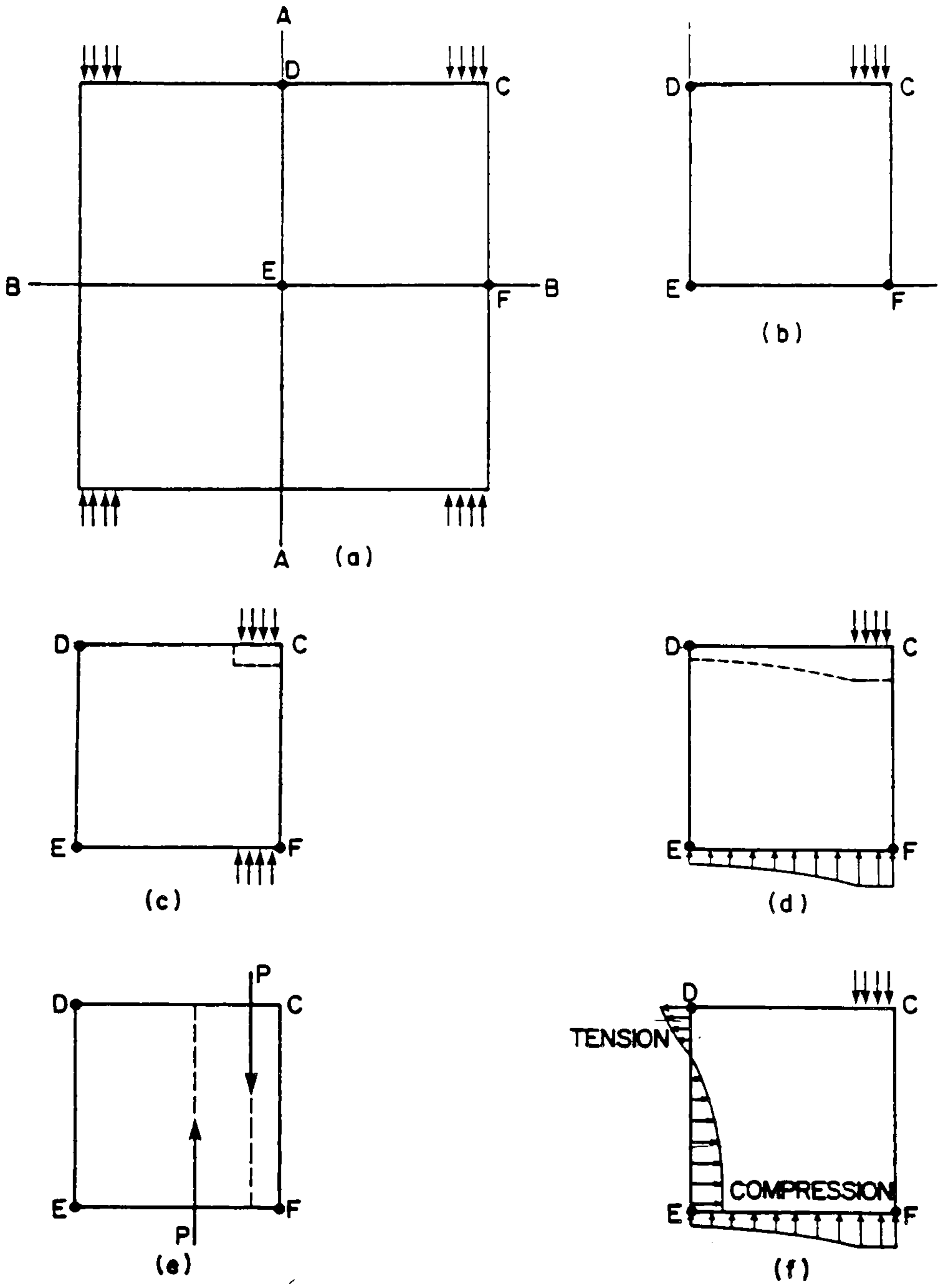

FIGURE 3.1 FAILURE MECHANISM OF FACE-SHELL BEDDED MASONRY (after Shrive, N.G., Refrence 104)

of the web is presently unknown and more detailed information on material properties and detailed experimental evidence is required to develop and check more rigorous solutions.

3.1.3 Objectives and Scope

The objective of this part of the research program was to investigate factors affecting the behaviour and strength characteristics for face shell mortared concrete block prisms. Specifically the influence of prism height, capping material, capping configuration, bearing plate thickness, pinned versus flat end conditions, and stack versus running bond were factors included. Using one combination of block and mortar as a constant, it was intended that strain data and failure mechanism observations would provide an in depth assessment of the factors affecting the apparent strength characteristics of blockwork. It was also the intent of this research to report on specimen height and testing method for adoption as standard test for design and compliance requirements.

Four block high prisms were used as the standard and were compared with 2 block high prisms where both were built in running bond. The types of capping were limited to Hydrostone (representing hard capping) and fibreboard (representing soft capping).

To achieve a satisfactory level of confidence in the results of testing concrete masonry, it has been suggested that a minimum of ten replications are needed[71]. However in a large test program where a large number of variables are included, this implies an enormous effort and cost. Based on the results of previous research at McMaster University[43,116], a maximum coefficient of variation of up to 10 percent was reported for 4 replications[43,116], and 3 replications[116]. Assuming that this consistency was maintained, for a derived confidence of 95%, 5 repetitions would yield a tolerable error of 10.7% according to the student t- distribution (the t-distribution was employed instead of the normal since the number of replications is small, less than 30). It is worthwhile mentioning that in CAN3-S304-M84[26] a minimum of 5 tests are required and if the coefficient of variation exceeds 10% a second set of tests must be performed. Hence it was decided to prepare 5 prisms for each combination of variables.

3.2. PRISM FABRICATION AND TEST PROCEDURE

3.2.1. Prism Configuration

Running bond construction was adapted for the standard prism in this research program since it represents normal construction practice.

The Background review, Section 3.1.2, revealed that for 3-course prisms the failure mode approached the proper tensile cracking in the central unit while for 4-course and 5-course prisms the failure mode more closely resembled a wall compression failure[51]. In addition, no significant decrease in prism compressive strength was achieved with heights beyond 4- or 5-courses.

In this study a 4-course high, 1-block long prism built in running bond was adopted to ensure that the central failure zone includes one head joint and one bed joint while being free of platen restraint. Running bond was also adopted for 2-course high, 1-block long prisms prepared for comparison purposes.

3.2.2 Fabrication of Prims

Hollow 190 mm concrete block stretcher units used for prism fabrication were stored inside the laboratory to achieve uniform dryness. The prisms were constructed by an experienced mason, who was told to build according to his normal practice. Half units needed at every second course to achieve a running bond were saw cut at the middle web of stretcher units. They were placed with the cut end exposed to the outside.

Mortar Type S2, described in Chapter 2, was used. No retemperting of the mortar was allowed. To achieve a consistent workmanship, small 60 to 70 kg batches of mortar were employed. The mortar joint thickness was around 10 mm for bed and head mortar joints.

The prisms were constructed near the end of April with the temperature in the laboratory being around $20^{0}C$ with a relative humidity of approximately 50%. Prisms and mortar cubes were air cured in the laboratory until testing. Testing started after one month of curing.

3.2.3 Instrumentation

Strain measurements were carried out at 14 different locations on the prism. Deformations were monitored in the three orthogonal directions near the platens and at mid-height of the specimen. As indicated earlier, for every combination of parameters investigated 5 similar prisms were tested. However strain measurements were recorded for two prisms only. For each of these prisms, the deformations were taken on opposite sides and ends to achieve greater confidence in the data.

The gauge locations for the different strains measurements were shown in Figure 3.2 for 2-course prisms and in Figure 3.3 for 4-course prisms. The mechanical gauge points mounted on the prism faces provided gauge lengths of 50 mm and 200 mm. For the 50 mm gauge length, a "Huggenberger" mechanical strain indicator having a resolution of 0.001 mm was used. This resolution provided a precision of 20 micro-strain for the readings. For the 200 mm gauge length, a "DEMEC" mechanical strain indicator with a precision

Note: all dimensions are in millimeters
strains are slso measured on opposite sides

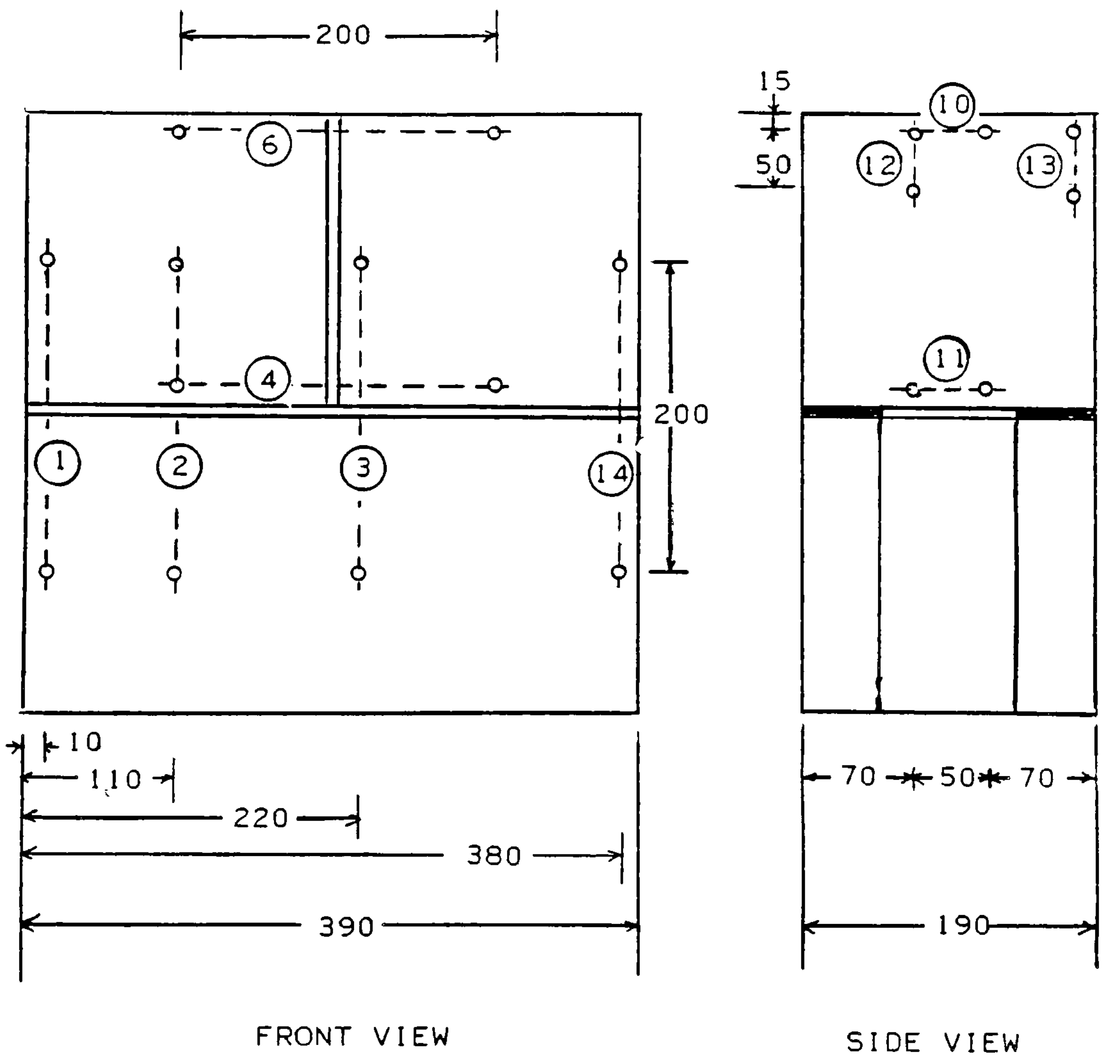

FIGURE 3.2 STRAIN MEASUREMENT LOCATIONS IN 2-COURSE PRISM TEST

Note: all dimensions are in millimeters
strains are slso measured on opposite sides

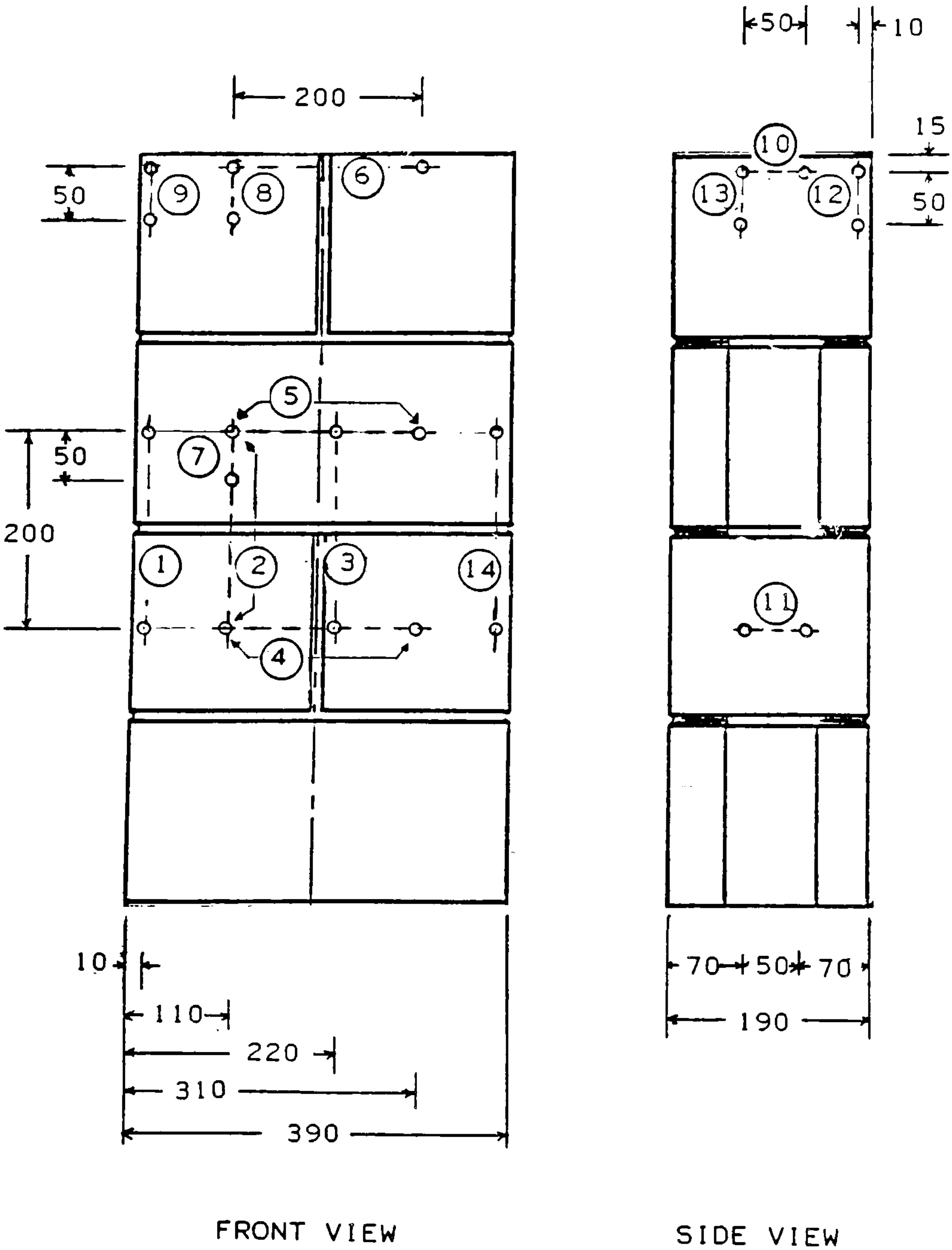

FIGURE 3.3 STRAIN MEASUREMENT LOCATIONS IN 4-COURSE PRISM TEST

of 10 micro-strain was used. A comparison between the two strain indicators was provided in Appendix B.

Vertical (axial) deformations over 200 mm gauge length including a block and a joint in the prism were measured over the central portion of the prisms (strain no.2) and were considered to be representative of the prism assemblage deformation. Similar measurements were also performed at locations 1, 3 and 14 to examine the uniformity of strain distribution.

Vertical deformations on blocks were also taken near the platens and at prism mid-height on both the face shells and the webs.

Lateral (horizontal) deformations were measured across block and head joint in the central portion of the prism and as close as possible to the bearing plate to identify the influence of platen restraint. In addition, lateral strain measurements were taken on the face shells and the webs of blocks.

Finally, in a separate study, the vertical cracking of webs for face shell mortared 4-course prisms were monitored over the height of central unit webs as shown in Figure 3.4.

3.2.4 Specimen Preparation and Test Set-Up

For full bed hard capping, the prism was set into the Hydrostone mix which had been poured on a leveled steel

Note: all dimensions are in millimeters
strains are also measured on opposite sides

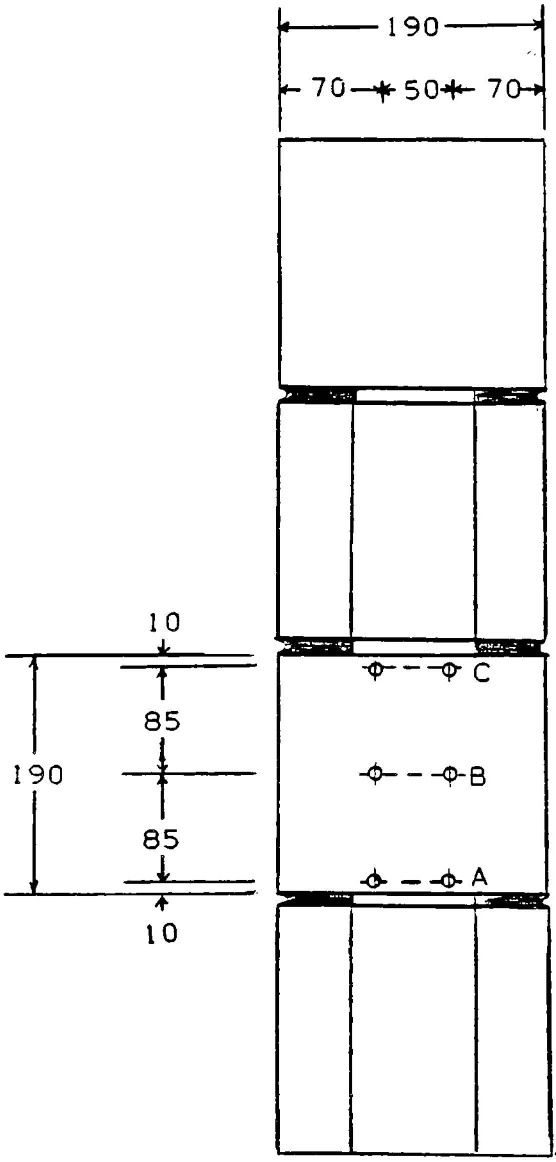

SIDE OF PRISM

FIGURE 3.4 STRAIN MEASUREMENT LOCATIONS IN WEB OF 4-COURSE PRISM TEST bearing plate. Hydrostone was then spread on the top of the prism and the top bearing plate was placed using a level. The thickness of the capping layer was no more than 3 mm.

To achieve face shell hard capping, cardboard was used to cover all but 32 mm strips along the face shells. To hold the wet Hydrostone on the two 32 mm wide strips, a frame was formed around the steel plate and the specimen was then set over the plate. A similar procedure was adopted for capping the top end of the prisms. Before adopting the approach described above, several alternatives were examined and it was learned that there is no easy way to properly achieve face shell hard capping.

For soft capping, the specimens were fully capped first with Hydrostone to provide uniform loading surfaces. After placing the prism in the test machine with the steel bearing plates still attached at both ends, the bond between the prism and the plate was gently broken by tapping with a rubber hammer. Then the specimen was lifted so that the fibreboard sheet could be placed at the bottom interface. Capping of the top surface was achieved in a similar manner. Full bed capping required that the fibreboard sheet cover the whole loading area while for face shell capping, fibreboard strips of 32 mm width were placed along the edges of the face shells.

The test set-up for specimen with pinned-end loading and full bed hard capping was shown in Figure 3.5. Line loading was achieved through the use of a 50.8 mm x 50.8 mm steel bar on the top and a 25.4 mm roller at the bottom. The use of the square steel bar at the top (instead of roller) should not affect the pinned-end conditions since the spherical machine head is moveable. The use of the roller at the bottom facilitated the placement of the specimen in the testing machine and provided flexibility for alignment. Wooden wedges were employed to hold the specimen upright. These wedges were removed after a small load was applied.

The load was transferred to the prisms through the 75 mm thick steel bearing plates used to cap the prisms. The influence of the plate thickness was investigated by also using steel plates of 50.8 mm thickness.

For flat-ended conditions, the capping plate at the base of the prism was entirely supported by the base of the test machine while the 225 mm diameter spherical seat transferred load directly to the top capping plate.

The prism axial compression tests were carried out by a RIEHLE Universal Testing Machine with a 2500 KN capacity. The prisms were loaded at a convenient rate for up to 50% of the ultimate load. For the rest of the loading the rate was kept constant. The total time for testing a prism was about 3 minutes. For prisms with strain gauges, the total time

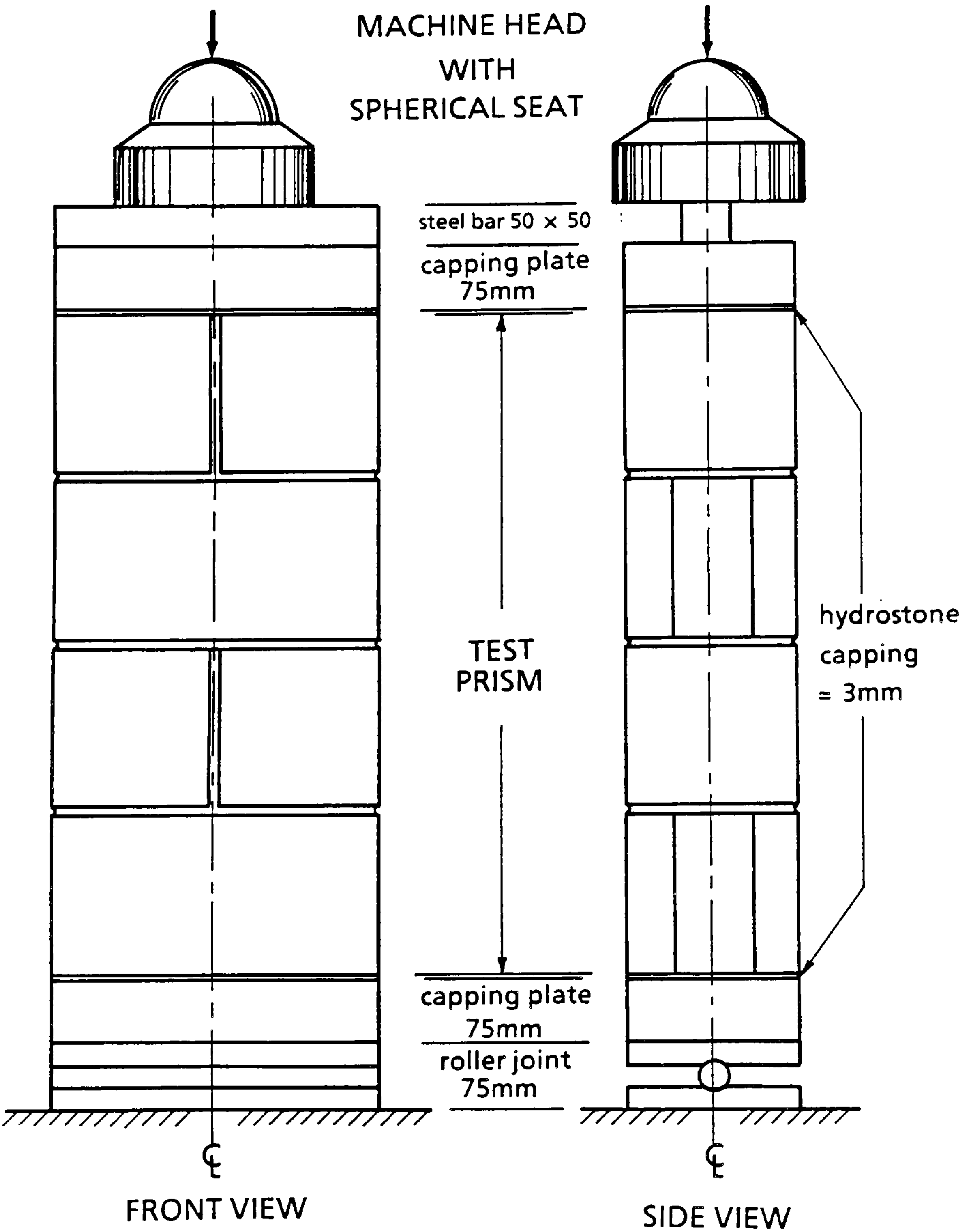

FIGURE 3.5 PRISM TEST SET-UP

ranged from 30 to 40 minutes. Normally, strain measurements were taken at 50 KN load increments but in some cases the load increment was reduced. Strain measurement was stopped at about 90 percent of the ultimate load. This was necessary due to the explosive failure of the prisms. Following development of extensive cracking in the prism, it is doubtful if local strain readings provide meaningful information on stress-strain behaviour. Therefore no attempt was made to investigate the post-ultimate behaviour.

3.3 EXPERIMENTAL RESULTS AND INTERPRETATION

3.3.1 Introduction

3.3.1.1 General

The results for 2 and 4 course prism tests were listed in Table 3.2. This table includes the results from the various testing techniques and procedures. The strain results from these tests were tabulated in Appendix B where each strain is the average of four readings. The block compressive strengths were reported in Chapter 2 and the tensile splitting strengths of the blocks and the mortar cube compressive strengths were listed in Appendix B.

The moduli of elasticity from these tests, obtained at 0.3 of the ultimate strength were listed in Table 3.3. The assemblage modulus of elasticity was determined from the prism central portion (strain no. 2 in Figure 3.2 and 3.3). The

TABLE 3.2: PRISM COMPRESSION TEST RESULTS

Description of Test Conditions	2 Block High Prisms					4 Block High Prisms				
	Series No.	Ult. Load (kN)	Mean Load (kN)	f'm* (MPa)	COV (%)	Series No.	Ult. Load (kN)	Mean Load (kN)	f'm* (MPa)	COV (%)
Full Bed Hydrostone Capping	PH2-1	751 689 682 709 675	701	22.8	4.4	PH4-1	560 536 586 599 600	576	18.8	4.8
Flat-ended Conditions: Full Bed Hydrostone Capping	PH2-2	690 726 700 729 719	713	23.2	2.4	PH4-2	585 578 600 588	588	19.1	1.6
50 mm Thick Bearing Plate: Full Bed Capping	PH2-3	615 618 630 689 664	643	21.0	5.0	PH4-3	566 561 545 534 553	552	18.0	2.3
Face Shell Hydrostone Capping	PH2-4	801 729 799 763 748	768	25.0	4.1	PH4-4	644 584 610 513 570	584	19.0	8.4
Full Bed Fibreboard Capping	PH2-5	490 530 480 497 479	495	16.1	4.2	PH4-5	430 482 498 464 506	476	15.5	6.4
Face Shell Fibreboard Capping	PH2-6	705 687 717 697	702	22.9	1.8	PH4-6	610 626 602 584 584	601	19.6	3.0
Face Shell Stack-Bond: Face Shell Fibreboard Capping	PH2-7	659 655 612 665	648	21.1	3.7					

* f'm = Compressive strengths based on an effective mortar bedded area of 30,700 mm^2 or equivalent face shell thickness of 39.4 mm.

TABLE 3.3: PRISM SECANT MODULI OF ELASTICITY AND POISSON'S RATIOS*

Descrip. of Test	2 Block High Prisms			4 Block High Prisms		
	Series no.	Modulus of Elas. (MPa)	Assemb. Poisson Ratio v	Series no.	Modulus of Elas. (Mpa)	Assemb. Poisson Ratio v
Full Bed Hydrostone Capping	PH2-1	14800	0.20	PH4-1	14400	0.20
Flat-ended Conditions Full Bed Hydrostone Capping	PH2-2	14600	0.28	PH4-2	15800	0.34
50 mm Thick Bearing Plates: Full Bed Capping	PH2-3	16600	0.51	PH4-3	11800	0.29
Face-shell Hydrostone Capping	PH2-4	15100	0.24	PH4-4	15800	0.33
Full Bed Fibreboard Capping	PH2-5	16000	0.12	PH4-5	16700	0.16
Face-shell Fibreboard Capping	PH2-6	13500	0.10	PH4-6	16900	0.24
Face-shell Stack Bond: Face-shell Fibreboard Capping	PH2-7	12700	0.12			

* Elastic properties were determined at 0.3 of ultimate strength

assemblage Poisson's ratios also listed in Table 3.3, were taken as the ratio of the lateral strain (strain no. 4) to vertical compressive strain (strain no. 2).

The results from every testing procedure are examined separately in terms of the differences between the 2-course and 4-course prism compressive strengths, failure modes, deformations and elastic properties.

3.3.1.2 Mortar Bedded Area for Strength Calculation

As indicated in the Background the mortar bedded area should be used for strength calculations. However, there is a need to define a consistent method to determine this area.

As illustrated in Figure 3.6, direct measurements of the mortar joints between two courses in face shell mortared construction showed that the width of this layer varied from 37 mm up to 60 mm. The overall average width, based on measurements of five different mortar layers, was around 50 mm. It was also observed that the mortar was not necessarily confined to the face shell area alone but extended into parts of the cross-webs. The mortar contact area between the lower and upper courses in running bond hollow concrete construction was shown in Figure 3.7. The cross-hatching indicates the effective mortared area where the thickest part of the block is the top surface. The actual dimension for one strip of effective mortared area were shown in Figure 3.7(b).

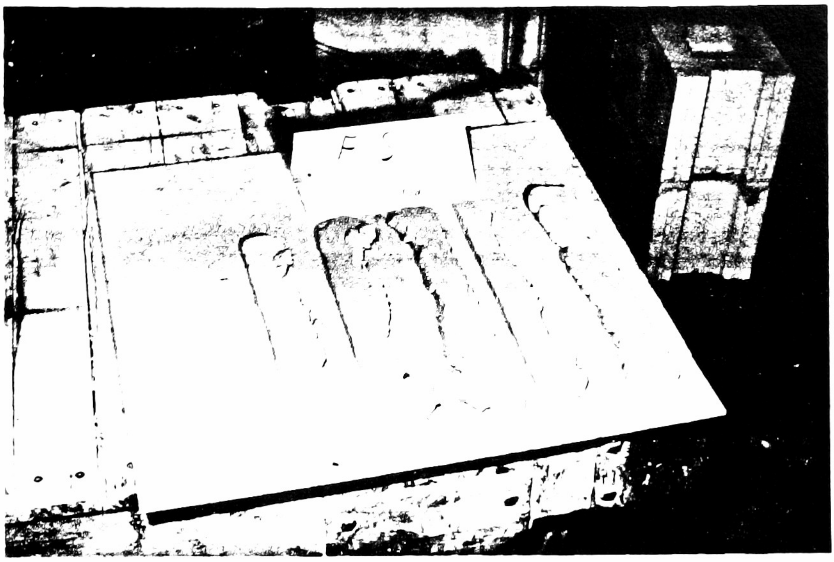

FIGURE 3.6 TYPICAL MORTAR JOINTS IN RUNNING BOND BLOCK MASONRY

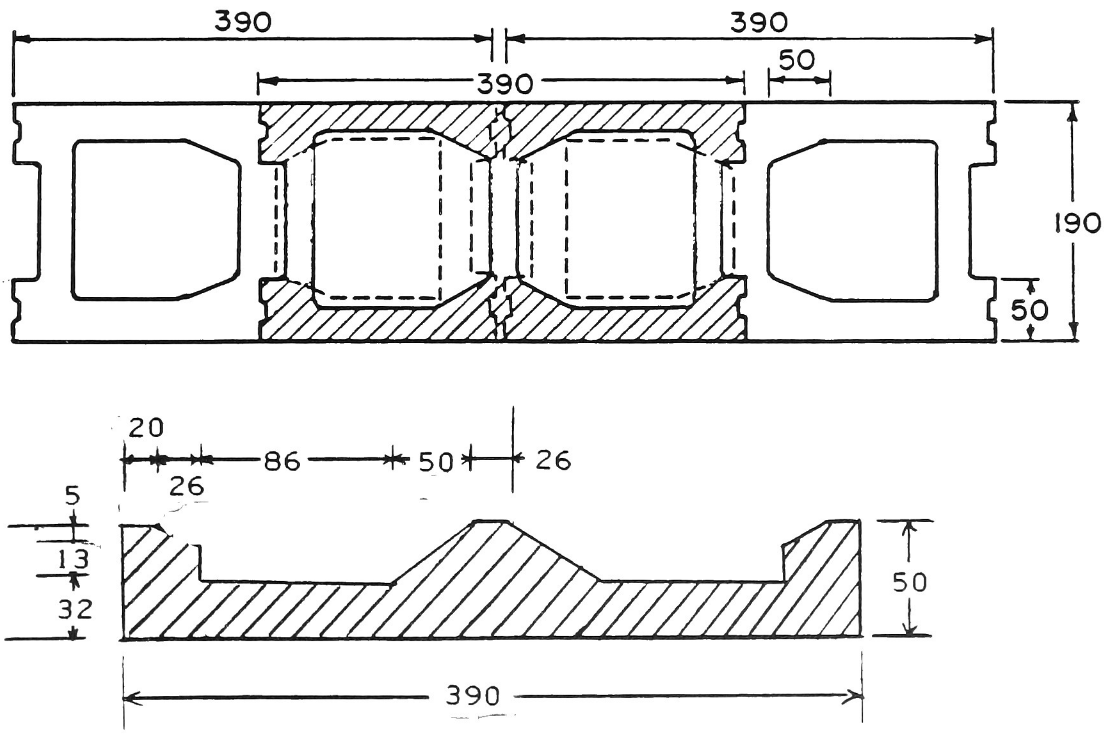

FIGURE 3.7 MORTAR BEDDED AREA FOR RUNNING BOND BLOCK MASONRY

The calculated effective mortar area in face shell mortared concrete masonry was found to be 30748 mm^2/block length. This corresponds to 23.2 percent increase over the mortar area based on the minimum face shall thickness of 32 mm. The calculated effective mortared area yields an equivalent face shell thickness of 39.4 mm.

Throughout this research work, the compressive strength of prisms built in running bond, will be calculated based on an adopted effective mortared area of 30700 mm^2 corresponding to an equivalent thickness of mortared face shell of 39.36 mm or a 23% increase over the minimum face shell thickness of 32 mm.

3.3.2 Detailed Test Results

3.3.2.1 Pinned-End Conditions (Full Bed Hydrostone Capping)

2-Course Prisms (Series PH2-1)

Prisms failed by extensive shearing of one or both face shells accompanied by crushing of the mortar. The failure mode was mainly explosive as shown in Figure 3.8. Large web crackings were also observed in some instances but only in the top course.

The influence of platen restraint can be observed by comparing lateral strains in the face shells at the specimen/platen interface and at the prism central portion as

FIGURE 3.8 TYPICAL FAILURES OF 2 AND 4 COURSE PRISMS (SERIES PH2-1 AND PH4-1)

shown in Figure 3.9. Lateral strains at the prism central portion were about 60%, on average, more than those at the prism/platen interface. The lateral strains in the webs were also shown in Figure 3.9. These strains were negative (compressive) at the top of the web (prism/platen interface) and positive (tensile) at the bottom of the web. The lateral strains at the top of the web became positive (tensile at around 43% of the ultimate strength where the strain at the bottom of the web registered 3000×10^{-6}. It is suggsted at this level of stress, cracking reached the top of the web. In addition the vertical compressive strain at the top of the web, along the centerline, began to drop at this same load level (See Table B1.1 in Appendix B).

4-Course Prisms (Series PH4-1)

The prism mean compressive strength was about 18% less than for the 2-course prisms. Prisms failed by vertical web cracking which became visible at around 80% of the ultimate load. Spalling of the face shells was also observed near the failure load and in some instances mortar crushing was also observed at the joint surface. The final failure was the result of an instability in the prism which resulted from the situation where web cracking propagated along the prism height.

Vertical web cracking initiated at the bottom of the web and specifically in the mid thickness of the block indentation. The crack usually started in the third web from the prism top surface and propagated mainly along a more or less vertical line as shown in Figure 3.8. While fine cracks were observed in the webs of the top and bottom blocks. they did not propagate all the way to the prism ends. Lateral tensile cracking of the face shells was not observed.

The secant modulus of elasticity was about 3.0 percent less than that of the 2-course prisms. However this difference became more significant at higher stress levels.

The lateral strains at 3 different locations in the face shells were shown in Figure 3.10. As shown, near failure lateral strain near mid-height were over 300 percent more than those at the platen interface. In comparison with a difference of 60 percent obtained from 2-course prisms, the influence of prism height on reduction of platen restraint is quite evident. In addition, comparison of lateral strains in the prism central portion between 4-course and 2-course prisms showed that lateral strains in 4-course prism were some 60% more than those in 2-course prism. The measurements shown in Figure 3.10 indicated that vertical mortar joints had little influence on the overall lateral strains. The lateral restraint by the concrete units on both sides may explain this observation.

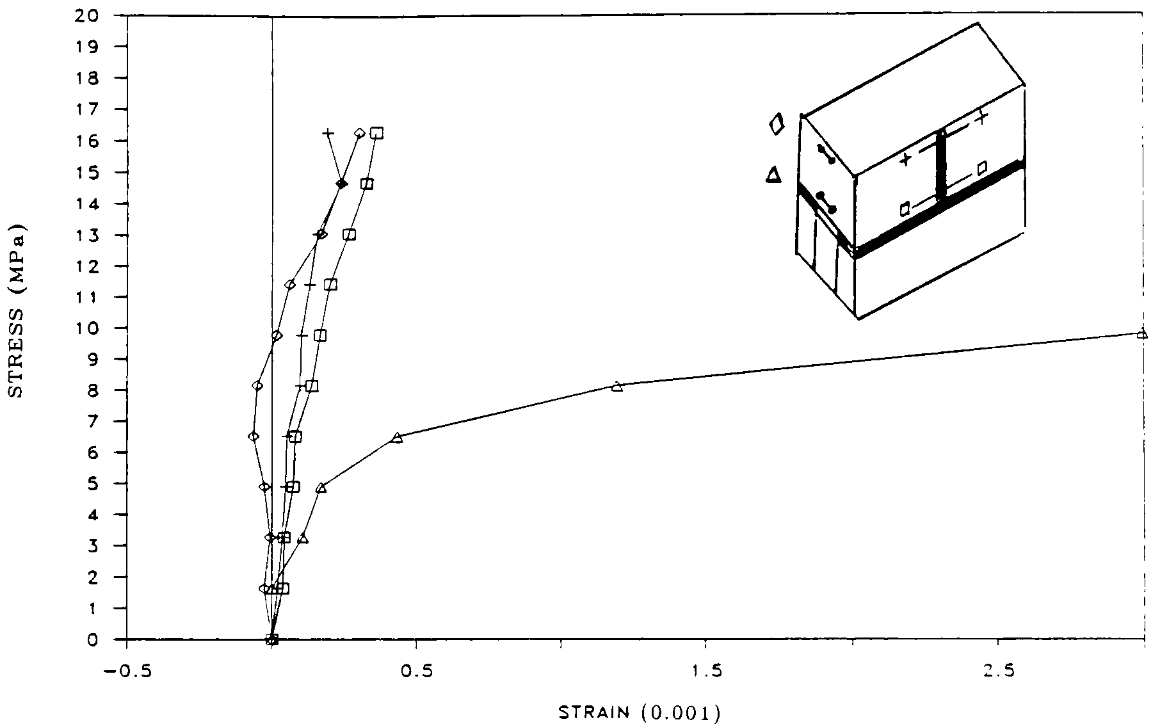

FIGURE 3.9 LATERAL STRAINS AT PLATEN INTERFACE AND CENTRAL PORTION OF 2-COURSE PRISM (SERIES PH2-1)

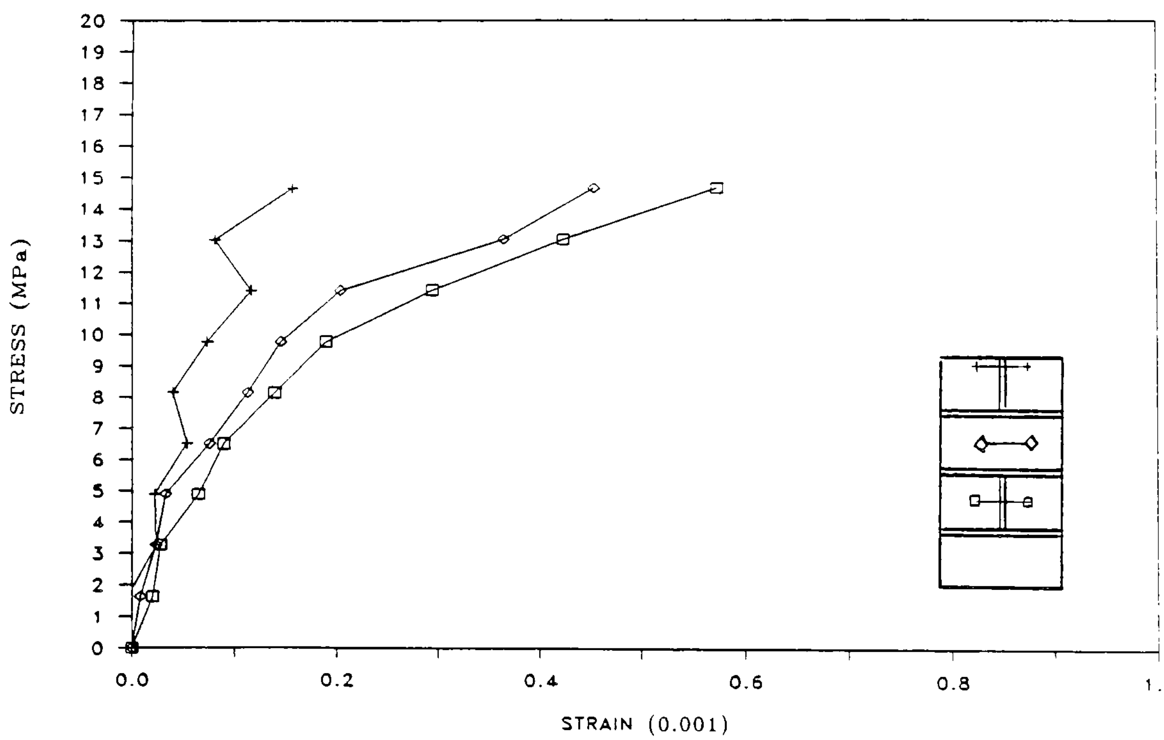

FIGURE 3.10 LATERAL STRAINS IN FACE-SHELLS OF 4-COURSE PRISM (SERIES PH4-1)

The vertical compressive strains near the platen interface, within a block at the prism central portion and across a block-and-joint were all shown in Figure 3.11. The concept of uniform vertical strain distribution along the prism height is not applicable when strains at the platen interface and in the central portion were compared. The axial strain distribution appears to be highly nonuniform. A similar trend has been reported in some analytical work[45]. If the concept of direct superposition of deformation is assumed to be valid for block masonry, the deformation within the mortar joint can be obtained from strains no. 2 and no. 7 in Figure 3.3. The resulting deformation within mortar was shown in Figure 3.12. It is interesting to observe that the mortar strain at failure greatly exceeded its maximum strain under uniaxial compression which was reported to range between 2000 and 3000 micro-strains[43]. It can also be observed that the mortar exhibited nearly constant stiffness from about 50 percent of the ultimate stress.

Contrary to the readings for 2-course prisms, lateral strains in the web at the platen interface were tensile (positive), but small in magnitude. This seems to suggest that the magnitude of platen restraint at the interface may be reduced by increasing the specimen height. Figure 3.13 contains a plot of the lateral strains in the prisms webs near the platen interface and in the central portion. It can be

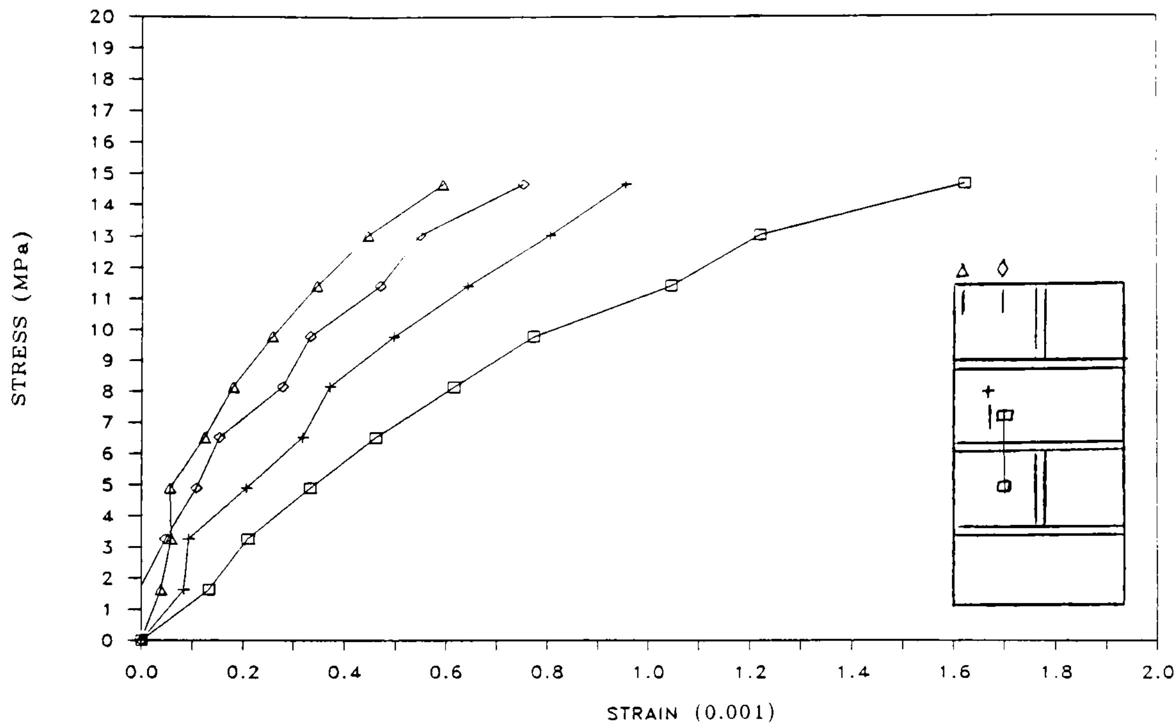

FIGURE 3.11 VERTICAL COMPRESSIVE STRAINS IN FACE-SHELLS OF 4-COURSE PRISM (SERIES PH4-1)

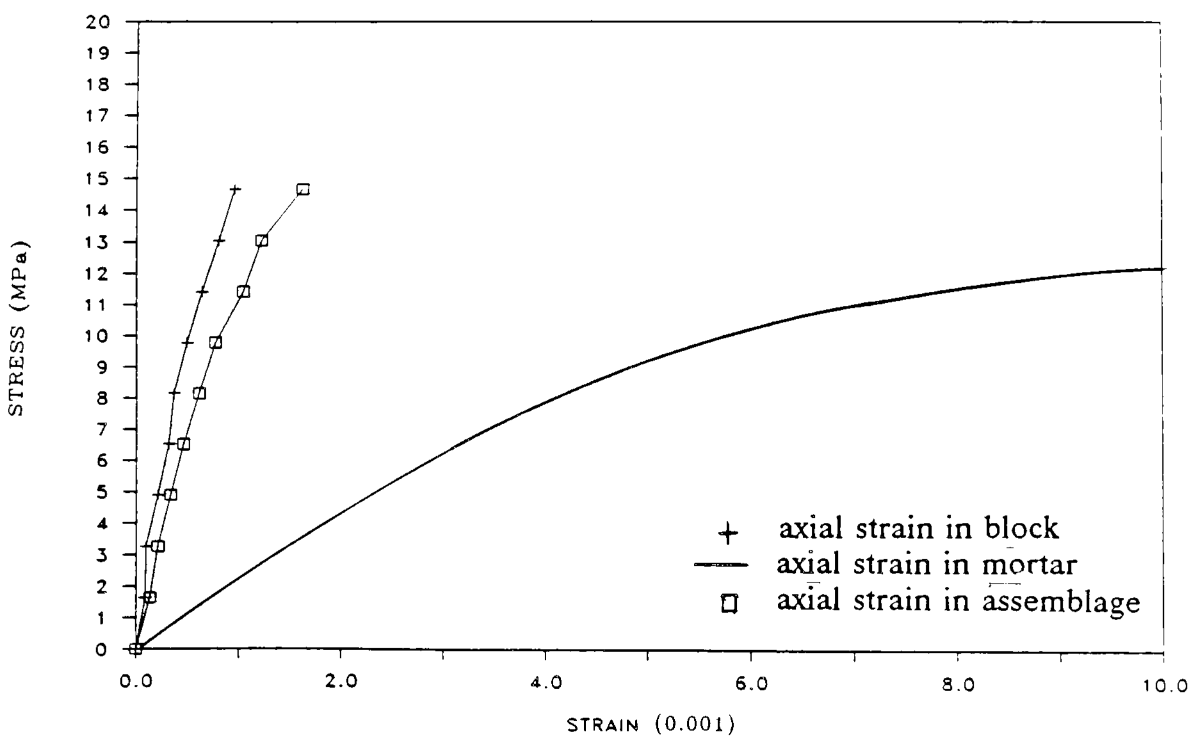

FIGURE 3.12 STRESS-STRAIN RELATIONSHIPS OF BLOCK, MORTAR AND PRISM UNDER AXIAL COMPRESSION (SERIES PH4-1)

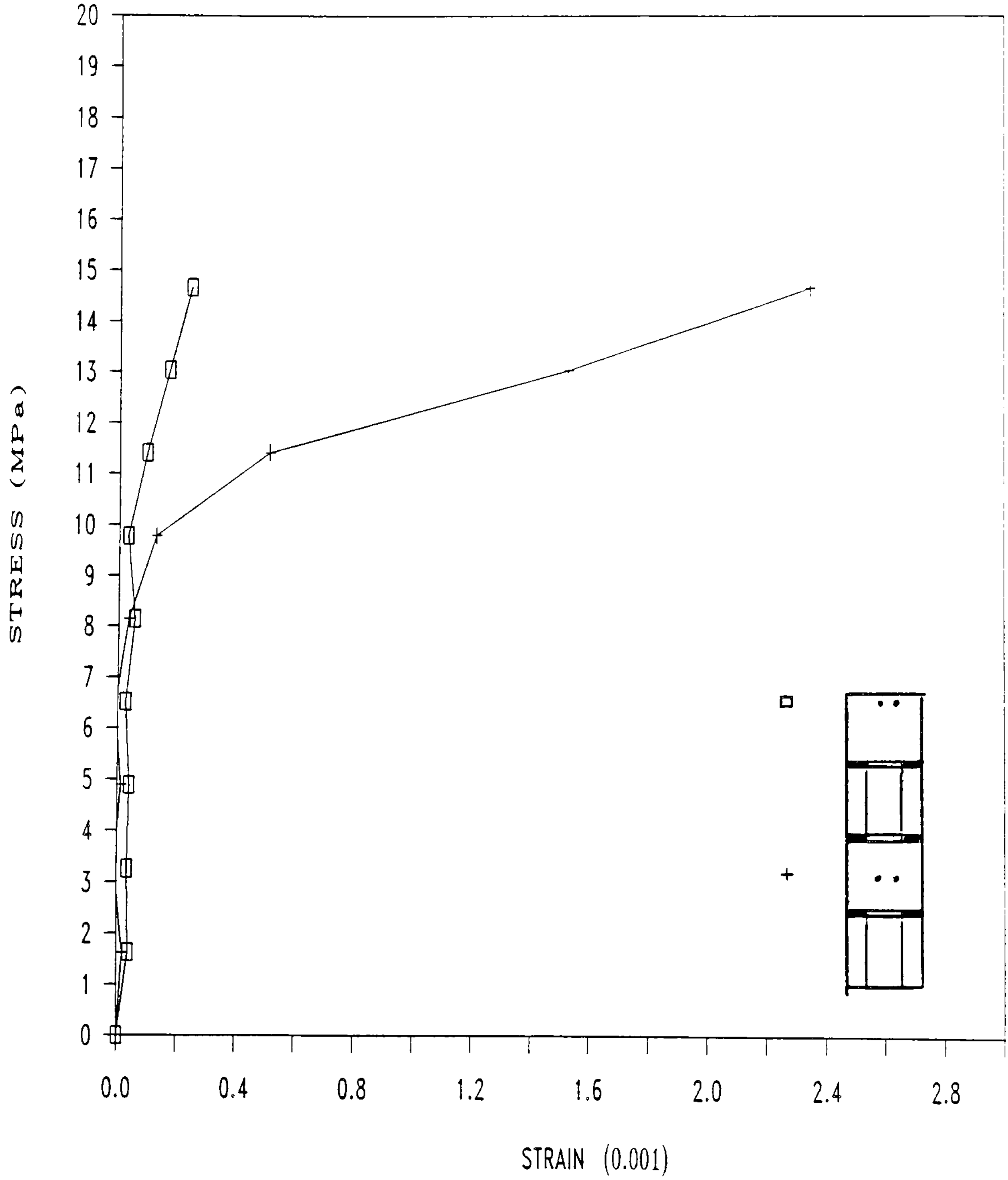

FIGURE 3.13 LATERL STRAINS IN WEBS OF 4-COURSE PRISM (SERIES PH4-1)

observed that these strains are small for most of the loading, however at high stresses (around 70% of the ultimate stress) large strain were experienced at mid-height of the third web from the top surface. Web cracking was observed to initiate in the third web, starting at the bottom and propagating upward. Hence cracking of the web must have initiated at a lower stress level than 70% of the ultimate load.

3.3.2.2 Flat End Conditions

2-Course Prisms (Series PH2-2)

The prism mean compressive strength was about 2% higher than the mean obtained from pinned-end loading. This difference is statistically insignificant at the 95% confidence level. The mode of failure was similar to that in Series PH2-1.

Compressive strains at the prism corners, near the platen interface (strains no. 12 in Figure 3.2), were much less than those for line loading. This may suggest that line-loading resulted in the specimen whole bearing area being loaded while for flat-end conditions the central portion transmitted more load than the corners.

Lateral strains at the prism central portion (strain no. 4 in Figure 3.2) were higher than those from line-loading. This may be attributed to the fixed conditions imposed by flat end loading. Lateral strains in the webs continued to be high however they were much less than those from line-loading. With line loading, the bearing plates may have experienced a slight bending and as a result the web section in the plane of the line load would be subjected to a bending action but only to the extent of the plates bending.

<u>4-Course Prisms</u> (Series PH4-2)

In general, prisms failed in a similar manner to those under line loading (Series PH4-1). However, splitting in the face shells was also observed to develop in the second course then travel downwards through the vertical mortar joints.

a) <u>comparison to 2-course prisms</u>

The prism mean compressive strength was about 18% less than that of 2-course prism. Increasing the prism height significantly reduced the lateral strains in the webs in comparison to 2-course prisms (See Tables B1.1 and B1.2).

b) <u>comparison to pinned-end conditions</u> (Series PH4-1)

The mean compressive strength was only 2% higher than that from line-loading. However for all practical purposes the compressive strength can be considered equal in both cases.

The mode of failure differed by the fact that flat-end loading resulted in the development of lateral tensile cracking in the face shells. This may be attributed to the fact that, with flat-end conditions, end rotation was prevented and the tendency to develop lateral tensile stresses along the prism face shells was greater. This is supported by the fact that lateral strains at the prism/platen interface were higher than those developed from line-loading. Judging from the lateral strains measured at mid height of the third web from the top surface (strain no. 11 in Table B1.2) it appears that web cracking initiated at lower stress level under line-loading.

3.3.2.3 50 mm Thick Steel Bearing Plates

2-Course Prisms (Series PH2-3)

The prism mean compressive strength was 8% less than the mean strength of prisms tested using 75 mm thick bearing plates. The mode of failure continued to be shearing of the face shells, however, in this instance the shearing action extended to the prism top corners. Lateral strains measured at the prism/platen interface, in both face shells and webs, were over 100 percent more than those reported when the 75 mm plate thickness was used. In addition, the lateral deformations in the prism central portion were also over 100 percent higher.

To examine the uniformity of the stress distribution, the vertical compressive strains were measured at 4 different locations in the prism central portion (strains no. 1, 2, 3 and 14 in Figure 3.2). The strain distribution was quite non-uniform with an overall average difference, between strains at the centreline and the prism corners of around 60% based on all stress levels where readings were taken. The vertical compressive strains on the prism face shells were plotted in Figure 3.14 along with the corresponding standard deviations where the lower strains at the corners of the prisms are evident. Worth noting that each data point plotted in Figure 3.14 was the average of 4 readings and the observed difference in the compressive strains at locations 1 and 14 may be explained by the natural scatter of the strain results as well as the variability of the materials.

Use of a 50 mm plate thickness resulted in lower strains in the prism corners than for a plate thickness of 75 mm. Vertical compressive strains at the prism top corners were much less than those obtained with the 75 mm plate thicknesses.

<u>4-Course Prisms</u> (Series PH4-3)

Vertical cracking was observed to extend to the webs of end blocks in the prism, a phenomena not observed in prisms tested with 75 mm thick plates. Vertical cracking in the face shells was also observed to propagate up and down through the vertical mortar joints. In addition, the top corners of the

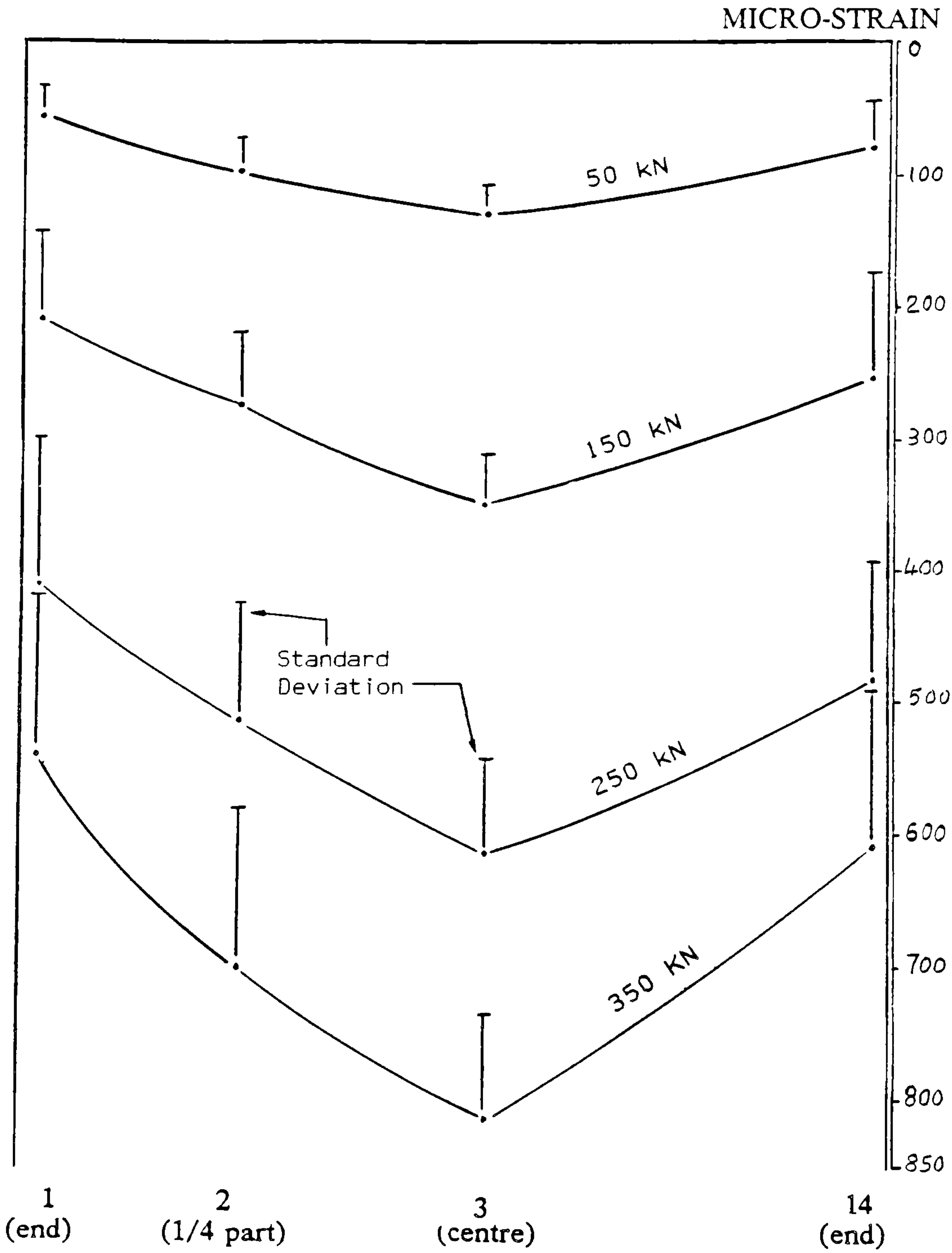

FIGURE 3.14 VERTICAL COMPRESSIVE STRAINS DISTIBUTION IN 2-COURSE PRISM WITH 50 mm THICK BEARING PLATES (SERIES PH2-3)

prism tended to come apart in some instances.

a) <u>comparison to 2-course prisms</u>

The prism mean compressive strength was 14% less than the mean strength for 2-course prisms. The vertical compressive strains were much higher than those reported from 2-course prisms and this in fact resulted in a secant modulus of elasticity which was around 30% less than the 2-course prisms. (See strain no. 2 in Tables B1.1 and B1.2).

The average difference between compressive strains measured at the centerline and corners (in the central portion of prism) was reduced to 24.1% by increasing the prism height to 4-courses, see Figures 3.14 and 3.15.

b) <u>comparison with tests using 75 mm thick plates</u> (Series PH4-1)

Reducing the bearing plate thickness by 25 mm resulted in 4% decrease in the prism mean compressive strength. Lateral deformations in the prism face shells and webs at the prism/platen interface were much higher when the 50 mm thick plates were used. This appears to suggest that 50 mm plates have experienced some bending which alleviate some of the restraint at the prism/platen interface. In addition, the lateral deformations in the face shells over the central portion of the prisms were also higher when thinner plates

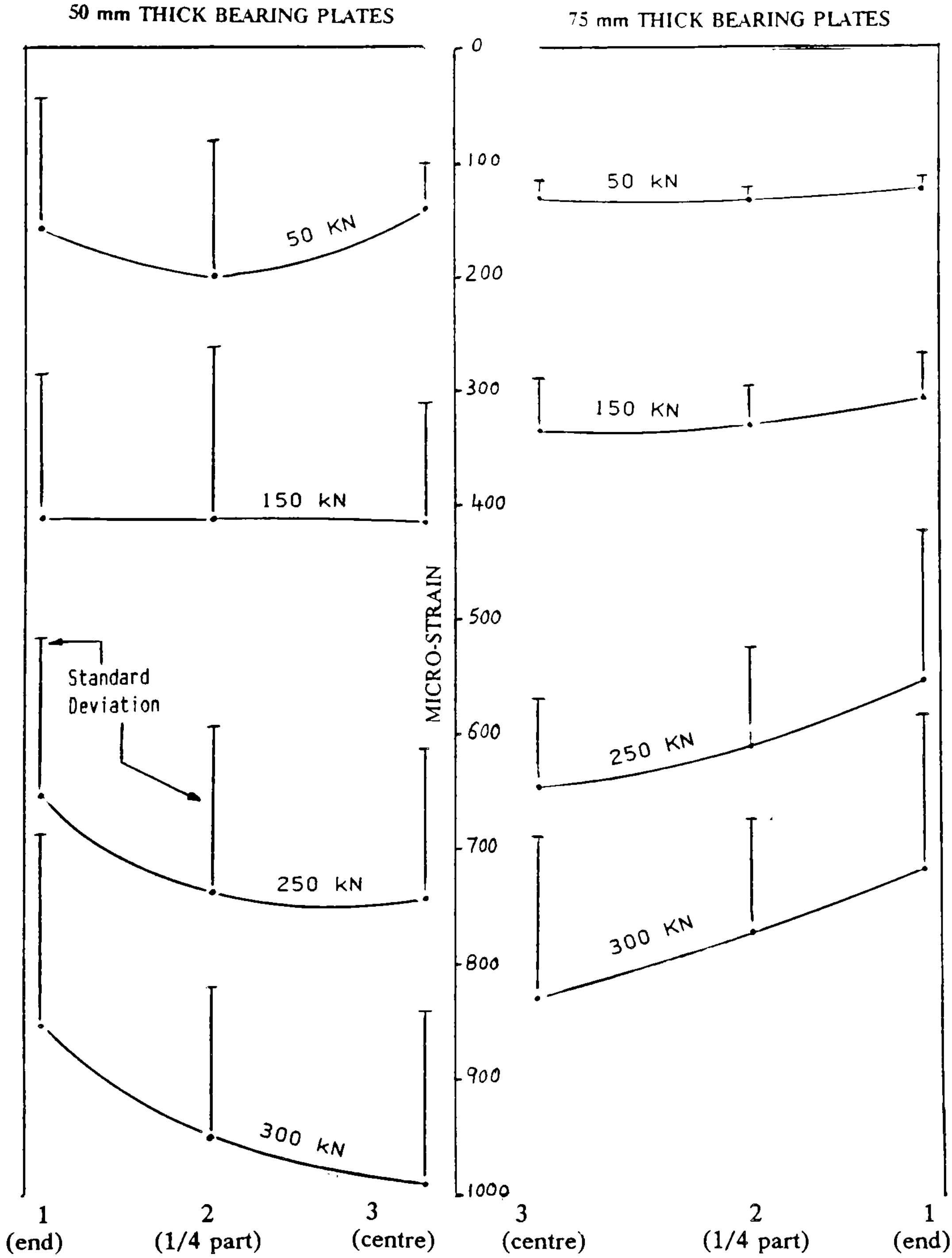

FIGURE 3.15 VERTICAL COMPRESSIVE STRAIN DISTRIBUTION IN THE CENTRAL PORTION OF 4-COURSE PRISMS WITH 50 mm AND 75 mm THICK BEARING PLATES (SERIES PH4-3 AND PH4-1)

were used.

The strain distributions under both cases were monitored through strain measurements in the prism central portion (strains no. 1, 2, 3 and 14 in Figure 3.3). For 75 mm thick bearing plates the overall difference in compressive strains (average of four sets of readings) measured at the prism corner and along the centre was 14.0 percent. The overall difference was calculated for the range up to 80 to 90% of the ultimate load. However for 50 mm thick plates, the overall difference in compressive strains was 24.0 percent. It appears that achieving a completely uniform stress distribution is difficult due to the nature of the loaded material[45], however using thick bearing plates can significantly improve the uniformity of the strain in the specimen. The vertical compressive strains across the central portion of 4-course prism were plotted in Figure 3.15 for 50 mm and 75 mm thick plates.

The influence of the bearing plate thickness on the prism compressive strength appears to be greatly reduced by increasing the specimen height from 2-course to 4-course. This was supported by the fact that, at 95% significance level, the 2-course prism compressive strength was significantly reduced by using thinner bearing plates. However, at the same significance level, the 4-course prism compressive strength appears to be unaffected.

3.3.2.4 Face Shell Hard (Hydrostone) Capping

__2-Course Prisms__ **(Series PH2-4)**

The prisms failed mainly by shearing of the face shell of the bottom course. This was accompanied by either an opening of the vertical mortar joint or the top prism corners shearing away. Curshing of the mortar was observed at around 85% of the ultimate load.

The prism mean compressive strength was about 10% more than the mean strength for prisms tested with full bed hard capping (Series PH2-1). The reason for this increase in strength was due to avoiding direct loading of the end webs. This can be clearly observed when the lateral strains in the web under both loading conditions are compared (See strains no. 10 and 11 in Table B1.1) These lateral strains were also plotted in Figure 3.16. With full bed capping, small lateral compressive strains (suggesting compressive stresses) existed in the web at the platen up and until cracking initiated at the bottom of the web (away from the platen). It appeared that cracking of the web initiated around 45-50% of the ultimate stress. At this stress level the lateral strains in the web at the platen became tensile and continued under higher stresses.

Under face shell loading, the lateral strains in the web at the platen were tensile but very small throughout the loading. The lateral strains at the bottom of the web increased with increasing load, however their magnitude was much smaller than those recorded under full bed capping. Further examination of these strain measurements appears to suggest that cracking of the web under face shell loading would be expected to occur at higher load level than under full capping.

<u>4-Course Prisms</u> (Series PH4-4)

Prisms tended to fail by developing vertical cracking along the webs and the face shells. Web cracking initiated at the bottom of webs of the central blocks and propagated upwards. Cracking of the face shells initiated in the middle of the second course from the top and then travelled downwards through the vertical mortar joint. In some instances the cracking line in the face shells travelled down all the way to the bottom course. It is worth noting that out of the five prisms, two prisms exploded suddenly without prior development of any visible cracks.

a) <u>comparison to 2-course prisms</u>

Increasing the prism height from 2-courses to 4-courses resulted in a 24% decrease in the mean compressive strength. In addition, the effect of platen restraint appeared to be greatly reduced by increasing the prism height. While lateral strains at the platen interface continued to be similar, lateral strain at the specimen central portion (in the face shell) increased significantly with increased specimen height.

It has been reported[104] that the strength of face shell mortared, face shell capped masonry should be relatively independent of the number of units in a prism. This does not appear to be true since a significant reduction in strength resulted from increasing the prism height. Even with face shell capping, platen restraint continued to significantly affect the prism compressive strength.

It has been analytically reported[37] that a condition of maximum lateral tensile stress exists in the web at the platen midway between the face shells under face shell loading. The observed mode of failure and the lateral strain measurements taken at the platen both showed that cracking would not be expected to occur at this location. Very small lateral strains were recorded at the platen in the web midway between the face shells. This suggests that for hard face shell capping platen restraint continued to exist.

b) comparison to full bed hard capping (Series PH4-1)

The 4-course prism compressive strength did not appear to be affected by the hard capping configuration. At failure, the prism showed no signs of vertical cracking in the top and bottom course webs. Cracking in the centre units' webs was observed but the lateral strains in the centre webs were highly lower than for fully hard capped prisms as can be seen in Figure 3.17. In the prism face shells, larger lateral deformations were recorded in the prism central zone in comparison to fully hard capped prisms (strain no. 4 in Table B1.2).

3.3.2.5 Full Bed Soft (Fibreboard) Capping

<u>2-Course Prisms</u> (Series PH2-5)

The prism failed by extensive vertical cracking of the webs over the full height of the prisms. Also in-plane splitting along the face shells resulted in 15 mm to 20 mm thick segments splitting away from the face shell as shown in Figure 3.18. This type of failure was previously observed to occur under eccentric loading[12]. Compression of the fibreboard resulted in more time being required to test the prisms. The final thickness of the fibreboard was reduced from about 11 mm to about 5 mm.

In comparison to hard capping, full fibreboard reduced the prism strength by about 30%. The vertical compressive strains (strain no. 2 in Figure 3.2) of full bed soft and hard capped prisms were plotted in Figure 3.19. The sudden surprising change of strains from being compressive to being tensile in soft capped prisms coincided with the propagation of cracking to the web ends (See also strains no. 2 and 10 in Table B1.1). After the web cracking had propagated through

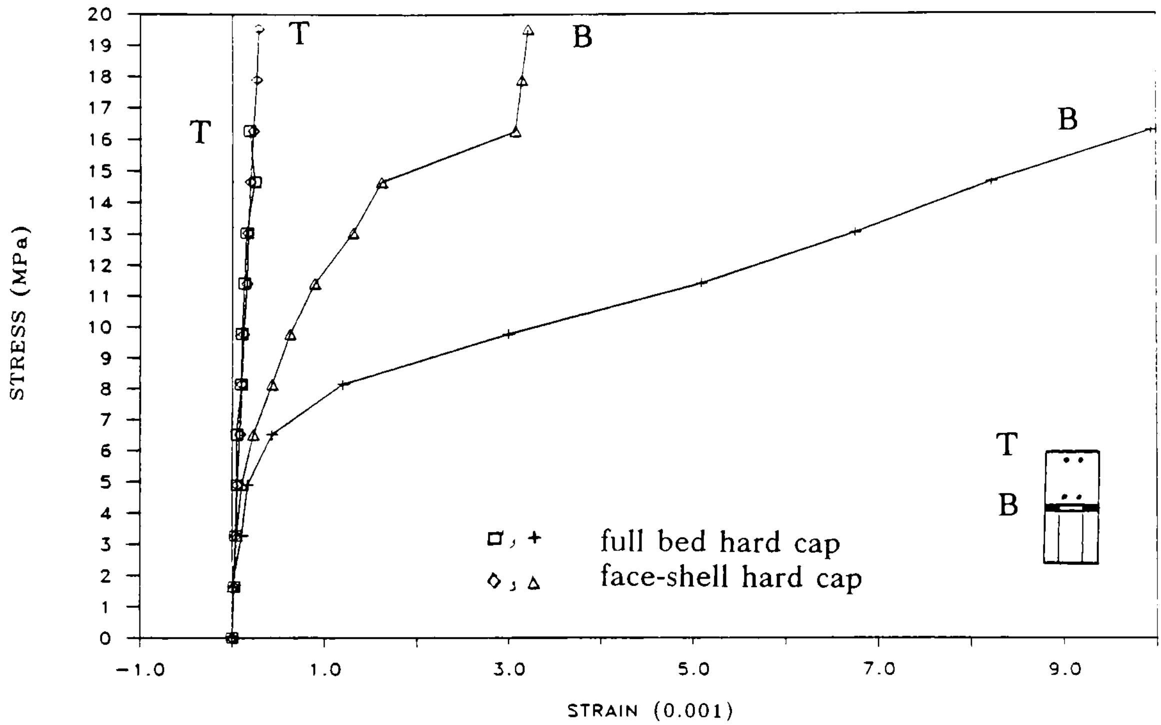

FIGURE 3.16 LATERAL STRAINS IN 2-COURSE PRISM WEBS UNDER FULL AND FACE-SHELL HARD CAPPING (SERIES PH2-1 AND PH2-4)

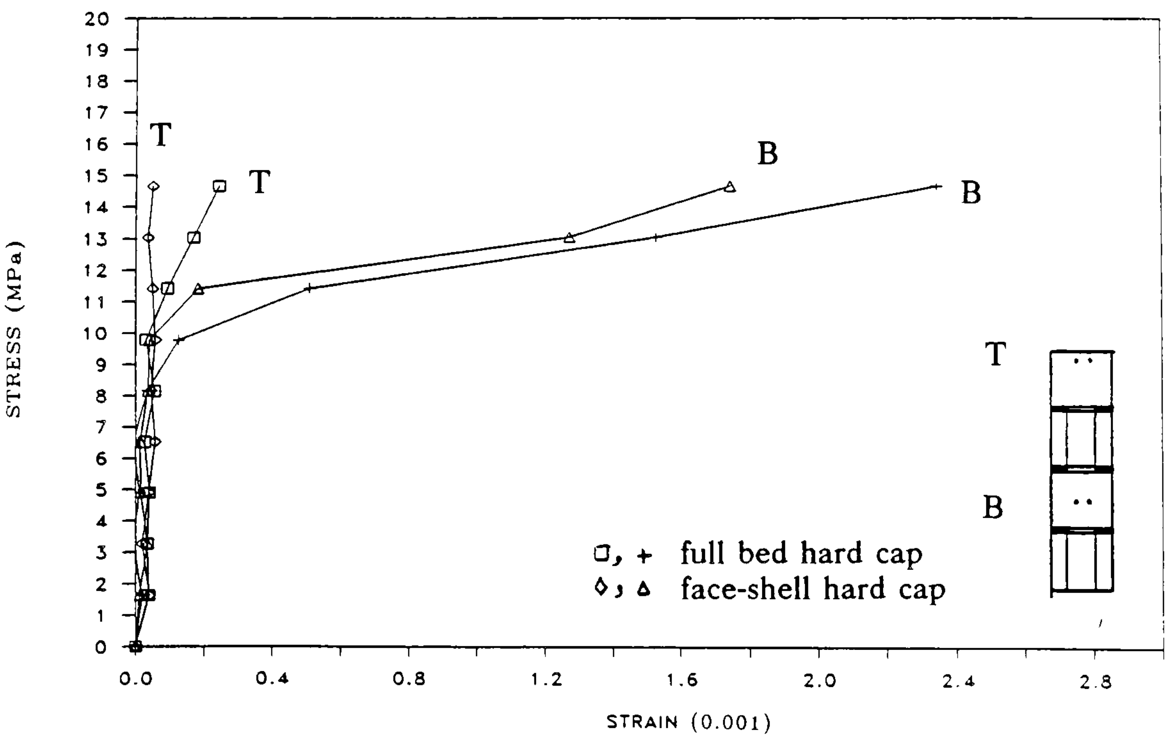

FIGURE 3.17 LATERAL STRAINS IN 4-COURSE PRISM WEBS UNDER FULL AND FACE-SHELL HARD CAPPING (SERIES PH4-1 AND PH4-4)

FIGURE 3.18 TYPICAL FAILURES OF 2-COURSE AND 4-COURSE PRISMS WITH FULL SOFT CAPPING (SERIES PH2-5 AND PH4-5)

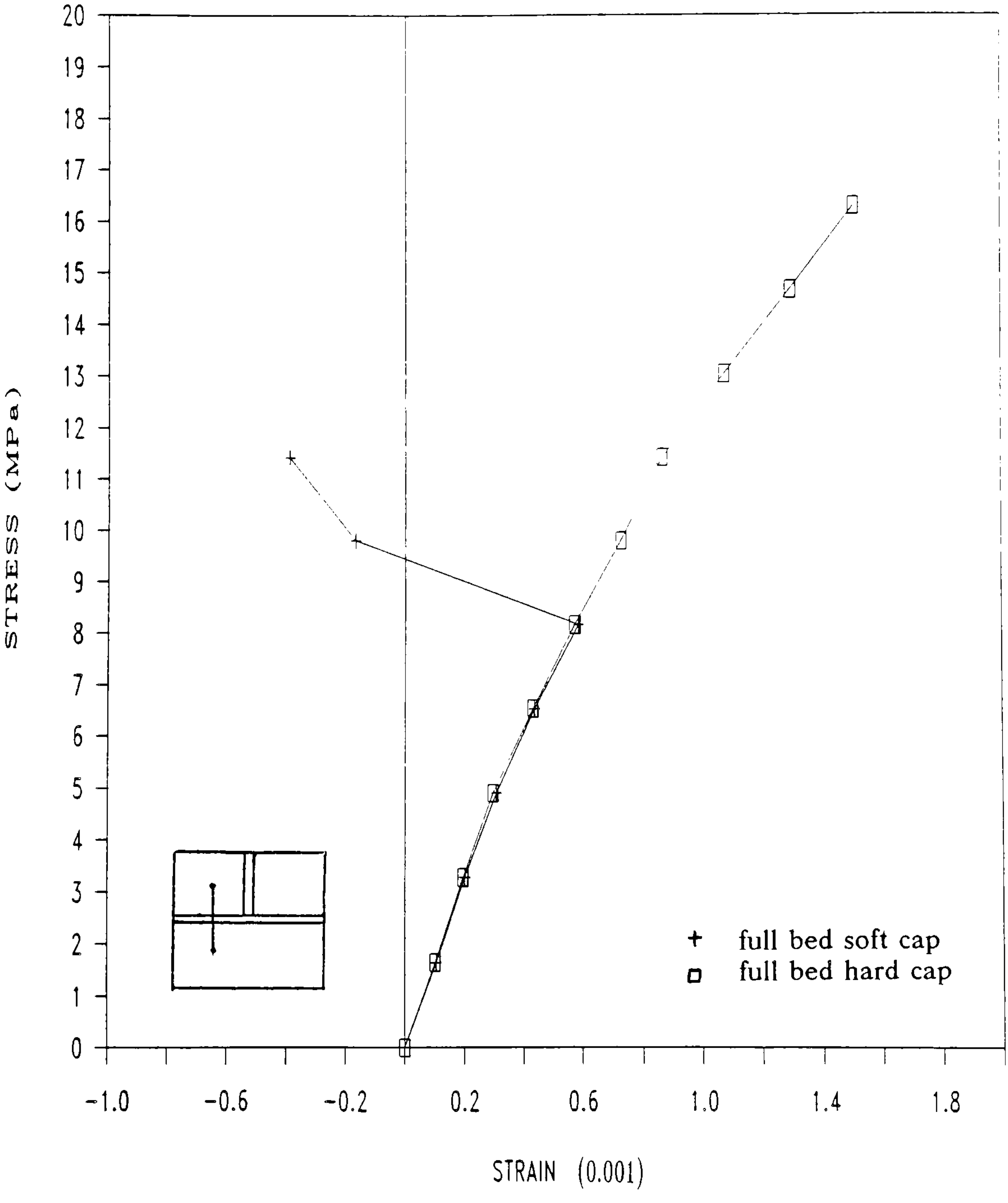

FIGURE 3.19 AXIAL COMPRESSIVE STRAIN IN HARD AND SOFT FULLY CAPPED 2-COURSE PRISMS (SERIES PH2-1 AND PH2-5)

the entire prism height, the assemblage splitted into two unsymmetric halves loaded eccentrically on the inside part of each half. As a result, opening at the mortar bed joint would be expected. In fact crushing of the inside edge of the mortar joint was observed. It is believed that the sudden change in the surface axial strains to tension was attributed to the opening at the mortar joint.

Lateral strains in the prism face shells at the platen interface exceeded those in the central portion of the prisms. This seems to suggest that fibreboard capping did not only reduce the platen restraint but appears to reverse the lateral stresses at the interface from being compression to tension stresses. These tensile strains were remarkably high at high load levels.

The lateral strains in the webs at the platen (strain no. 10) and at mid joint (strain no. 11 in Figure 3.2) were drawn in Figure 3.20 for hard and soft capped 2-course prisms. It can be seen that at a stress around 6.5MPa (40% of ultimate strength) large tensile strains developed at the mid joint of soft capped prisms and quickly increased in magnitude. With only small increases in load the cracks propagated upwards. However, while at the same stress level lateral strains developed at the mid joint of hard capped prisms, these strains did not increase quickly. Platen restraint in hard capped prisms seems to prohibit these cracks from propagating upwards.

4-Course Prisms (Series PH4-5)

The failure of 4-course prisms with full fibreboard capping was shown in Figure 3.18. Extensive vertical web cracking developed over the full height of the prism. After the initial web cracking, the load fluctuated up and down until failure occurred. No evidence of any crushing, splitting or shearing was observed in the prism face shells. In addition no crushing of the mortar was observed. It appeared that the extensive cracking in the webs constituted the sole cause for prism failure.

a) comparison to 2-course prisms

Increasing the prism height from two to 4-courses resulted in only 4% reduction of the mean compressive strength which, at a 95% significance level, was not significant. The most notable difference was the face shell splitting for the 2-course high prism.

Lateral strains in the face shells were similar but smaller (See strain no. 6 in Tables B1.1 and B1.2) but again seemed to indicate that fibreboard produced lateral tension at the platen.

b) <u>comparison to 4-course prisms: full bed hard capping</u> **(Series PH4-1)**

Vertical cracking of the webs was less opponent for hard capped prisms and did not extend through the top and bottom blocks nor was there any sign of damage to the face shells for soft capping. The 18% lower capacity for fibreboard capped prisms corresponded to higher vertical compressive strains near the platens and lower strains at mid height. The latter resulted in an apparent 18% increase in the modulus of elasticity for fibreboard capped prisms.

In contrast to Hydrostone, fibreboard capping resulted in lateral deformations, across the face shells, at the platen interface being higher than those in the prism central portion, away from the platen, even in 4-course prisms.

A close examination of the lateral strains developed at mid height of the third web from the top surface (strain no. 11 in Figure 3.3) showed that, as shown in Figure 3.21, large strains started developing at a similar stress level for both fibreboard and Hydrostone capped prisms. In fact the behaviour was similar to that shown in Figure 3.19 but the magnitudes of the lateral strains in the webs were much smaller than those for 2-course prisms, for both types of capping material. However, for fibreboard capped prisms, these strains rapidly increased to large magnitudes and after only small increases in the load the crack reached the top

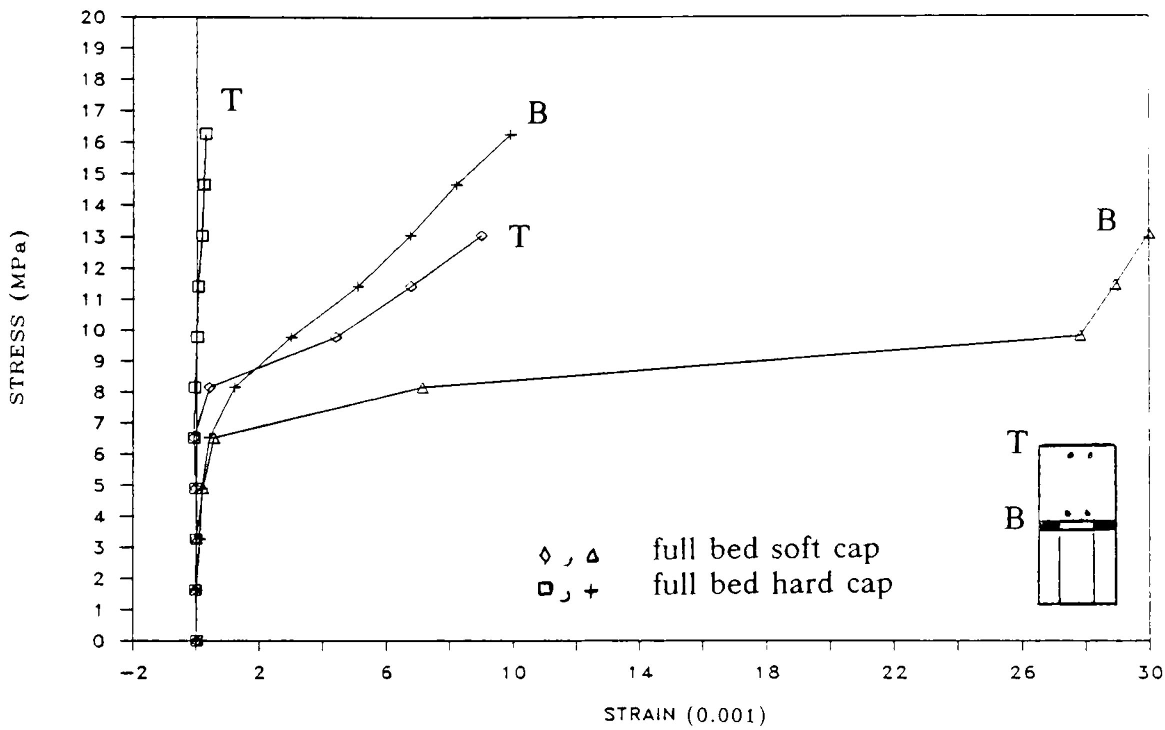

FIGURE 3.20 LATERAL STRAINS IN WEBS OF FULLY CAPPED HARD AND SOFT 2-COURSE PRISMS (SERIES PH2-1 AND PH2-5)

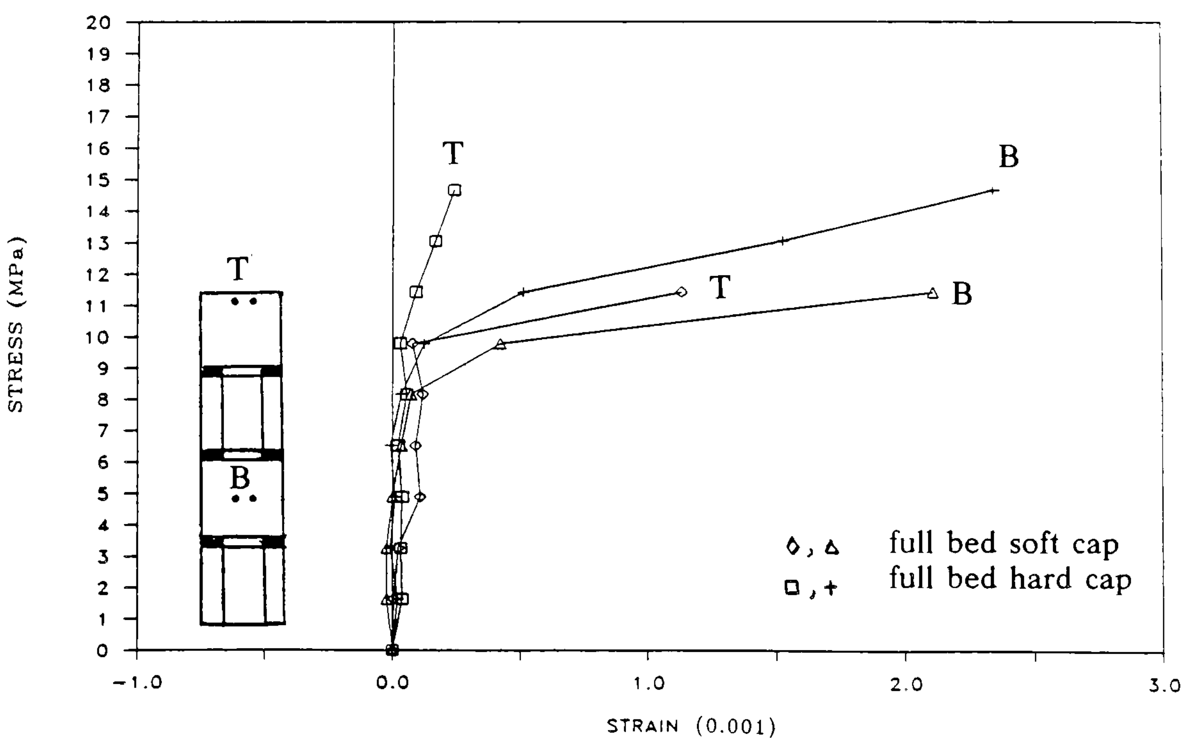

FIGURE 3.21 LATERAL STRAINS IN WEBS OF FULLY CAPPED HARD AND SOFT 4-COURSE PRISMS (SERIES PH4-1 AND PH4-5)

web. After the prism had split into two halves, the inability to resist more axial load because of instability may account for the reduced compressive strength.

3.3.2.6 Face Shell Soft (Fibreboard) Capping

2-Course Prisms (Series PH2-6)

The prism failure was shown in Figure 3.22 where two types of face shell cracking were observed.

1. Vertical tensile cracking initiated at the platen interface and travelled down in a diagonal path toward the prism corners. In some instances more than one crack was observed.

2. In-plane cracking caused a longitudinal 15-20 mm thick section of the face shell to split away.

In addition some fine cracking lines initiated in the web at the platen and not at mid joint as observed earlier. Cracking in the webs was also observed to initiate at the face shell-web intersection and not midway between the two face shells.

a) comparison to full fibreboard capped prisms (Series PH2-5)

Fibreboard face shell capping instead of full bed capping resulted in around 42% increase in the mean compressive strength. This increase in strength was mainly due to avoiding direct loading of the webs. Such a difference

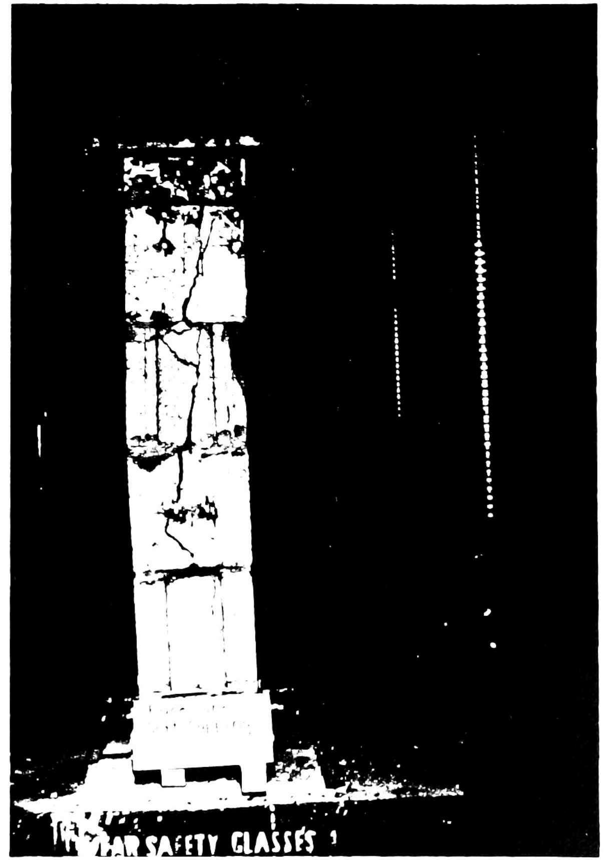

FIGURE 3.22 TYPICAL FAILURES OF 2 AND 4-COURSE PRISMS WITH FACE SHELL SOFT CAPPING (SERIES PH2-6 AND PH4-6)

can be detected when the lateral strains at mid top and mid bottom of the web shown in Figure 3.23 are compared for both capping configurations. In the prism face shells,the much larger lateral strains at the prism/platen interface than those near mid height was an indication that fibreboard produced lateral tension at the platen.

b) <u>comparison to face shell Hydrostone capped prisms</u> (Series PH2-4)

The prism mean compressive strength was about 9% less than the mean strength of prisms tested with face shell Hydrostone capping. This decrease was attributed to the diminishing effects of platen restraint due to using fibreboard. This can be observed when the lateral strains at the platen are compared for both capping materials as shown in Figure 3.24.

Of particular importance is the effect of face shell capping material on the vertical compressive strains. The axial stress-strain relationships in the web at the platen were shown in Figure 3.25 for two locations; a) at the face shell-web intersection (strain no. 12 in Figure 3.2) and b) midway between the face shells (strain no. 13 in Figure 3.2). Vertical compressive strains were higher in prisms tested with fibreboard (strain no. 12). However, (surprisingly) tensile axial strains were recorded midway between the face shells

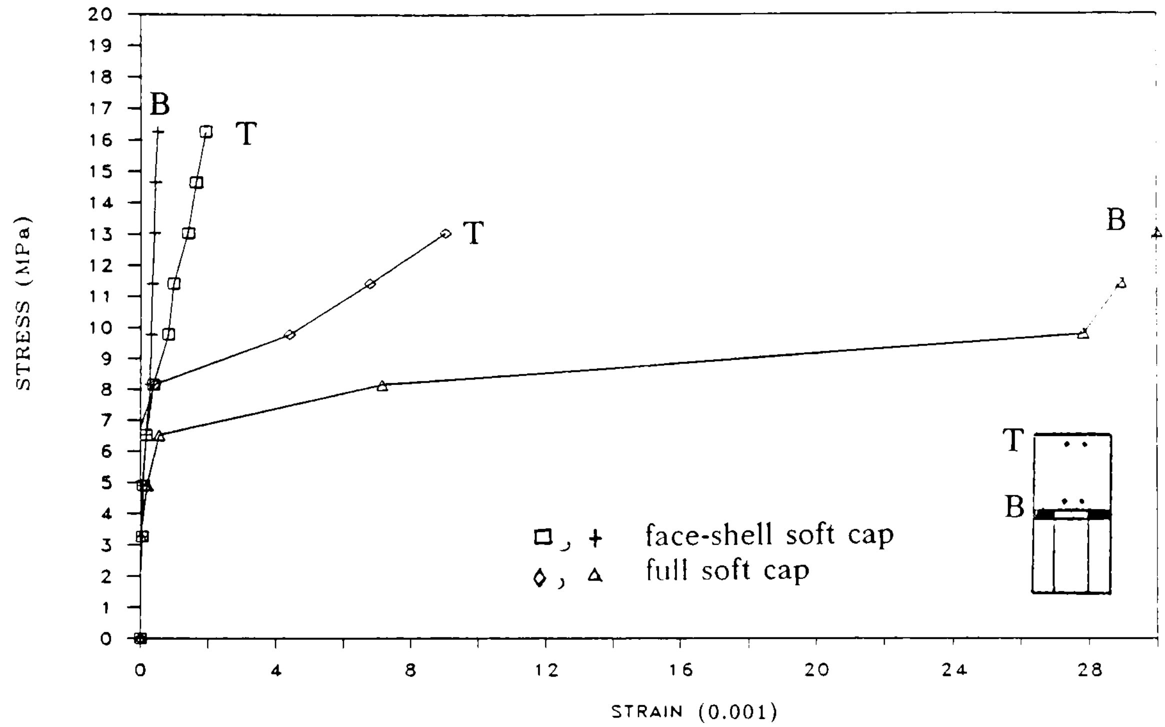

FIGURE 3.23 LATERAL STRAINS IN WEBS OF FACE-SHELL AND FULL SOFT CAPPED 2-COURSE PRISMS (SERIES PH2-6 AND PH2-5)

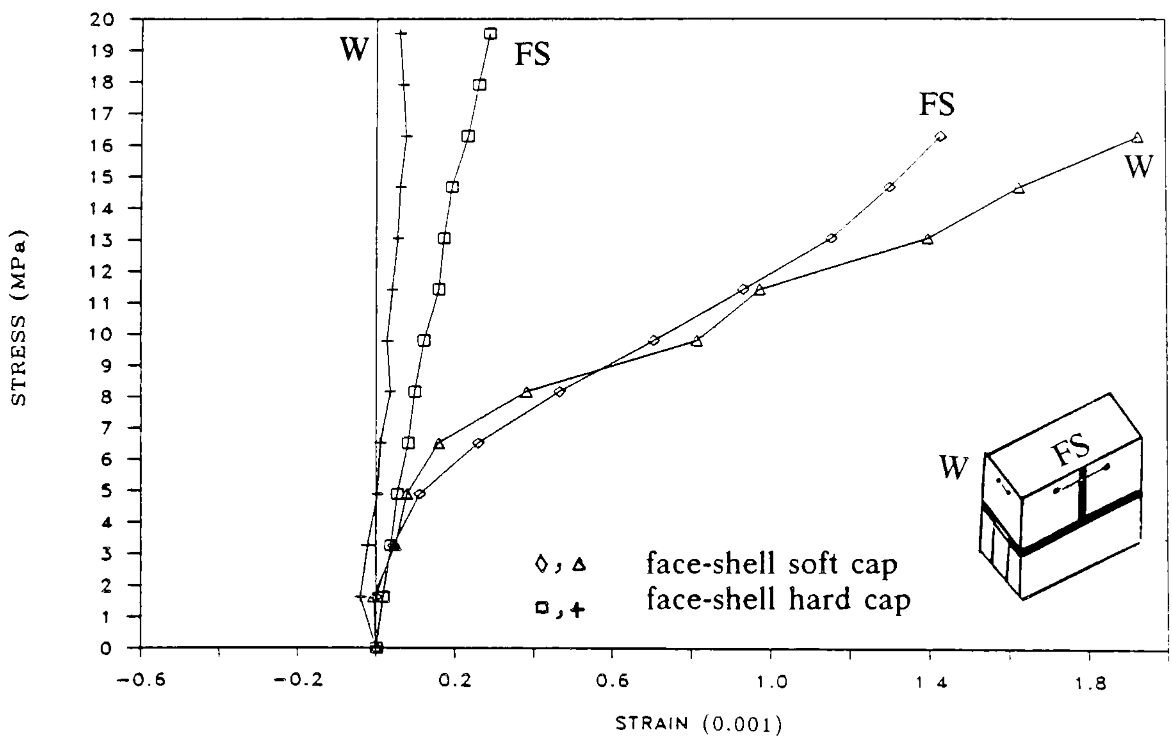

FIGURE 3.24 LATERAL STRAINS AT PLATEN IN SOFT AND HARD FACE-SHELL CAPPED 2-COURSE PRISMS (SERIES PH2-6 AND PH2-4)

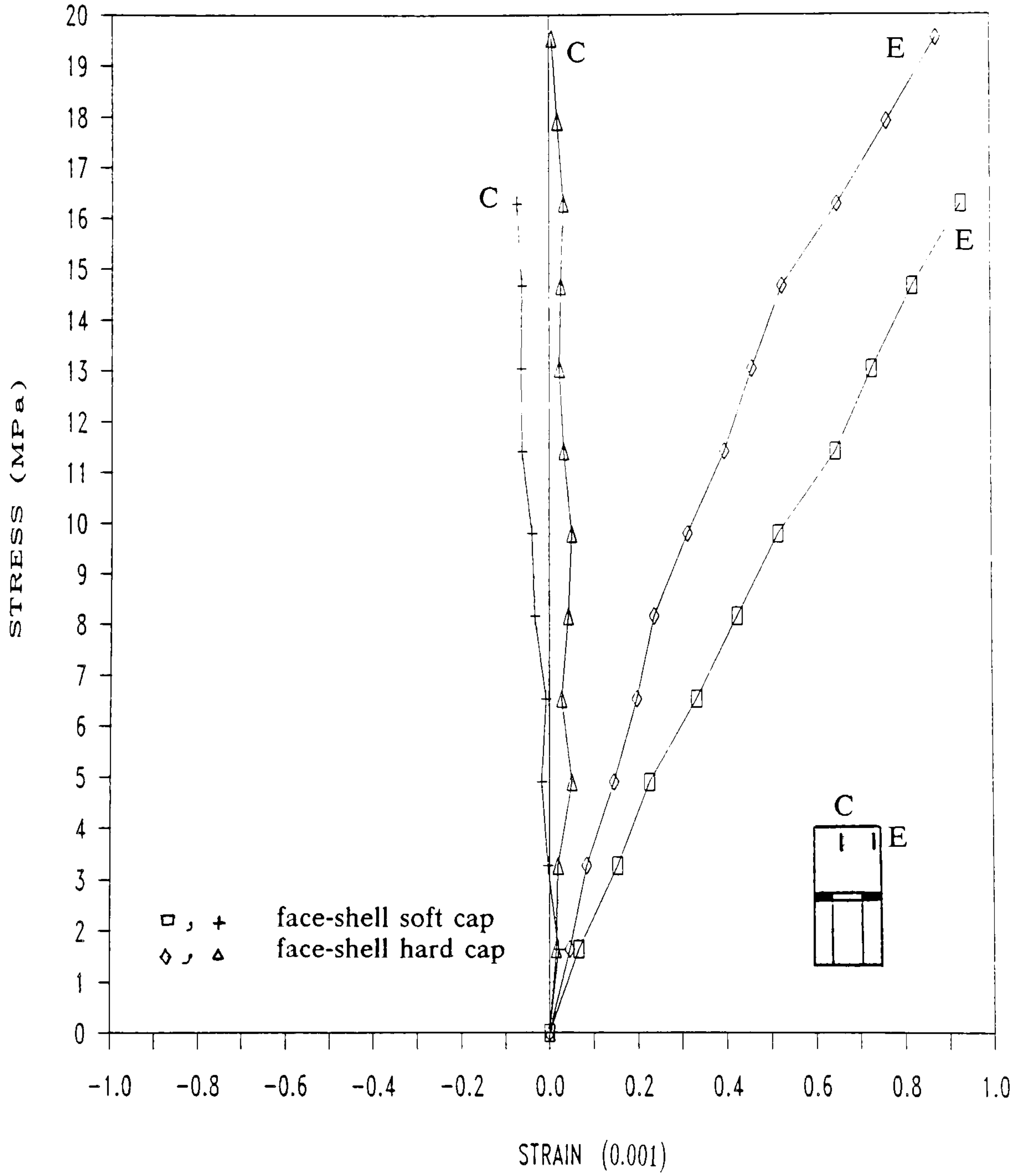

FIGURE 3.25 AXIAL COMPRESSIVE STRAINS AT PLATEN IN SOFT AND HARD FACE-SHELL CAPPED 2-COURSE PRISMS(SER. PH2-6 & PH2-4)

(strain no. 13) in fibreboard capped prisms. Such behaviour suggests that as a result of restraining forces at the interface, hard capping may have resulted in a greater transfer of the load to the unloaded webs.

4-Course Prisms (Series PH4-6)

Prisms in this series showed different modes of failure. One prism exploded suddenly without showing any signs of splitting or cracking. In another prism, mortar crushing was observed along with an unusual splitting line at the web-face shell intersection. This was also accompanied by a vertical splitting in the face shell of the second course which travelled down through the vertical mortar joint. A third prism showed upon failure only some vertical cracking of webs in both ends. For this prism, no evidence of any face shell splitting was observed but only sign of crushing of the mortar. A fourth prism showed large vertical cracking of the webs, including blocks at the top and bottom. Extensive splitting and spalling were also observed in the face shells even near the platen. This last failure mode was shown in Figure 3.22.

Common among these various failure modes is the tendency for the webs to develop vertical cracking. However, the location for the initiation of the crack in the web and its propagation along the web height varied. The large lateral strains observed in the webs suggest that web cracking would be expected even near the platens (Refer to Table B1.2 in Appendix B). Note that strain values listed in Appendix B are the average of four readings each. Lateral web strains near the platen from two sets of readings were very large (in the 2500 micro-strain range near failure). These large strains provided an indication of the magnitude of the tensile stresses developed at the platen interface due to the use of fibreboard capping material.

Cracking of the face shells was less common in the various observed failure modes. The lateral strains in the prism face shells were much higher at the platen interface than those in the central zone. The magnitude of these strains at the platen would suggest that splitting might occur in this region. In fact their magnitude was much higher than recorded strains in any of the other 4-course prims series.

a) comparison to 2-course prisms

Increasing the prism height from 2-courses to 4-courses resulted in a 13% decrease in the prism mean compressive strength. The assemblage elastic properties, however, were improved by increasing the height. The compressive modulus of elasticity increased by around 24% as a result of lesser tension due to fibreboard.

The prism failure modes differed by the tendency of the 2-course prism to develop more extensive splitting in the face shells than 4-course prisms. It appears that by increasing the height the tensile stresses at the platen interface were reduced. This can be detected by comparing the lateral strains at the platen for both 2-course and 4-course prisms (See strain no. 10 in tAbles B1.1 and B1.2). This was manifested by the tendency for the web to develop cracking at the top in 2-course prisms.

Axial strain results from the web zone near the platen continued to confirm what has been observed in 2-course prisms. The axial strains midway between the face shells were tensile instead of being compressive. In addition the compressive strains in the web-face shell intersection were also high as observed for 2-course prisms. These results again suggest that face shell fibreboard capping may not result in a sufficient transfer of the load to the webs (at least in the web area adjacent to the platen) in comparison with Hydrostone capping.

b) comparison to 4-course prisms with full fibreboard capping (Series PH4-5)

Face shell capping resulted in a 26% increase in the mean prism compressive strength compared to full fibreboard capping. The capping method also significantly affected the prism failure mode. With full bed capping, prisms failed by extensive cracking of the webs even at the prism ends. No damage in the face shells was observed. However, with face shell capping moderate splitting developed in both webs and face shells. The lateral strains in the webs were shown in Figure 3.26 for 4-course prisms with both capping configurations. It can be seen that the behaviour is somewhat similar to that observed in 2-course prisms as shown in Figure 3.23 but the magnitudes of these strains were much smaller. Again it appeared that direct loading of the end webs was the most important single factor affecting the prism failure mode as well as the compressive strength.

The magnitudes of the lateral strains in the prism face shells near the platen and in the central zone were much smaller in fully capped prism compared to face shell capped prisms. This tends to explain why no splitting (or damage) was observed in prisms tested with full capping. It appears that the prisms failed prematurely due to the extensive cracking developed in the webs without allowing the prism face shells' capacity to resist the axial load to be fully developed. This observation is supported by the low axial compressive strains recorded at the platen (strain no. 8 in Table B1.2) and in the prism central zone (strain no. 2 in Table B1.2).

c) <u>comparison to face shell Hydrostone capped 4-course prisms</u> **(Series PH4-4)**

The mean compressive strength of 4-course prisms increased only by about 3% by employing fibreboard instead of Hydrostone face shell capping. However, at the 95% confidence level, the type of capping material does not affect the compressive strength of 4-course prisms when face shell capping is used. [Note: An opposite conclusion was reached in the case of 2-course prisms]. As indicated in the Background, Section 3.1.2, hard capping materials were associated with higher specimen compressive strengths than soft capping materials. However it appears that beyond a certain height of face shell capped specimen, the type of capping material has little influence on the compressive strength.

While the prism compressive strength appears to be unaffected by the type of capping, the various strain results revealed some remarkable differences. With fibreboard capping, the lateral deformations near the platen were much more than those in the prism central zone. The reverse was true when Hydrostone capping was used. However when these strains were compared, Hydrostone capping material resulted in more lateral deformations in the prism central portion than fibreboard (strain no. 4 in Table B1.2). It may be suggested that with fibreboard capping, not only was the platen restraint removed but tensile stresses were also introduced at the platen interface.

The lateral strains at web midheight, in the third course from the top surface (strain no. 11 in Figure 3.3), were shown in Figure 3.27 for Hydrostone and fibreboard face shell capped prisms. Web cracking appeared to have initiated in prisms with Hydrostone capping earlier than in fibreboard capped prisms. This may explain why fibreboard capped prisms yielded a slightly higher compressive strength than Hydrostone capped prisms. As it will be discussed later, this observation may only be true for 4-course prisms.

3.3.2.7 Stack Bond 2-Course Prisms Using Face Shell Soft (Fibreboard) Capping (Series PH2-7)

Because stack pattern 2-course block prisms are commonly tested to determine compressive strength, Series PH2-7 was introduced for comparison with 2-course prisms constructed in running bond (Series PH2-6). Face shell fibreboard capping was employed.

For the stacked pattern prisms, the mean compressive strength was about 8% less than for running bond which is significant at the 95% confidence level. This suggests that the compressive strength of stacked and running bond 2-course prism cannot be taken as equal, It is suggested that this increase in strength can be attributed to the fact that for

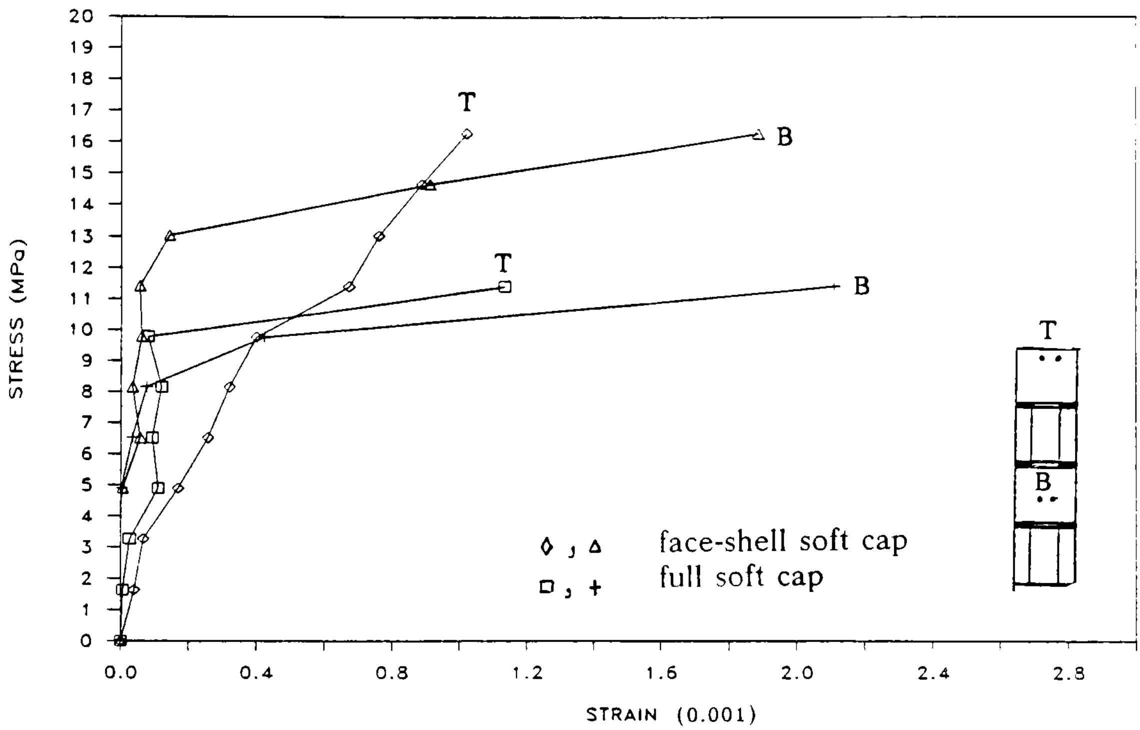

FIGURE 3.26 LATERAL STRAINS IN WEBS OF FACE-SHELL AND FULL SOFT CAPPED 4-COURSE PRISMS (SERIES PH4-6 AND PH4-5)

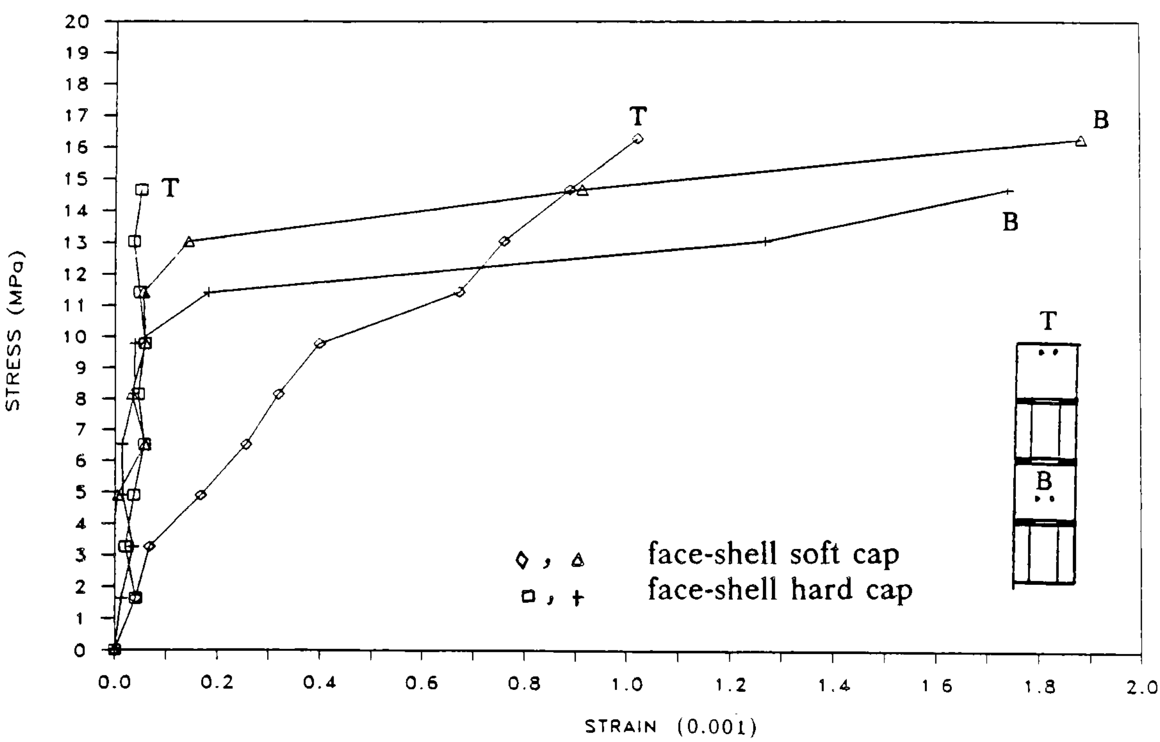

FIGURE 3.27 LATERAL STRAINS IN WEBS OF SOFT AND HARD FACE-SHELL CAPPED 4-COURSE PRISMS (SERIES PH4-6 AND PH4-4)

running bond prisms, there were 2 webs under the spherical machine head while for stacked pattern prisms there was only one web. However different behaviour may exist in prisms with more courses or different capping materials.

The failure was basically similar to that for running bond prisms. In addition, vertical cracking of the webs was observed in some instances. However, the cracking tended to initiate at the top of the web (near the platen) instead of the bottom as usually had been observed.

The lateral web strains at the platen and mid joint were shown in Figure 3.28 for stacked and running bond prisms. The large strains at the top of the web of the upper course suggest that cracking initiated at the top of the web as it was observed at failure. This indicates the extent of the lateral tensile stresses developed at the platen due to the use of fibreboard. While similar behaviour was observed for the running bond prisms, these lateral strains were only 1/3 to 1/2 of those recorded for stacked prisms (both at top and bottom of the web). The larger lateral strains in the face shells of running bond prism (in comparison to stacked prism) recorded at the platen across the mortar joint seemed to indicate that most of the lateral expansion due to fibreboard was absorbed by the relatively weak mortar joint(See strain no. 6 in Table B1.1). As a result, lower expansion would be expected to occur at the platen in the webs of running bond

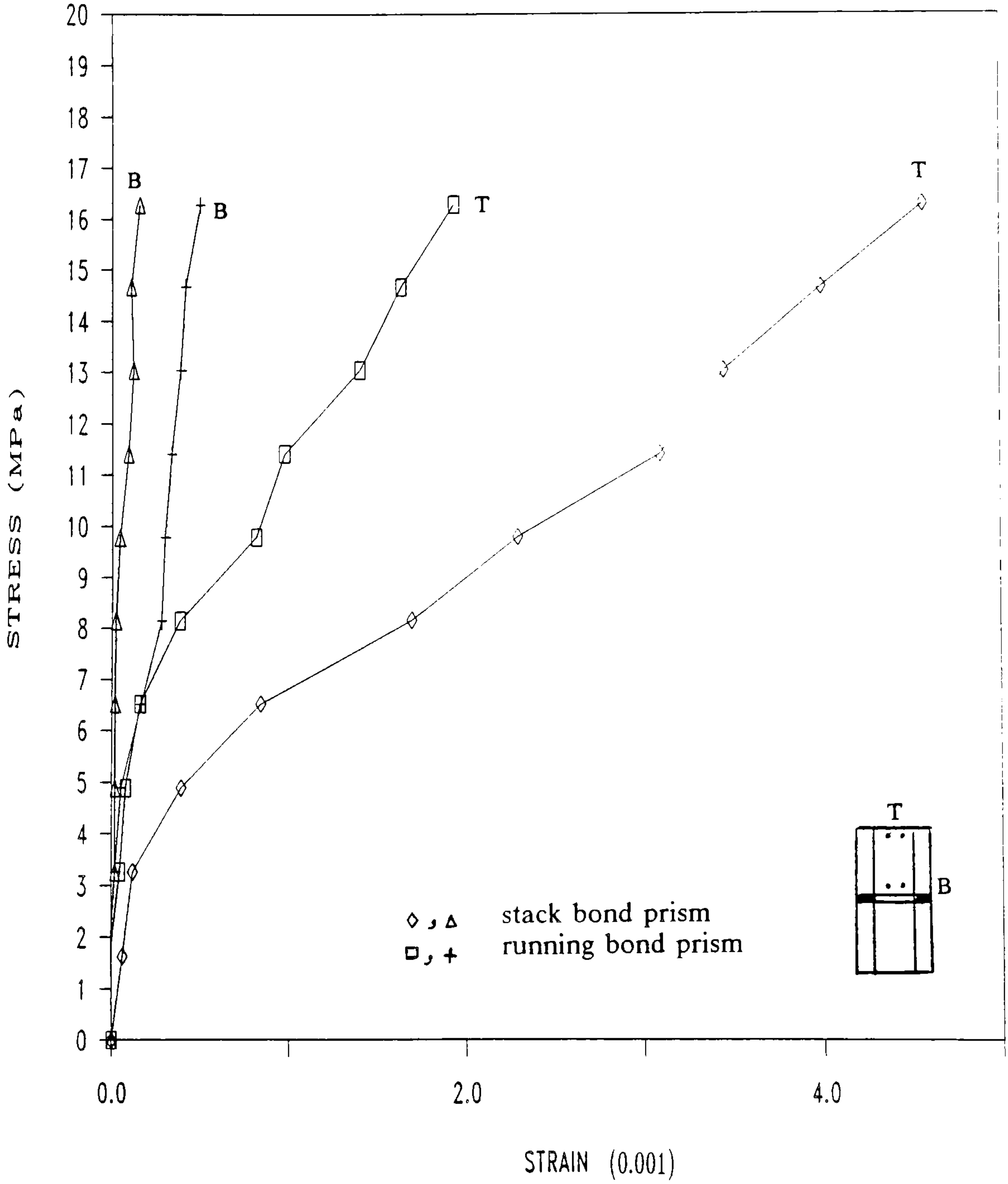

FIGURE 3.28 LATERAL STRIANS IN WEBS OF STACK AND RUNNING BOND 2-COURSE PRISMS; FACE-SHELL FIBREBOARD CAPPING (SERIES PH2-7 AND PH2-6)

prisms. This may explain why the lateral strains in the webs were much higher in stacked prisms.

The vertical compressive strains (strain no. 2 in Figure 3.2) in stacked prisms were about 20% higher than those developed in running bond prisms at the same stress levels. In fact these strains were also much higher than strains developed in any of the other six different series. Such large compressive strains may have caused an earlier failure and therefore inpart resulted in the compressive strength being lower than for running bond prisms.

3.4 DISCUSSION OF RESULTS

3.4.1 General

It was identified earlier that test methods and loading conditions significantly affect the overall behaviour of hollow blockwork prisms. The prism failure, compressive strength and elastic properties were affected by the degree of platen restraint versus lateral expansion at the ends, the instability of cracked portions of the prism which was controlled by the type and the configuration of the capping material, the non-uniformity of the loading and the specimen height. The effects of these parameters were briefly discussed in the following section.

3.4.2 Factors Affecting Strength Measurement of Face Shell Mortared Hollow Concrete Prisms

3.4.2.1 Influence of End Support Conditions

Flat end loading conditions did not result in any significant change in strength compared to pinned end conditions. However, greater difficulties in achieving proper alignment make it important to note the influence of alignment where if 5 mm of accidental eccentricity was assumed, this could translate into about 10% decrease in the axial load capacity. The other significant factor was that elimination of the 50 mm square bar along the top of the prism allowed greater unevenness of bending of the capping plate around the spherical seat. Hence lower strains were observed near the corners of the prism.

For the 4-block high prisms, it appeared that line loading for the pinned-end conditions resulted in a prism failure mode which resembled more clearly full-scale wall failure than did flat support loading[12].

3.4.2.2 Influence of Bearing Plate thickness

Bearing plates of 50 mm thickness experienced bending action and by increasing the plate thickness to 75 mm, the difference in bending was fairly obvious and affected the prism behaviour. The compressive strength of 2-course prisms was significantly increased however for 4-course prisms the strength was unaffected because the difference in bending of plates was distributed over 800 mm instead of 400 mm prism height. The distribution of axial strains across the prism cross-section was significantly improved by using thicker plates. Nevertheless, it appeared that achieving a truly uniform axial strain distribution in the prism central portion is unlikely given the complex geometry of face shell mortared masonry and the mode of load transfer from the webs to the face shells of the block[45].

3.4.2.3 Effects of Capping Configuration (Full vs. Face Shell) and Material (Soft vs. Hard)

In discussing the influence of full versus face shell capping, it is imperative that the type of capping material be taken into consideration since the results outlined earlier indicated that hard capping caused platen restraint while soft capping in fact induced lateral expansion in the block at the platen.

<u>**Full Capping**</u>

The load acting on the top of a web in a 2-course prism with full capping was illustrated in Figure 3.29 (a) and the lateral strains (measured at locations no. 10 and 11 in Figure 3.2) along the web centreline were shown in Figure 3.29 (b) for a specified stress level of 4.9 MPa prior to crack

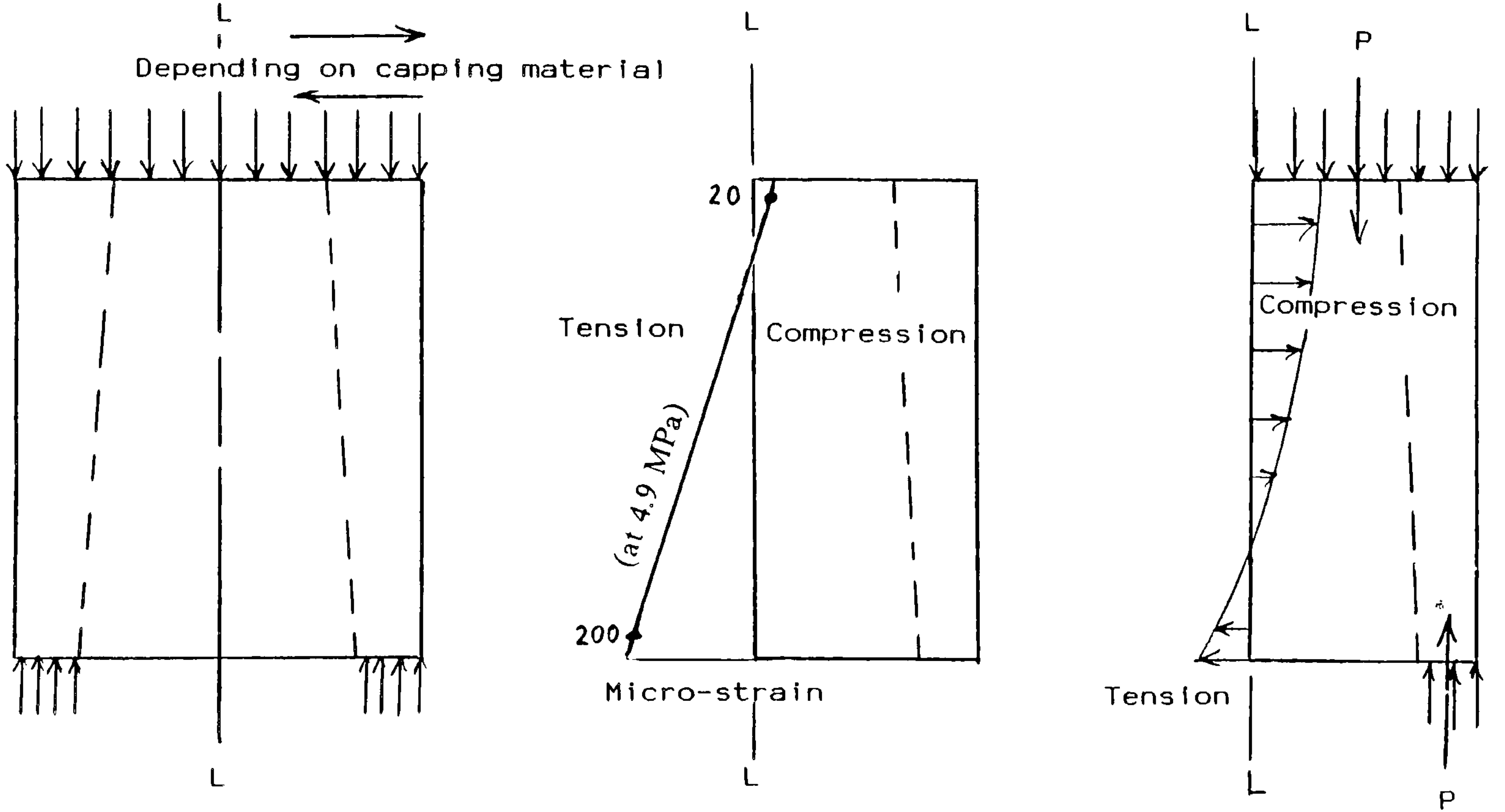

(a) loading

(b) lateral strain at centreline

(c) suggested stress distribution (from Reference 104)

FIGURE 3.29 LOADING ON THE TOP WEB OF A 2-COURSE PRISM WITH FULL BED CAPPING initiation. It is important to note that almost identical strain values were also recorded when full hard capping was employed (See Table B1.1). It has been suggested[104] that under full capping, bending of the webs would be expected and the stress distribution shown in Figure 3.29 (c) was conceptually assumed to be the case. However, such stress distribution would not satisfy equilibrium especially if the effect of lateral expansion due to fibreboard on the top surface is added, tensile stresses would have to be added to the distribution in (c). In addition, as can be seen in (b) the lateral compressive strains at the top are extremely small in comparison to the tensile strains at the bottom and if linear elastic behaviour was assumed to exist at such low stress level the web bending theory would even be harder to accept. Bending of the web is unlikely simply because curvature is prohibited if plane sections are assumed to remain plane and any bending that may exist is limited to the extent that the steel bearing plates bend under the load. However, any stress distribution that may exist along the web centreline would be expected to diminish once cracking has initiated at the bottom of the web and as indicated earlier cracks were initiated at low stress levels.

The large tensile strains developed in the bottom of the web of fully capped 2-course prisms can at best be assumed to be the result of principal stresses flowing from the top where the full surface is loaded then arching toward the two face shells. In fact this principal stress situation may look somewhat similar to the flow of stress in an arch problem. In 2-course prism, both blocks are pushing out at the mortar bed joint and from symmetry the shear force at the mortar joint is zero. Therefore tension must develop in the web to resist this outward force. This appeared to be true at small stress levels up to 6.5 MPa regardless of the capping material since similar strains were recorded in the webs of soft and hard capped prisms. The influence of capping material becomes extremely significant only after initiation of cracks. With soft capping, cracks propagated upwards quickly to the prism ends due to the absence of any platen restraint (in fact lateral expansion existed at the top due to fibreboard) and after only small increases in the load failure occurred. However with hard capping, cracks were remarkably slowed from propagating upwards due to platen restraint, therefore allowing the prism face shells' potential for resisting to the axial load to be utilized.

In prisms with more than 2-courses (such as the 4-course prisms), lower tensile stresses would be expected to develop at the webs near the bed joint next to the platen than at the same location in 2-course prisms (location no. 11 in Figure 3.2) possibly due to transmission of shear from one unit to another within the prism as shown in Figure 3.30.

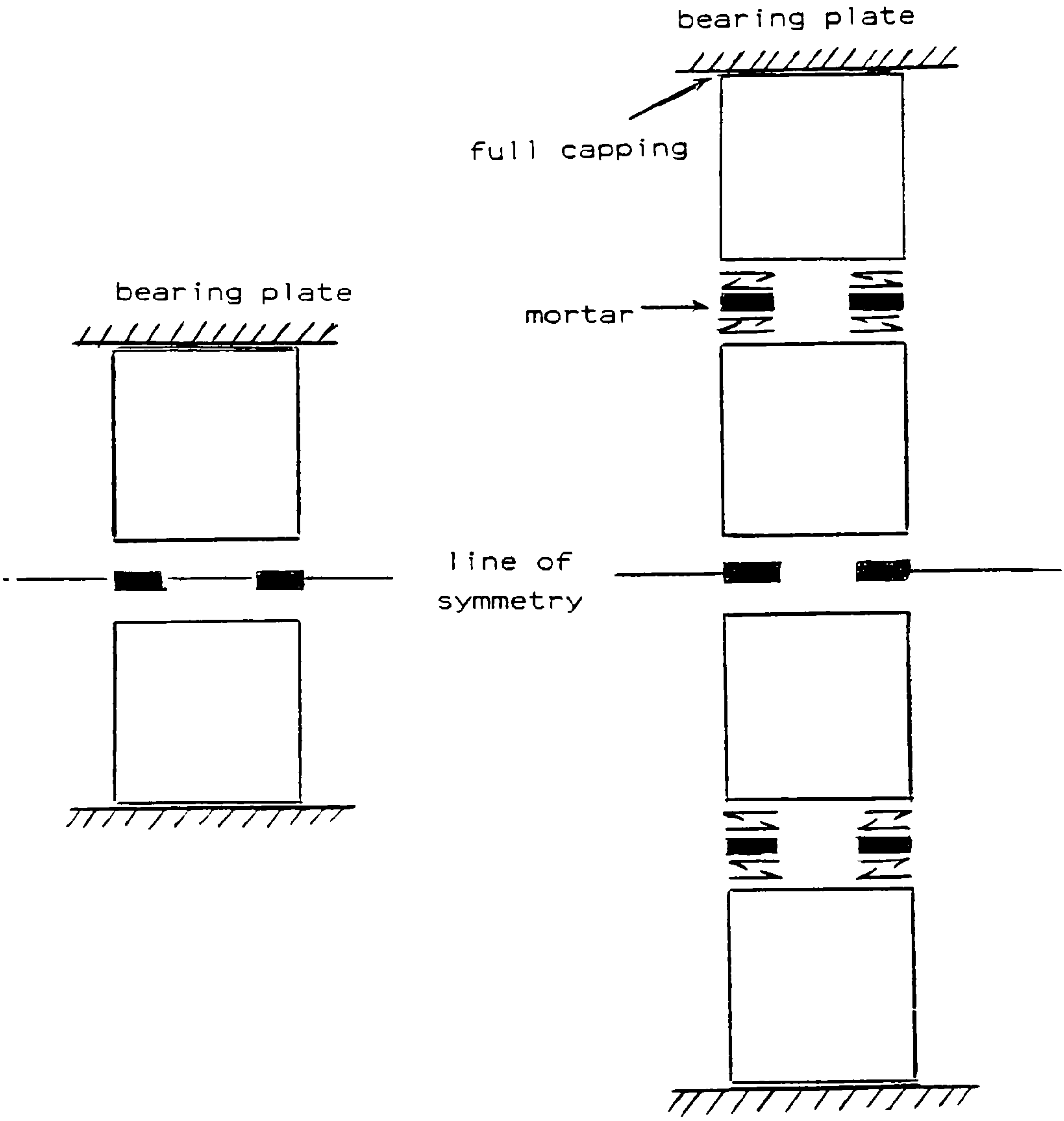

FIGURE 3.30 2-COURSE AND 4-COURSE PRISMS SEPARATED AT THE AT THE MORTAR / UNIT INTERFACE, FULL CAPPING

Shear transmission cannot occur in 2-course prism because equilibrium conditions cannot be satisfied about the line of symmetry. In 4-course prism, shears are transmitted from the end units through mortar to the centre units.

This shear transmission could occur through the mortar joints. This suggestion is supported by the fact that the strain measurements discussed earlier showed lower tensile strains in the webs of 4-course prisms than 2-course prisms and web cracking initiated at lower stress levels in 2-course prisms.

It must be noted, nevertheless, that this does not imply that a 2-course prism with full capping would fail at a lower load than a prism with more courses. The stability of the cracked portion of the prism which is much less insignificant in 2-course prisms as well as the change in the zone of cracking to the centre block webs in 4-course prisms would indicate that 2-course prisms would resist a higher load than prisms with more courses. In addition the observed increase in end effects influence with the decrease in the prism height (reported earlier) strongly supports such a suggestion. For example, with full hard capping the platen restraint increased significantly by decreasing the prism height.

Face Shell Capping

In face shell capped prisms, the lateral tensile stresses in the webs would be expected to be lower than those in fully capped prisms. This is simply because the flow of axial principal stresses in the end webs are completely different. By preventing direct loading of the webs adjacent to the platen, most of the load is now carried by the face shells. Nevertheless, transfer of the stresses to the web would be expected and at midheight of the web, appreciable axial compressive stresses are expected[37] but lower in magnitudes than in the case of full capping. The lateral strains recorded in the webs were much smaller for face shell capped prisms than their counterpart fully capped prisms.

It has been suggested that fully capped face shell mortared prisms are expected to be weaker than face shell capped prisms[104]. While this appears to be true for 2-course prisms, the results from this research indicate that this statement may not always be true. For hard capped 4-course prisms, the results strongly suggest that there was little influence of the capping configuration on the prism strength even though slightly higher lateral tensile strains were recorded in the centre webs of fully capped prisms. This suggests that little or no change of platen restraint occurred by employing either capping configuration. It is important to note, nevertheless, that the influence of platen restraint was greatly reduced in 4-course prisms in comparison to 2-course prisms.

Based on a finite element modelling of a 2-course prism with face shell capping and no restraint at the prism ends, it was reported[104] that for the top course, the lateral tensile stresses in the web are higher at the bottom than the top of the web. However, strain measurements taken at these locations (strains no. 10 and 11 in Figure 3.2) showed that under face shell soft capping (which can be considered to alleviate any platen restraint) larger expansion is expected at the top of the web and not at the bottom. In fact cracks were observed to develop in the web near the platen.

3.4.2.4 Effects of Prism Height

The results from this research program showed how significantly the various characteristics of concrete masonry were affected by different testing procedures and techniques. Introducing the height of the prism as an extra variable would further complicate the interpretation of the effect of testing methods. It was observed that for the same testing procedure/technique, changing the specimen height resulted in significant modifications to the axial and lateral strain distributions failure mode, compressive strength and elastic properties.

Regardless of the type of capping material, capping configuration and support condition, 2-course prisms did not produce a failure mode which resembled that of full-scale masonry walls. It is concluded that a 2-course high prism does not provide a central zone where uniform stresses occur. Furthermore the end effects would significantly affect the state of stress in the prism. The end effects do not always imply platen restraint; soft capping materials such as fibreboard may very well introduce lateral expansion at the platen. Increasing the specimen height reduced the zone of influence near the platen created by the end effects and provided a central zone relatively free of such effects.

Two-course prisms provided significantly higher compressive strengths than 4-course prisms for most of the various testing methods examined in this research program. Face shell Hydrostone capped 2-course prisms were 31.5% higher strength which was the largest increase. Full fibreboard capping exhibited least effect with 2-course prism strengths only 4% higher than for 4-course prisms. Nevertheless as discussed earlier, with full fibreboard capping it is the splitting tensile strength of the web which controls the prism failure. However, on average (average of various testing methods), 2-course prisms resulted in a compressive strength which was around 22% higher than for 4-course prisms.

The relationship between the specimen strength and aspect ratio, h/t, was shown in Figure 3.31 for the six different testing procedures/methods. The block strengths were also determined according to each of these testing methods (See Chapter 2, Section 2.2.3). The individual hollow block had an aspect ratio of one. As can be seen, the influence of testing technique on the specimen compressive strength is quite evident. It is also obvious that this influence was very much reduced by increasing the specimen

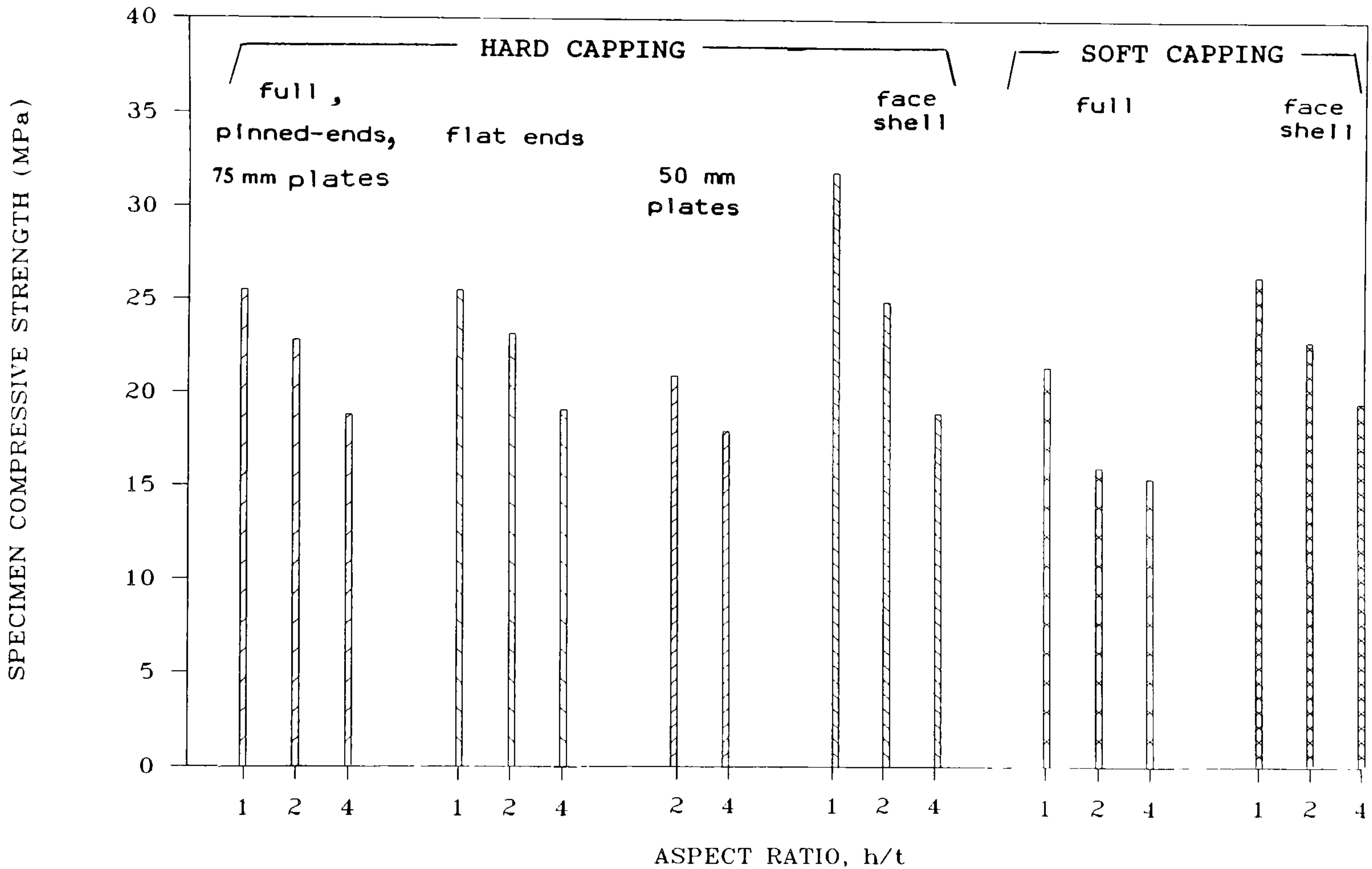

FIGURE 3.31 SPECIMEN COMPRESSIVE STRENGTH VERSUS ASPECT RATIO

height.

3.4.3 Recommended Set-Up for Prism Compression Tests

It has been shown that regardless of the test technique, 2-course prisms cannot be taken as directly representative of full-scale blockwork since they are significantly affected by the end effects, do not produce a representative failure mode and yield higher compressive strength. Therefore for representative strength measurements, use of 4 block high prisms can be more directly and reasonably related to full-scale walls. For research, use of pinned-end loading conditions is recommended because it resembles closely conditions in full-scale masonry and it is easier to ensure proper alignment. Also it allows direct correlation with eccentric loading tests where it is necessary to employ line loading. Bearing plate thicknesses of not less than 75 mm are recommended because of the adverse effects due to bending of thinner plates. Hard capping is recommended because it does not introduce any lateral expansion at the prism ends nor will it result in a premature failure. Even though platen restraint will be present its influence is relatively small in 4-course prisms. Full bed capping is recommended along with sufficiently high specimens since little difference in strength was found in comparison to face shell capping and failure was more representative. In addition such capping procedure is easier to produce.

It is believed that the prism test set-up recommended above (See also Figure 3.5) would provide the most reasonable and accurate results in addition to being practical. Therefore, this set-up was employed throughout the rest of this research program.

3.4.4 Failure of Face Shell Mortared Block Masonry

The observed failure mode of 4-course prisms as well as the various strain measurements monitored throughout the test program showed that:

1. Vertical cracking of the web was observed in all six series. However the extent of the crack propagation and its location in the web was affected by the testing procedure.

2. Cracks were observed to initiate at bottom of the centre block web, midway between the face shells and propagate upward.

3. Initiation of cracks does not constitute immediate failure nor determine the ultimate capacity of the prism.

4. Higher lateral tensile strains were recorded in the webs than in the face shells. This was true in all six series regardless of the testing procedure.

To understand how web cracks develop, webs in a central block of a 4-course prism were gauged along the vertical centreline as shown in Figure 3.4. The lateral strains at the bottom, mid height and top of the webs were monitored during the loading using the set-up shown in Figure 3.5 and conditions similar to Series PH4-1.

The lateral strains along the web centreline were shown in Figures 3.32 and 3.33 for 10% increments of the axial load up to failure. Each figure represents one set of data instead of an average which might obscure the actual behaviour.

The main observations from this data are:

1. Extremely large tensile strains were present in the webs.

2. The larger lateral strains at the bottom of the web (location A in Figure 3.32) confirms the observed crack initiation at the bottom. As discussed previously the web is narrower at the bottom and in some cases has some indentation or small crack all of which could cause cracking to initiate at this point.

3. Cracks appeared to have initiated at the bottom (location A in Figure 3.32) of the web somewhere between 0.4 and 0.5 of the ultimate stress then propagated slowly upward.

4. The cracking tensile strain of concrete masonry appeared to range between 300 and 500 micro-strain .

5. The vertical crack is expected to propagate along the full height of the web and in a direction parallel to the

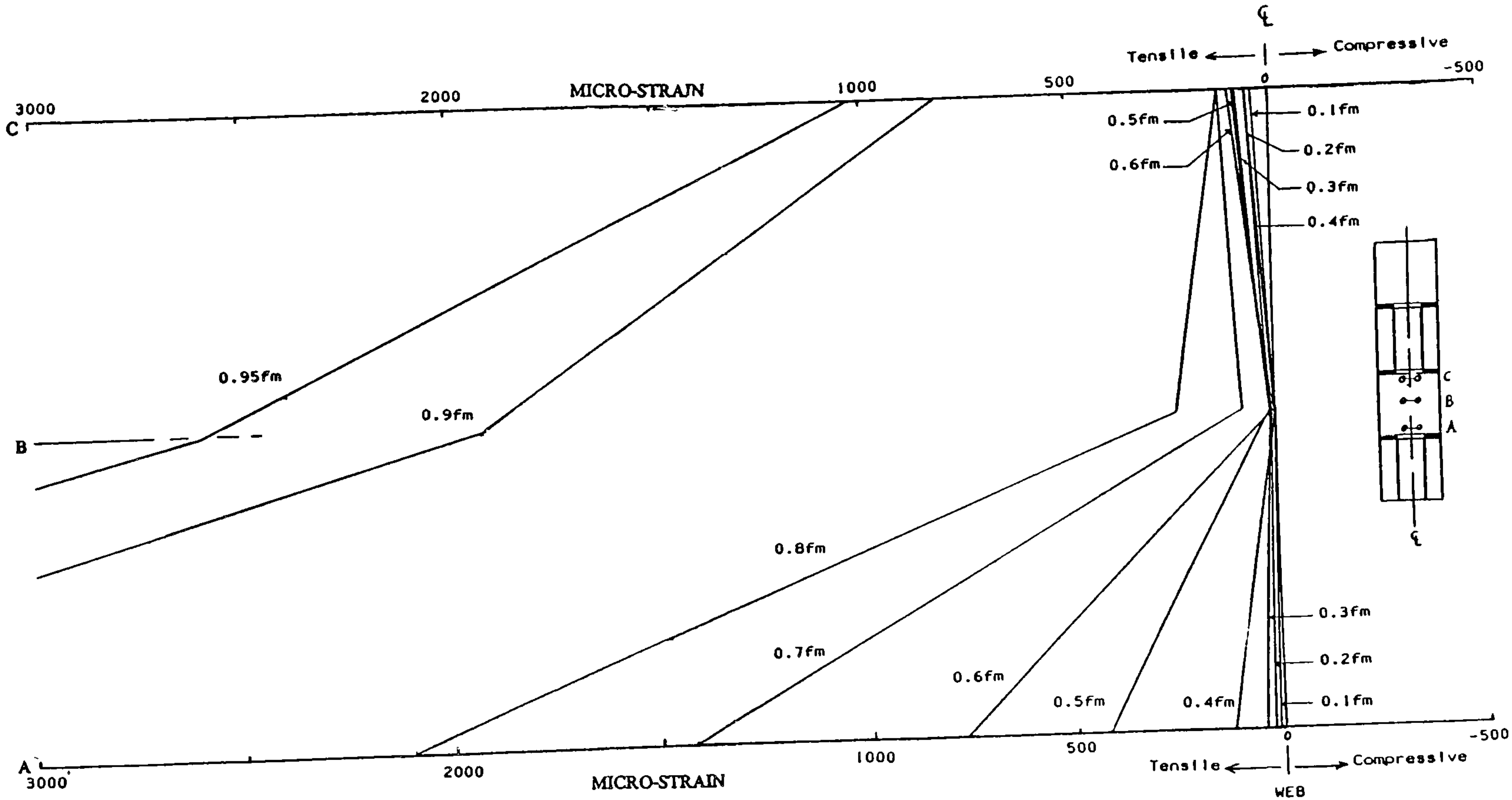

FIGURE 3.32 LATERAL STRAIN DISTRIBUTION IN A CENTRE WEB OF 4-COURSE FACE-SHELL MORTARED PRISM

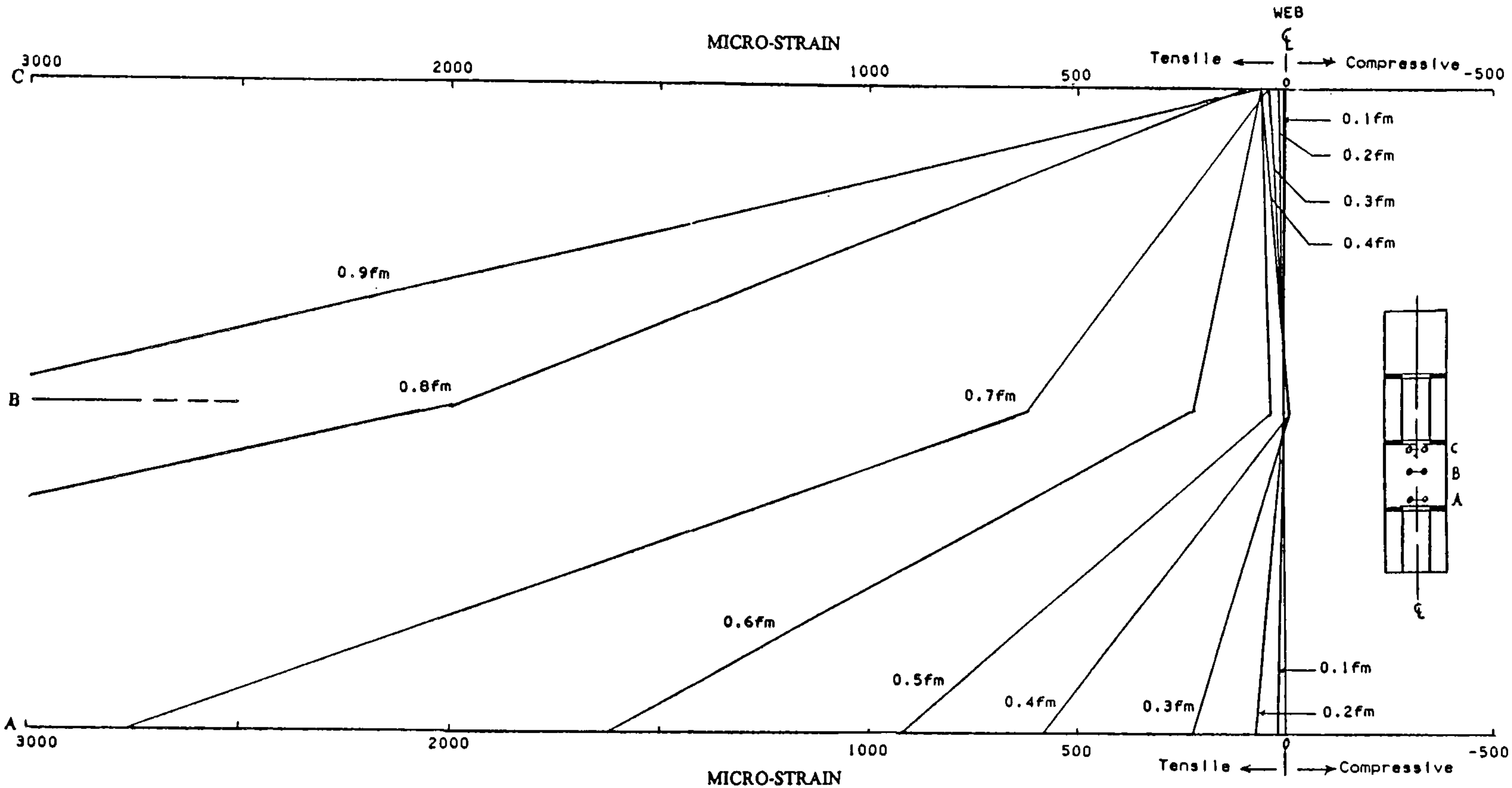

FIGURE 3.33 LATERAL STRAIN DISTRIBUTION IN A CENTRE WEB OF 4-COURSE FACE-SHELL MORTARED PRISM

axial load line.

Discussion of Failure

As indicated earlier in the Background, Hilsdorf's theory of "lateral tensile splitting" has been assumed in some instances to be applicable to face shall mortared masonry. Application of this theory would suggest that the face shells should crack when the prism is loaded in axial compression. However since cracks develop in the webs, Hilsdorf failure criteria is not applicable. In addition, several other factors which affect the validity of this and other recently proposed failure criteria have been identified as follows:

1. Lateral stresses in both horizontal principal axes cannot be assumed to be equal. Web strains were found to be much higher than face shell strains.

2. The axial strain distribution along the specimen height suggests that the vertical stress distribution is highly non-uniform. This is also true for the lateral stress distribution along the height.

3. Assumption of linear behaviour of block masonry is not justified. The response of the secant modules of elasticity to increased load was plotted in Figure 3.34. Significant reductions in modulus of elasticity, indicative of non-linear behaviour, were observed at stress levels well below the suggested[10] linear range of up to 50% of strength.

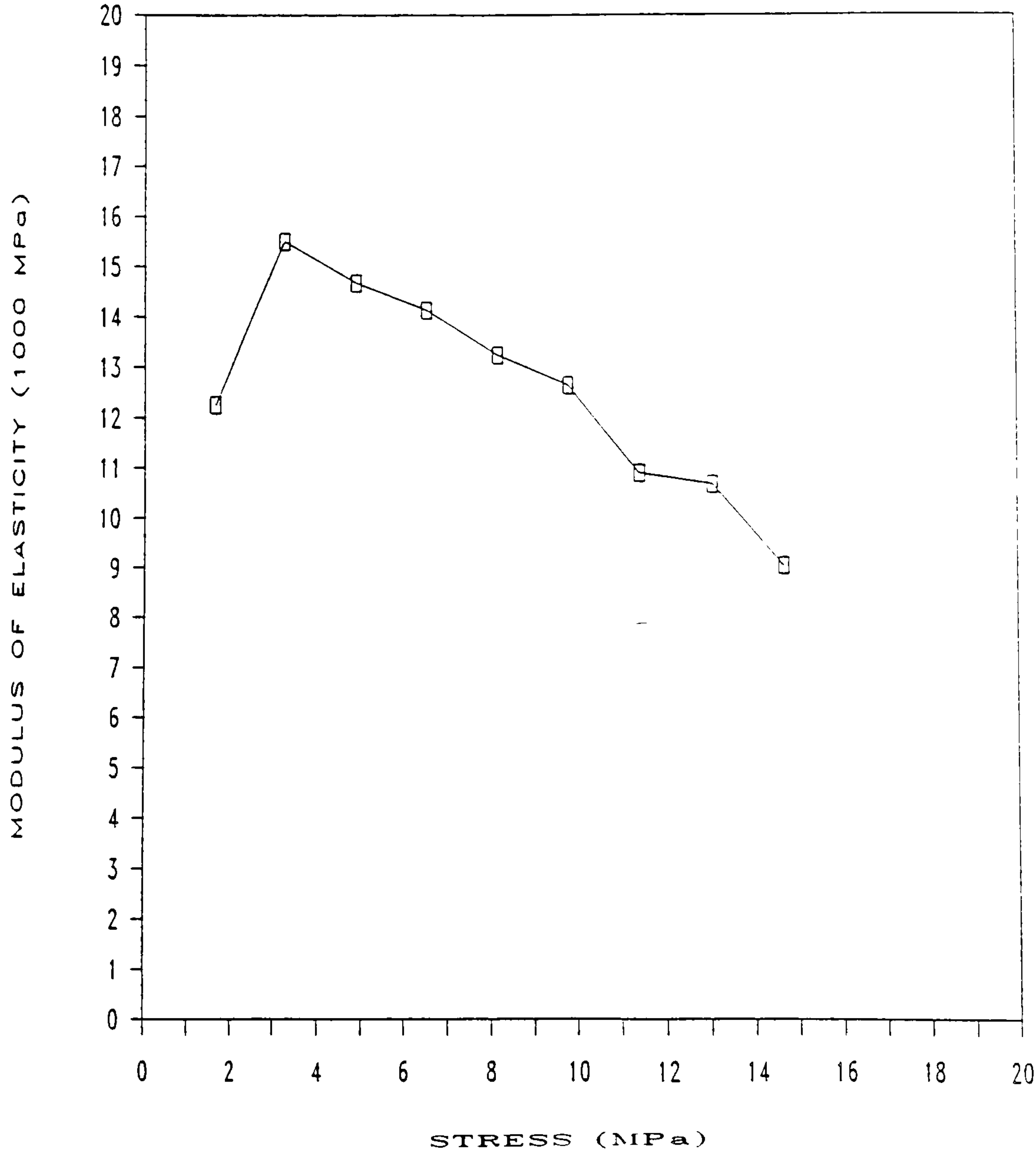

FIGURE 3.34 RESPONSE OF ASSEMBLAGE SECANT MODULUS OF ELASTICITY TO INCREASED AXIAL STRESS

It is perhaps of significance to note that in various analytical works a Poisson's ration of a certain value has been used. However as was observed in Section 3.3 such property fluctuated widely depending on the testing procedure and prism height. After all, once cracking has occurred, this property is of little significance and dilation could very well be the case. Therefore caution is required in the use as well as the significance of published values of Poisson's ratio.

4. Since cracking of the web involves the tensile strength of the unit (or maybe the web) this would be expected to affect the prism compressive strength. The degree to which tensile strength can be correlated to prism strength will be discussed in greater depth in later Chapters.

Testsindicate that web cracking is not the same as ultimate strength since there is much reserve strength after initial observation of cracking. Therefore models which predict cracking (whether linear of non-linear models) should not necessarily be expected to predict ultimate strength. The problem is much more complex than many give it credit for being. "Deep beam bending" models (discussed in Background) are an unfortunate diversion from looking at the actual behaviour.

Finally, as mentioned earlier, cracking was always observed to initiate at the indentation in the bottom of the web. It had been suggested[88] that in all brittle materials such as masonry, failure in compression is caused by the initiation and propagation of cracks. This argument has been based on the fundamental concepts of Griffith cracking theory[103] which requires that tension exists at the tip of a crack (defect) in order to break bonds and that tensile stresses can be found around flaws and defects. Hence it may be argued that since tensile stresses develop at the bottom of the centre webs in face shell mortared masonry, the indentation is the most likely location where bond would break. This does not imply that the indentation is the cause for breaking but could be attributed to a premature crack development.

Although currently there are no rigorous models, the observed phenomena and generalized conceptual ideas of how failure occur lead to the conclusion that there is potential for enhancement in the strength characteristics of face shell mortared masonry through a study of an optimum shape of the hollow concrete unit.

3.5 CONCLUSIONS

The following are the conclusions drawn from the results presented in this chapter:

1. Use of pinned-end loading resulted in a more uniform stress distribution over the loading surface. It is also easier to achieve proper alignment.

2. Thickness of end bearing plates is quite important. Use of 50 mm thick plate experienced some bending and reduced prism strength.

3. Full fibreboard capping resulted in a premature prism failure and reduced the prism compressive strength significantly.

4. Fibreboard capping material induced lateral expansion at the platen.

5. For face shell capped 4-course prisms, the capping material had little effect on the prism compressive strength.

6. Contrary to previous suggestions[104], the compressive strength of face shell mortared, face shell capped blockwork was not independent of the number of the units in the prism.

7. The suggestion that fully capped, face shell mortared masonry gives lower strength than face shell capped masonry[104] is limited only to 2-course prisms and soft capping material. No difference in strength was observed in 4-course prisms with either face shell or full hard capping.

8. Increasing the specimen height produced a central zone relatively free of end effects.

9. On average, tests of 2-course prisms yielded a compressive strength 22% higher than 4-course prisms.

10. Axial compression tests of 4-course prisms with line-loading, 75 mm thick bearing plates, Hydrostone capping material and full bed capping is the most practical test set-up among the six methods examined. This test set-up would also yield the most reasonable and accurate results.

11. Cracking of the web is the expected cracking pattern in face shell mortared masonry. Cracks initiated at loads as low as 40% of the ultimate stress and extremely large tensile strains were recorded in the webs.

12. Theories developed for solid masonry are not applicable to face shell mortared hollow masonry.

13. The compressive modulus of elasticity decreased rapidly with increasing load at loads as low as 30% of the ultimate load.

3.6 RECOMMENDATIONS

1. There is a need for a compression test which predicts masonry compressive strength with an acceptable degree of accuracy. To measure the strength of face shell mortared masonry, it is recommended that a prism representative of actual construction practice be employed.

2. Two-course prisms cannot be considered to be representative of full-scale masonry wall. 4-course prisms

should be considered for adoption as a standard prism height. Only in some cases where it is necessary to employ 2-course prisms, such practice may be allowed if a strong and accurate relationship can be established between 2-course prisms and higher course prisms (or walls).

3. It is recommended that the prism test procedure recommended earlier in Section 3.4.3 be employed in prism compression tests.

4. Current specifications[25] on prism compression tests are in need of re-evaluation, especially regarding the specified fibreboard capping material.

5. A study into an optimum geometry of the hollow concrete block could improve the strength characteristics of face shell mortared blockwork. Elimination of the web indentation should be considered. Changes to the actual shape of the block could offer the potential for improvement to the structural response.

6. In running bond construction using standard 190 mm hollow blocks, the mortar bedded area to be used in strength calculation should be determined by increasing the minimum block face shell area by 23 percent.

CHAPTER 4

PARAMETRIC STUDY OF THE VARIABLES INFLUENCING THE COMPRESSIVE STRENGTH OF FACE SHELL MORTARED BLOCK PRISMS

4.1 INTRODUCTION

4.1.1 General

For well defined test conditions and specific prism height, prism compressive strength could be affected by variables which interact to either alter the mechanism of failure or modify the stress pattern in the prism. Possible factors include block compressive and tensile strengths, mortar strength, type and composition of mortar, workmanship, age, type of mortar bedding, type of bond and change in the actual geometry of the standard hollow unit. The influence of these factors on the compressive strength of brick masonry prism was reviewed in Monk[75] and Mayes and Clough[72]. Numerous researchers have examined the effects of some of these factors on the compressive strength of concrete masonry[14,27,29,49,63,71,72,97]. However most of these studies were carried out on solid or hollow fully mortared concrete masonry and, in many instances, 2-course high prisms were used. As discussed in Chapter 3, the initial failure of face shell mortared masonry was by web cracking, a mechanism different than the failure of solid or fully bedded concrete masonry. Therefore there is a need to examine the effects of the above variables on the behaviour of face shell mortared block prisms using specimens representative of the full-scale walls.

4.1.2 Objectives

It was concluded in Chapter 3 that 2-course high prisms would not yield a representative failure and would overestimate the strength of full-scale masonry. It was also found that the failure of 4-course prisms was more representative and provided a good measure of the compressive strength.

Taking into consideration the findings of Chapter 3, it was the objective of the study reported in this chapter to investigate the influence of the following range of variables on the axial load behaviour of 4-course high face shell mortared hollow block prisms built in running bond:

- unit compressive strength
- unit tensile strength
- mortar strength
- mortar type
- mortar composition
- type of masonry bond pattern
- type of mortar bedding

- geometry of the standard hollow unit
- age of prism.

4.1.3 Background

<u>Unit Compressive Strength</u>

Researchers have often attempted to relate masonry unit compressive strengths to wall or prism strengths by employing an "efficiency ratio"[27,29,72]. The "efficiency ratio" was expressed as the ratio of the wall or prism strength to the strength of the masonry unit. As shown in Chapters 2 and 3, the influence of the method of testing on the strengths of both single units and prisms can be very significant. Unfortunately such influences have not been accounted for when the efficiency ratio was employed. This is evident in the Canadian code[25] which specifies different testing methods for the measurement of the unit and prism compressive strengths. Cranston and Roberts[29] reported that over a wide range of block strengths the wall strength was reasonably constant, generally falling between 0.7 and 0.8 times the unit strength. They also added that the relationship between the wall strength and the block strength depended on the variation of the strength of individual blocks. For 15 percent coefficient of variation in the block strength, the average wall strength was found to be 85 percent less than would be the case if there were no variation at all in unit strength.

Copeland and Timms[27] concluded that for a given mortar, the strength of walls was directly proportional to the strength of the individual units. In the National Concrete Masonry Association, TEK Note 15[81], the compressive strength of block was found to be the most important factor in influencing wall strength. However Mayes and Clough[72] reported results of a study by the National Bureau of Standards which concluded that the strength of solid walls was more clearly related to the shear strength than any other strength property. Other opinions were also presented by Mayes and Clough[72] who concluded finally that only statistical and not functional correlations have been obtained between the unit and wall compressive strength.

Unit Tensile Strength

Full mortared block masonry (solid and hollow) has been observed to crack vertically on the wide face when subjected to axial compression[17,97,109]. Face shell mortared masonry fails also by developing cracks in the webs, although in a different mechanism than for full mortared bed joints. Hence cracking failures are prevalent in masonry and therefore capacity is likely related in some way to the material tensile strength.

The tensile splitting of masonry under axial compression has been recognized for many years[72]. The theory presented by Hilsdorf[54] for the failure of masonry (solid and fully bedded) under axial compression was based on the tensile strength of the unit in combination with the triaxial state of stresses in the mortar as controlling the failure. However the analytical formulation presented by Hilsdorf for determining the prism compressive strength does not appear to fully reflect the importance of the unit tensile strength on the prism strength. Independent calculations showed that a substantial decrease in the unit tensile strength would only result in insignificant decrease in the prism compressive strength while an equivalent percentage of decrease in the unit compressive strength would result in an appreciable decrease in the prism compressive strength. Hamid[43] used the same approach for hollow blockwork. Again, the predicted capacity was not sensitive to tensile strength.

Shrive[102] argued that the formulations presented by Hilsdorf and Hamid cannot explain the vertical cracking of masonry under axial compression since the tensile stresses obtained from such formulations are too small in comparison to the uniaxial tensile strength obtained experimentally.

Given the nature of web cracking in face shell mortared masonry, suggestions have been made for changes in the standard hollow unit for possible improvements in the compressive strength of walls[37,44,88]. Such suggestions are mainly concerned with increasing the tensile strength of the web. Some[55] have indeed suggested that the webs are too thin to adequately transfer the load from the face shells. However, there is no information in the literature on the influence of increasing the unit (or web) tensile strength on the compressive strength of face shell mortared blockwork. In fact there is no information in this regard for any type of masonry.

Mortar Type and Strength

While the mortar compressive strength determined by tests on 50.8 mm standard cubes provides a valuable means of comparing mortar, it does not necessarily indicate the strength of the mortar as it occurs in the wall[27]. The reasons for this were discussed in Chapter 2.

Numerous tests have been performed to examine the influence of mortar type and strength on the compressive strength of face shell mortared block[27,32,63,67,95,97,104]. Most of these tests showed that the compressive strength of prisms was relatively independent of the mortar type or strength. However it is worthwhile mentioning that in some of these tests, the prisms were 2-course or 3-course high[12,32,95,97] and therefore the effects of the mortar strength may be overshadowed by the influence of end platen effects. Page and Shrive[88] suggested that the small influence of mortar properties on the failure of hollow masonry may be attributed, in part, to the high ratio of the unit height to joint thickness. In addition, they indicated that the initial failure of face shell mortared block is by web cracking, a mechanism independent of mortar strength. There is no information on the influence of significantly weaker mortar on the strength of face shell mortared block where the mortar might fail before initiation of the web cracking.

Mayes and Clough[72] reported that the influence of the mortar type on brick prism strength was very marked. The prism strength was shown to be reduced by more than half by using Type O instead of Type M mortar. The prism strength was also reduced by over 30% by using Type N mortar. Hamid[43] indicated that the assemblage compressive capacity was affected by the mortar strength relative to the masonry unit and not the absolute value of the mortar strength. He also added that lower mortar-masonry unit strength ratio resulted in lower prism compressive strength. Self[97] compared the prism efficiency (ratio of prism strength to block strength) with mortar strength to show the effect of mortar strength. He concluded that the influence was insignificant and that an increase in mortar strength of 200 percent produced an increase in efficiency of only 11 percent.

Mortar Composition

While there has been some discussion in the literature on the influence of the mortar composition (mainly the use of masonry cement) on the tensile bond strength of masonry[28,41,58,108], no particular information was found on the compressive strength of masonry.

Type of Bond Running Versus Stack (Only Face Shell Bedding)

Mayes and Clough[72], in a review on brickwork, indicated that running bond would give lower strength than stack bond prisms. They attributed this to the influence of the vertical mortar joint. According to Stafford-Smith and Carter[109] the peak values of horizontal tensile stress in compression loaded walls were associated with the vertical joints. However, Hamid[43] reported that the conclusion by Stafford-Smith and Carter[109] is questionable. He also concluded that there was no significant effect of the bond type on the prism compressive capacity for either ungrouted or grouted specimens. It is important to indicate that in Hamid's work both stack bond and running bond prisms had fully mortared bed joints and 3-course high prisms were employed. A similar conclusion was also reported by Hedstrom[49]. However test results by Hegemier et al[51] tend to contradict the conclusion offered by Hamid[43]. Grouted prisms laid in running bond were shown to yield significantly lower compressive strength than stack bond prisms. Other tests also have shown that consistently lower strengths were observed in running bond compared to stack bond face shell mortared prisms[63,70,87,97]. The secant modulus has also been observed to be lower for running bond than stack bond prisms[63].

Finally, it is worthwhile mentioning that when examining the influence of bond pattern on the compressive strength, running bond should be compared only against stack bond with face shell mortaring. Employing stack bond with fully mortared bed joints would confuse such a comparison.

Mortar Bedding: Face Shell versus Full Mortaring

The failure of face shell mortared hollow block prisms was discussed in detail in Chapter 3. The traditional approach for measuring the compressive strength of hollow concrete masonry (usually built in running bond) was based on testing stack bond prisms with full mortaring[27,33,43,93,95,97]. However, the recent awareness of the fundamental difference in the failure mechanism (and eventually all characteristics) between face shell and fully mortared masonry have attracted some attention to this area[67,777,97,104]. In a study on 2-course prisms, Nacos[77] reported that face shell mortaring increased the prism strength by as much as 18% over full mortaring (based on mortar bedded area). Maurenbrecher[67] indicated that data from Nacos contradicted the results of a survey which showed little or no influence due to the type of bedding. He also stated that the high difference reported by Nacos could be partly attributed to the value of mortar bedded area. Different opinions have also been reported[81,97]. The prism height as well as the type of capping configuration have been reported to influence the comparison between the two types of mortar bedding[70,104].

Geometry of the Standard Hollow Block

Standard 190 mm hollow blocks are available in two forms, one with recessed or "frogged" ends the other with plain ends. In addition there are standard "stretcher" units and "splitter" units. The latter normally have 1 frogged end and 1 flat end plus 2 central webs on either side of the fracture line for splitting. Both types of units have the same face shell area.

Given the nature of initial failure in face shell mortared blockwork, suggestions have been made for a study of the optimum shape of the unit for improvements of the strength characteristics[37,88]. Hamid and Abboud[44] concluded that the shape of the standard hollow unit had a significant effect on its strength and deformational characteristics. They also added that tapering of the unit face shells and webs would result in a large reduction in the compressive strength of blockwork.

In almost all investigations hollow stretcher units or plain end units with only 3 webs have been used. There is no information on the influence of introducing an extra web to the unit on the failure or compressive strength of face shell mortared blockwork.

Age of Prisms

Concrete blocks will continue to gain strength after manufacture[67,88,97]. Self[97] reported an increase in the unit compressive strength for up to 200 days. However Wong[116] showed that no significant increase in strength have been achieved in units tested at 9 and 19 months. The gain in the unit's strength has been attributed to gain in the strength of concrete with time and also from the drying of the block[67]. Increases in strength are also a function of the type of curing. For example, autoclave cured units would not be expected to increase significantly in strength with time[116]. However, an increase in the moisture content have been found to decrease the block strength[88,95,97].

Mortar strength would also be expected to increase with time. However, data on Type S2 mortar, as detailed in Chapter 2, showed no significant increase beyond the 28 day strength of air cured webs. Maurenbrecher[67] reported that the small effect of mortar on blockwork strength implies that any increase in strength with age is mainly due to the block.

While there is some information on the influence of age on the unit strength, little is known with regard to the assemblage strength.

Modulus of Elasticity

Current Codes[1,26] specify a modulus of elasticity $E_m = 1000f'_m$ where f'_m is the prism compressive strength. Hamid et al[47] suggested that this relation is a carry-over from a similar for concrete. Some researchers have shown that the modulus values for concrete masonry based on $E_m = 1000\ f'_m$ were high[47,63] while others reported that such relationship is likely to be an underestimation[116]. However, Maurenbrecher[68] suggested that this relationship agreed with values for the hollow concrete masonry.

The actual elastic modulus of concrete masonry can be a function of the same variables that affect the prism compressive strength. Some investigators have indicated the uncertaintly of estimating the elastic modulus using a single equation for all material combinations[47,96].

Experimentally, the elastic modulus may be defined by the initial tangent, tangent or secant lines. Some have suggested that the high variation in strains at low stress levels makes the initial tangent method unreliable[90,116]. In fact, the experimental work carried out for Chapter 3 tended to confirm this suggestion. Many have used the secant method although the stress level at which to base the secant has varied[43,63,80,116]. Stress levels of 40% and 50% have been used[43,90]. However, as shown in Chapter 3, the modulus of elasticity starts decreasing at stress levels lower than 50% of the ultimate stress. According to Amney et al (in Wong[116]), it is practical to use the secant modulus at 0.225 f'_m because it is the code allowable stress level. The secant modulus at 0.225 f'_m has been found to be around 10% higher than at 0.5 f'_m for face shell mortared blockwork[116]. In addition the experimental stress-strain curve was reported to be linear up to about 0.3 of the ultimate strength.

It has been argued that the modulus of elasticity cannot be explicitly related to the compressive strength since the states of stress and strain existing at low stress levels are quite different from those existing at or near failure[43,116]. Hence attempts have been made to calculate the modulus as a function of the component properties[43,92,96]. Such an approach would require a prior knowledge of the mechanical properties of the constituent materials. However, the behaviour of these materials under the conditions of uniaxial compression would differ greatly from the conditions that exist within the masonry assemblage[43]. Furthermore, it is not an easy task to develop test methods to determine the properties of the constituent materials under conditions similar to those existing in an assemblage.

4.1.4 Outline of Investigation

The test program for this parametric study was shown in Table 4.1. Standard one block long, 4-block high prisms were built in running bond using face shell mortaring on 190 mm standard stretcher units. In most cases the five repetitions for each test condition were repeated for two different blocks representing bubble cured (No. 10) and autoclaved (No. 21). Units with a specified 15 MPa compressive strength were requested. The Type S2 mortar described in Chapter 2 was used. The following series of tests were performed.

Series S0 - This standard series was used as the basis of comparison.

Series S1 - For the effect of unit compressive strength, a 30 MPa specified block strength was obtained from Company 10.

Series S2 - To investigate influence of unit tensile strength, blocks with nearly identical compressive strengths were obtained from 2 different companies (No. 13 and No. 26) at two different times.

Series S3 - Type S2 mortar was modified to try to provide 5 MPa and 20 MPa mortar strengths to study the influence of mortar strength.

TABLE 4.1: DETAILS OF PRISM INVESTIGATION PROGRAM

SERIES NO.	BLOCK COMPANY NO. 10	21	OTHER	PARAMETER	DESCRIPTION OF SERIES	NUMBER OF PRISMS
S0	Y	Y		Standard	15 MPa specified unit strength, running bond, 12 MPa specified mortar strength (Type S2), stretcher unit, prism age of 6 momths	5
S1	Y			Unit compre-ssive strength	30 MPa specified unit strength	5
S2			13 & 26	Unit tensile strength	Change in tensile strength for the suppo-setly same specified compressive strength of units received at two different periods, blocks from two different new companies; 2 sets of prisms for each companies	5 5
S3	Y	Y		Mortar strength	5 MPa mortar strength 20 MPa mortar strength	5 5
S4	Y	Y		Type of mortar	Type N2 mortar	5
S5	Y	Y		Mortar composition	Portland cemene-lime mortar	5
S6	Y	Y		Bond pattern	Stack bond with face-shell mortar bedding	5
S7	Y	Y		Full bedding	Stack bond with full mortar bedding	5
S8	Y	Y		Unit geometry	Hollow splitter units	5
S9	Y	Y		Age of prism	- Prisms tested at age of 7 days Prisms tested at age of 36 days	5 5
S10	Y	Y		Height comparison	2-Course stack bond prisms, face-shell bed-ding; for comparison with 4-course prisms	5

Y= units used in prisms pertain to this company.
Standard = all other Series will be compared to the Standard Series-S0, except Series S2.

Series S4 - Type N2 mortar was used to investigate the influence of mortar type.

Series S5 - Type S Portland Cement-Lime mortar was used to investigate the influence of mortar composition.

Series S6 - A series of prisms were built in stack pattern with face shell mortaring to provide data on influence of bond pattern.

Series S7 - Stack pattern prisms with fully mortared bed joints were provided for comparison purposes.

Series S8 - Prisms were made with splitter units in running bond pattern to investigate the influence of an extra web.

Series S9 - Prisms were tested at 7 and 36 days to provide information on effect of age.

Series S10 - 2-course high stack pattern prisms with face shell mortaring were tested to measure influence of prism height for that configuration.

4.2. PRISM FABRICATION AND TEST PROCEDURE

4.2.1 Fabrication of Prisms

The prisms were constructed by professional mason in a manner similar to that described in Section 3.2.2. Construction of the prisms took place during the last week of

January with temperature in the laboratory being around 20^0C. The relative humidity was around 20 to 30%. Local Hamilton masonry sand, designated as McMaster Masonry Sand, was used throughout.

4.2.2 Instrumentation and Testing

Vertical (axial) deformations across a block-and-joint in the prism were measured using a DEMEC mechanical indicator with a 200 mm gauge length. These strain measurements were monitored on the central portion of the prism away from the platen at strain location No. 2 in Figure 3.3. For every set of 5 prisms, strains were monitored in 3 prisms with measurements taken at opposite sides of each prism. Strain measurements were recorded up to 80% to 90% of the ultimate load.

Based on the findings in Chapter 3, line loading was used with 75 mm thick steel bearing plates employed to transfer the line load to the prism. Full bed Hydrostone capping was used. The prism test set-up was as shown in Figure 3.5. Capping procedure, preparation of prism and actual testing were all carried out as described in Section 3.2.4. To avoid the influence of age on most of the comparisons, prisms were tested over a period ranging between 5 to 6 months age.

4.2.3. Tests of Constituent Materials

Unit Compressive Strength: Ten stretcher units for each company were tested in axial compression. The blocks were fully capped with Hydrostone and 75 mm thick steel bearing plates were used. Details of the test procedure can be found in Appendix A (Series C10-1). The block mean compressive strengths were 31.0 MPa and 24.5 MPa for Companies 10 and 21, respectively. The individual results were listed in Table C1.1 in Appendix C.

Unit Tensile Strength: Splitting tests were carried out on ten half units with the load applied across the face shells. The splitting test set-up was shown in Figure A2.1 in Appendix A. Details of the test procedure are in Appendix A. The block mean tensile splitting strengths were 2.6 MPa and 2.3 MPa for Companies 10 and 21, respectively. The individual results were listed in Table C1.1 in Appendix C.

Mortar Strength: Three standard mortar cubes were made for every batch. The cubes were left for the first few days in a room where the heat was left on accidently. This adversely affected the cement hydration and may have resulted in low mortar compressive strengths. The mortar cubes were tested at an age comparable with the prism tests.

4.3 EXPERIMENTAL TEST RESULTS

Tables 4.2 and 4.3 contain summaries of the prism compression test results for Series S1 and S3 to S10, for Companies 10 and 21, respectively. For these series, units with a 15 MPa specified compressive strength were used. Tables 4.2 and 4.3 also include the mortar mean compressive strengths (based on 3 cubes). The results for Series S1 were listed in Table 4.4 separately because units with different specified compressive strength were used. The results related to Series S2, where blocks form different sources (Companies 13 and 26) were used, were listed in Table 4.5.

The net mortar bedded area was used in the strength calculation for running bond prisms. More details on the value of this area can be found in Chapter 3. Independent calculations showed that for stack bond prisms with face shell mortaring, the same mortar bedded area can be used. However, for stack bond prisms with full bedding the unit minimum net area of 38028 mm^2 was used (See Table 2.1 for details). This value is equivalent to the mortared area in contact with the upper and lower units.

For each Company, the results from each series, except Series S2, were compared with the standard series, Series S0. Results from Series S2 were compared only against each other.

TABLE 4.2: SUMMARY OF RESULTS FOR COMPANY 10

SERIES NO.	VARIED PARAMETER	MORTAR		PRISM COMPRESSION TEST			
		STRENGTH (MPa)	C.O.V. (%)	ULTIMATE LOAD (kN)	MEAN LOAD (kN)	MEAN STRENGTH (MPa)	C.O.V. (%)
S0-10	Standard	7.1	11.5	593.0 568.0 585.0 624.0 591.0	593.0	19.3	3.4
S3-10	5 MPa Mortar	1.3	1.7	375.0 382.0 423.0 295.0 325.0	360.0	11.7	14.0
	20 MPa Mortar	24.8	11.4	660.0 681.0 705.0 637.0 668.0	670.2	21.8	3.8
S4-10	Type N2 Mortar	1.9	4.9	503.0 515.0[a] 504.0 463.0 517.0	500.4	16.3	4.4
S5-10	Portland Cement-Lime Mortar	10.1	13.7	656.0 639.0 650.0 669.0 576.0[b]	638.0	20.8	5.7
S6-10	Stack Bond Face-shell Bedding	9.9	7.3	691.0 704.0 710.0 729.0 731.0	713.0	23.2	2.4
S7-10	Stack Bond Full Bedding	9.0	14.6	809.0 829.0 783.0 771.0 759.0	790.2	20.8	3.6

TABLE 4.2: continued

SERIES NO.	VARIED PARAMETER	MORTAR		PRISM COMPRESSION TEST			
		STRENGTH (MPa)	C.O.V. (%)	ULTIMATE LOAD (kN)	MEAN LOAD (kN)	MEAN STRENGTH (MPa)	C.O.V. (%)
S8-10	Splitter Units	8.4	10.9	692.0 693.0 630.0 638.0 702.0	671.0	21.9	5.1
S9-10	7 Days Prism Age			607.0 714.8 712.6 620.0 718.4	674.7	22.0	8.3
	36 Days Prism Age	11.9	10.9	615.3 657.3 651.6 671.1 592.4	637.5	20.8	5.1
S10-10	2-Course Prism	6.1	0.2	725.0 760.0 715.0 697.0 735.0	726.4	23.7	3.2

C.O.V.= coefficient of variation

a= Second batch of mortar was used; mortar strength was 2.9 MPa

b= Second batch of mortar was used; mortar strength was 8.5 MPa

TABLE 4.3: SUMMARY OF RESULTS FOR COMPANY 21

SERIES NO.	VARIED PARAMETER	MORTAR		PRISM COMPRESSION TEST			
		STRENGTH (MPa)	C.O.V. (%)	ULTIMATE LOAD (kN)	MEAN LOAD (kN)	MEAN STRENGTH (MPa)	C.O.V. (%)
S0-21	Standard	7.9	11.0	512.0 498.0 493.0 509.0 525.0	507.4	16.5	2.5
S3-21	5 MPa Mortar	1.3	2.9	300.0 299.0 341.0 349.0 327.0	323.2	10.5	7.1
	20 MPa Mortar	25.0	8.6	538.0 543.0 585.0 528.0 553.0	549.4	17.9	4.0
S4-21	Type N2 Mortar	2.1	7.7	391.0 424.0 381.0 348.0 388.0	386.4	12.6	6.0
S5-21	Portland Cement-Lime Mortar	8.2	2.1	455.0 503.0 528.0 517.0 510.0	502.6	16.4	6.5
S6-21	Stack Bond Face-sh. Bedding	8.6	6.7	484.0 542.0 515.0 569.0 511.0	524.2	17.1	6.2
S7-21	Stack Bond Full Bedding	11.9	16.4	649.0 628.0 562.0 649.0 647.0	627.0	16.5	6.0

TABLE 4.3: continued

SERIES NO.	VARIED PARAMETER	MORTAR		PRISM COMPRESSION TEST			
		STRENGTH (MPa)	C.O.V. (%)	ULTIMATE LOAD (kN)	MEAN LOAD (kN)	MEAN STRENGTH (MPa)	C.O.V. (%)
S8-21	Splitter Units	8.6	7.8	592.0 617.0 594.0 540.0 552.0	579.0	18.9	5.5
S9-21	7 Days Prism Age			497.4 483.7 580.3 593.4 515.6	523.3	17.0	7.3
	36 Days Prism Age	11.3	7.6	480.5 442.3 555.7 485.6 533.7	499.6	16.3	9.0
S10-21	2-Course Prism	6.1	0.3	661.0 601.0 565.0 599.0 549.0	595.0	19.4	7.2

C.O.V.= coefficient of variation

4.4 DISCUSSION OF PARAMETERS AFFECTING PRISM STRENGTH CHARACTERISTICS

4.4.1 Standard Series (Series S0)

In general, the prisms failed in the manner described in Sections 3.3.2.1 and 3.4.4. Initially, fine cracks at the bottom of the webs of the 3rd block were observed at low load levels. With the increasing load, the cracks propagated along the full height of the webs. Audible cracking was heard just prior to cracking of the central portion of the prisms into 2 halves. This happened around 80%-85% of the ultimate load for Company 10 prisms and little above 90% of the ultimate load for Company 21 prisms.

The "efficiency ratio" (prism strength to unit strength) were 0.62 and 0.67 for Companies 10 an 21, respectively, and the stress-strain relationships indicated that the linear range only extended to about 40% of the ultimate strength. As shown in Figure 4.1, the non-dimensionalized stress-strain relationships were almost equal for the two companies.

4.4.2 Influence of The Block Strength Characteristics

4.4.2.1 Influence of Block Compressive strength (Series S1)

The results were listed in Table 4.4 along with those from Series S0, where units with 15 MPa specified compressive strength were employed. It is worthwhile mentioning that the

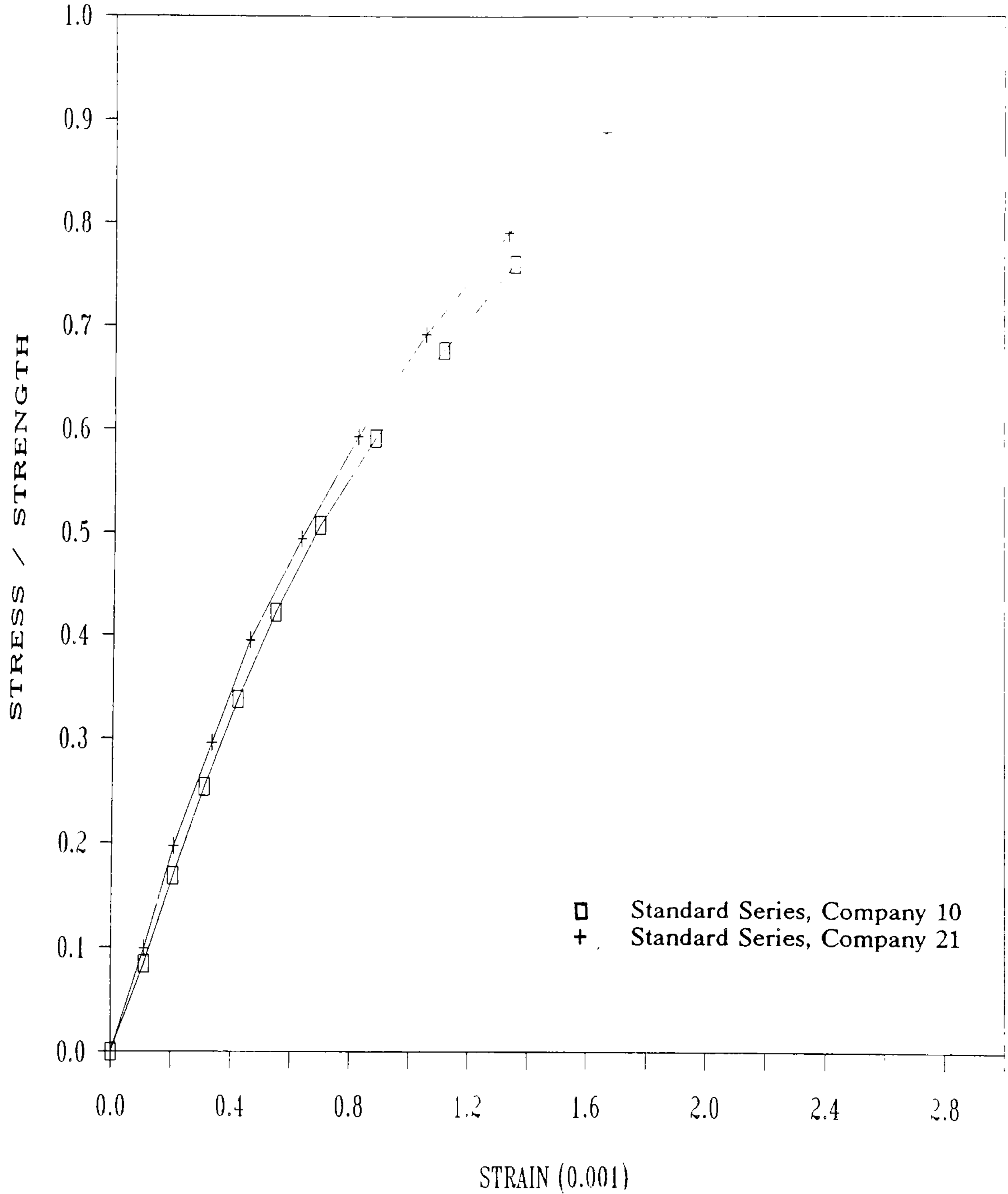

FIGURE 4.1 AXIAL COMPRESSIVE STRAINS OF STANDARD PRISMS FOR COMPANIES 10 AND 21 (SERIES S0)

TABLE 4.4: INFUENCE OF UNIT COMPRESSIVE STRENGTH (Company 10)

SERIES NO.	PARAMETER	UNIT STRENGTH		MORTAR COMP. STRENGTH (MPa)	PRISM COMPRESSION TEST			
		COMPR. (MPa)	TENSILE (MPa)		ULT. LOAD (kN)	MEAN LOAD (KN)	MEAN STRENGTH (MPa)	C.O.V. (%)
S0-10	15 MPa Specified Unit comp. Strength	31.0 [6.5]	2.6 [14.1]	7.1 [11.5]	597 568 585 624 591	593.0	19.3	3.4
S1-10	30 MPa Specified Unit comp. Strength	38.4 [4.0]	3.7 [11.0]	8.2 [14.6]	646 781 788 707 798	744.0	24.2	8.8

C.O.V.= coefficient of variation
[ ]= value inside brackets is the coefficient of variation (%)

block manufacturer was asked to supply blocks with these specified strengths (15 MPa and 30 MPa). However as will be shown in Chapter 6, the unit strengths determined from compression tests were often much higher than the specified strengths.

Employing units with higher compressive strength does not appear to affect the general mode of failure, except that near failure some crushing of the mortar was observed. As a result, shearing of the face shell near the crushed mortar occurred in some instances. However, the prism compressive strengths were remarkably improved by using units with higher compressive strength. The prism strength was increased by around 25% for an increase in block strength of 24%. Since it is the webs where cracking first occurred, it may be suggested that the increase in the prism strength can be in part attributed to the increase in the splitting tensile strength of the web. The stronger units had a tensile splitting strength over 40% higher than the standard units.

Of a particular importance, is the relatively lower stiffness exhibited by the prisms built with the stronger units (See Figure 4.2). The secant modulus of elasticity (determined at 0.3 of the ultimate strength) can be expressed as $E_m = 576\ f'_m$ in comparison to the 1000 f'_m value specified in CAN3-S304[26].

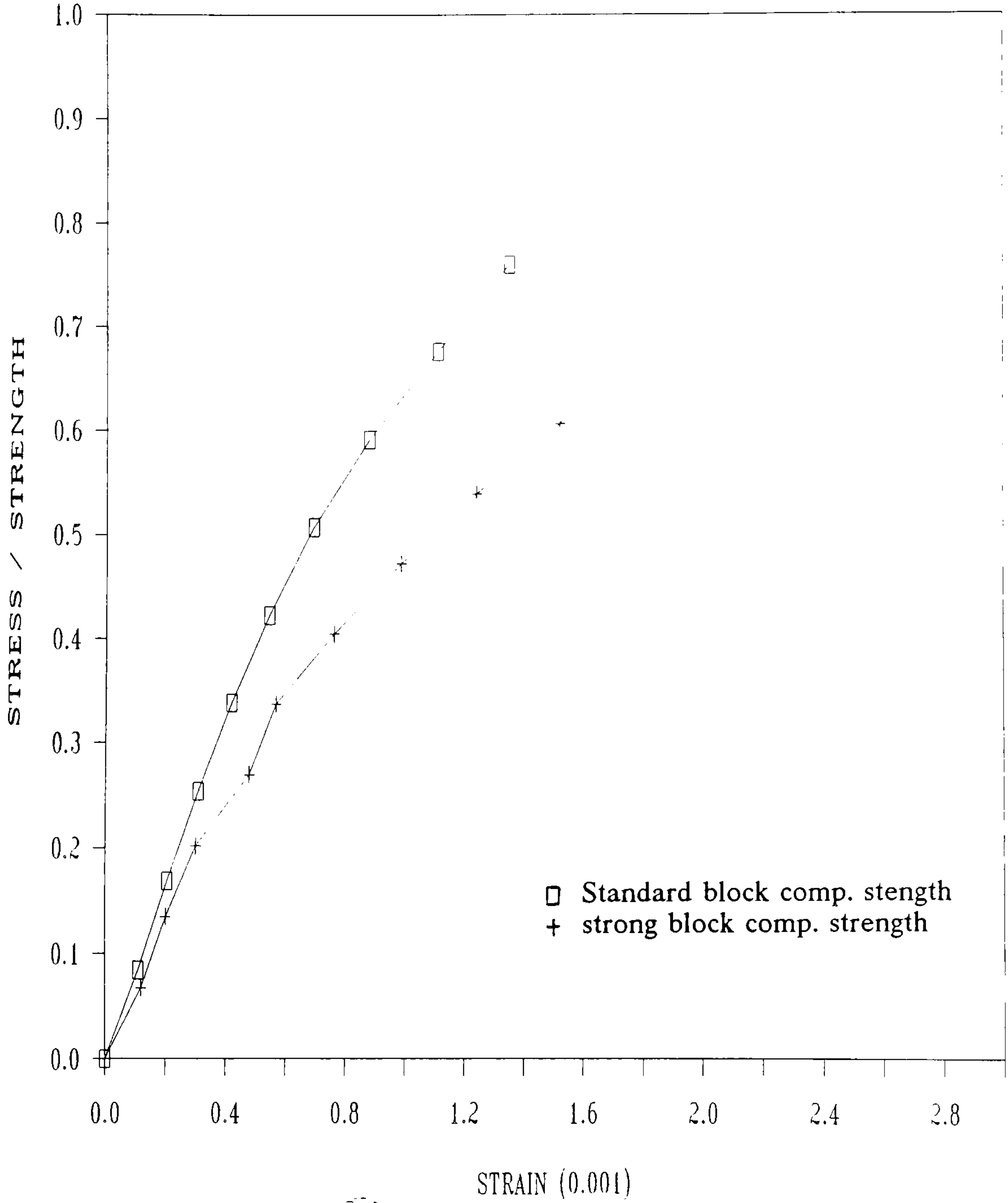

FIGURE 4.2 STRESS/ STRENGTH-STRAIN RELATIONSHIPS OF PRISMS WITH 15MPA AND 30MPA SPECIFIED UNIT COMPRESSIVE STRENGTHS (SERIES S0-10 AND S1-10)

The similar efficiency ratio of 0.63 for the higher strength blocks suggests a strong dependence of the prism compressive strength on the unit compressive strength and for the limited range of results, indicates that the mortar strength to unit strength ratio was not a major factor.

4.4.2.2 Influence of Block Tensile Strength (Series S2)

Table 4.5 contains the results from prism tests using concrete blocks with a specified 15 MPa compressive strength obtained at two different times (A and B) from manufacturing plants 13 and 26.

Company 13

The prism mean compressive strength for blocks delivered at time B was 67.6% higher than for blocks delivered at time A, even though the mortar strength was lower. This increase in prism strength corresponded to a 73.0% increase in the tensile splitting strength and a 17.4 increase in the compressive strength of the blocks. These results appear to indicate that the large improvement in the prism strength can be attributed to the substantial increase in the unit tensile splitting strength since the increase in the unit compressive strength was relatively small. Improvement in the unit tensile splitting strength would be expected to delay cracking in the webs.

TABLE 4.5: INFUENCE OF CHANGE IN UNIT TENSILE STRENGTH (SERIES S2)

COMPANY NO.	PARAMETER		UNIT STRENGTH COMP. (MPa)	UNIT STRENGTH TENSILE (MPa)	MORTAR COMP. STRENGTH (MPa)	PRISM COMPRESSION TEST ULT. LOAD (KN)	PRISM COMPRESSION TEST MEAN LOAD (KN)	PRISM COMPRESSION TEST MEAN STERNGTH (MPa)	PRISM COMPRESSION TEST C.O.V. (%)	EFFI-CIENCY RATIO	PRISM / UNIT TENSILE STRENGTH	SECANT MODULUS OF ELAS. E (1000 MPa)
13	Effect of Change in Unit Tensile strength	A	19.5 [3.0]	1.1 [23.9]	10.0 [5.5]	309.0 306.0 310.0 318.0 316.0	311.8	10.2	1.6	0.52	9.3	12.9
		B	22.9 [7.7]	1.9 [12.0]	8.7 [4.7]	522.0 545.0 542.0 501.0 512.0	524.4	17.1	3.6	0.74	9.0	15.7
26	Effect of Change in Unit Tensile strength	A	34.8 [3.9]	2.8 [5.4]	7.1 [7.2]	561.0 458.0 487.0 524.0 541.0	514.2	16.7	8.1	0.48	6.0	9.6
		B	31.6 [4.5]	3.3 [5.2]	10.1 [11.7]	662.0 694.0 690.0 651.0 674.0	674.2	22.0	2.7	0.70	6.7	17.2

C.O.V.= coefficient of variation

[ ]= value inside brackets is the coefficient of variation (%)

efficiency ratio= ratio of prism strength to unit compressive strength

The influence on the modulus of elasticity at 0.3 f'_m was shown in Figure 4.3 where E_m = 15700 MPa corresponded to the higher prism strength (B) compared to 12600 MPa for the lower prism strength (A).

As discussed in Chapter 2, the improvement in the tensile strength of the unit can be attributed to many factors, such as a higher degree of compaction[55] and better curing during the initial period of production. Other possible factors may include stronger aggregate materials and/or increase of the cement content. However, no confirmation was obtained for these possible factors.

Company 26

The prism mean compressive strength for blocks deliverd at time B was 31.7% higher than for blocks delivered at time A, even though the unit compressive strength decreased by about 10%. This increase in prism strength was accompanied by an 18% increase in the blocks' tensile splittting strength and 42% increase in the mortar strength. Eventhough the mortar strength was substantially higher, it is not expected to greatly affect the prism strength. Therefore it is suggested that the enhancement in the prism strength can be mainly attributed to the improvement of the blocks' tensile strength. The stress-strain curves in Figure 4.3 also indicate that the prisms stiffness was improved as a result

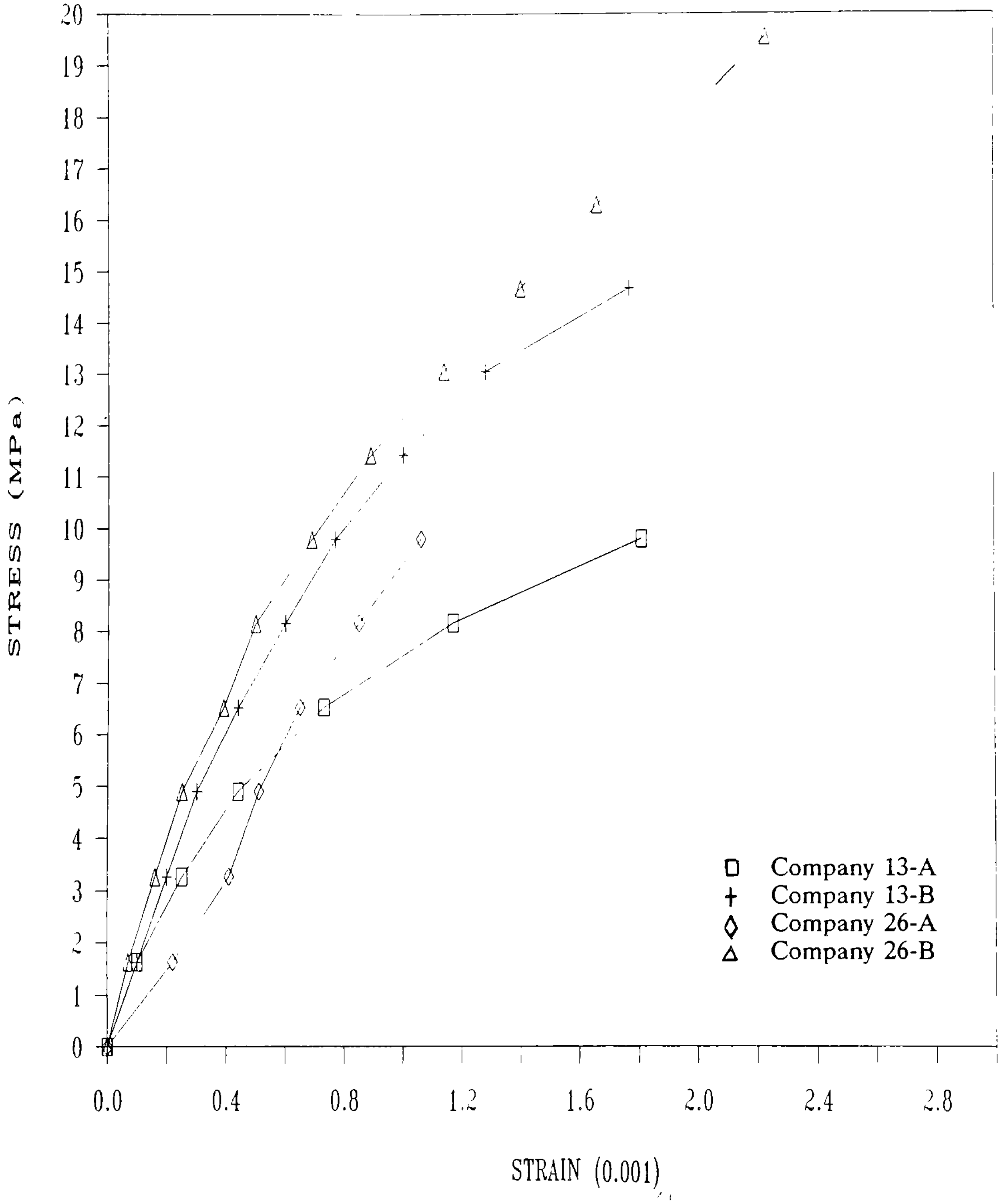

FIGURE 4.3 STRESS-STRAIN RELATIONSHIPS OF SERIES S2 PRISMS (COMPANIES 13 AND 26)

of enhancement to the unit tensile strength. The higher stiffness at higher stresses probably reflects the influence of delayed web cracking.

In Table 4.5, the ratios of prism strength to the unit compressive strength and to the unit tensile strength appear to suggest that a strong direct relation exists between prism strength and unit tensile strength. In addition, it can be seen that the "efficiency ratios" were also greatly improved as the direct result of an increase in the unit tensile strengths.

4.4.2.3. Overall Influence of the Block Strength Characteristics

To better understand the relation between the assemblage strength and the unit compressive and tensile strength, a regression analysis was done on Series S0, S1 and S2. The analysis showed that while the prism compressive strength related well to the unit compressive strength (correlation coefficient, r = 0.81), a stronger linear relationship existed with the unit tensile strength (r = 0.94). These relationships along with the least square fit lines were shown in Figure 4.4 (a) and (b). The overall results clearly indicate the importance of the unit tensile properties on the strength of face shell mortared blockwork. In addition, the apparent influence of the unit compressive

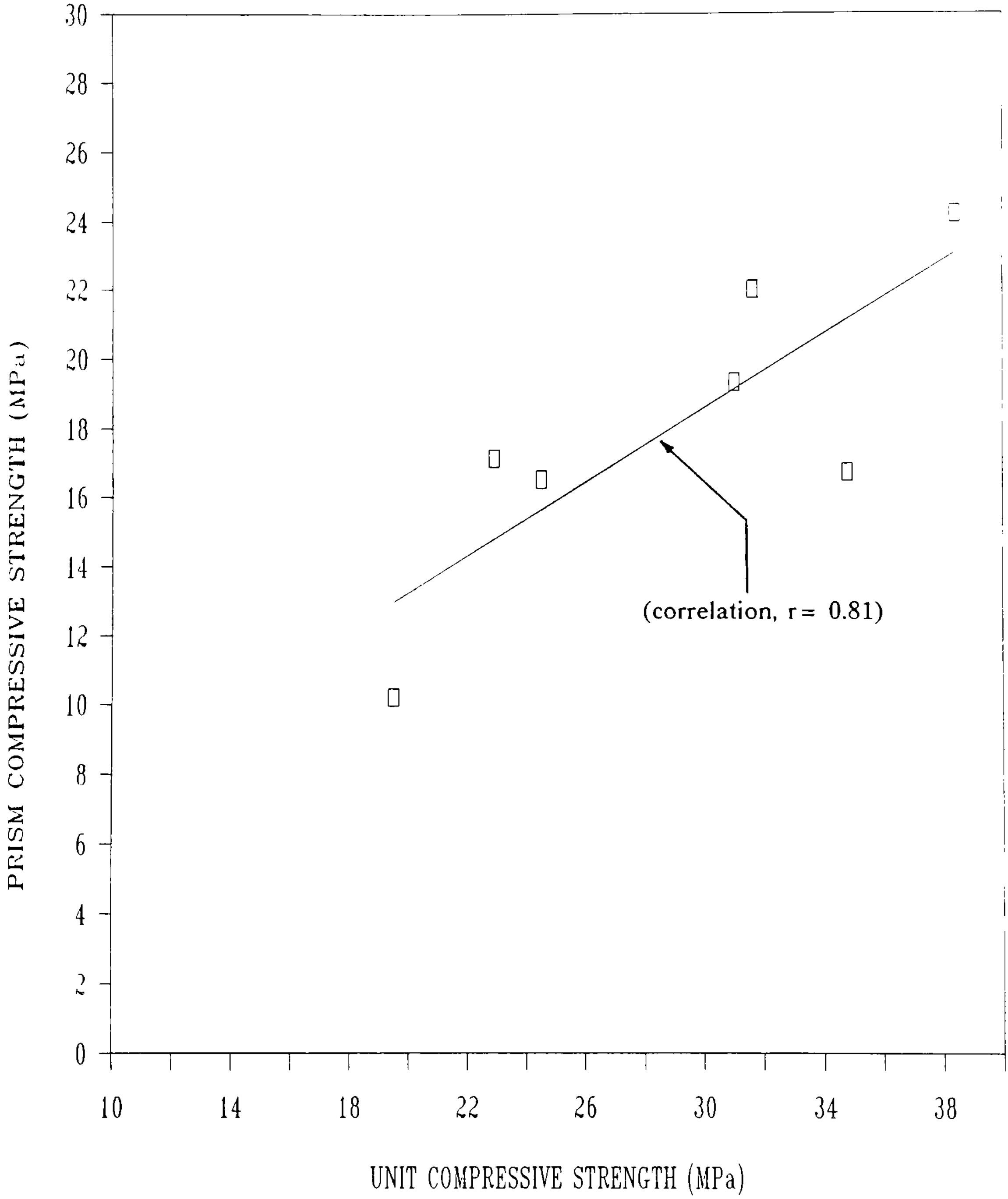

FIGURE 4.4 a) RELATIONSHIP BETWEEN PRISM COMPRESSIVE STRENGTH AND UNIT COMPRESSIVE STRENGTH

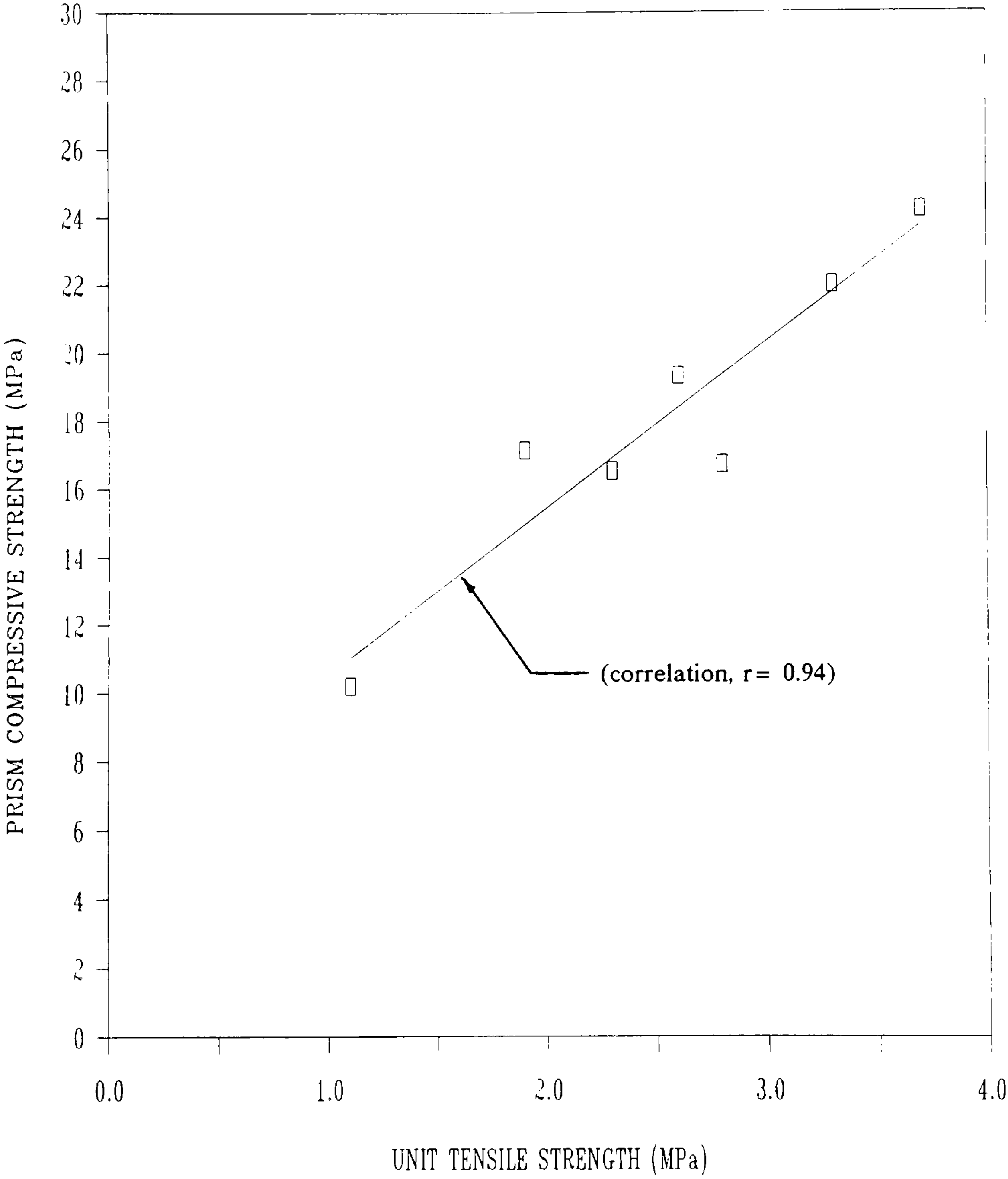

FIGURE 4.4 b) RELATIONSHIP BETWEEN PRISM COMPRESSIVE STRENGTH AND UNIT TENSILE STRENGTH

strength is suggested to be mainly attributed to its direct relationship with the unit tensile strength and not to its own effect, within reason of course. In fact, a correlation coefficient of 0.93 showed that a strong relationship existed between the units' cmpressive and tensile strengths.

It is of importance to indicate that, while the reference is always to the "unit" tensile strength, it is actually intended to imply the "web" tensile strength. This difference was discussed in Chapter 2.

For a given normal strength mortar, it appears that the relative modulus of elasticity would decrease for an increase in the block compressive strength while an enhancement in the relative value would be expected with an increase in the unit tensile strength. By improving the unit tensile strength, the cracking of the webs which initiated at around 40% of the ultiamte load was delayed resulting in a higher modulus of elsticity.

4.4.3 Influence of Mortar Strength (Series S3)

While for normal strength mortar (specified 12 MPa) and high strength mortar (specified 20 MPa) the strength of face shell mortared blockwork appeared to be only moderately affected by the mortar strength, the use of extremely weak mortar had a much more significant effect on prism strength. Using mortar with a specified 5 MPa strength (actual 1.3 MPa for air cured cubes) resulted in reduction in prism strength by 40% and 46% in comparison with normal and strong mortars for Company 10 and 36% and 41% reduction for Company 21. The relationships betwen the actual air cured mortar strengths and the prism strengths for the 2 companies were plotted in Figure 4.5.

Prisms built with normal and strong mortar failed in the manner described ealier. However, for prisms built with weak mortar the failure was completely different. Large deformations occured in the mortar joint at very low stress levels. In fact, as can be seen in Figures 4.6 and 4.7, the stress-strain relationships do not show any linear range. Mortar started to crush before cracking developed in the webs. Almost no web cracking was observed. As a result of the mortar crushing, an uneven surface existed in the bed joints. This uneven surface along with the openning in the vertical mortar joints introduced a situation by which the units within the prism were subjected to bending stresses. Large cracks were observed through the face shells as shown in the photograph of the prism failure in Figure 4.8.

The stress-strain relationship for the prisms built with weak mortar was quite non-linear. Obtaining the modulus of elasticity from the initial tangent would result in a serious misrepresentation. The secant moduli at 0.3 of the ultimate strength for Companies 10 and 21, respectively, were

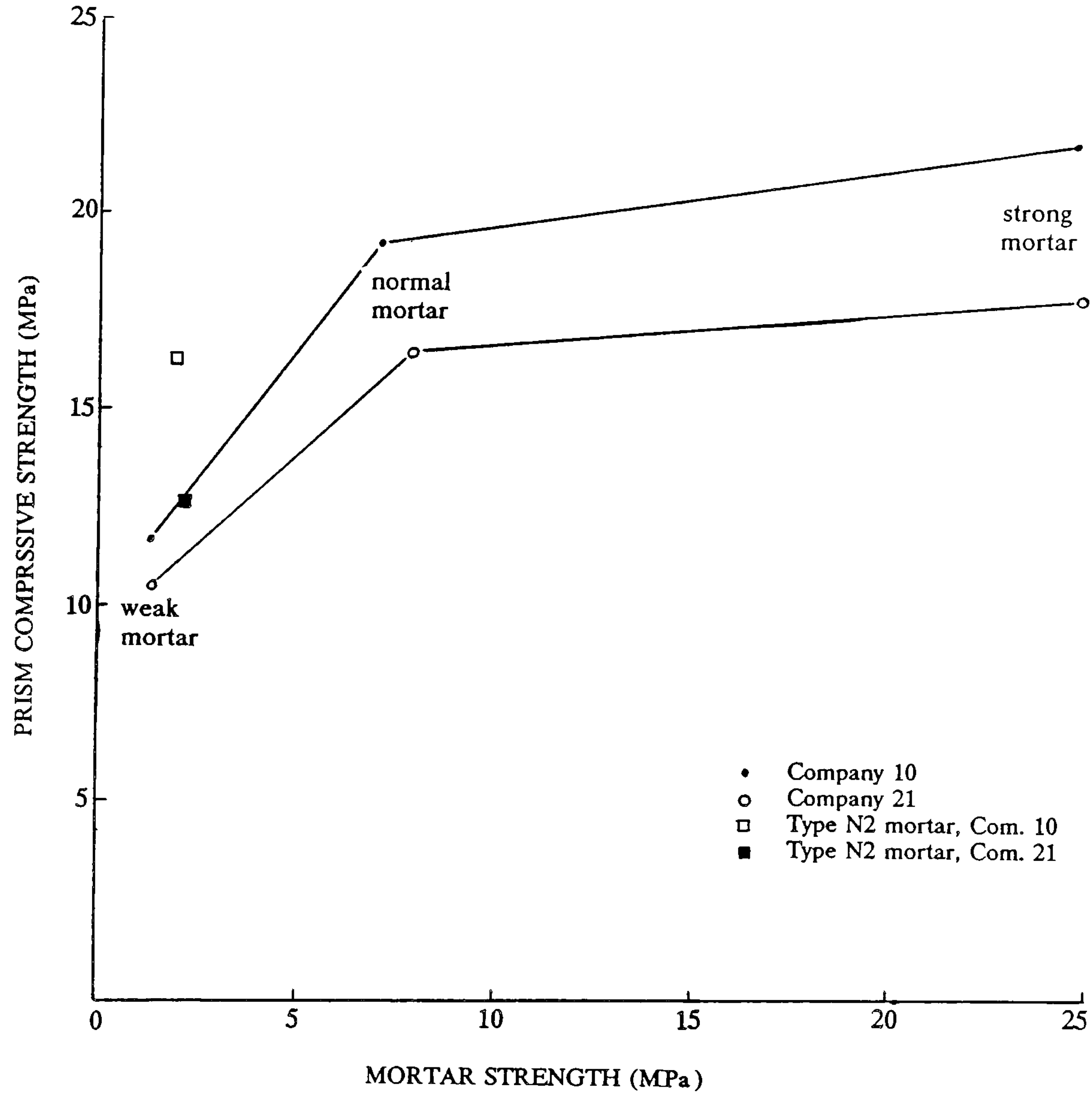

FIGURE 4.5 INFLUENCE OF MORTAR STRENGTH ON PRISM COMPRESSIVE STRENGTH

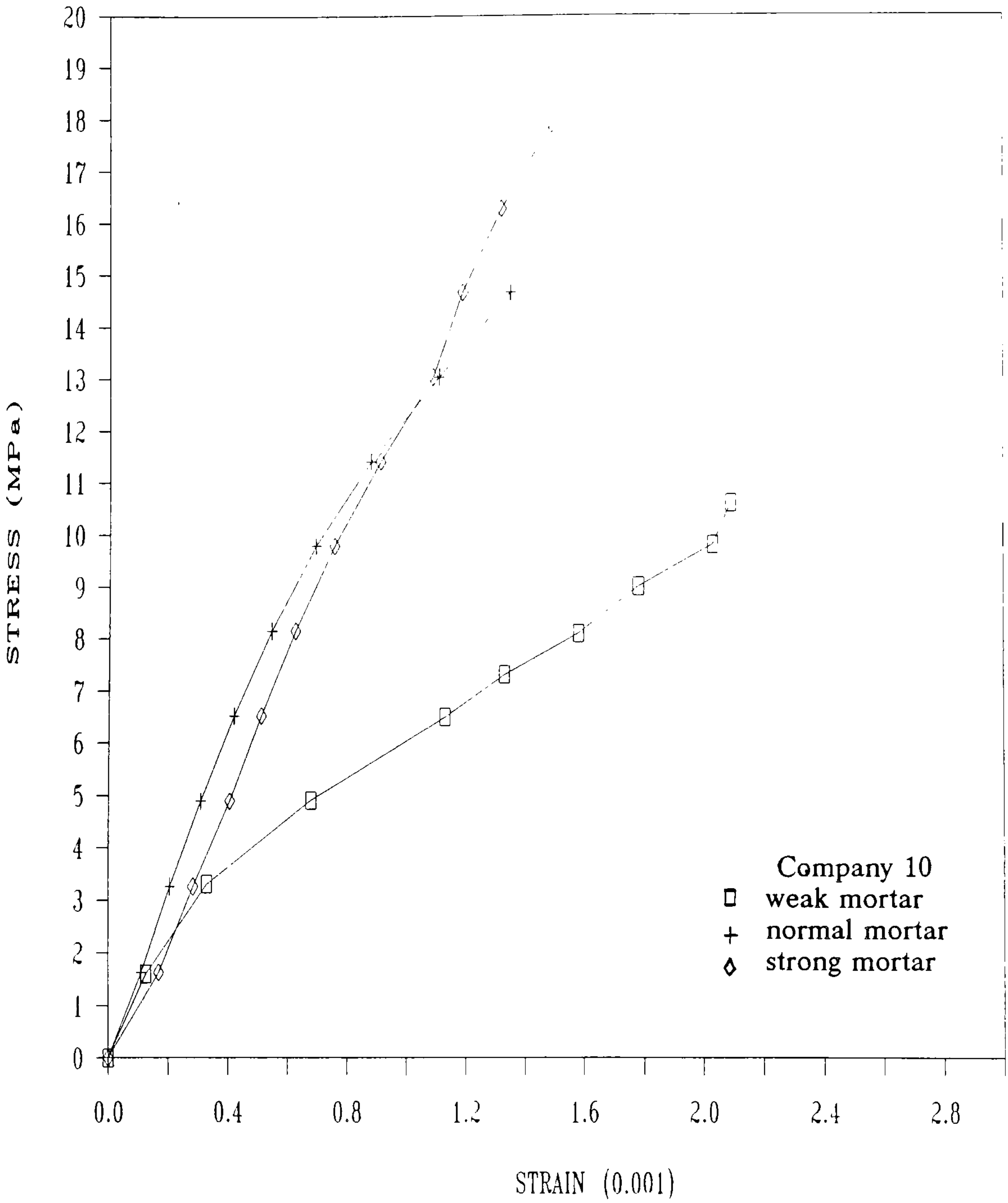

FIGURE 4.6 STRESS-STRAIN RELATIONSHIPS OF PRISMS WITH DIFFERENT SPECIFIED MORTAR STRENGTHS (SERIES S0-10 AND S3-10)

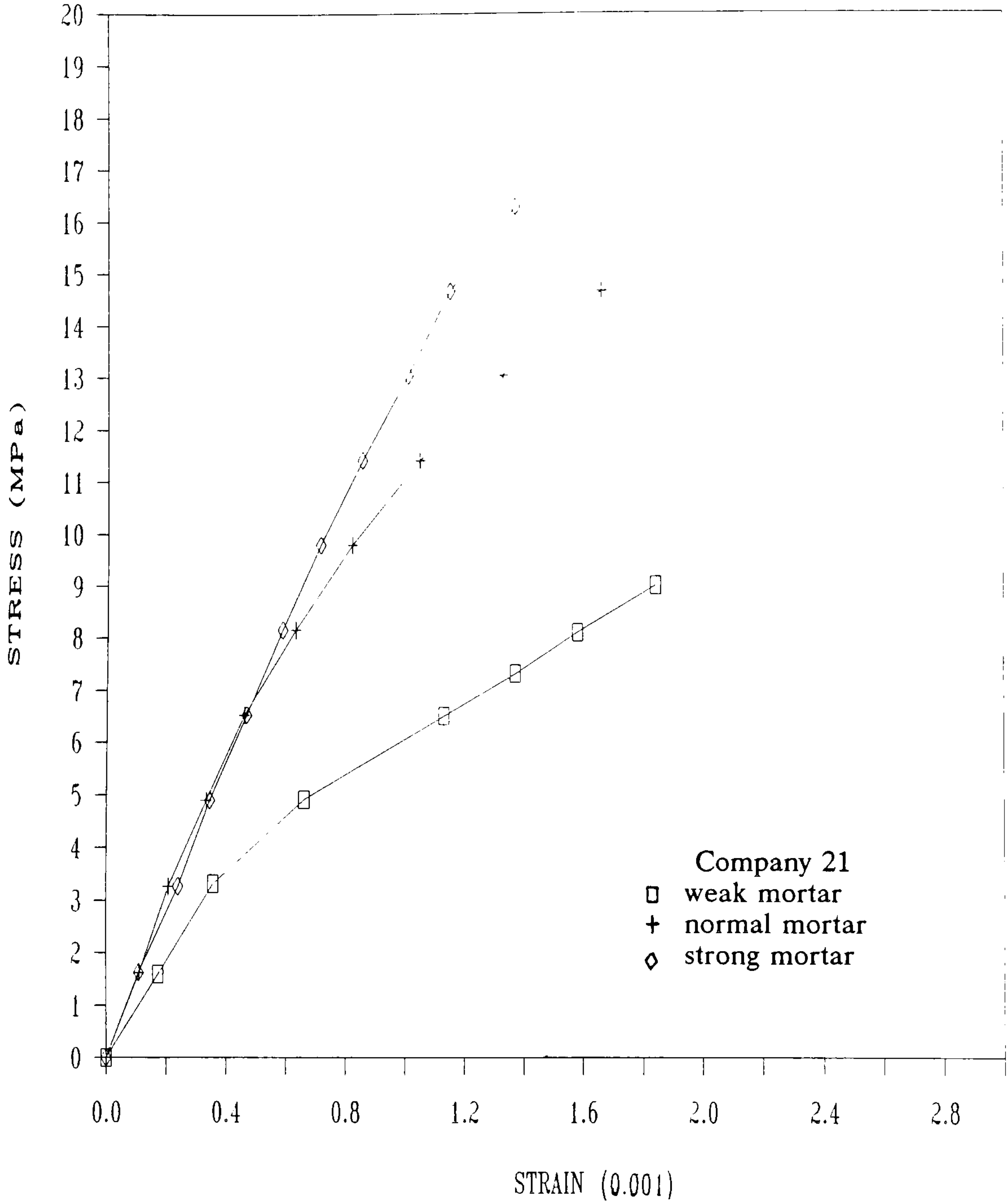

FIGURE 4.7 STRESS-STRAIN RELATIONSHIPS OF PRISMS WITH DIFFERENT SPECIFIED MORTAR STRENGTHS (SERIES S0-21 AND S3-21)

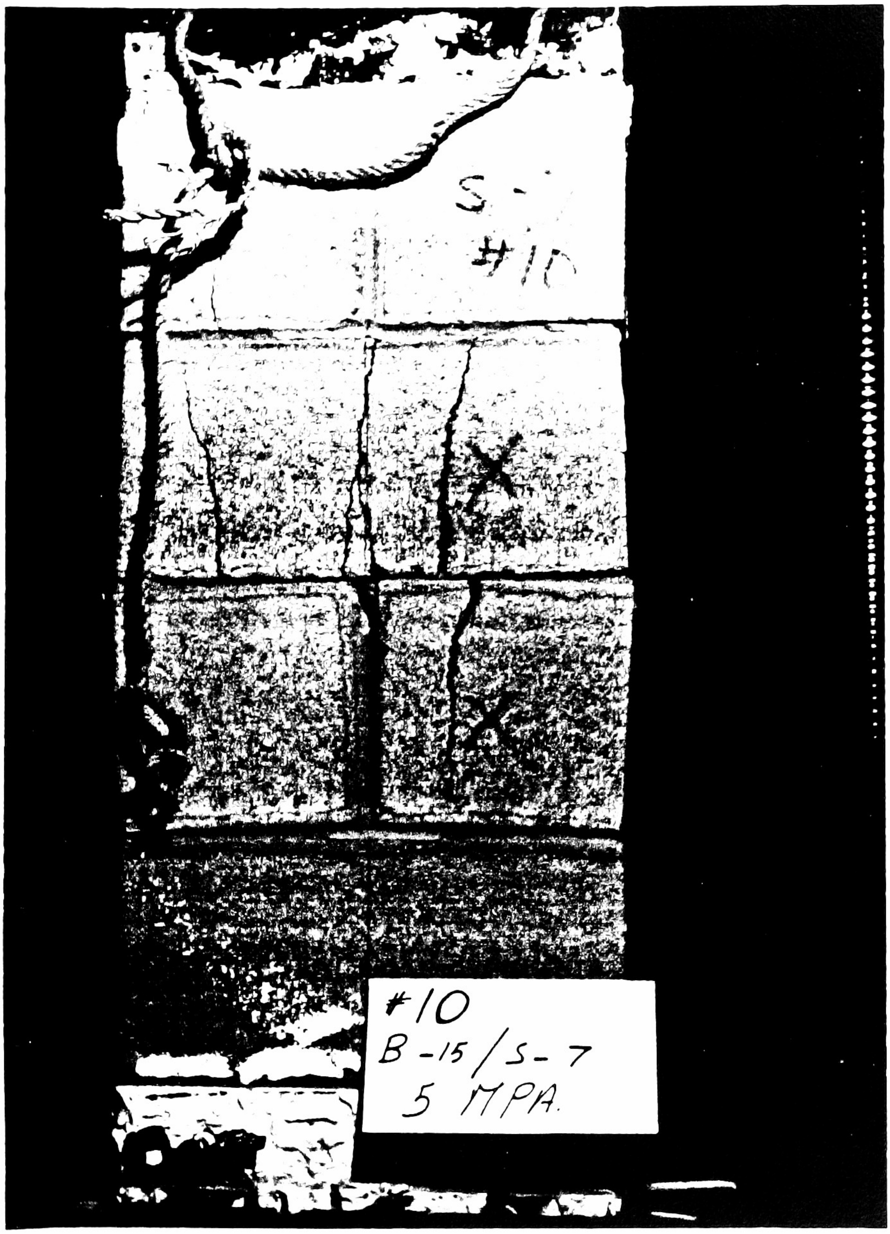

FIGURE 4.8 TYPICAL FAILURE OF PRISMS BUILT WITH LOW STRENGTH MORTAR (SERIES S3-10)

4800 MPa and 9200 MPa which is comparably low.

Based on a statistical assessment, at the 95% confidence level, the strength of prisms built with normal mortar was significantly lower than for prisms built with strong mortar. A difference of 13% and 8.5%, respectively for Companies 10 and 21, was obtained. It is of importance to indicate that such a difference in prism strength was caused by over 300% increase in the mortar strength. The prism strengths were not completely insensitive to increases in the mortar strength beyond the normal strength. While such increases would not be expected to affect the initial assemblage failures (by web cracking) it certianly influenced the secondry failure which occured after the prism has split in two halves. As can be seen in Figure 4.6 and 4.7, the use of strong mortar increased the linear range in the stress-strain relationships.

When the results from both companies were compared, prisms built with weak mortar had statistically equal strengths at the 95% confidence level. Given the fact that the blocks from both companies had somewhat different strength characteristics, it may be suggested that the weak mortar was the controlling factor in the failure of these prisms. This argument was substantiated when the prism strengths from both companies were tested for equivalence for the normal and strong mortars. It was found that the prisms from Company

10 had significantly higher strengths than those from Company 21.

Eventhough face shell mortared blockwork normally fails by a mechanism unrelated directly to mortar, it cannot be said that the blockwork strength is independent of mortar strength[104]. Extremely weak mortar was found to be the major cause of failure and the assemblage strength was reduced by around 50%. It was also found to be generally true that lower mortar to block strength ratios result in lower prism strengths[43]. However for the same strong mortar, the influence of the mortar to block strength ratio appeared to be more significant when high strength blocks were used as opposed to blocks with normal strength.

4.4.4 Influence of Mortar Type (Series S4)

The actual proprotion for mortar Type N2 as well as the individual results can be found in Chapter 2. The results from this series can be used to examine the influence of the type of mortar on the prism strength by comparison with the results from Series S0 where Type S2 mortar was used. It is also interesting to compare the results with the low strength mortar from Series S3.

In comparison to use of Type S2 normal strength mortar, use of Type N2 mortar resulted in reductions in prism strength of about 16% and 24%, respectively, for Companies 10 and 21. Such large decreases contradict the suggestion that the type of mortar has little influence on the strength of face shell mortared blockwork[104]. In addition, the prisms mainly failed by crushing of mortar, opening the vertical joints and the development of cracks in the blocks' face shells. In only one instance was web cracking observed in the one prism where a second batch of slightly higher strength mortar was used (See Table 4.2). The stress-strain relationships for prisms built with Type N2 and S2 mortars were plotted in Figure 4.9. The non-linear behaviour at the initial part of the curve is quite evident for Type N2 mortar. The curves also show that large deformations occurred in the mortar joints and the prism appeared to experience a fairly constant stiffness beyond the initial stage. The secant moduli of elasticity at 0.3 of the ultimate stress were 7300 MPa and 5300 MPa for Companies 10 and 21, respectively, yeilding values of 450 ad 418 for the stiffness coefficients, K, ($K = E_m / f'_m$, modulus to prism strength ratio) in comparison with K values of 811 and 893 for prisms with normal Type S2 mortar. Much higher strains were recorded at stresses near failure. For example, for Company 21 the axial strains at 90% of the ultimate stress were 3700 micro-strain in comparison with 1700 micro-strain for prisms with Type S2 mortar.

In comparison with the use of low strength mortar (Series S3) where the decreases in the prism strength were

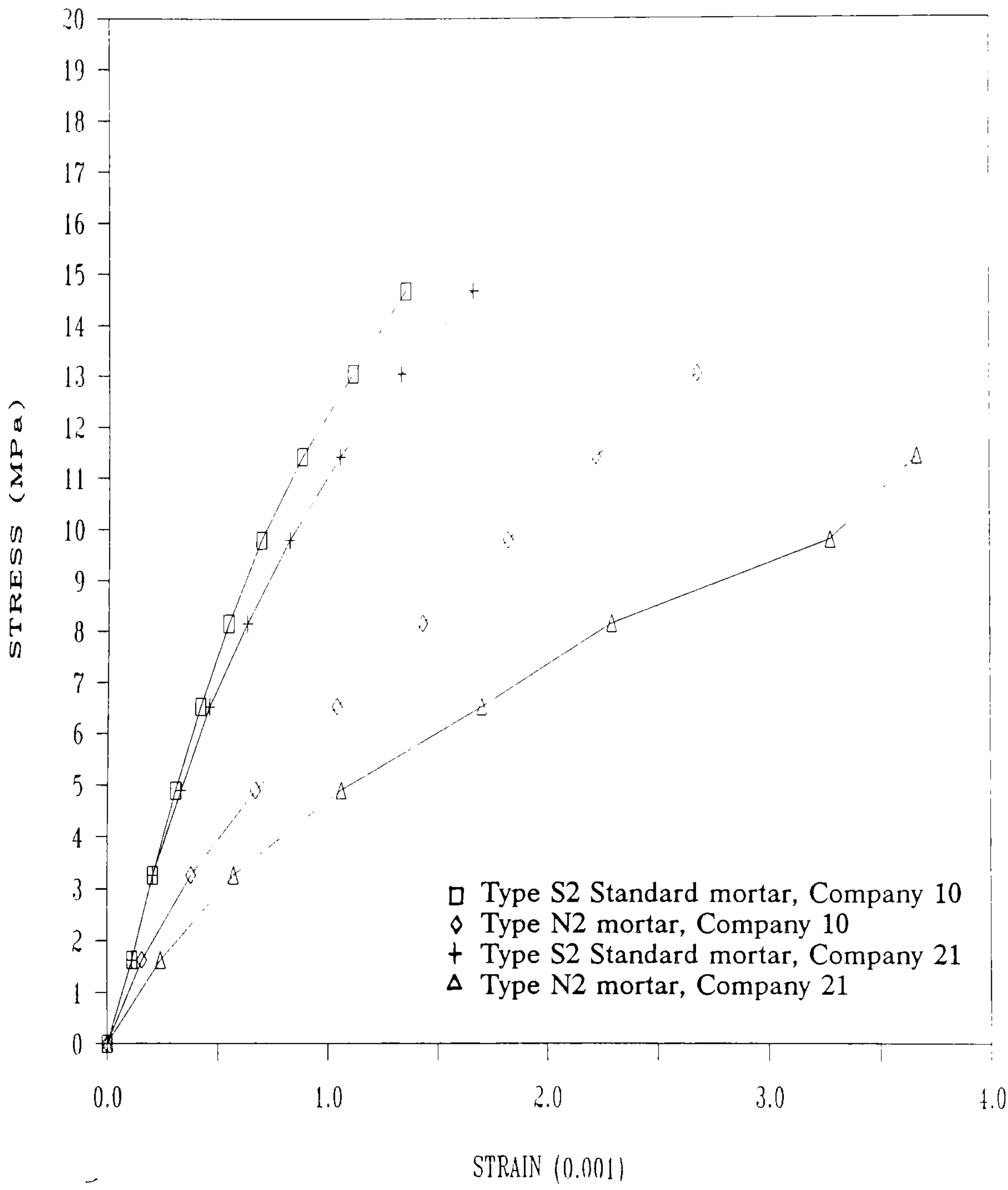

FIGURE 4.9 STRESS-STRAIN RELATIONSHIPS OF PRISMS BUILT WITH TYPE S2 AND N2 MORTARS (SERIES S0 AND S4)

about 40%, reductions in prism strength due to the use of Type N2 mortar were relatively small. These results clearly indicate the importance of the mortar on the development of the masonry strength where very weak mortar is used. The increases in the prism strengths were from 11.7 MPa to 16.3 MPa for Company 10 and from 10.5 MPa to 12.6 MPa for Company 21 for going from weak/poor Type S2 mortar to standard N2 mortar. These increases reflect the significance of altering the proportion/composition of weak mortar on the prism strength. For Type N2 mortar, the joints accommodated large deformations but spalling of the mortar occurred at higher stresses than for the low strength mortar (Series S3), therefore allowing for more of the blocks' potential to be developed.

4.4.5 Influence of Mortar Composition (Series S5)

In building the prisms for this Series, the mortar batch for Company 10 was sufficient to build only 4 prisms. Therefore a second mortar batch was made for the fifth prism. The mortar cubes from the first batch had a strength of 10.2 MPa while for the second batch the mortar strength was 8.5 MPa.

For Company 10, prisms built using Portland Cement-Lime (PC-L) mortar had a mean strength 8% higher than those built with Portland Cement-Masonry Cement (PC-MC) mortar. This difference is statistically significant at the 95% confidence level but is not significant at the 98% confidence level. However, before arriving at any conclusions, it is important to examine the mortar strengths. This difference in prism strength corresponded to a 42% increase in mortar strength (comprising mortar strength from the 1st batch of PC-L and the PC-MC batch in Series S0). Such a large difference in mortar strength would be expected to cause some difference in prism strength. For Company 21, identical prism strengths were obtained for the two mortar compositions which also had very similar strengths. Therefore it was concluded that these test results did not indicate any influence of Lime versus Masonry Cement mortar content on prism strength.

There was no apparent influence of the mortar composition on the failure of the prisms. The stress-strain curves were similar to the relationships obtained from prisms with PC-MC mortar. The linear range in the curves were more marked for prisms with PC-L mortar and slightly lower axial strains were recorded at higher stresses. The secant moduli at 0.3 f'_m were almost equal to those from prisms with PC-MC mortar.

4.4.6 Influence of Bond Pattern (Series S6)

The failure mechanism for face shell mortared stack bond prisms was similar to prisms built in running bond. At failure, minor cracks were also observed in the webs of the end units. Audible cracks were heard at loads over 90% of the ultimate load in compression with around 85% for prisms in running bond (Series S0).

For Company 10, the compressive strength of stack bond prisms was 20.2% higher than the strength for running bond prisms. In order to explain such a difference in strength, it is important to note that the strength of the mortar used in stack bond prisms was 40% higher than for the mortar used for running bond prisms. Eventhough the initial web cracking failure in prisms with both types of bond pattern was basically independent of mortar strength, such large difference in mortar strength would be expected to have some effect on the prism strength. This difference in mortar strength may not explain the whole 20.2% increase in strength of stack bond prisms. However, it is likely to affect the secondary failure which occurs after the prism has cracked in two halves.

For Company 21, stack bond prisms with face shell mortaring had only a 3.6% increase in strength compared to the running bond prisms. This increase was statistically insignificant. Further examination of the data indicated that the strength of the mortar for the stack bond prisms was only

8.8% higher than for the running bond prisms. While the results for these two companies seem to indicate that there is some benefit to excluding the head joint, a conclusive result was not obtained. Other factors not investigated such as differences in tensile stresses in the 2 webs of the half units at the centre of the prisms may have obscured the results of this comparison. However, as shown in Figure 3.10 in Chapter 3 the lateral tensile strains across the block and head joint combination were around 26% higher than strains within blocks. This seems to indicate, as it has been suggested[109], that peak values of horizontal tensile stresses are associated with vertical joints. Nevertheless it should be emphasized that this is limited only to the prism face shells since in Chapter 3 the maximum lateral strains were found to develop in the webs for face shell mortared prisms. As a result it may be suggested that running bond prisms should result in slightly lower strength than stack pattern prisms.

In Figure 4.10, the stress/strength-strain relationships were plotted for prims with both types of bond from both companies. Very similar relationships existed for prisms with the two different bonds with stacked prisms exhibiting slightly higher strains for the same stress/strength ratio.

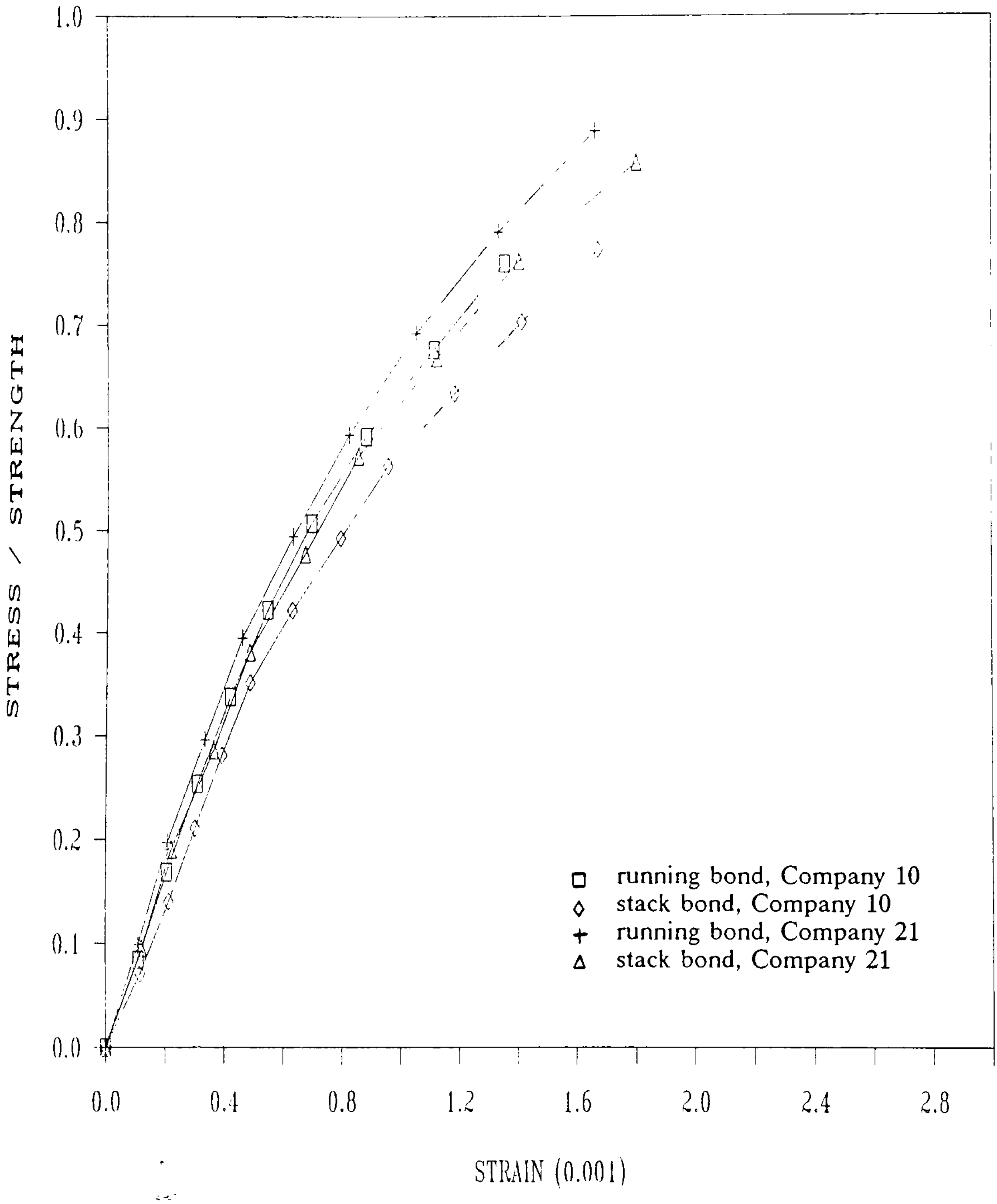

FIGURE 4.10 STRESS/ STRENGTH-STRAIN RELATIONSHIPS OF RUNNING AND STACKED BOND PRISMS (SERIES S0 AND S6)

4.4.7 Influence of Full Mortar Bedding (Series S7)

4.4.7.1 General

Prisms built in a stack pattern with fully mortared bed joints failed in a manner completely different from prisms with face shell mortaring. No web cracking was observed for either company. The failure can be described by the inability of the prisms to carry further load after crushing of the mortar has occurred. In some instances cracking and shearing of the face shells was observed. The failure mechanism for prisms with fully mortared bed joints was discussed in Chapter 3.

4.4.7.2 Full Bed Versus Face Shell Mortared Joints (Series S7 versus S6)

Full mortaring of bed joints increased the prism capacity by 11% and 19%, respectively, for Companies 10 and 21 compared to face shell mortared prisms. Fully mortared joints corresponded to an increase of 24% in the mortared area. For Company 21, the relatively higher increase in capacity in comparison to Company 10 may inpart be attributed to the comparably higher mortar strength for prisms built with full mortar joints (40% higher than mortar for face shell mortared prisms). The axial load capacity of hollow block prisms does not appear to be directly related to net mortared area, implying that an increase in the mortared area would not result in a equivalent increase to the axial load capacity.

This difference could be attributed to the two different mechanisms which cause the failure in the two differently mortared prisms. Joining the webs with mortar creates continuity in the vertical direction of the prisms. As a result , the axial stress distribution in fully mortared prisms can be expected to be more uniform across the cross-section and in both vertical orthogonal planes of the prism[45]. Hence the mechanism which initiated and caused the failure in face shell mortared prisms will have changed.

As indicated in Section 4.1.3, test data were often reported in terms of strength. If such an approach was used in this comparison, it would appear that full mortaring had decreased the prism strength by 10% and 3.5% for Companies 10 and 21, respectively [Again it is worthwhile noting that for Company 21 the mortar strength was relatively higher for fully mortared prisms than face shell mortared prisms.] Hence based on this limited range of result it does appear that use of fully mortared joints would result in slightly lower prism strength than for face shell mortared prisms[77].

The stress-strain relationships for fully mortared and face shell mortared stack pattern prisms were shown in Figure 4.11. The linear range of the curves extended up to about 60% of the ultimate stress for fully mortared prisms in comparison to 40% for face shell mortared prisms. This may be attributed to reducing the effect of the complicated geometry in face

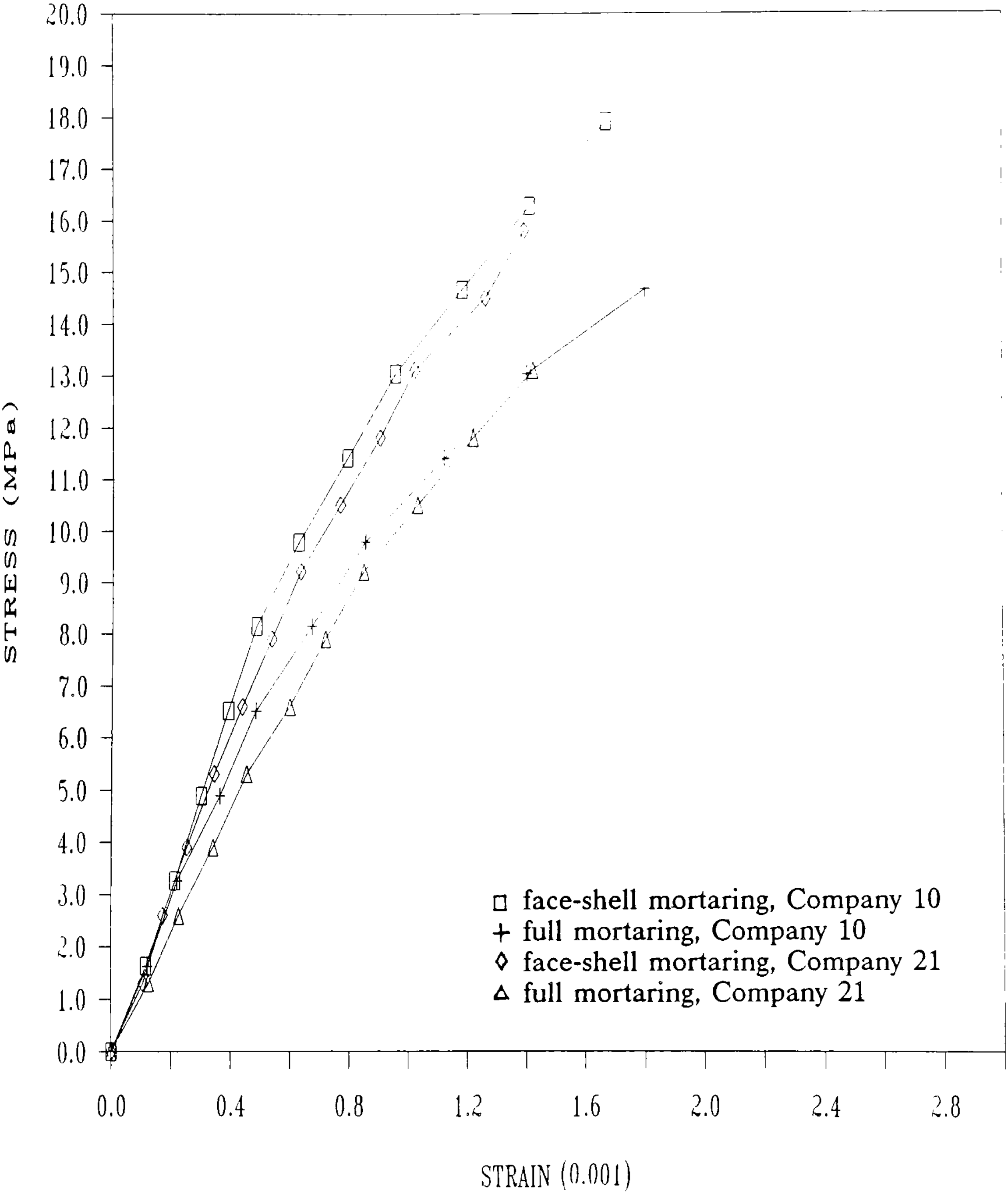

FIGURE 4.11 STRESS-STRAIN RELATIONSHIPS OF STACKED PRISMS WITH FACE-SHELL AND FULL MORTARING (SERIES S6 AND S7)

shell mortared prisms. The secant moduli of elasticity from fully mortared prisms were 10% and 13% lower, respectively, than face shell mortared prisms for Companies 10 and 21.

4.4.7.3 Stacked Prisms with Full Mortared Joints versus Running Bond Prisms (Series S7 versus S0)

Stack pattern prisms with full mortared joints yielded axial load capacities 33% and 24% higher than running bond prisms for Companies 10 and 21 respectively. This increase in load capacity corresponded to 24% increase in the loaded area. It is of interest to note that such increases in capacity can be attributed to a change in the bond pattern and an increase in the mortared area. Hence if the influence of the increase in the mortared area is eliminated (See Section 4.4.7.2) it can be seen that stacked prisms would generally yield higher capacities than running bond prisms. It is perhaps worth repeating that the different failure mechanisms occur. Hence, this factor should also be considered in comparing these results. In addition, a review of the results listed in Table 4.2 and 4.3 shows that the mortar strengths for fully mortared prims were higher than these for running bond prisms for both companies. However this latest factor is not expected to greatly affect this comparison.

If the prism strengths were compared, it can be seen that the prism strengths were relatively equal. Fully mortared prisms yielded a compressive strength 8% and 0% higher than running bond prisms for Companies 10 and 21, respectively.

The stress-strain relationships shown in Figure 4.12 indicate that fully mortared prisms result in a more linear relationship than running bond prisms. Again this may be attributed to the difference in flow of axial stresses which tended to be more uniform in fully mortared prisms. However, fully mortared prisms appear to have exhibited lower stiffness than running bond prisms. The moduli of elasticity for fully mortared prisms were 4% and 20% lower than running bond prisms for Company 10 and 21, respectively.

4.4.8 Influence of Block Geometry-Splitter Units (Series S8)

The introduction of an extra web into the courses of running bond prisms, by using splitter units, significantly improved the prism compressive strength. Prisms with splitter units had 13% and 14% higher strengths than prisms with stretcher units for Companies 10 and 21, respectively. Such improvements over the standard prism strength are simply attributed to the increase in the web area capable of resisting the lateral tensile stresses which develop along the web centreline in face shell mortared blockwork. The addition of an extra web in the unit resulted in a more significant increase in the prism strength then employing very strong

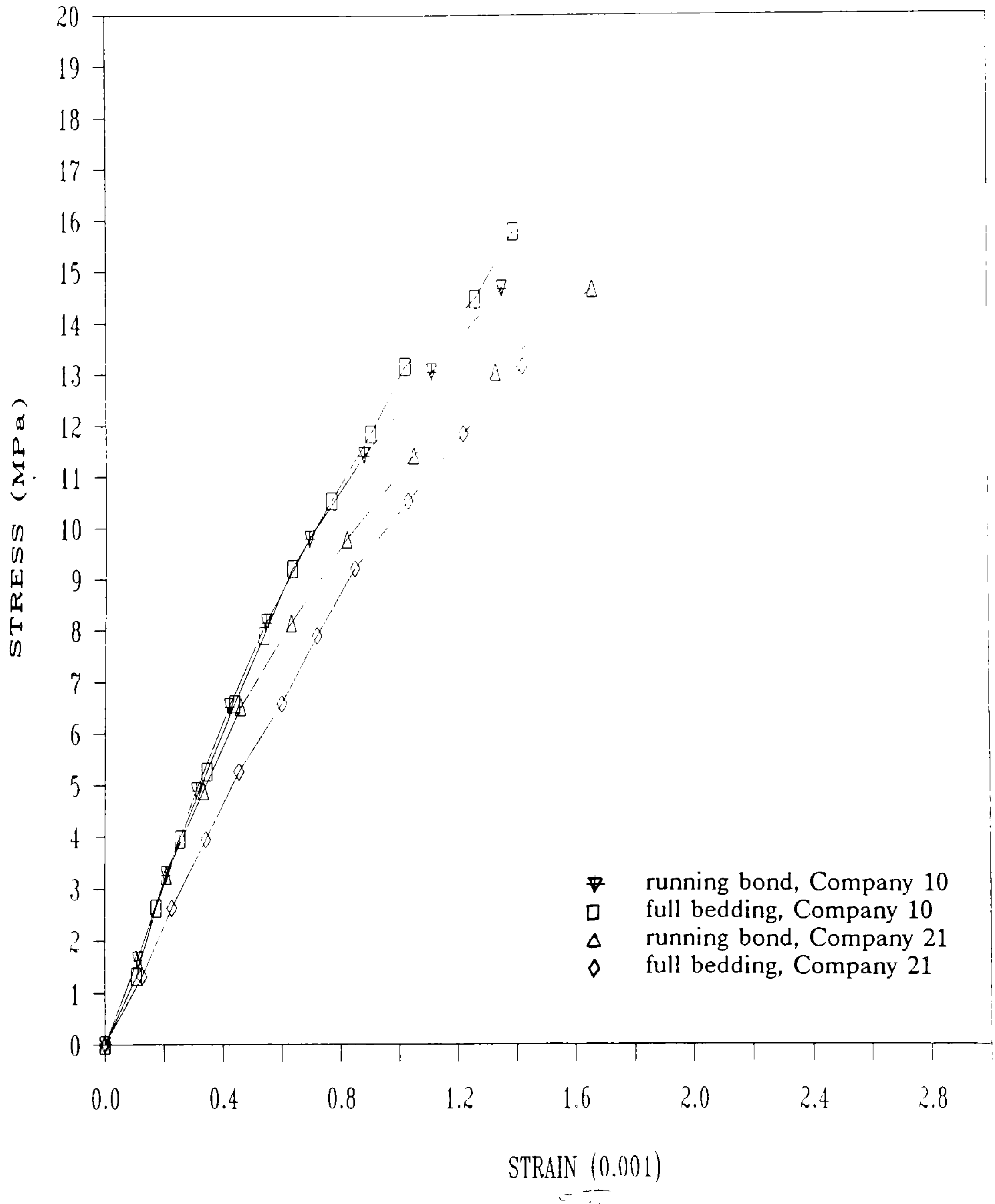

FIGURE 4.12 STRESS-STRAIN RELATIONSHIPS OF RUNNING AND FULL MORTAR STACKED PRISMS (SERIES S0 AND S7)

mortar. The failure pattern remained the same as for Series S0.

For both companies, the stress-strain relationships were generally similar to those from prisms with stretcher units with the exception that prisms with splitters exhibited slightly lower axial deformations at high stress levels. For Company 10, identical moduli were obtained for prisms with both types of units. Similar moduli would have been expected for Company 21, however a lower initial slope of the experimental curve for prisms with splitters may have been due to closing initial cracks in the mortar joints. This would have caused a secant modulus somewhat lower than for the stretcher unit prisms.

4.4.9 Influence of Prism Age (Series S9)

For Company 10, ("bubble" - low pressure cured blocks) prisms tested at 7 days of age had a compressive strength 5.6% and 13.8% higher, respectively, than those tested at ages of 36 days and 6 months. However, the coefficient of variation decreased from 8.3% to 3.4% by testing at 6 months of age instead of 7 days.

A statistical assessment was carried out at the 95% confidence level to interpret the results from this Series. The variances of the results examined first were equal for the prisms tested at the three different ages. However different variances between those tested at 7 days and 6 months can be found at the 90% confidence level. The analyses also showed that the mean strength of prisms tested at 6 months is statistically different than those tested at 7 and 36 days. Since no blocks were tested at 7 days, no explanation was offered for the unexpected decrease in prism strength with age. However worth noting that a compatible bonding between the mortar and the blocks in the prisms, changes in the mortar properties [Note that mortar for prisms tested at 6 months had a relatively low strength], variation in the blocks' material and/or possible drying shrinkage with time may in part explain the decrease in prism strength with time.

For Company 21 (Autoclave - high pressure cured blocks), the statistical assessment revealed that there was no difference among the strengths of prisms tested at ages of 7 days, 36 days and 6 months. Autoclave cured blocks were reported to develop their strength within the first couple of days with little or no change in strength with time[82].

Since it is expected that the prism strength would increase with age, no conclusion regarding the age influence can be made. It is suggested that this parameter be investigated in the future.

The stress-strain relationships for the prisms tested at 3 different ages were shown in Figure 4.13 for both companies. For Company 10, the curves show almost identical

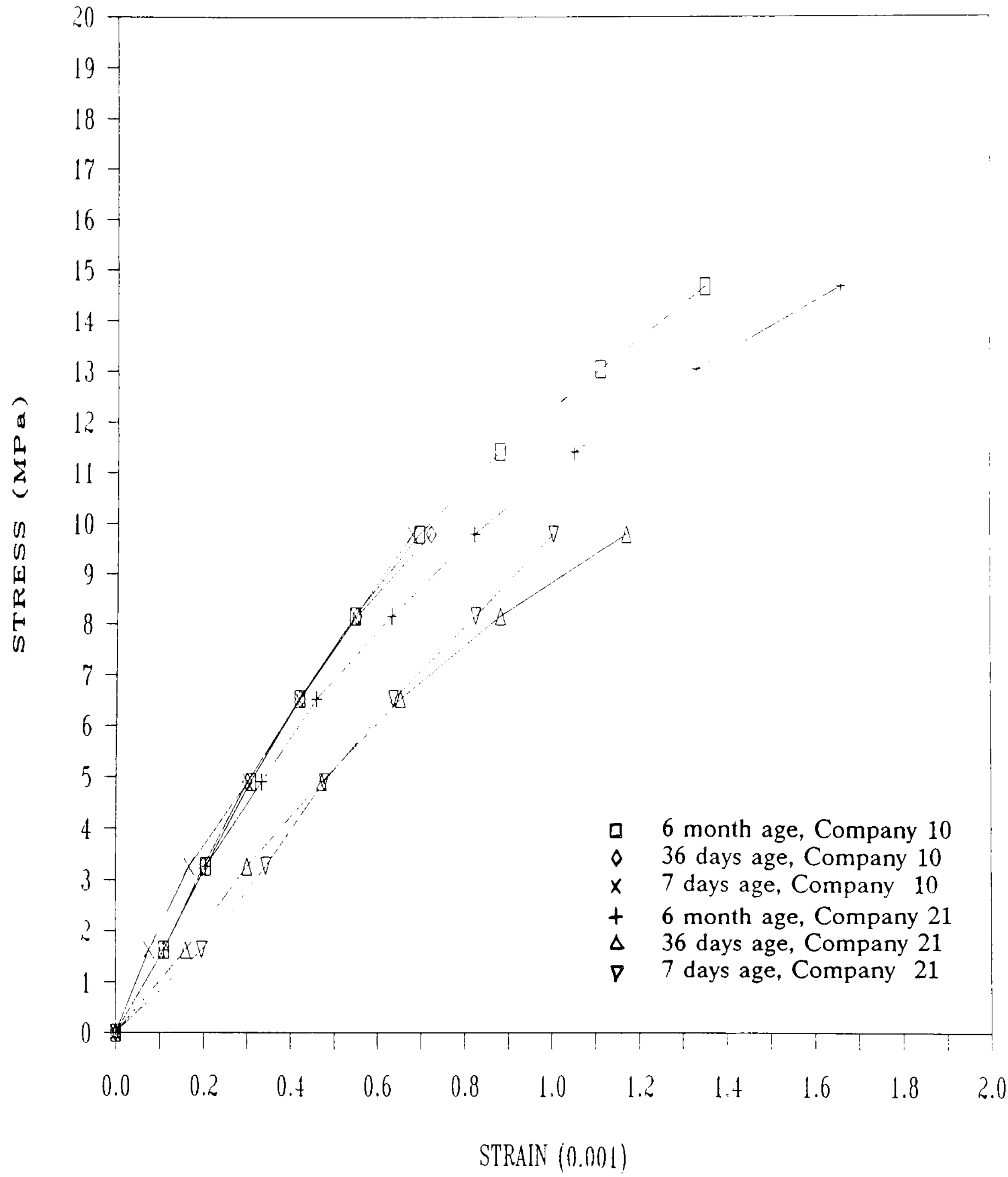

FIGURE 4.13 STRESS-STRAIN RELATIONSHIPS OF PRISMS TESTED AT 7 DAYS, 36 DAYS AND 6 MONTHS OF AGE (SERIES S9 AND S0)

behaviour and similar secant moduli were obtained from the three different ages of tests. For Company 21, the stress-strain relationships suggest a possible increase in prism stiffness with time. The secant modulus for prisms tested at 6 months was considerably higher than those from prisms tested 7 days and 36 days. Neville[82] reported that an increase in the modulus of elasticity of autoclave cured specimens would be expected with age although the compressive strength would not change.

4.4.10 Influence of Prism Size (Series S10)

The influence of prism height on the compressive strength was discussed in detail in Chapter 3. However, employing 2-course stack pattern prisms with full Hydrostone capping for measuring the compressive strength of blockwork, as commonly is the case, was not included in Chapter 3.

Two-course stack pattern prisms with face shell mortaring failed by shearing action in one or both face shells and were 22.6% and 17.6% stronger than Series S0 for Companies 10 and 21, respectively. The secant moduli of elasticity were lower than those reported for prisms in the standard series.

Again, the results from this series clearly show that employing 2-course prisms would result in a misrepresentation of the characteristics of face shell mortared blockwork.

4.5 MODULUS OF ELASTICITY

The high variation of strains at the very early stress levels would result in the modulus of elasticity, E_m, based on the initial tangent method being unreliable. Large initial strains could occur as a result of closing of initial cracks in the mortar joint. The modulus of elasticity at around 50% of the ultimate stress would not be a representative measure of the assemblage elasticity since the range of linearity does not extend to this stress level in face shell mortared masonry. Slightly lower moduli values were obtained even from determining E_m at 40% of the ultimate stress.

The secant moduli determined at 0.3 of the ultimate stress from all series for Companies 10 and 21 were listed in Table 4.6. In addition, the stiffness coefficient, K, (secant modulus to compressive strength ratio) were also tabulated. The results showed relatively low modulus of elasticity for prisms with low strength and Type N2 mortars. The results also indicated that the prism stiffness in fact decreased when high strength blocks (Series S1) or high strength mortar (Series S3) were used. The secant moduli listed in Table 4.5 for Companies 13 and 26 suggest a possible direct relationship between the assemblage stiffness and the unit tensile strength. The modulus of elasticity increased substantially by improvement to the unit tensile strength.

TABLE 4.6: SECANT MODULI OF ELASTICITY AT 0.3 ULTIMATE STRESS

SERIES NO.	VARIED PARAMETER	COMPAANY 10		COMPANY 21	
		MODULUS OF ELAS.- E (1000 MPa)	STIFF. COEFF. K	MODULUS OF ELAS.- E (1000 MPa)	STIFF. COEFF. K
S0	Standard	15.7	811	14.7	893
S1	30 MPa Unit Comp. Strength	13.9	576		
S3	5 MPa Mortar	4.8	407	9.2	630
	20 MPa Moratr	12.8	585	14.1	788
S4	Type N2 mortar	7.3	450	5.3	418
S5	Portland Cement-Lime Mortar	15.1	725	14.5	886
S6	Stack Bond Face Shell Bedding	16.6	717	13.5	787
S7	Stack Bond Full Bedding	15.1	728	11.7	708
S8	Splitter Units	15.6	712	13.4	708
S9	7 Days Test Age	15.6	708	10.3	606
	36 Days Test Age	15.6	749	10.4	640
S10	2-Course Stack, Face-Shell Bedd.	13.1	552	13.5	698

K= Stiffness Coefficient
= ratio of modulus of elasticity to prism compressive strength

Figure 4.14 is a plot of secant moduli versus prism compressive strengths for all the tests reported in this chapter. The evident scatter of the data indicate a high degree of uncertainty in the estimation of the elastic modulus using a single equation for all material and variable combinations. The range of the relationship between the modulus of elasticity and the prism strength vary between an upper bound of 1260 f'_m (Company 13-A) and a lower bound of 407 f'_m (Company 10 - weak mortar), with the upper bound value, 1260, being the only exception above 1000. A regression analysis was employed to examine the relationship between these two parameters. The least square fit curve, shown in Figure 4.14, resulted in a correlation coefficient, r, of 0.68. Exponential relationships did not provide any better correlations. The linear relationship can be expressed by

$$E_m = 700 \quad f'_m \tag{4.1}$$

Eventhough the correlation between the modulus of elasticity and the prism strength is not very strong, a relationship can be drawn. Nevertheless, this relationship clearly shows that the values of modulus of elasticity based on the code equation[26], $E_m = 1000\ f'_m$, are quite high, especially for weak mortar. These findings tend to contradict what has been reported that the modulus of elasticity based on the code equation was either in agreement[68] or an

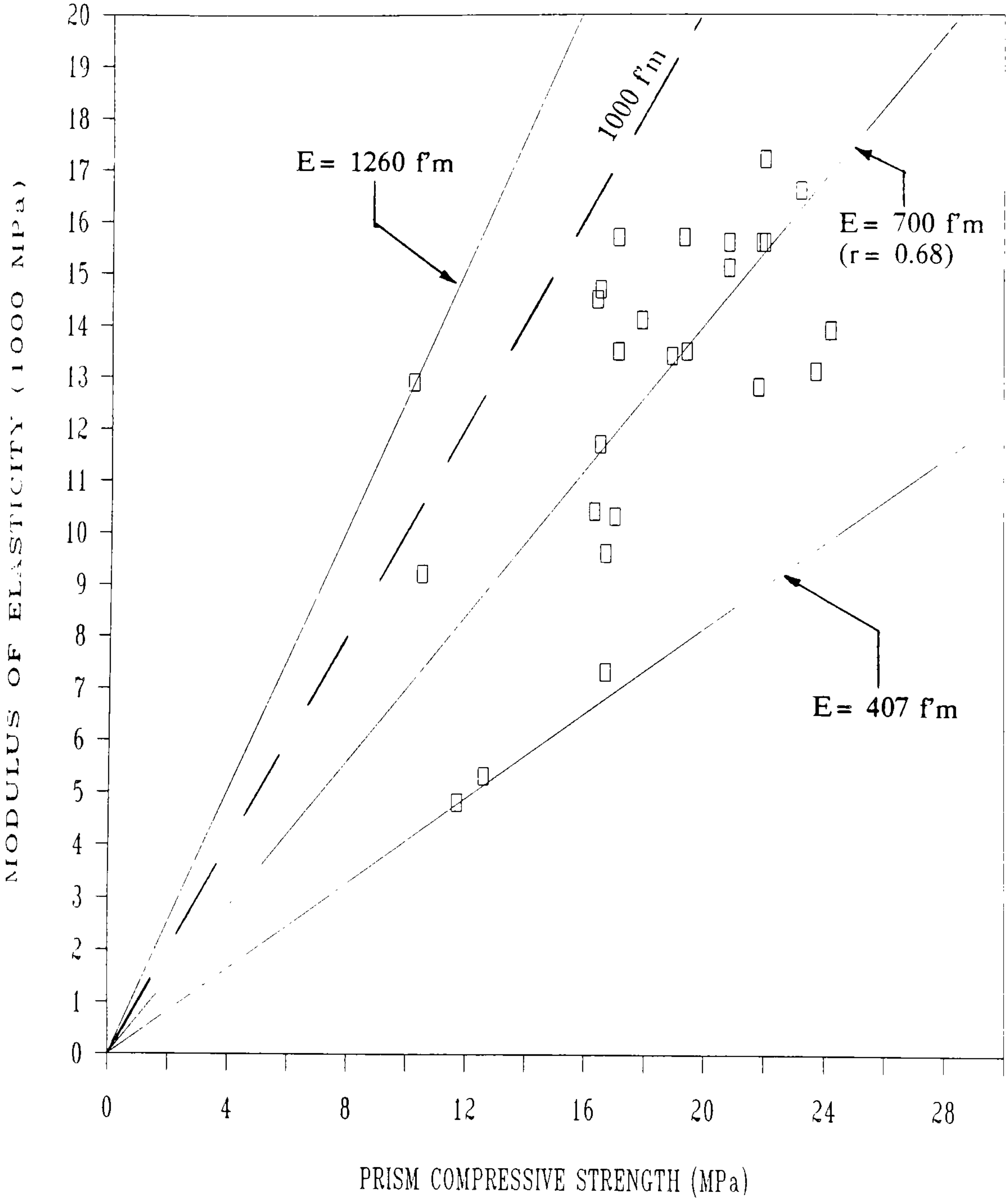

FIGURE 4.14 RELATIONSHIP BETWEEN MODULUS OF ELASTICITY AND PRISM COMPRESSIVE STRENGTH

underestimation[116]. However, recent research work[47] reported findings similar to those in this investigation.

4.6 SUMMARY

As a result of this research, the following summary outlines the importance of various parameters on the characteristics of face shell mortared concrete blockwork loaded under axial compression:

1. Increasing the unit compressive strength resulted in a significant increase in the prism strength for the same strength of mortar, while the assemblage efficiency ratio remained unchanged. In addition for this series the secant modulus of elasticity decreased slightly.

2. Improving the unit tensile strength corresponded to an appreciable increase in the assemblage strength and the efficiency ratio. The secant moduli also increased. While the strength of face shell mortared blockwork can be related to the unit compressive strength, a stronger relationship existed with the unit tensile strength.

3. The apparent influence of the unit compressive strength on the strength of face shell mortared blockwork could at least partially be attributed to its correlation with the tensile properties of the block.

4. Weak mortar resulted in around a 50% reduction in prism strength. The mode of failure was also dramatically altered by the use of weak mortar. Even-though the initiation of failure in face shell mortared masonry was independent of mortar (excluding the case where the mortar actually failed), the ultimate strength was not independent of the type or strength of mortar. While it was generally true that a lower mortar to unit strength ratio corresponded to a lower prism strength, the use of high strength units as opposed to normal strength units may affect such a relation.

5. For extremely weak mortar the strength of face shell mortared prisms was relatively independent of the block strength.

6. Mortar composed of Portland Cement-Masonry Cement as opposed to Portland Cement-Lime does not appear to affect the compressive strength and axial deformation of face shell mortared block prisms.

7. Although no conclusive results were obtained, it appears that running bond would result in lower prism strength than stack pattern because of the head joint. Larger lateral tensile strains across the head joint were obtained.

8. Fully mortared stack prisms failed in a different mechanism than face shell mortared prisms. Full mortaring resulted in an average 15% increase in the load capacity in comparison to face shell mortaring while the prism compressive

strength decreased slightly.

9. The combined effects of stack pattern and full mortaring of the bed joints resulted in an average 28.5% increase in the load capacity over running bond prisms.

10. Improvement to the unit geometry, by adding an extra web significantly improved the strength of face shell mortared masonry. This increase in masonry strength is attributed to the increased capability of web area in resisting the tensile stresses in face shell mortared blockwork.

11. Prisms built with bubble cured block units unexpectedly showed a decrease in strength with age while prisms built with autoclave cured units showed no sign of change in strength with time.

12. Determining the strength of face shell mortared masonry based on compression tests of 2-course stack bond prisms resulted in around a 20% overestimation of the masonry strength. The failure mode was not representative of the failure of actual masonry and lower secant moduli were obtained.

13. Modulus of elasticity

a) Employing the secant method at 0.3 of the ultimate stress appeared to be the most consistent approach for experimentally obtaining the modulus of elasticity.

b) Most of the variables that affected the masonry compressive strength also appeared to affect the modulus of elasticity. However the magnitude and direction of such effects were not always the same.

c) The modulus was much lower for weak mortar. There may be some relationship between the assemblage modulus of elasticity and the unit tensile properties.

d) Possible correlation between the strength of face shell mortared blockwork and the modulus of elasticity can be obtained. However using the code equation[26], $E_m = 1000 \; f'_m$, would result in a considerable overestimation.

4.7 RECOMMENDATIONS

For an efficient use of face shell mortared blockwork and for design purposes, the following suggestions can be made.

1. Hollow concrete masonry prisms should be built with the same mortar bedding and bonding as the corresponding walls to better simulate the behaviour and to have a more representative value of the compressive strength.

2. For low strength mortar, care should be taken in specifying the mix proportion and composition since the masonry strength is sensitive to the properties of weak mortars.

3. There appears to be merit in investigating the possible direct relationship of the blocks' tensile properties to the compressive strength of masonry.

4. A study into the optimum shape of the hollow concrete unit would be expected to result in improvement on the strength characteristics for face shell mortared construction.

5. Further examination of the effects of age on the strength characteristics of blockwork should be considered.

6. It is recommended that lower values of the elastic modulus should be specified for face shell mortared blockwork. The relationship, $E_m = 700 \quad f'_m$ was found to fit the data in this chapter reasonably well.

CHAPTER 5

EFFECTS OF BLOCK SIZE, PERCENTAGE SOLID, GROUT FILLING AND ECCENTRICITY ON PRISM COMPRESSIVE STRENGTH

5.1 INTRODUCTION

5.1.1 General

Concrete blocks are available in 90 mm, 140 mm, 190 mm, 240 mm and 290 mm widths. As indicated earlier, according to CAN3-S304[26] the strength of concrete masonry can be based on the compressive strength of the unit for a given mortar. Therefore for a specified unit strength an increase in the loaded area should lead to a corresponding increase in the compressive capacity. In face shell mortared blockwork, as was found earlier for 190 mm blocks, the assemblage failure was initially affected by the tensile properties of the web. Therefore by changing the block's web dimension, the principal tension stresses may be affected. Furthermore, the ratio of the block's net area to the effective mortar bedded area increases as block width increases. Hence the assumption that a constant masonry strength can be achieved regardless of the size of the unit should be investigated. Most research test data reported in the literature employed standard 190 mm blocks and the behaviour of blockwork built with various block sizes has rarely been examined.

Blocks with 75 percent and 100 percent solid have been used to increase the axial capacity of blockwork [CAN3-S304-M84[26] specifies that the terminology solid units be applied to units with 75% or higher percentage of solid cross-section]. As was discussed in Chapter 3, solid blockwork has been observed to fail in a different mode than hollow face shell mortared blockwork[37,45,104,116] and lower strengthsare specified[26] for solid blockwork. It has been reported that no difference in strength would be expected between fully mortared hollow and solid blockwork[43] while other test data showed substantial difference[33,116]. Furthermore, some test data[33] raises the question about the code[26] approach of equating 75% and 100% solid blockwork since 75% solid running bond construction is neither face shell mortared nor fully mortared.

In CAN3-S304[26] the compressive strength of grouted blockwork is equated to the strength of solid blockwork provided that the grout strength is at least equal to that of the unit. Such an approach seems questionable since grouted blockwork is a three phase material with the grouted cores providing a continuity in the direction of loading and therefore this could have a significant effect on the assemblage behaviour[43]. Test data showed that grouted prisms yielded higher[33], lower[43] and equal[116] strengths in comparison to solid prisms. Based on the net loaded area, grouted prisms were also found to result in lower compressive strength in comparison to hollow prisms[35,43].

For face shell mortared blockwork under eccentric loading, it has been found that little change in the failure mode would be expected for loading within the central third region of the specimen[33,37]. However, others have suggested that the failure mode would change from web cracking to crushing at an eccentricity of the order of t/20[48] and the strain gradient effect is an inevitable occurrence even at low eccentricity[104]. Elastic analysis has often been used to calculate the strength of eccentrically loaded prisms[12,33,37,48] and some have suggested that eccentrically loaded face shell mortared blockwork would fail when the unit compressive strength is reached[48]. Based on this analysis and for an eccentricity of t/6, a wide range of ratios of eccentric to axial strength varying from 1.12 up to 1.93 has been reported[33,104]. Maurenbrecher[69] suggested that some of these results may have been incorrect possibly owing to ill defined conditions. He suggested that an ultimate strength analysis, using a rectangular stress block, would give better results[68]. Other alternative analysis methods have been suggested[12].

5.1.2 Objectives and Scope

An outline of the investigation program was listed in Table 5.1. The objective from this investigation was to examine the following aspects:

1. The influence of the block size on the strength characteristics of hollow concrete blockwork.

2. The relationship between the strength characteristics of hollow, 75% and 100% solid blockwork.

3. The relationship between grouted, solid and hollow blockwork.

4. The influence of eccentric loading on face shell mortared blockwork.

5. An evaluation of the Canadian code[26] provisions with respect to the aspects listed above.

6. The applicability of a proposed analytical formulation[43] to predict the compressive strength of grouted and fully mortared blockwork.

As indicated in Table 5.1, blocks from 2 companies (No. 10 and 21) with different curing processes (bubble curing and autoclave) were employed to provide more confidence in the results. For each Company, a set of 5 four-course high prisms was included for every parameter. Where different block's size or shape was introduced, the unit compressive strength was determined from tests on 10 single units. The unit tensile strength was obtained from splitting tests on 10 half units.

TABLE 5.1: DETAILS OF PRISM INVESTIGATION PROGRAM

SERIES NO.	BLOCK COMPANY		PARAMETER	DESCRIPTION OF TEST SERIES	NO. OF PRISMS PER COMPANY
	10	21			
S0	Y	Y	Standard	390mm x190mm x190mm standard hollow units, 4-course high prism, ungrouted, concentric loading; Series S0 also in Chapter 4	5
DS1	Y	Y	Various Unit Sizes	390mm x190mm x90mm hollow unit	5
DS2	Y	Y		390mm x190mm x140mm hollow unit	5
DS3	Y	Y		390mm x190mm x240mm hollow unit	5
DS4	Y	Y		390mm x190mm x290mm hollow unit	5
DS5	Y		Unit's Percent Solid	75 % solid standard size units	5
DS6	Y			100 % solid standard size units	5
DS7	Y	Y	Grout	Prisms with standard size units	4
DS8	Y	Y	Eccent-ricity	Eccentric loading at e = t/6	5

Y= units used in prisms pertain to this Company.
Standard= all other Series will be compared to the Standard Series S0

5.2 MATERIALS AND PRISM TESTING

5.2.1 Material Properties

Concrete blocks: All the types of blocks were received from the manufacturers at the same time and had 15 MPa specified compressive strengths. Table 5.2 contains a summary of some of the physical properties of these various units where the net areas were obtained from the Concrete Block - Metric Technical Manual, OCBA[85].

Compressive strengths were determined by testing 10 full blocks fully capped with Hydrostone. Tests were carried out at an age comparable to the corresponding prism tests. The net areas shown in Table 5.2 were used in calculating the strengths.

Splitting tensile strengths of the face shells were determined from 10 tests as described in Chapter 2. The average maximum and minimum face shell widths shown in Table 5.2 were used in these calculations.

Mortar: Mortar Type S2 was used throughout along with McMaster Masonry sand. More details can be found in Chapter 2. The compressive strength was determined from testing three air cured standard cubes at an age comparable to the corresponding prism tests.

TABLE 5.2: NET AND MORTARED AREAS FOR DIFFERENT BLOCKS

UNIT SIZE L H W	DESCRIPTION	FACE SHELL THICKNESS(mm)		WEB THICKNESS(mm)		NET AREA (mm^2)	MORTAR BEDDED AREA (mm^2)
		MIN.	MAX.*	MIN	MAX.*		
390 x190 x90 mm	Hollow	26	30	26	30	25600.0	24336.0 (a)
390 x190 x140 mm	Hollow	26	30	26	30	31700.0	24336.0 (a)
390 x190 x190 mm	Hollow	32	36	26	30	41500.0	30700.8 (b)
390 x190 x240 mm	Hollow	35	39	28	32	49600.0	32760.0 (a)
390 x190 x290 mm	Hollow	38	42	32	36	57700.0	35568.0 (a)
390 x190 x190 mm	75 (%) Solid	60	64	30	34	57800.0	56160.0
390 x190 x190 mm	100 (%) Solid	-	-	-	-	74100.0	74100.0

Net area was used for calculating unit compressive strength
Mortar bedded area was used for calculating prism compressive strength
Mortar bedded area= area of mortar in contact between upper and lower units
(a)= plus 20 % of minimum face-shell area
(b)= plus 23 % of minimum face shell area
* flares not included

Grout: A medium strength grout with an intended 250 mm slump was used. Details on mix proportion, curing and testing of grout control specimens can be found in Appendix D. The compressive strength was determined by testing three 75 x 75 x 150 mm grout prisms cast according to CSA-A179-1976[23]. The block molded grout had an average compressive strength of 36.7 MPa.

5.2.2 Test Prism and Test Procedure

Prisms were built, in running bond construction, at the same time and in the same manner as those included in the investigation reported in Chapter 4. For prisms built with 75% and 100% solid blocks full mortaring of the bed joint was employed. Prisms similar to those used in the standard series, S0, were employed for grouting.

The prism test set-up was shown in Figure 3.5. Full bed Hydrostone capping was used throughout. Capping procedure, preparation and actual testing were all carried out as described in Section 3.2.4 and the prisms were tested over a period ranging between 5 and 7 months. Axial deformations across blocks and mortar joints were measured as indicated in Section 4.2.2 for 3 prisms out of the 5 replications. Measurements were terminated at 80% to 90% of the ultimate load.

5.3 EXPERIMENTAL RESULTS

5.3.1 General

The test results from concentrically loaded prisms were listed in Tables 5.3 and 5.4 for Companies 10 and 21, respectively. These tables include the block and mortar strengths as well as the prism compression results. As indicated earlier, the standard Series S0 was the same S0 Series reported in Chapter 4 where "standard" implies prisms built with standard 190 mm hollow units, ungrouted and loaded concentrically. The eccentric loading results are presented later on in this chapter.

5.3.2 Mortar Bedded Areas

Since running bond was employed throughout, the various prism compressive strengths were calculated based on the effective mortar bedded areas shown in Table 5.2. These areas were obtained by placing the units in running bond and then calculating the mortar area in contact between the upper and lower units. For the 90 mm hollow blocks, almost full bedding can be achieved leaving only around 5% of the net area unloaded. The same is true for 75% solid blocks where only around 3% of the net area was not loaded. For these two types of units full mortar bedding would be required in order to achieve effective transmission of the axial load.

TABLE 5.3: SUMMARY OF TEST RESULTS FOR COMPANY 10

SERIES NO.	PARAMETER	BLOCK STRENGTH		MORTAR STRENGTH (MPa)	PRISM COMPRESSION TEST			
		COMP. (MPa)	TENSILE (MPa)		ULT. LOAD (kN)	MEAN LOAD (kN)	MEAN STRENGTH (MPa)	C.O.V. (%)
S0-10 same as in Chap.4	Standard 190 mm Unit Wide	31.0 [6.5]	2.6 [14.1]	7.1 [11.5]	597 568 585 624 591	593.0	19.3	3.4
DS1-10	90 mm Unit Wide	21.9 [4.6]	2.5 [11.7]	9.1 [16.4]	382 412 377 384 378	386.6	15.7	3.7
DS2-10	140 mm Unit Wide	26.0 [6.0]	2.6 [11.3]	7.5 [5.4]	467 461 426 437 459	450.0	18.5	3.9
DS3-10	240 mm Unit Wide	31.9 [3.3]	3.1 [12.2]	7.0 [5.1]	733 728 707 743	727.8	22.2	2.1
DS4-10	290 mm Unit Wide	30.6 [5.7]	3.2 [12.9]	7.0 [3.1]	848 854 827 754 819	820.4	23.1	4.9
DS5-10	75 (%) Solid	38.1 [5.2]	3.0 [9.3]	7.5 [4.0]	1227 1273 1454 1304 1318	1315.2	23.4	6.5
DS6-10	100 (%) Solid	28.4 [6.4]	2.2 [6.6]	7.5 [3.9]	1303 1345 1263 1247 1311	1293.8	17.5	3.0
DS7-10	Grouted	Same as Series S0-10		7.8 [10.2]	1185 1062 887 899	1008.3	13.6	14.1
Number of Tests		10	10	3				

[]= value inside brackets is the coefficient of variation (%), C.O.V.

TABLE 5.4: SUMMARY OF TEST RESULTS FOR COMPANY 21

SERIES NO.	PARAMETER	BLOCK STRENGTH		MORTAR STRENGTH (MPa)	PRISM COMPRESSION TEST			
		COMP. (MPa)	TENSILE (MPa)		ULT. LOAD (kN)	MEAN LOAD (kN)	MEAN STRENGTH (MPa)	C.O.V. (%)
S0-21 Same as in Chap.4	Standard 190 mm Unit Wide	24.5 [5.2]	2.3 [7.3]	7.9 [11.0]	512 498 493 509 525	507.4	16.5	2.5
DS1-21	90 mm Unit Wide	18.2 [5.9]	1.7 [8.3]	7.3 [3.2]	320 360 344 325	337.3	13.9	5.4
DS2-21	140 mm Unit Wide	19.3 [3.8]	1.8 [11.5]	7.1 [3.0]	347 345 350 347 343	346.4	14.2	0.8
DS3-21	240 mm Unit Wide	19.9 [8.9]	2.4 [6.8]	7.9 [10.9]	402 458 428 456 451	439.0	13.4	5.4
DS4-21	290 mm Unit Wide	23.1 [7.3]	2.1 [8.2]	7.9 [5.7]	563 521 498 466	512.0	14.4	8.0
DS7-21	Grouted	Same as Series S0-21		9.1 [10.1]	808 864 754 734	790.0	10.7	7.4
Number of Tests		10	10	3				

[ ]= value inside brackets is the coefficient of variation (%), C.O.V.

For 140, 190, 240 and 290 mm blocks, vertical alignment of the webs is not achieved in running bond. Therefore the effective loaded area is significantly lower than the block's net area. For 140, 240 and 290 mm block construction, the mortar bedded area can be correctly obtained by increasing the minimum face shell area by about 20%. For 190 mm block construction, the mortar bedded area was discussed in Section 3.3.1.2.

5.3.3 Influence of Block Size

5.3.3.1 Failure Modes

The effective area for prisms built with 90 mm blocks was nearly the same as the net area and there was much less length of unloaded web to share the load between mortar joints. Both of these factors would tend to reduce the principal tensile stresses in the webs. Hence vertical cracking of the webs would not be expected. The observed failures showed almost no signs of cracking. Failure tended to be explosive and in some instances a wedge of face shell was observed to spall away in the lower courses. However it is suggested that the high aspect ratio, $h/t = 8.5$, may have led to an instability condition once the failure load was exceeded. Figure 5.1 is a photograph of this face shell spalling failure mode.

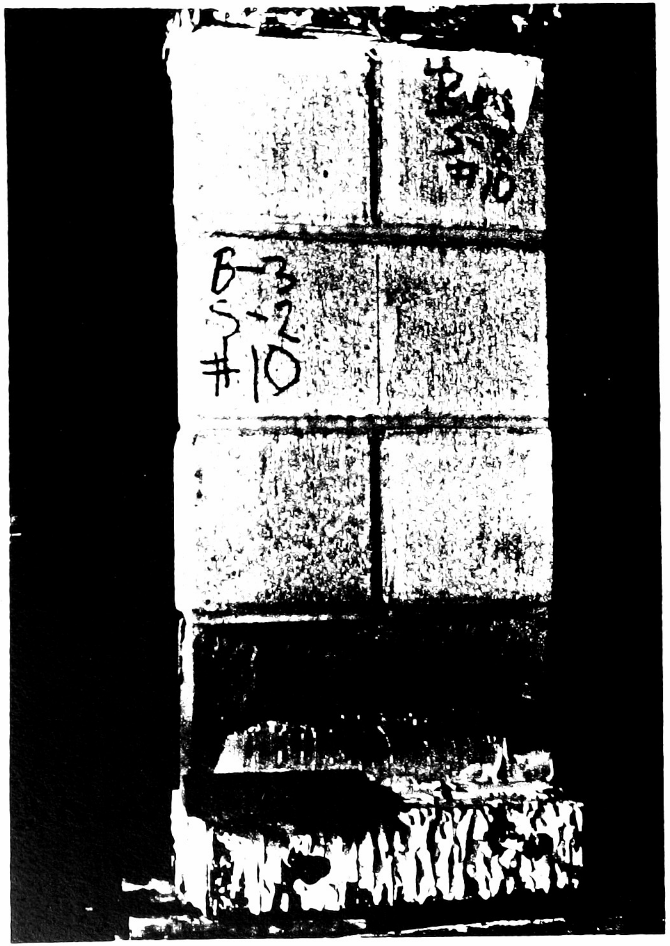

a) 90 mm Wide Prism

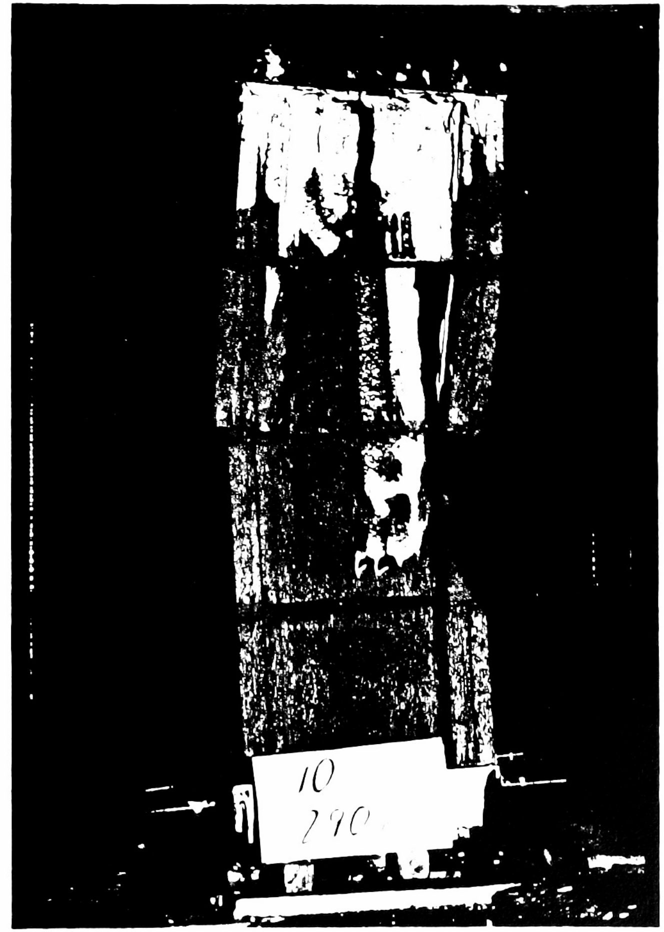

b) 290 mm Wide Prism

FIGURE 5.1 TYPICAL PRISM FAILURE FOR 90 mm AND 290 mm BLOCKS

For prisms built with 140 mm blocks, web cracking occurred in the same manner as described in Chapters 3 and 4 for 190 mm blocks but at a later stage of loading. In fact, as indicated in Table 5.5, the audible cracks were reported to occur very near failure for Company 10 prisms, in comparison with around 85% for 190 mm prisms (Audible cracking seems to indicate that cracks have propagated through the webs of one of the central blocks). Secondary failure occurred by shearing in one of the face shells.

The failure mode for prisms made with 190 mm blocks was discussed in detail in Chapters 3 and 4. A photograph of the prism failure for 290 mm blocks shown in Figure 5.1(b) is representative of both the 240 mm and 290 mm block prisms which all developed extensive cracks through the webs. The extent of these cracks was much more evident than for the 190 mm block prisms but the audible cracking was reported at lower load levels than for the 190 mm block prisms. For prisms built with 240 mm and 290 mm blocks, more than one line of cracking was observed with cracks developing at the web - face shell interaction after initial cracking at the centre of the webs. The final failure appeared to be instability of the crack separated parts of the assemblage.

The development of full cracking of the webs of the middle blocks at lower loads for larger blocks seems logical since larger principal tension stresses would be expected for webs spanning a larger distance between face shells. Also worth noting is the difference between Companies 10 and 21 in reserve strength following cracking or, looking at it differently, the fact that cracking occurred much nearer failure for Company 21.

TABLE 5.5:OCCURRANCE OF CRACKING IN PRISMS WITH VARIOUS WIDTHS

PRISM WIDTH	OCCURRANCE OF WEB CRACKING			
	COMPANY 10		COMPANY 21	
	PERCENT OF ULT. LOAD (%)	CORRESPONDING STRESS (MPa)	PERCENT OF ULT. LOAD (%)	CORRESPONDING STRESS (MPa)
140 mm	98	18.1	-	-
190 mm	85	16.4	93	15.0
240 mm	75	16.6	91	12.0
290 mm	52	12.0	82.4	11.2

Cracking in the webs was observed to initiate at loads between 30 - 40% of the ultimate load. However, contrary to what may be expected for larger blocks, where the effects of plate restraint would seem to have a greater impact, web cracks propagated all the way to the ends of the prisms - a behaviour not observed for hard capped 190 mm block prisms.

Regardless of the increment of load between complete cracking of the webs and prism failure, final failure occurred with shearing of the face shell of the bottom block. However shearing of the face shell in larger block prisms may be related to the relatively low aspect ratio, for 290 mm block prisms. The aspect ratio is h/t = 2.6, where platen restraint effects could be expected to affect the failure.

There is a need to understand why for Company 10, larger block prisms continued to resist increases in the load after webs had developed full cracks whereas Company 21 prisms failed shortly after web cracking. After full web cracking, the prisms made with 240 mm and 290 mm blocks completely split in two halves with the load being resisted by these two relatively thin columns with complicated geometry. Comparisons between the block strengths from the 2 companies may provide a partial explanation for the different behaviours observed. As listed in Tables 5.3 and 5.4, the compressive strength of the 240 mm blocks from Company 10 was around 60% higher than that of Company 21. Furthermore the axial compressive strains at similar stress levels for Company 10 prisms were much lower than those from Company 21. For example, at a stress level of 11.9 MPa for 240 mm block prisms the axial strain for Company 10 was 1000 micro-strain versus 1500 micro-strain for Company 21. This is a relatively large difference in axial strains and thus may have contributed to the different behaviour.

5.3.3.2 Compressive Strength

Figure 5.2 shows the hollow block prism test results for Companies 10 and 21 where strength was normalized first in terms of compressive strength of blocks and then in terms of the blocks' splitting tensile strength. As can be seen in terms of block compressive strength, the results are reasonably consistent over the full range of sizes and between companies. However it is worth noting that the comparisons shown in Figure 5.2 do not take into account the influence of the prism aspect ratio. For example, for 290 mm block prism h/t = 2.62 while for 90 mm block prism h/t = 8.4 and as indicated earlier, the secondary failure of wide prisms by shearing of the face shells may reflect the increased effects of platen restraint in wider block. Figure 5.2 indicates that for 90 mm and perhaps 140 mm where tensile strength is not as important, [Note: the failure mode of 90 mm wide prism was not initiated by web cracking therefore the unit compressive strength is of more significance], higher ratios of prism strength to block compressive strength existed. Maurenbrecher[67] indicated that for wider blocks the ratio of prism to block strength decreased. This appears to be generally true as can be seen in Figure 5.2 . However for 290 mm block prisms from Company 10, where a higher ratio was obtained, it may be suggested that for these prisms which have cracked around 50% of the ultimate load the failure load can

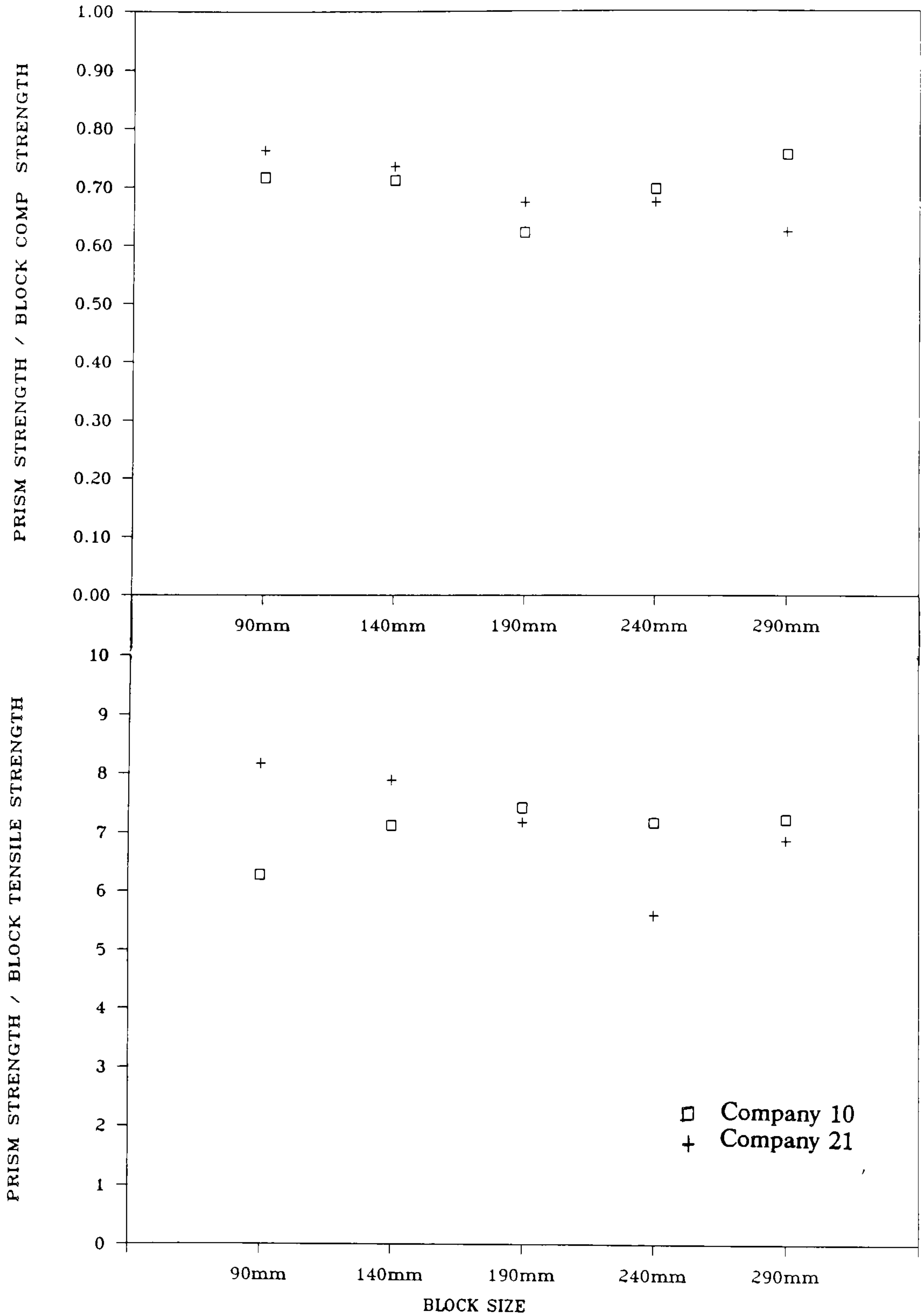

FIGURE 5.2 HOLLOW BLOCK PRISM STRENGTH NORMALIZED IN TERMS OF BLOCK COMPRESSIVE STRENGTH AND TENSILE STRENGTH

possibly be considered to occur at lower loads than the obtained ultimate capacity. Platen restraint may have attributed in causing such artificially high strength and prisms with higher aspect ratio could possibly yield a lower strength.

The relationship between the hollow block prism strengths and the blocks' tensile strength was drawn in Figure 5.3. As can be seen, a reasonably good correlation exists. As indicated earlier, since for 90 mm block prisms the tensile strength is not as important, if these two data points (Companies 10 and 21) were removed from the relationship in Figure 5.3, the correlation coefficient would increase to 0.964 and the relationship is nearly linear.

5.3.3.3 Stress-Strain Characteristics

Figures 5.4(a) and (b) are the stress-strain relationships for the prisms for Companies 10 and 21, respectively. With the exception of the 290 mm prisms, the stress-strain relationships are generally similar. It also appears that 90 mm block prisms had a more linear relationship than the other prisms. This is expected since with 90 mm blocks almost full bedding is achieved and hence a more uniform axial stress transfer would occur. The lower initial slope for the 90 mm prism curve, Company 21, is attributed to closing cracks in the mortar joints. Prisms with such small

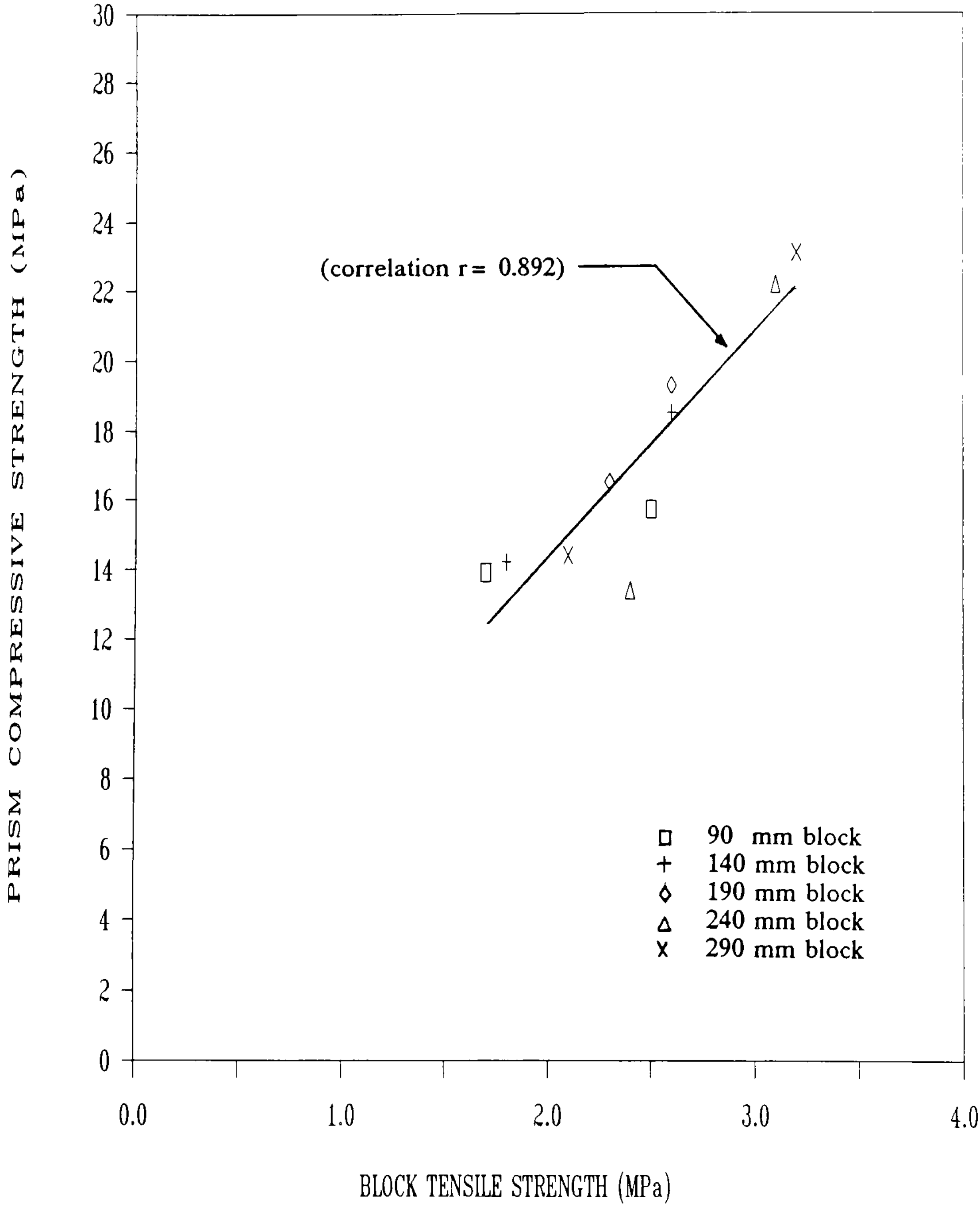

FIGURE 5.3 RELATIONSHIP BETWEEN HOLLOW BLOCK PRISM STRENGTH AND BLOCK SPLITTING TENSILE STRENGTH

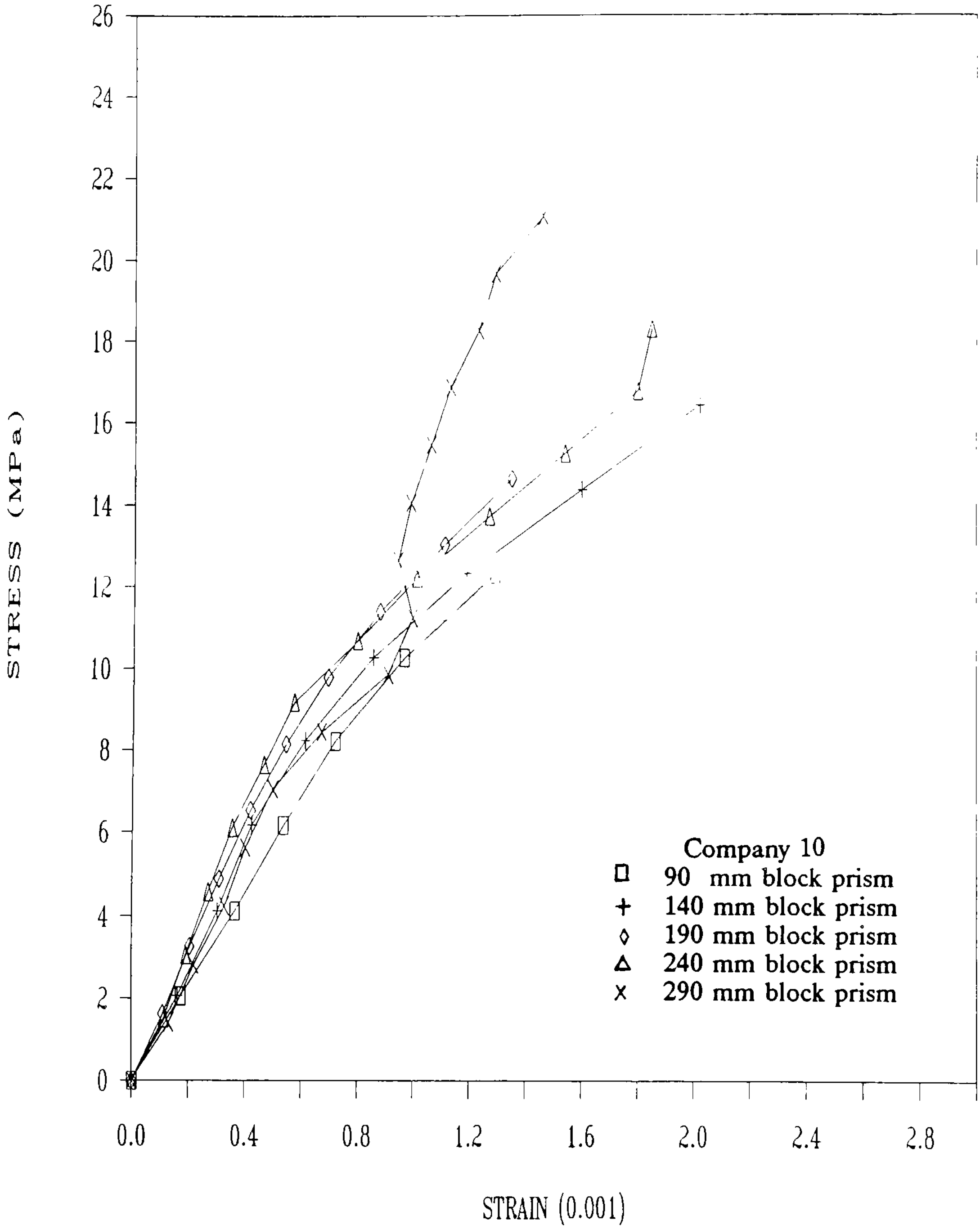

FIGURE 5.4 a) STRESS-STRAIN RELATIONSHIPS FOR HOLLOW BLOCK PRISMS FOR COMPANY 10

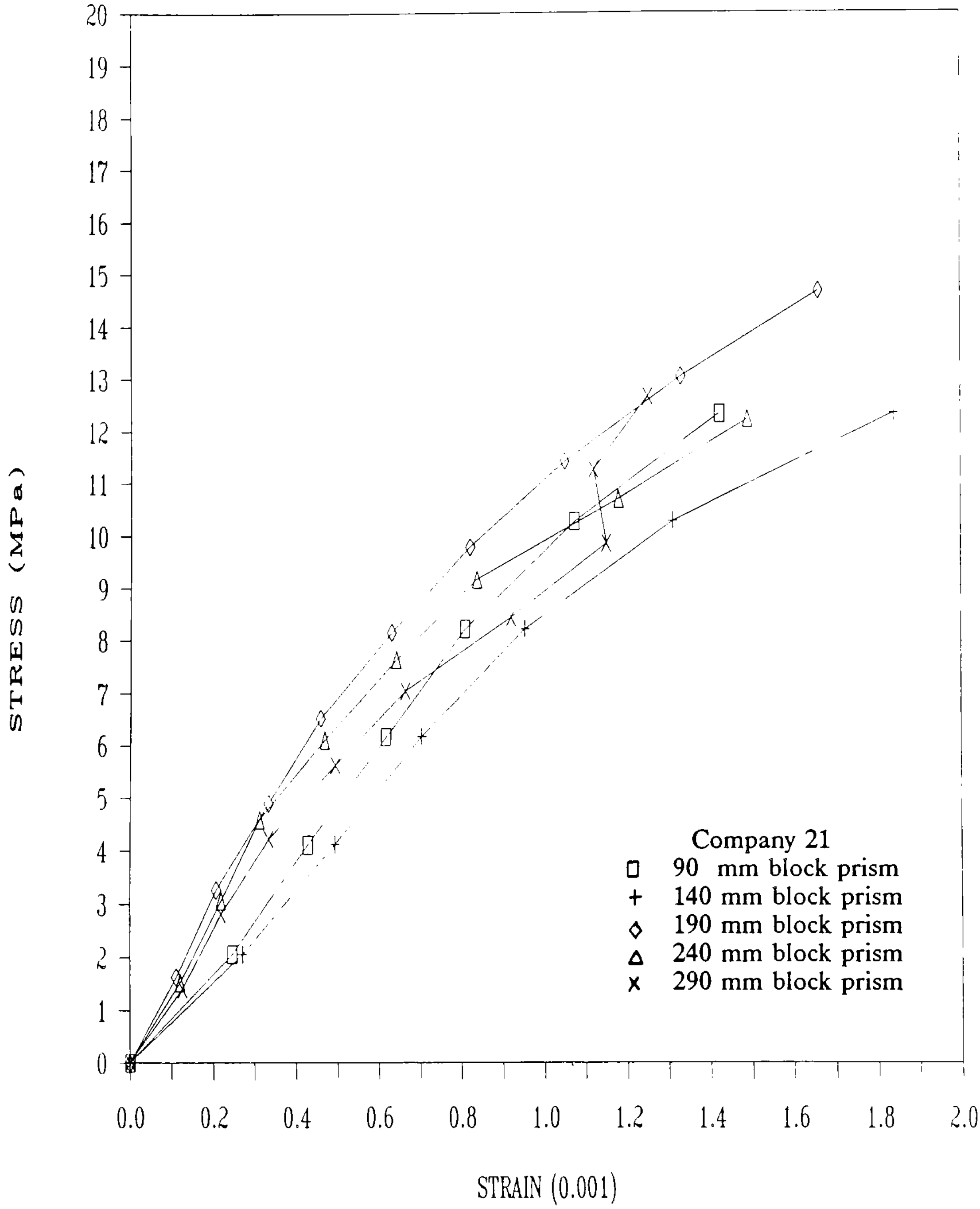

FIGURE 5.4 b) STRESS-STRAIN RELATIONSHIPS FOR HOLLOW BLOCK PRISMS FOR COMPANY 21

width are sensitive to moving and in some instances the bonding between the mortar and the unit was broken.

Of a particular interest is the stress-strain relationship of the 290 mm prisms. The sudden change in the curves coincided with the occurrence of full web cracking as indicated in Table 5.5. The distinct stiffening in the upper portion of the curve may be a reflection of the face shell stiffness and not of the whole assemblage because after the web had cracked, the load was resisted by the two unsymmetric halves of the prism. A similar behaviour was observed for the 240 mm block prisms for Company 10 where the sudden change in the top portion of the curve occurred at the audible cracking load of around 78% of the ultimate load.

In order to obtain a meaningful comparison between the various stress-strain relationships for prisms made with different blocks, it is sometimes better to normalize the stress with respect to the strength. Figure 5.5 is a repeat of the results in Figure 5.4 but with stress expressed as a ratio of prism strength. As can be seen, the stress-strain curves are somewhat more consistent when presented in this manner.

The secant moduli of elasticity taken at 0.3 of the ultimate stresses were listed in Table 5.6 for the various series of tests. For Company 10, the modulus of elasticity increased with increasing prism strength which also happens

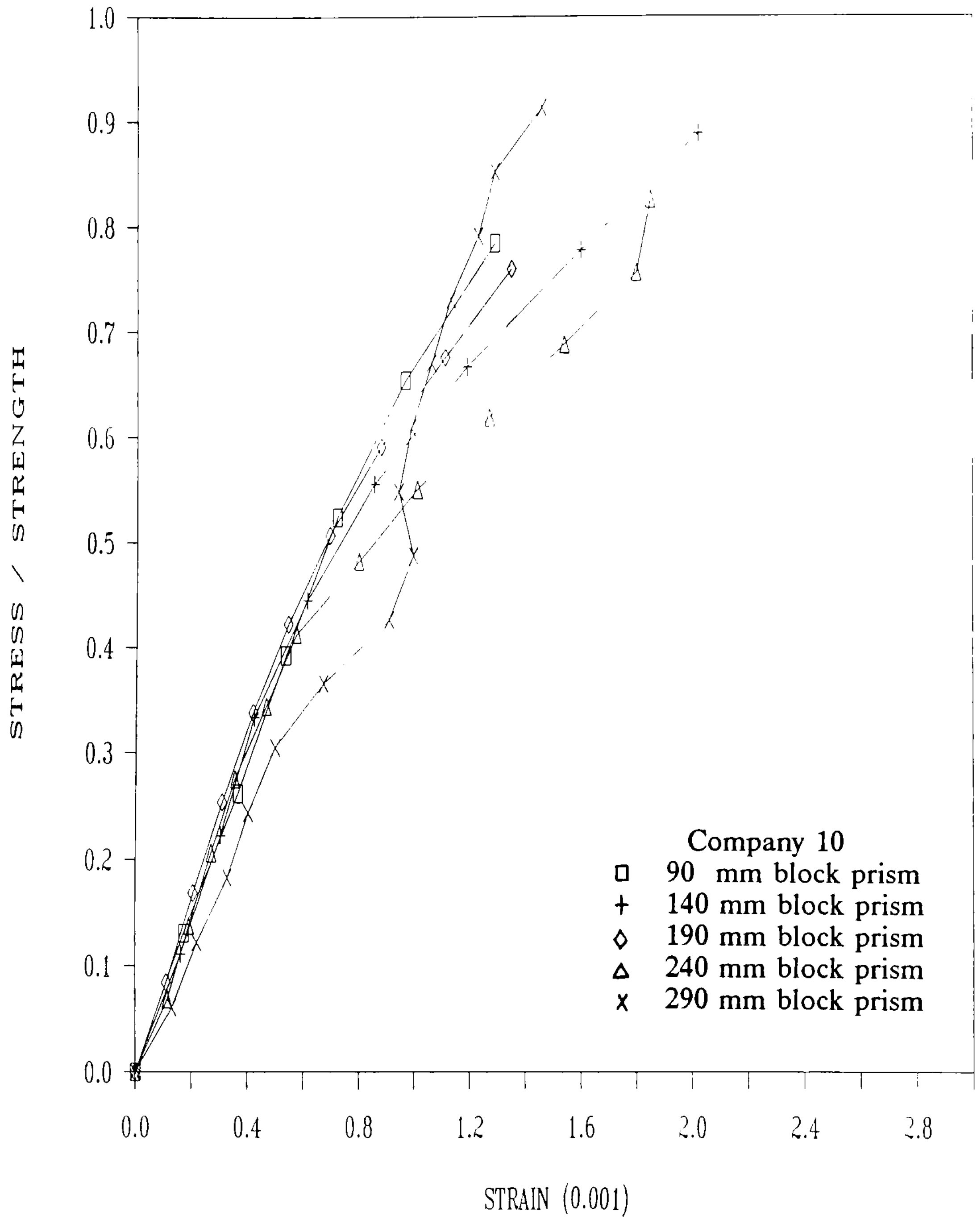

FIGURE 5.5 a) STRESS/STRENGTH-STRAIN RELATIONSHIPS FOR HOLLOW BLOCK PRISMS FOR COMPANY 10

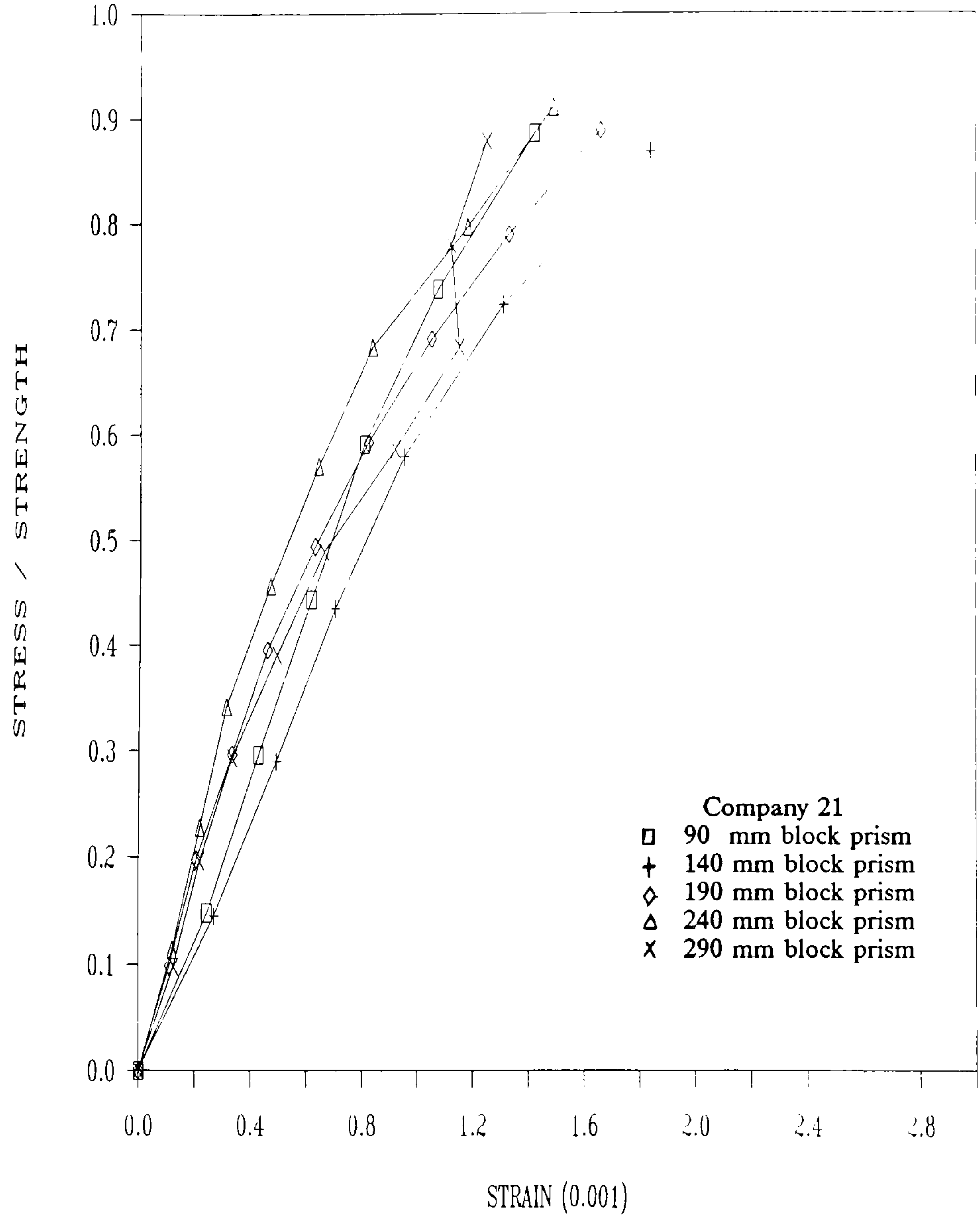

FIGURE 5.5 b) STRESS/STRENGTH-STRAIN RELATIONSHIPS FOR HOLLOW BLOCK PRISMS FOR COMPANY 21

TABLE 5.6: SECANT MODULI OF ELASTICITY AT 0.3 OF ULTIMATE STRESS

SERIES NO.	PARAMETER	DESCRIPTION	COMPANY 10		COMPANY 21	
			SECANT MODULUS Em (1000 MPa)	STIFF. COEFF. K	SECANT MODULUS Em (1000 MPa)	STIFF. COEFF. K
S0	Standard	190 mm Wide Unit	15.7	811	14.7	893
DS1	Various Unit Sizes	90 mm Wide Unit	11.4	724	9.6	692
DS2		140 mm Wide Unit	14.4	777	7.6	532
DS3		240 mm Wide Unit	16.9	760	14.5	1083
DS4		290 mm Wide Unit	14.1	610	12.5	868
DS5	Unit's Percent Solid	75% solid	16.8	718		
DS6		100% solid	13.6	777		
DS7	Grout		13.8	1018	11.5	1072

K= Stiffness Coefficient
 = ratio of modulus of elasticity to prism compressive strength

to coincide with increasing block size for this Company. However the modulus for 290 mm prisms was lower than the others even though the prism strength was the highest. As shown in Figure 5.4(a) 290 mm prisms experienced larger strains at lower stress levels than the other prisms. It was observed that, in 290 mm block prisms, web cracking initiated at very low stress level, 0.2 to 0.3 f'_m, and this could have affected the axial strains at these low stress levels. For almost all the various prism sizes for both companies, the stiffness coefficients, K, defined as E_m/f'_m were lower than the 1000 value specified in CAN3-S304-M84[26]. For Company 21, while the highest modulus corresponded to the highest prism strength (190mm prism), the various prisms' moduli fluctuated even when the prism strengths were statistically equivalent. For 90 mm and 140 mm prisms the moduli could be artificially low as a result of the closing of the initial cracks in the mortar joints, as discussed earlier.

5.3.4 Influence of Percentage Solid of Blocks

Figure 5.6(a) is a photograph at failure of a prism built with 75% solid units. In 75% solid block construction, little or no gap exists between the webs of the blocks constructed in running bond. Therefore for face shell mortaring, the load is nearly uniformly distributed across the block area and development of principal tension stresses is

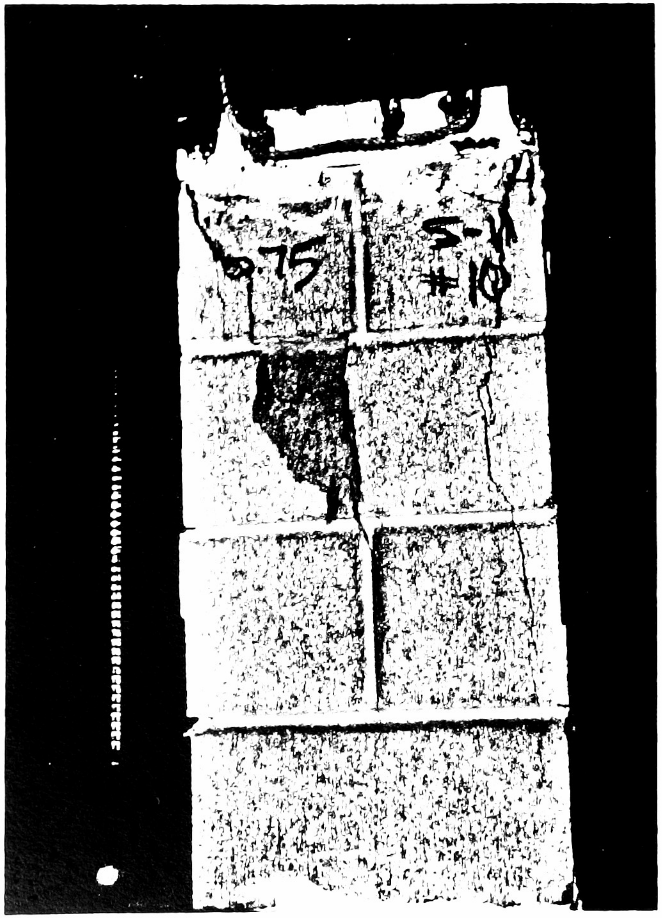

a) 75 % Solid Block Prism

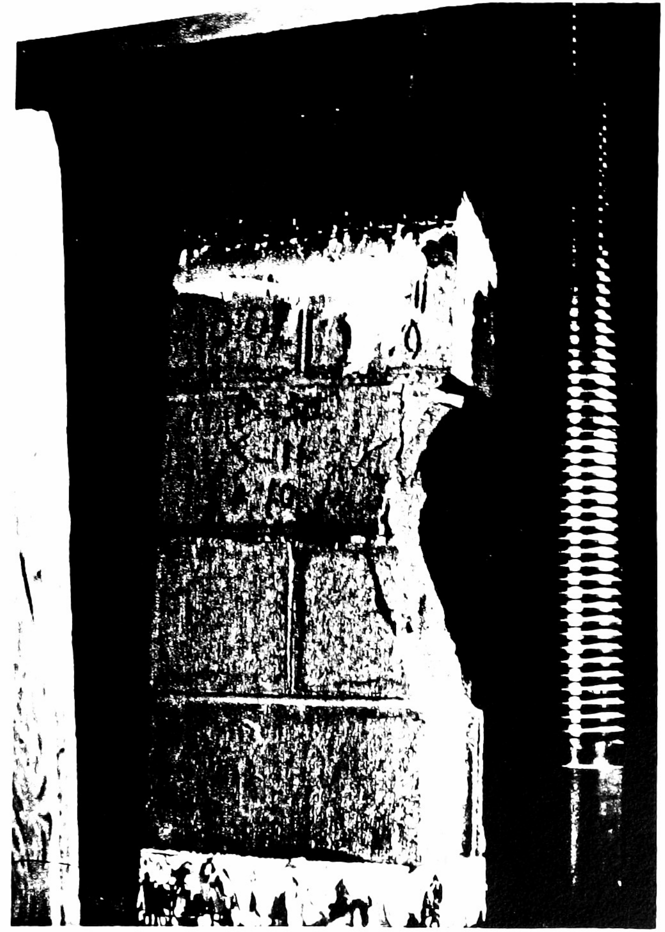

b) 100 % Solid Block Prism

FIGURE 5.6 TYPICAL PRISM FAILURE FOR 75 % SOLID AND 100 % SOLID BLOCKS not as significant as for hollow block prisms. After initial web cracking, the prism failed by developing cracking in both corners of the face shells. Shearing of a part of the face shell was also observed. The nature of the failure suggests an apparent influence of platen restraint, simply because of the large cross-sectional area subject to confinement at the ends. This was similar to the conical failure usually observed for concrete cylinders. The web cracking also observed in some instances may be attributed to the fact that the web constitutes the weak link in the unit (ratio of face shell thickness to web thickness = 2) and is subject to the influence of mortar dilation causing transverse lateral stresses. The observed difference in failure mode between hollow block and 75% solid prisms suggests that different mechanisms caused the failure. These mechanisms were discussed in Chapter 3.

Prisms built with 100% solid blocks had only a slightly different failure mechanism from 75% solid block prisms, with the failure being explosive. The conical shape failure shown in Figure 5.6(b) resulted from vertical cracks which, near ultimate load, formed the conical failure zone because the top block did not crack. This type of failure was also evident in full wall tests conducted by Suwalski[110]. There was no evidence of any cracks in the narrow faces as had been observed by Wong[116] or of mortar crushing. Such behaviour may be attributed to the fact that the narrow face has a depth of 390 mm while the wide face has only a depth of 190 mm. This implies that for the interaction between the mortar and the solid blocks, there were different stress distributions according to the width of the prism face. Cracking and spalling mainly occurred in the face shells.

It was apparent that with the increase in the block solid percentage from 56% (standard hollow) to 75% and 100%, the failure gradually was transferred from web cracking to a combination of face shell and web cracking and finally to face shell cracking alone.

The prism strengths for 75% and 100% solid blocks as a ratio of either block compressive or tensile strength were essentially the same. These ratios were also very close to those for the prisms built with 190 mm hollow blocks.

The stress-strain relationships for hollow, 75% and 100% block prisms for blocks supplied by Company 10 were shown in Figure 5.7. The relationship for 75% solid block prisms was distinctly different from the two others. In fact the stress-strain relationship was linear up to around 60% of the ultimate strength. Furthermore, as indicated in Table 5.6, while the secant modulus of elasticity was substantially higher than for 100% solid block prisms, based on prism strength, the two values were reasonably comparable. Again, as was the case for hollow block prism, the secant moduli of

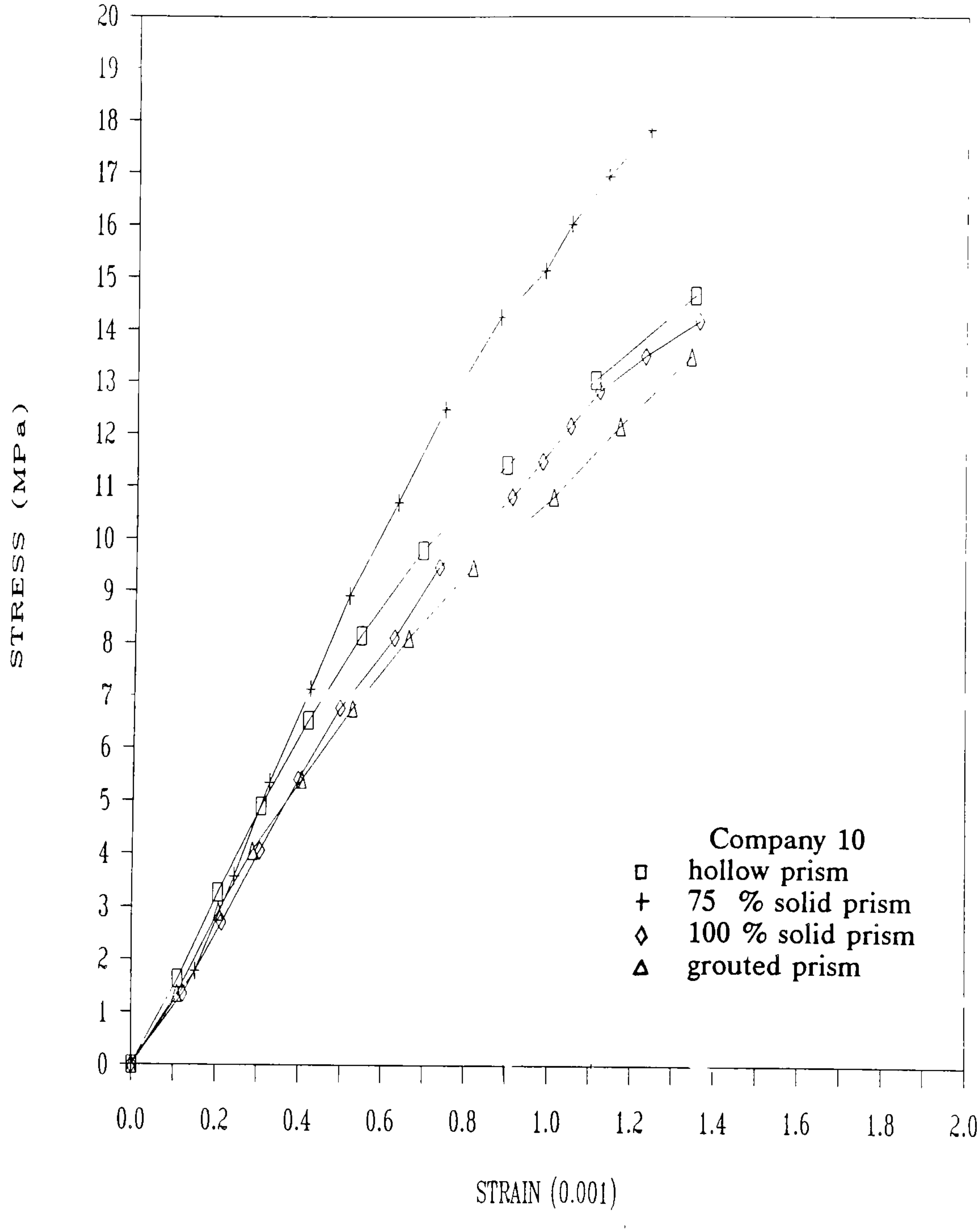

FIGURE 5.7 STRESS-STRAIN RELATIONSHIPS FOR DIFFERENT PERCENT SOLID BLOCK PRISMS AND HOLLOW BLOCK PRISMS

elasticity were far below the specified code[26] value of 1000 f'_m.

5.3.5 Influence of Grouting on Prism Strength

Grouted prisms failed in a distinctly different mode and mechanism than hollow block prisms. A photograph of the failure of a grouted prism was shown in Figure 5.8. The failure can be described as the development of vertical cracks in both webs and face shells. The cracks in the webs mainly occurred at the prism corners and not in the middle as was the case for hollow masonry. Also the cracks appeared to be localized and not continuous. The cracking in grouted masonry has been attributed to the inelastic deformations of the grouted core in the horizontal direction which result in high bilateral tensile stresses in the block unit as it tends to confine the grout[43]. The observed prism failure appears to support this suggestion, especially the splitting in the web corners where highest lateral tensile stresses would be developed.

Comparison of the grouted prisms results, listed in Table 5.3 and 5.4, from Companies 10 and 21 showed that even though the same grout was used the prism strengths were different (Note that grout strength was higher than the compressive strength of units from both companies). This led to the suggestion that the grouted prism strength depends

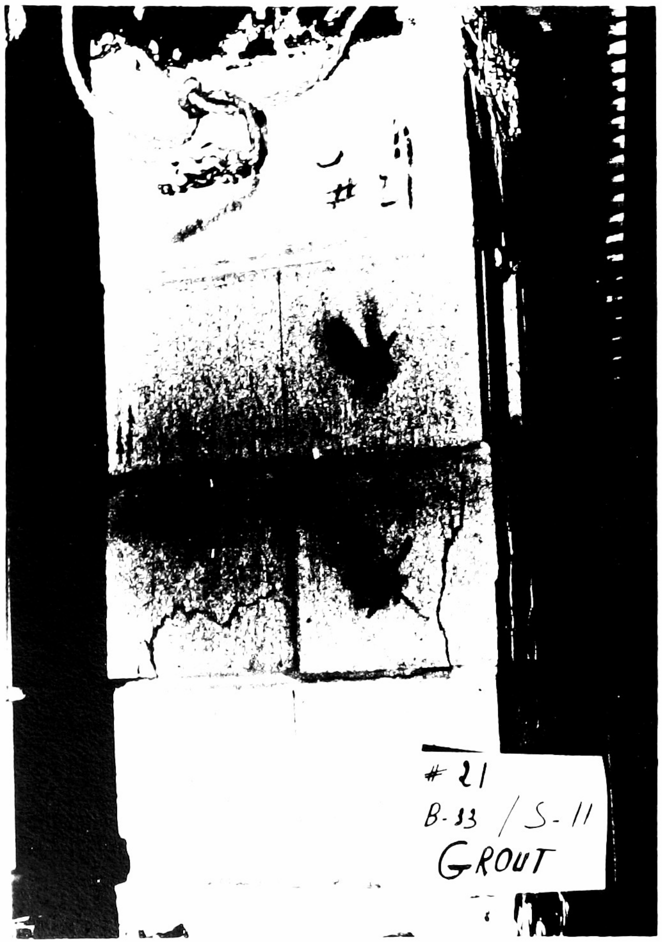

Plane View

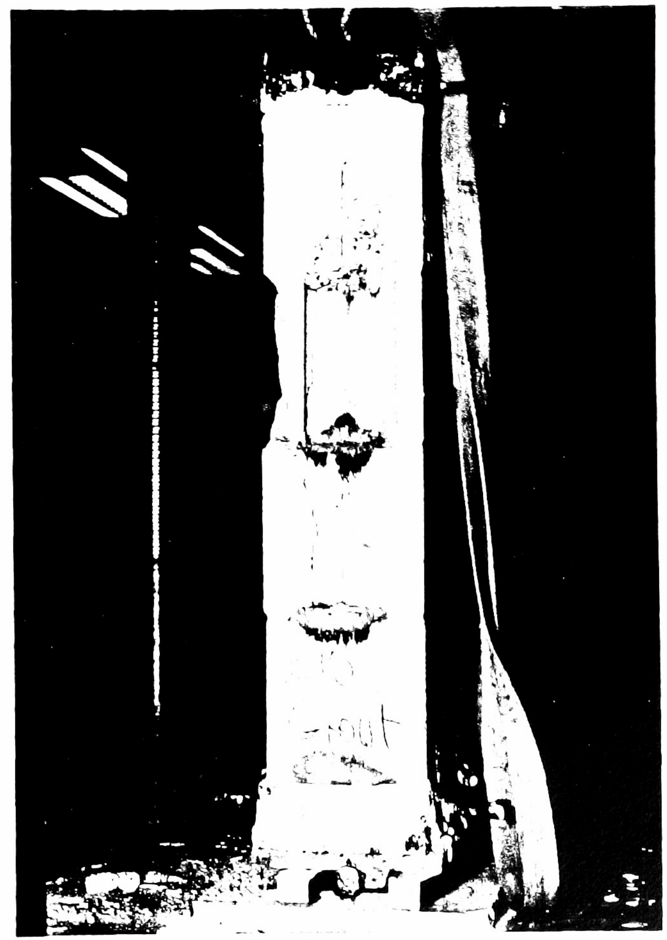

Side View

FIGURE 5.8 TYPICAL FAILURE OF GROUTED PRISMS primarily on the block strength, particularly the tensile properties. Failure occurred after the limiting block strengths under biaxial compression-tension conditions were reached. In fact, after the failure, grouted cores were observed to be intact and could be recovered as solid pieces.

Based on effective area, the compressive strengths of grouted prisms were significantly lower (30%-35%) than the strengths of hollow prisms. This confirms the previously described failure mechanism.

Results from Company 10 prisms also showed that the compressive strength of the grouted prisms was significantly lower than for the 100% solid block prisms even though the solid blocks were slightly weaker than the hollow blocks used to build the grouted prisms. Therefore equating the strength of grouted blockwork to that of masonry built with solid units is certainly an overestimation.

The stress-strain relationships for hollow and grouted prisms for Companies 10 and 21 were plotted in Figure 5.9. While the similarity of the stress-strain relationships is apparent, it can be seen that grouted prisms had less axial stiffness and, as indicated in Table 5.6, lower moduli of elasticity than for hollow prisms. However, compared to the low prism strength, the ratio of 1000 f'_m in the code[26] appears to be reasonable. In Figure 5.7, the stress-strain relationships for grouted prisms were also shown for Company

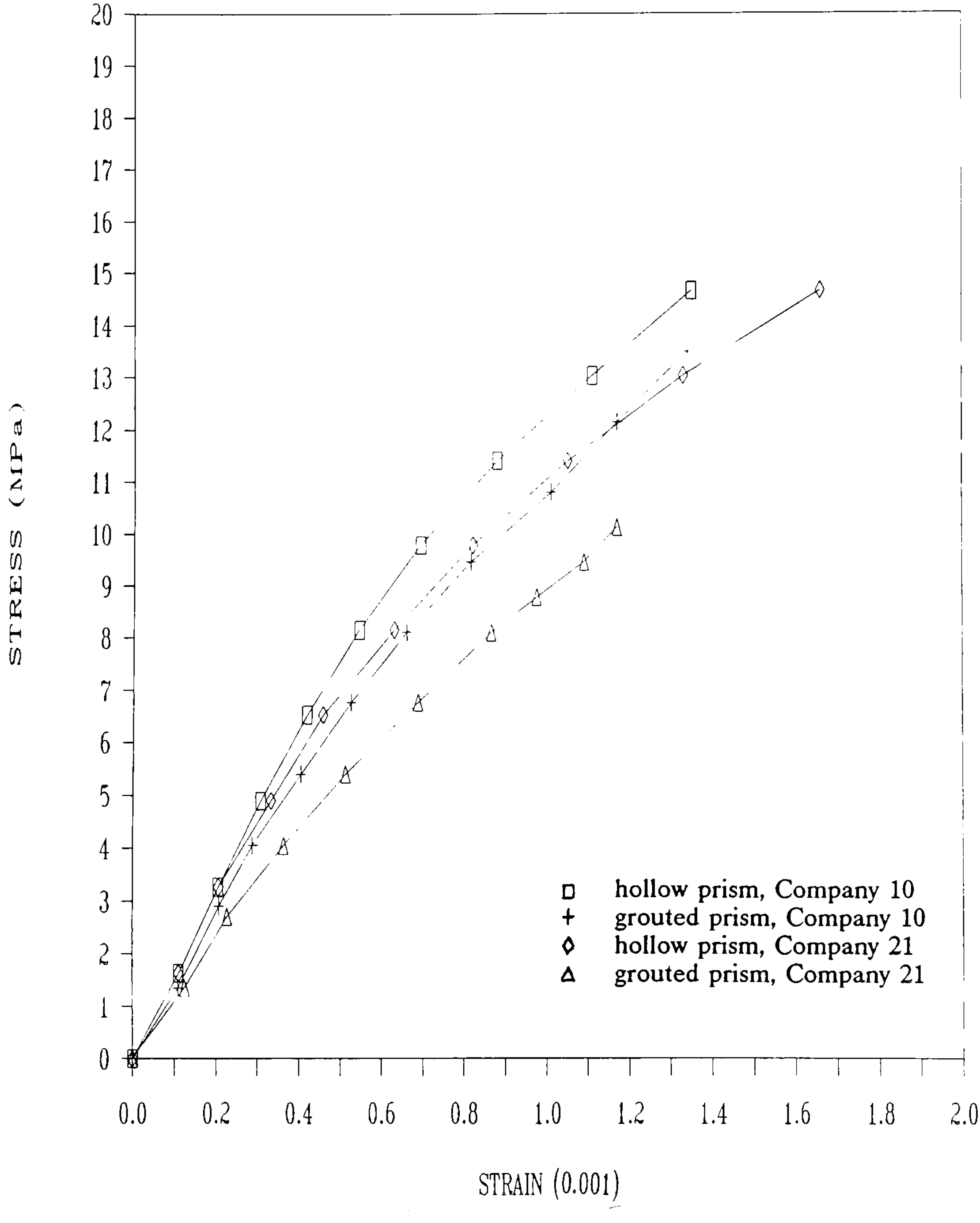

FIGURE 5.9 STRESS-STRAIN RELATIONSHIPS FOR GROUTED AND HOLLOW PRISMS FOR COMPANIES 10 AND 21

10 so that it can be compared to prisms built with blocks having various percents solid.

5.3.6 Influence of Eccentric Loading on Prism Strength

For eccentricities of one sixth of the block thickness, t/6, web cracking continued to be observed in eccentrically loaded prisms. However, the location of cracks and the path shifted toward the most heavily loaded face shell[104]. In some instances there was a tendency for the crack to cross the web. Final failure was observed to occur by shearing of a large section of the face shell as shown in Figure 5.10. Similarly to what has been reported[116], no cracking in the face shells was observed. For Company 10 prisms, the failure was more explosive and the web cracking was less apparent than for Company 21.

As indicated in Table 5.7, loading at an eccentricity of $e = t/6$ significantly reduced the axial capacity of the prisms, especially for Company 21. The eccentric to axial load ratios, Pe/Po, agree with some test data where similar construction and unit size were used[33,116], while a surprisingly high ratio with a value over 1.0 was reported elsewhere[104]. However a review of the latter data showed that this high value of Pe/Po = 1.3 may have been due to the fact that full fibreboard capping was used. Therefore for the test with the load at e=o, premature failure occurred and as a result low

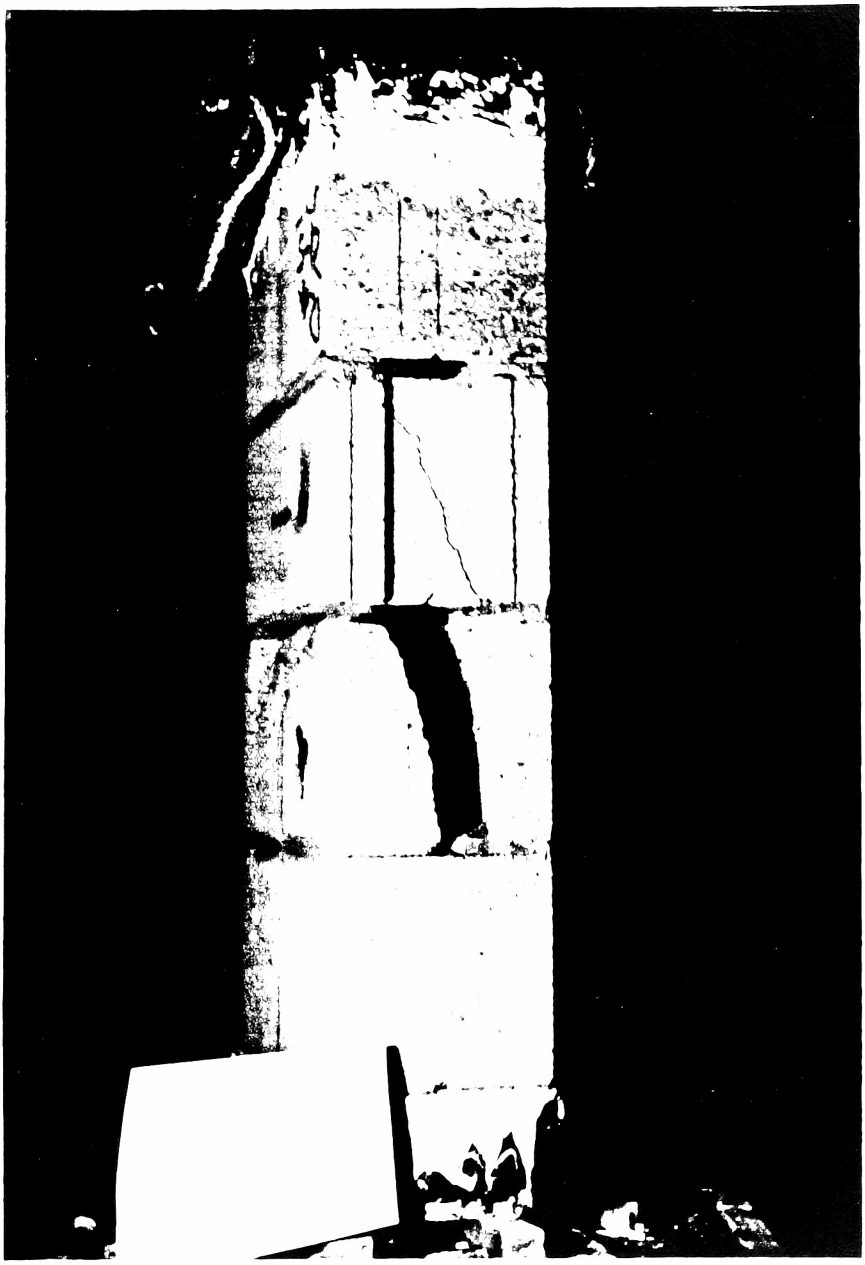

FIGURE 5.10 FAILURE OF PRISM UNDER ECCENTRICITY e = t/6

axial capacity was obtained (See Chapter 3).

TABLE 5.7: RESULTS OF ECCENTRIC LOADING TESTS (SERIES DS8)

SERIES NO.	MORTAR STRENGTH (MPa)	ECCENTRIC COMPRESSION TEST ULT. LOAD (kN)	MEAN LOAD-Pe (kN)	C.O.V. (%)	Pe/Po
DS8-10	7.4 [11.7]	511.0 510.0 514.0 482.0	504.3	3.0	0.85
DS8-21	10.2 [10.4]	405.0 373.0 376.0 416.0 350.0	384.0	6.9	0.76

Po= mean concentric load from Series S0

As was expected, because the eccentricity was within the kern point, no axial tensile strains were recorded at the less highly compressed side of the prism. The stress-strain relationships for the eccentrically loaded prisms were plotted in Figure 5.11. Near failure and at the same load level, the axial strains at the extreme fibre of the compression face of eccentrically loaded prisms were around 60% and 90% higher than those in axially loaded prisms for Companies 10 and 21, respectively. Such differences are much higher than the 30% difference reported in test data[69] for the same eccentricity but agree with other data[116].

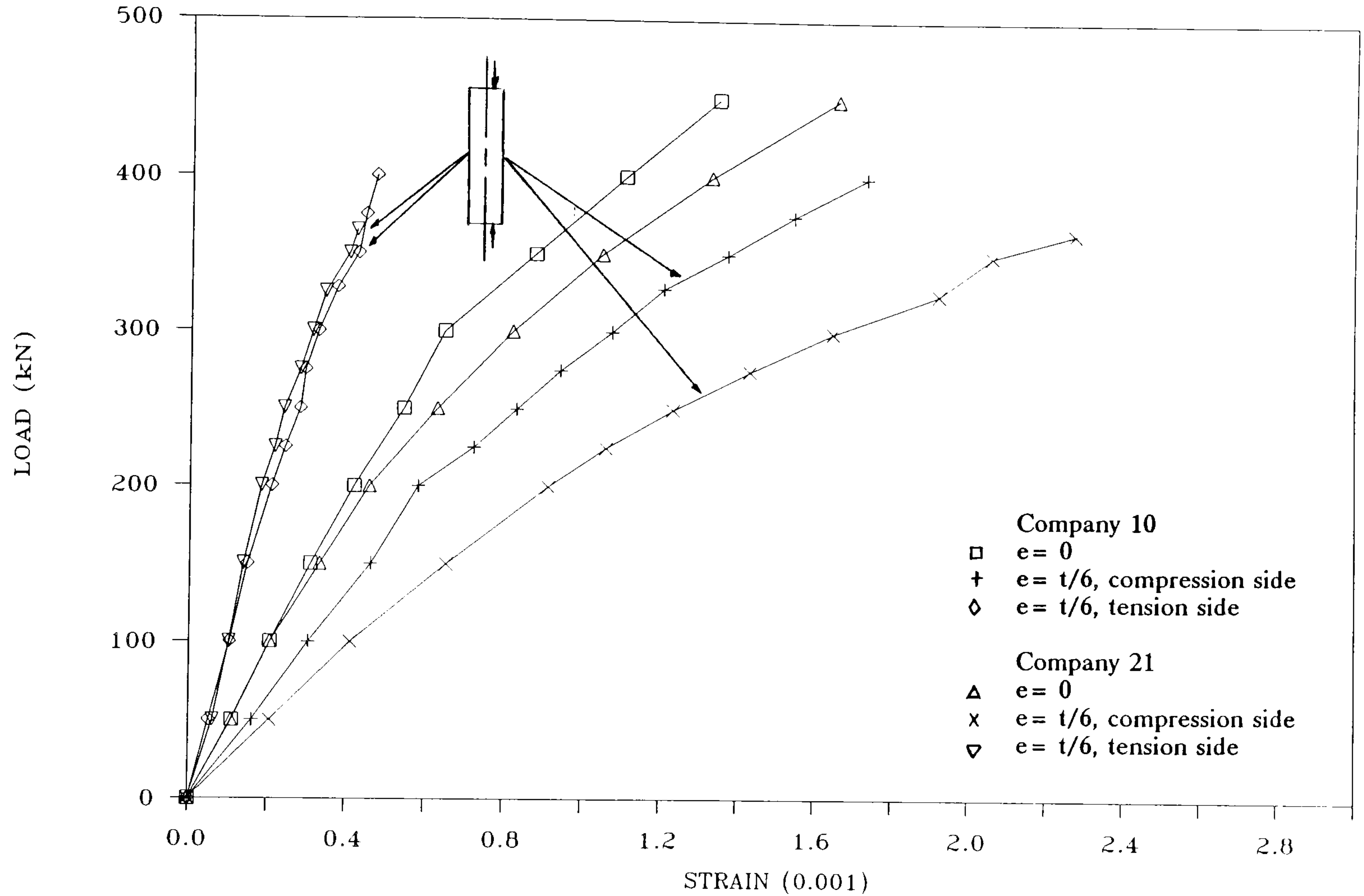

FIGURE 5.11 LOAD-STRAIN RELATIONSHIPS FOR ECCENTRICALLY (e=t/6) AND CONCENTRICALLY LOADED PRISMS

5.4 EVALUATION OF CODE PROVISIONS

5.4.1 Hollow Concrete Blockwork

The 4-course prism strength data presented for hollow block sizes shown in Figure 5.12 as a function of block compressive strength indicates reasonable correlation between the two strengths independent of block size. The code provisions[26] also plotted indicate a somewhat conservative approach for high strength blocks. When it is considered that the code provisions were based on 2 block high prisms, the code is even more conservative. However as indicated earlier, the strength of 240 mm and 290 block prisms from Company 10 may be artificially high since large cracks developed at 50-70% of the load. Furthermore, once the coefficients of variation are incorporated into the results to obtain the characteristic strengths as specified by CAN-3-S304-M84,[26] Clause 5.3.2.2, the points shown in Figure 5.12 are expected to fall slightly.

5.4.2 Solid Blockwork

The evident difference in the behaviour of hollow (face shell mortared) and solid blockwork justify the treatment of each type separately as specified in CAN3-S304-M84[26]. However, as shown in Figure 5.13, based on the results in this research (obtained from 4-course prism tests) and

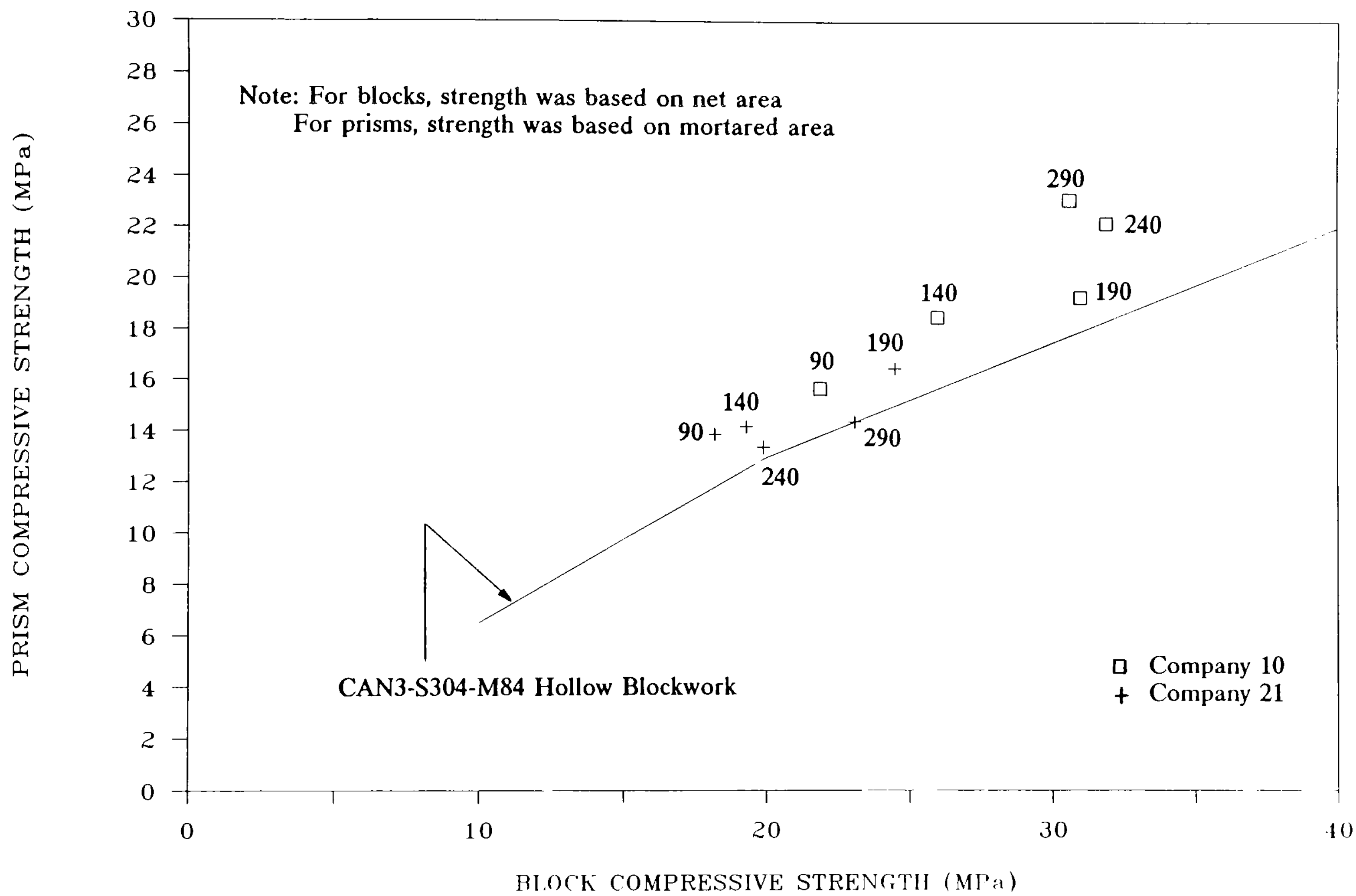

FIGURE 5.12 HOLLOW BLOCK PRISM COMPRESSIVE STRENGTH VERSUS BLOCK COMPRESSIVE STRENGTH

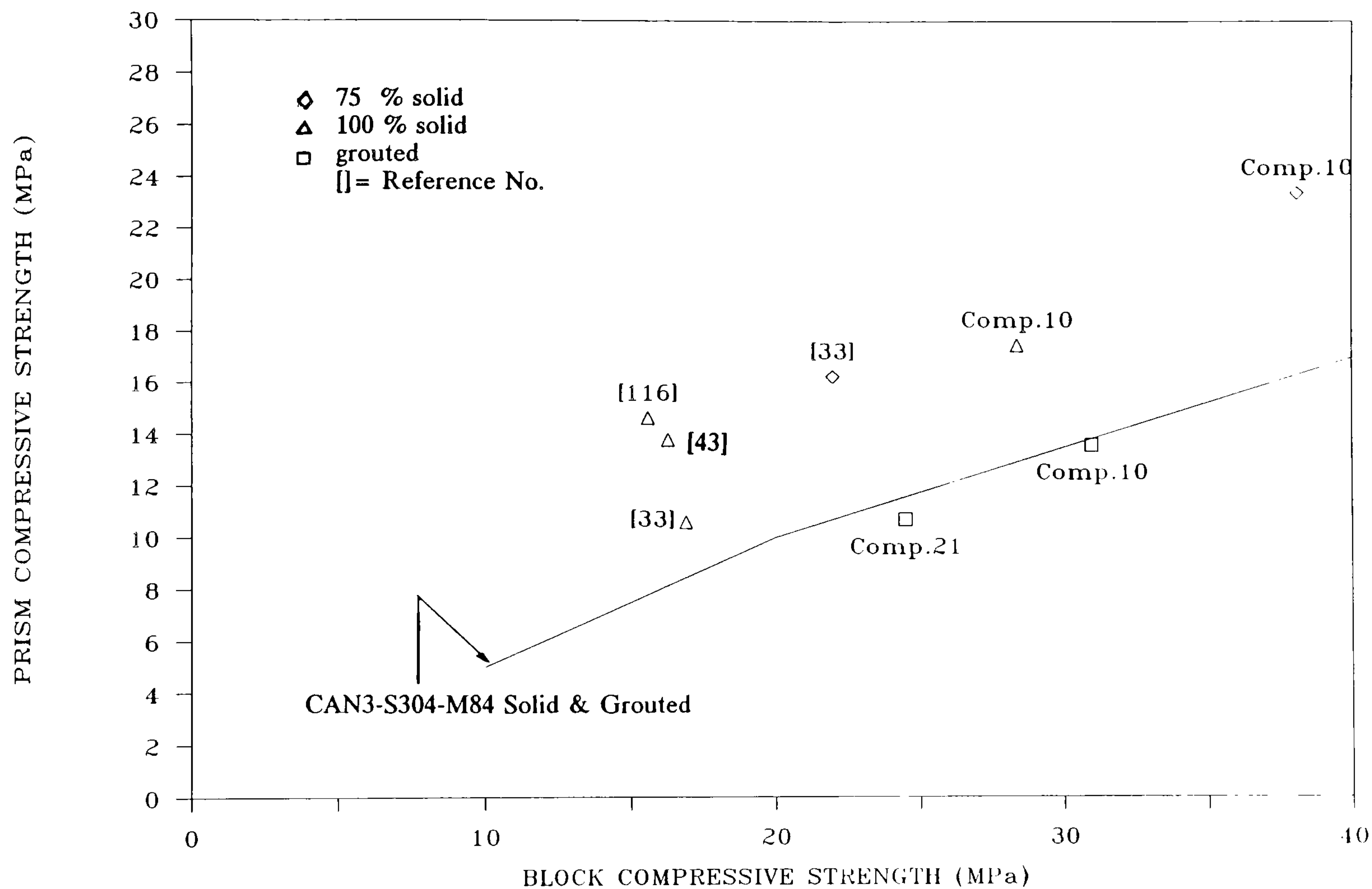

FIGURE 5.13 SOLID BLOCK AND GROUTED PRISM COMPRESSIVE STRENGTHS VERSUS BLOCK COMPRESSIVE STRENGTH

other test data[33,43,116] the allowable strength values for solid blockwork as specified by the code[26] are fairly conservative. The allowable strength values for solid blockwork are 23% lower than those specified for hollow masonry in comparison with only 10% lower in the 1978 edition of the code[26]. It appears that a reinstatement of the 10% difference in the tabular code values for solid blockwork would be reasonable. In a discussion with A.H.P. Maurenbrecher of the National Research Council of Canada, he indicated that lower values for solid masonry were specified to account for the common practice by masons not to lay mortar over the full surface of solid blockwork. Increases to the current allowable compressive strength may be possible along with strict workmanship control.

5.4.3 Grouted Blockwork

As indicated earlier and as shown in Figure 5.13 where the grouted prism strengths fell below the code allowable strength values for solid blockwork, there is no apparent merit in equating grouted and solid blockwork as specified by the code[26]. An alternative approach of relating the strength of grouted blockwork to that of hollow blockwork would be more acceptable since while there is no relationship between the characteristics of the units used in solid and grouted blockwork, the same hollow units are used in hollow and grouted construction. In addition, it is common to employ partial grouting in hollow construction. The ratio of strength for grouted to hollow blockwork ranged between 0.60 and 0.77[33,116]. Therefore a reduction factor of, for example, 0.6 could possibly be employed. Different factors may be derived for different grout strengths. This alternative would also permit separate allowable compressive strengths to be derived for solid blockwork without having such values artificially lowered to accommodate strength values for grouted blockwork.

5.4.4 Modulus of Elasticity

Table 5.6 contains the moduli of elasticity for the various prisms examined in this research along with the ratios of the modulus E_m, to the prism strength, f'_m, (stiffness coefficient K). Only for grouted prisms did the code[26] equation, $E_m = 1000 f'_m$ appear to be valid in contrast to some suggestions indicating otherwise[47]. For various block size and solid prisms, this equation appeared to result in a significantly overestimated modulus of elasticity. A statistical analysis was used to assess the relationship between the modulus of elasticity and compressive strength, except for grouted prisms. It appears that a moderate relationship (correlation = 0.70) can be drawn between the two parameters. This relationship was found to be $E_m = 770 f'_m$.

5.4.5 Eccentric Loading

The current Canadian code[26] provisions regarding eccentric loading were based on data for solid brick masonry[35,69,113]. These may be used for all masonry types including solid, grouted and hollow blockwork and are based on linear elastic stress distribution. Elastic analysis has been found to underestimate the load capacity of eccentrically loaded masonry prisms. Therefore an empirical magnification factor has been applied to the failure stress derived from axially loaded prisms[26]. This magnification factor was introduced to take into account the effect of the so-called "strain gradient". This effect is characterized by higher apparent compressive value stresses for eccentrically loaded prisms than for concentrically loaded prisms.

For hollow blockwork (mainly face shell mortaring), the ratio of eccentric to axial failure stress obtained from various test data varied widely. Some have suggested that the strain gradient effect on hollow blockwork is quite small, with ratio being around 1.10[33,35]. Others have reported large ratios, sometimes over 2.0[37,104]. An elastic analysis, presented in Appendix D, was used to obtain the compressive stress under eccentric loading of $e = t/6$. On this basis, the eccentric failure stress and the ratio of eccentric to axial load based on different interpretations of the location of the controlling stress and the area in use for the calculation were listed in Table 5.8. It can be seen that the ratio varied according to the method of calculation. It is logical to obtain the stress at mid-width of the mortared face shell instead of the extreme fibre since the stress across the width of the more compressed face shell can be assumed to be nearly uniform up to an eccentricity beyond the centre of this face shell[33]. The use of the minimum face shell area would result in significantly higher failure stress for eccentric loading. As a result, some researchers have concluded that in eccentrically loaded prisms, failure would occur when the unit compressive strength is reached[48]. It appears that the high ratios of eccentric to axial stress reported can be attributed to different methods used to calculate such stresses. Furthermore, improper testing procedure and ill defined end conditions would further increase such ratios[69]. The stress averaging approach suggested by Beccia[12] provided stress ratios similar to that using the mortar bedded area with uniform stress across the face shell.

In determining the strength of eccentrically loaded prisms using an elastic design method, it appears that an empirical magnification factor is needed to modify the axial strength. However if the mortar bedded area is used in the calculation, the code value of 1.30 is high for eccentric loading at $e = t/6$. Perhaps a lower value should be

TABLE 5.8: COMPRESSIVE FAILURE STRESS AT AN ECCENTRICITY e= t/6

DESCRIPTION OF STRESS CALCULATION UNDER ECCENTRIC LOADGING	COMPANY 10		COMPANY 21	
	ECCENT. FAILURE STRESS (MPa)	RATIO TO AXIAL STRESS	ECCENT. FAILURE STRESS (MPa)	RATIO TO AXIAL STRESS
Mid Side Stress; Motared area	23.18	1.20	17.65	1.07
Extreme Fibre Stress; Mortared Area	24.94	1.30	19.00	1.15
Mid Side Stress; Minimum Area	28.20	-	21.47	-
Extreme Fibre Stress; Mortared Area	29.80	-	22.71	-
Stress Averaging Method (Ref. 12)	23.34	1.21	17.77	1.08
	COMPANY 10		COMPANY 21	
Axial Stress,e= 0; Mortared area (MPa)	19.3		16.5	
Block Compressive Strength (MPa)	31.0		24.5	

considered. In terms of the ultimate capacity, the experimental results were compared against the code specified reduction factors, for an equal eccentricity top and bottom, as shown in Figure 5.14. The reduction factor for an eccentricity of e = t/6 based on ultimate strength analysis using a rectangular stress block (See appendix D) was also shown in Figure 5.14. It appears that there is little difference in the code reduction factor based on elastic analysis versus plastic analysis for face shell mortared blockwork. This is mainly because the compression face shell is at nearly uniform compression across its width in both types of analysis. Nevertheless it appears that the code correction factor is slightly conservative.

5.5 EVALUATION OF PROPOSED ANALYTICAL FORMULATION FOR DETERMINING CONCRETE MASONRY COMPRESSIVE STRENGTH

Based on an approach developed by Hilsdorf's[54] to analytically determine the compressive strength of solid brick masonry prisms, Hamid and Drysdale[32] proposed a formulation employing strength analysis to predict the compressive strength of grouted concrete masonry using the properties of its constituents. Formulations were also derived to predict the strength of solid and hollow concrete masonry. Discussion regarding Hilsdorf's and Hamid and Drysdale approaches can also be found in Chapter 3.

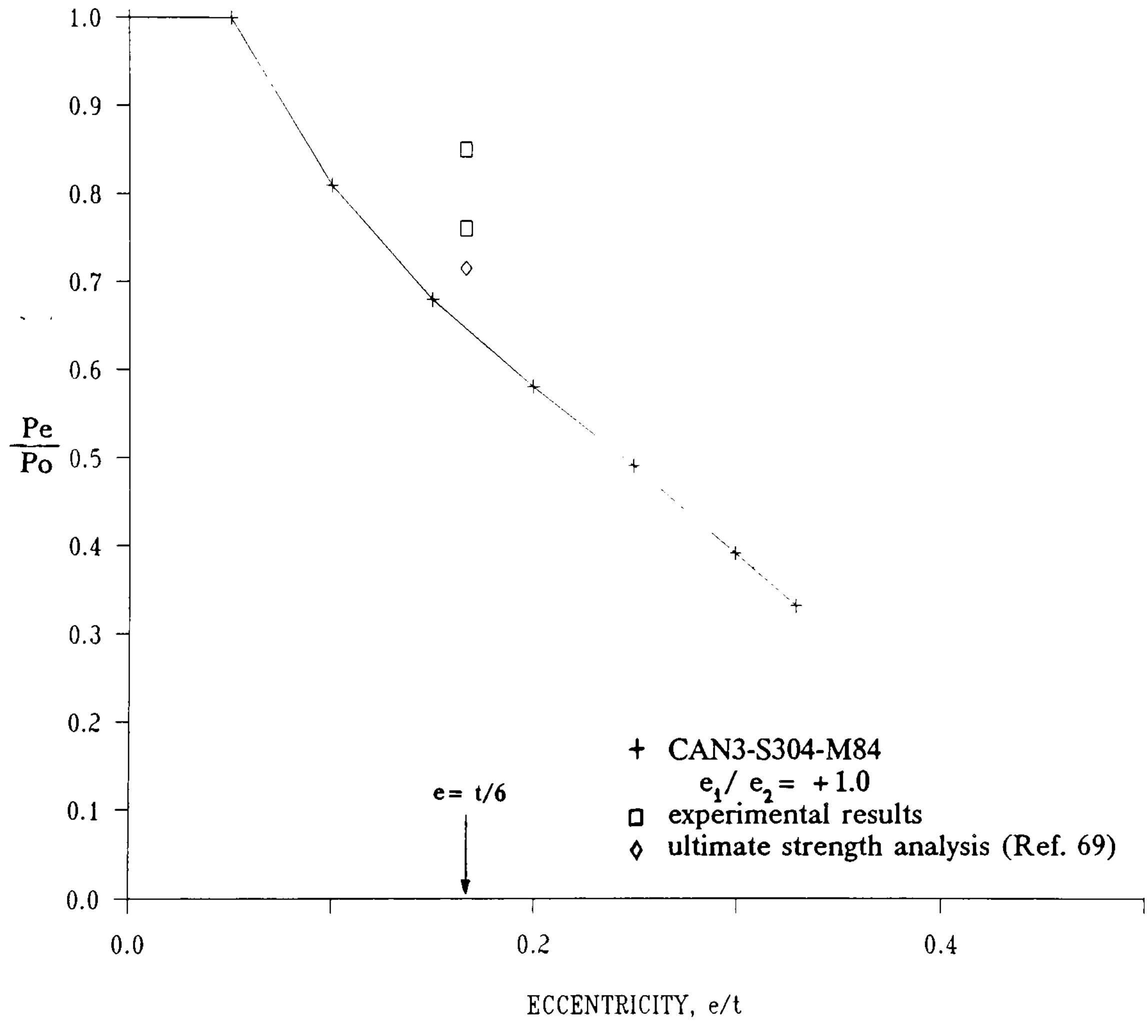

FIGURE 5.14 CAPACITY OF ECCENTRICALLY LOADED PRISMS

These formulas present the only analytical approach available for evaluating grouted masonry. However because the formulations presented for hollow and solid masonry assume fully mortared joints, they are not applicable to face shell mortared masonry. The proposed formulations[32] for grouted and solid masonry were examined by comparing the predicted strengths with the results in this investigation. Detailed calculations were reproduced in Appendix D.

Figure 5.15 contains both the predicted compressive strengths using the analytical formulations[32] and the experimental prism strengths for grouted and plain blockwork with full mortar bedding. For grouted masonry, the analytical formulations predicted relatively high strength values, around 55% higher. Examining the formulations indicated that the unit compressive strength was the most significant parameter influencing the compressive strength of grouted prisms. However given the observed cracking mode of failure, it can be suggested that the unit tensile properties should be the most significant parameter[17,55,72] and the fact that relatively high strengths were predicted is attributed to the insensitivity of the formulations to the unit tensile strength. For example, by reducing the unit tensile strength by 50% the predicted prism strength is only reduced by around 10%, however reducing the unit compressive strength by 50% would result in around 50% reduction of the predicted

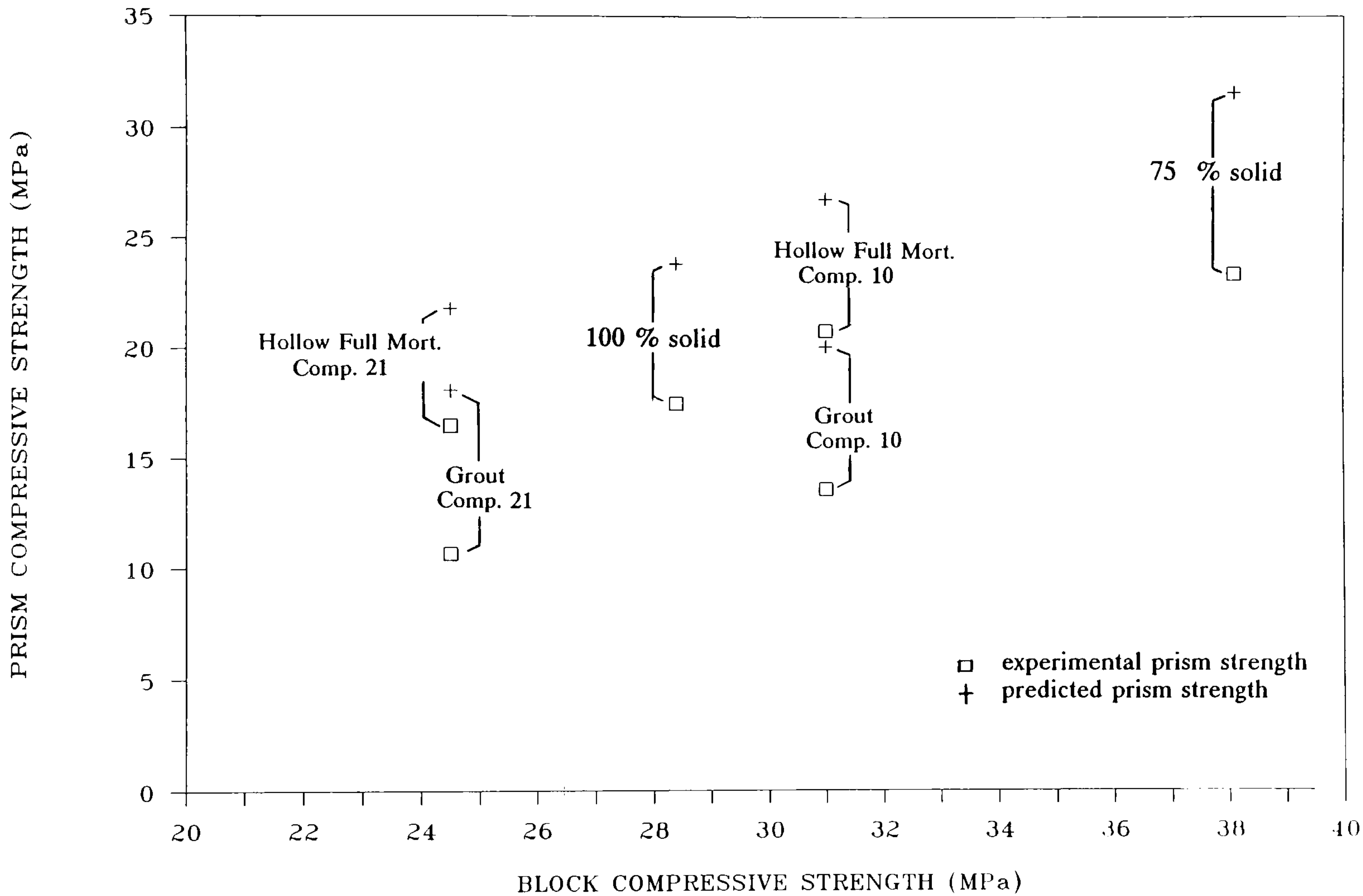

FIGURE 5.15 COMPARISON BETWEEN EXPERIMENTAL AND ANALYTICALLY PREDICTED PRISM COMPRESSIVE STRENGTHS

prism strength.

The above trend was also found for solid and fully mortared hollow blockwork. Predicted strengths were around 33% higher than the experimental results. Again it can be argued that the formulations do not fully reflect the importance of the block's tensile strength.

Suggestions have been made[98] that using approaches similar to Hilsdorf's method results in relatively low ratios of lateral tensile stress of failure in the units to the applied vertical stress. Ratios of 1:50, 1:33, 1:20 were calculated[98,109,33] in comparison with experimentally obtained ratios of the unit tensile strength to the prism failure stress of 1:3 to 1:10[98]. Therefore it is suggested that failure criteria should place more emphasis on tensile properties.

5.6 CONCLUSIONS

1. Regardless of the hollow block size, cracking of the web is the failure pattern in face shell mortared masonry. More extensive web cracking occurred in prisms made with larger blocks. There was a tendency for full web cracking to occur at lower stress levels for larger blocks.

2. Prisms built in running bond with 90 mm blocks failed in a different mechanism than larger block prisms since full mortar bed joints were usually achieved in the former.

3. The efficiency ratio for hollow block face shell mortared prisms appears to be reasonably consistent, around 0.70, for different block sizes.

4. A strong relationship existed between the compressive strength of hollow block face shell mortared prisms and tensile splitting strength of the blocks.

5. Solid masonry fails in a different mode than face shell mortared masonry. With the increase in the block solid percent the failure gradually transferred from web cracking to face shell cracking alone. The block strengths for 75% and 100% solid blocks as a ratio of the block strength were essentially the same.

6. For 75% and 100% solid blocks, the code specified strength values for solid masonry are conservative especially for 75% solid prisms. Other test data confirms this observation.

7. Grouted prisms had significantly lower compressive strengths compared to hollow block prisms. For the same strong grout, the compressive strength of grouted prisms improved appreciably by using blocks with higher strength characteristics.

8. Based on a difference in failure modes, compressive strengths and axial deformations, the behaviour of grouted prisms was significantly different from that of solid masonry especially 75% solid prisms. Therefore the code

approach of specifying the same compressive strengths for both types of blockwork is questioned. In fact this approach results in overestimated strength values for grouted masonry.

9. A reasonably good relationship can be established between the modulus of elasticity and compressive strength (correlation r = 0.70), for face shell mortared prisms made with various block sizes. However the relationship is far below the code equation, $E_m = 1000\ f'_m$. Only data from grouted prisms agreed with the code relationship for modulus of elasticity.

10. Face shell mortared prisms under eccentricity e = t/6 failed by developing web cracking first then spalling of the most highly compressed face shell. Under eccentric loading axial compressive strains were 60% higher than those under eccentric loading. The capacity of prisms under eccentric loading appears to depend on the unit strength characteristics. Based on mortar bedded area and uniform stress across the face shell width, ratios of 1.20 and 1.07 were obtained at an eccentricity of e = t/6.

11. Predicting the strength of grouted masonry prisms on the basis of its constituent materials using proposed analytical formulations[32] resulted in relatively higher strength values.

5.7 RECOMMENDATIONS

1. Further work is needed to examine the influence of prism height for larger blocks. Prisms higher than 4 courses may be considered.

2. Increasing the code[26] allowable strengths for solid masonry appears to be justifiable.

3. The modulus of elasticity for various block sizes and solid blockwork determined by multiplying the prism compressive strength by a factor between 700 and 800 is more representative than the code specified value of 1000.

4. Inclusion of a clause in the code requiring full mortar bedding in solid masonry is needed along with some strict workmanship control requirements.

5. There is a merit in treating solid and grouted masonry separately. Determining allowable strength values for grouted masonry based on the strength of hollow blockwork offers a promising alternative.

CHAPTER 6

QUANTITATIVE ASSESSMENT OF COMPRESSIVE STRENGTH OF FACE SHELL MORTARED CONCRETE BLOCK PRISMS

6.1 INTRODUCTION

6.1.1 General

The current edition of the Canadian masonry design standard[26] incorporated changes which affected the load-bearing capacity of face shell mortared hollow concrete block construction. In the 1978 edition, the allowable compressive strengths were not directly based on tests on concrete masonry. In fact the tabulated values were based on relatively old data obtained from ASA-A41.2-1960, "Building code requirements for reinforced masonry" which specified one set of tabular values for masonry using solid or hollow clay or concrete units[67]. In addition, the axial load capacity of walls was based on the net cross-sectional area of the units used in the wall whereas the effective mortar bedded area is now specified. This has meant that if the old allowable stress values in the 1978 edition were retained, lower axial load capacities would have resulted for face shell mortared masonry; a concern shared by designers and the masonry industry. Therefore, other changes were also introduced in the current edition to accommodate this concern. Based on test data on concrete block masonry from North American research, a new set of tabular values was drafted[26,67]. Essentially, there was little change in the strength values for blockwork using 15 to 20 MPa blocks while relatively higher allowable strengths were introduced for blockwork with high strength units. Discussion of the revisions to CAN3-S304-M78 was provided by Maurenbrecher[67].

To further offset the influence of using the mortar bedded area, the allowable axial compressive stress was increased from 0.225 to 0.25 of the strength in the 1984 edition. The allowable stress was further increased to 0.30 in a subsequent revision so that there is no distinction between allowable axial and flexural compressive stresses for hollow blockwork. In part this recognized that the "strain gradient effect" was not very significant for hollow blockwork[33,35].

For 15 MPa hollow 190 mm concrete blocks, which accounts for the majority of plain concrete construction, the compressive strength changed from 10 MPa in the 1978 code to 9.8 MPa in the current edition. Combined with the smaller area, the axial load capacity of walls determined according to the current code would be lower despite the increase in allowable stress. This is mainly attributed to a decrease of around 35% in area from that of the net block area. The mortar bedded area based on the minimum face shell area would give an axial capacity 20% lower than obtained using the 1978 code. Therefore a further adjustment to use the effective mortared area was introduced. For standard stretcher units with pear shaped cores, this resulted in a 23% increase in area for face shell mortaring and running bond (See Chapter 3).

To develop compressive strength values for the building code, it is necessary to have data which

1. Incorporates a broad base of materials representative of manufacturing differences.
2. Uses representative specimen configurations.
3. Employs reasonably accurate test methods and well defined boundary conditions.
4. Represents current manufacturing technology since quality control and curing processes have improved substantially in the past decade.

In order that old data may be excluded, it is necessary to provide new data which incorporates the above requirements. Although the investigations outlined in the previous Chapters have covered almost every aspect of the behaviour of face shell mortared concrete masonry (along with some other aspects of concrete masonry in general), the overall impact on the Canadian design code[26] will be somewhat limited by the fact that only two different sources of blocks were used. Therefore it was necessary to expand the scope of the test program to include many more sources of blocks but tested only in standard configurations.

6.1.2 Objectives and Scope

In addition to providing confirmation of some of the other important findings of this research program, it was the intent of this part of the investigation to evaluate the compressive strengths specified in the current code[26] for face shell mortared hollow concrete masonry. Based on blocks from 29 different manufacturing plants, it was the objective of this investigation to:

.evaluate the current specified compressive strengths for hollow face shell mortared masonry in the Canadian masonry design standard[26],

.develop representative compressive strength values, covering a broad base of materials, for future implementation in CAN3-S304[26],

.examine the relationship between the prism compressive strength and the tensile and compressive strengths of the blocks,

.quantitatively study the correlation between the assemblage modulus of elasticity and its compressive strength,

.quantitatively determine the relationship between the compressive strengths of 4-course prisms in running bond and 2-course stack bond prisms with face shell and full mortared bed joints.

Nominal 15 MPa compressive strength blocks account for the majority of blockwork construction in Canada. Therefore, in co-operation with the Ontario Concrete Block Association (OCBA), 29 block manufacturing plants each supplied one pallet of their 15 MPa, 190 mm hollow blocks. Each Company was also asked to provide a sample of the common masonry sand from their area. For every company a set of 4-course high, one unit long prisms were built in running bond using mortar made with the corresponding company sand [Note: Only 19 companies supplied their own sand. For the other 10 companies McMaster masonry sand was used]. These prisms were to be tested in axial compression. A Portland Cement-Masonry Cement mixture was used in making mortar to reflect the growing preference for masonry cement in the construction industry in Ontario (See Chapter 2).

To quantitatively determine the relationship between the strengths of 4-course running bond prisms and the commonly used 2 course stack bond prisms, several sets of five 2-course stack bond prisms were also built. For 7 different companies (out of the 29 companies) 2-course stack bond prisms with face shell mortaring were made. In addition for 5 out of these 7 companies, sets of 2-course stack bond prisms with fully mortared bed joints were also built.

To relate the mechanical properties of the component materials to those of the assemblage it was decided that compression and tensile tests on the units and mortar would have to be performed for every company. Compression tests on 10 single units, fully hard capped and loaded flatwise were performed. Splitting tension tests on 10 half units with the load applied across the face shells were also carried out to obtain the unit tensile strength. In view of the already large investigation program, it was decided not to also test for web tensile splitting strength but as discussed in Chapter 2, the potential differences should be kept in mind.

Axial deformations were measured across a block-and-joint in three out of the five prisms, for every company, in order to develop the characteristic experimental modulus of elasticity.

6.2 MATERIALS, FABRICATION AND PRISM TESTING

6.2.1 Materials

Concrete Blocks: Among the 29 different block sources, two distinct shapes can be identified. For most, the units had pear shaped cores and flared tops while for some companies units with a pear shaped cores but without flares were also identified. Discussion regarding the unit shape can be found in Chapter 2. The physical characteristics including the block shape, nominal area used in calculating the unit compressive strength, manufacturing curing process and weight were listed in Table E1.1 in Appendix E.

Compression tests were carried out as described in Section A1.2 (Series C10-1) at an age comparable to the prism tests. The date of receiving the blocks as well as that of testing were listed in Tables E2.1 to E2.29 for every Company numbered from 1 to 29.

Splitting tension tests were carried out as described in Appendix A and shown in Figure A2.1. The tensile strength was calculated using Equation A2.1 in Appendix A and the individual results were listed in Tables E2.1 to E2.29.

Mortar: Type S2 mortar using the sand supplied by each individual company was employed throughout. Analyses of the various sands can be found in Chapter 2. The mortar compressive strengths based on three air cured, standard size cubes were listed in Tables E2.1 to E2.29 for each company.

6.2.2 Prism Fabrication and Test Procedure

The various units were stored inside the laboratory for a sufficient period of time to allow to dry before construction began. The prisms were built by an experienced mason as described in Section 3.2.2. Construction took place during the first week of February with temperature in the laboratory being around 20^{0}C and relative humidity around 20%. Mortar was mixed to achieve a consistency desired by the mason. Further details regarding the various aspects of mortar were presented in Chapter 2 where the same numbering system regarding the sand and mortar properties was also used. Prisms were air cured under laboratory conditions for a minimum one month period or until testing. Prism fabrication and test dates were also shown in Tables E2.1 to E2.29.

Testing with full bed Hydrostone capping was used throughout as described in Section 3.2.4. The prism test set-up was shown in Figure 3.5. Axial deformations across block-and-joint (strain no.2 in Figure 3.3) were monitored in 3 out of every 5 prisms with measurements taken at opposite sides. Strain measurements were recorded up to around 50% of the ultimate load.

6.3 EXPERIMENTAL RESULTS

6.3.1 General

The individual block, mortar and prisms test results for every block company were listed in Appendix E. A summary of these results including the units' mean compressive and tensile strengths and the 4-course prism mean strengths along with the coefficients of variation was listed in Table 6.1. The prism strength was based on the mortar bedded area which corresponds to the minimum face shell area plus 23% or an equivalent 39.4 mm thick face shell.

TABLE 6.1: SUMMARY OF BLOCK AND 4-COURSE PRISM TEST RESULTS FOR 29 BLOCK COMPANIES

BLOCK COMPANY NO.	BLOCK MEAN STRENGTH		4-COURSE PRISM COMPRESSION		SECANT MODULUS OF ELAS. E (MPa)
	COMP. (MPa)	TENSILE (MPa)	MEAN STR. (MPa)	C.O.V. (%)	
1	28.8	2.20	20.4	3.4	12900
2	29.3	2.90	20.5	5.9	16600
3	30.5	2.50	19.9	9.6	16000
4	27.1	2.10	18.8	6.6	13600
5	27.0	2.30	18.4	5.1	12900
6	18.8	1.30	11.7	6.0	11200
7	22.9	2.10	13.8	7.9	14900
8	20.6	1.80	13.2	5.3	8800
9	30.1	2.50	20.0	3.6	15200
10	31.0	2.60	20.8	5.1	15600
11	23.8	2.20	16.2	10.7	13600
12	22.0	2.00	12.8	0.6	13700
13	19.5	1.10	10.2	1.6	12900
14	26.6	2.10	16.7	4.6	13000
15	36.5	2.90	21.3	8.1	17100
16	39.1	3.30	24.2	7.5	15700
17	30.6	2.20	18.3	11.6	12300
18	32.0	2.70	22.7	9.5	18200
19	29.3	2.10	16.5	6.9	9600
20	22.3	1.60	12.7	8.2	14400
21	24.5	2.30	16.3	9.0	10400
22	30.6	1.80	17.3	8.0	5300
23	38.5	2.60	22.8	2.2	15700
24	38.6	2.70	22.5	4.8	14500
25	23.4	1.90	13.9	3.7	12400
26	34.8	2.80	16.7	8.1	9600
27	25.8	2.50	18.4	4.0	10900
28	30.0	2.60	19.0	7.2	15600
29	21.0	1.80	14.8	8.5	12000
n	10	10	5		

n = number of tests
individual results are found in Tables E2.1 to E2.29

The summary of the results for the 2-course prisms built with face shell and full mortaring for the selected block plants was listed in Table 6.2. For prisms with fully mortared bed joints, the minimum net area was used in strength calculations. If net area defined in other ways was used instead, strength values would be lower depending on the shape of individual company blocks (See Table E1.1).

6.3.2 Prism Failure Patterns

The observed failure modes for the 4-course prisms confirmed that web cracking is the expected crack pattern in face shell mortared blockwork. Nevertheless the crack pattern varied with the individual company prisms. For most, web cracking was limited to the second and third courses and often in a direction parallel to the applied load. For some companies, small web cracks were observed in the end blocks. In general the webs developed cracks at around 80% of the ultimate load. However it appears that for prisms with high-strength units, cracks would occur at a lower percentage of the ultimate load. However prisms continued to resist increasing load after the webs cracked. Splitting and spalling of the prism face shells were also observed in some instances.

The 2-course stack bond prisms tended to fail by developing a shearing action in one or both face shells. For

TABLE 6.2: TWO-COURSE STACK PATTERN PRISMS TEST RESULTS

COMPANY NO.	PRISM COMPRESSION TEST					
	FACE SHELL MORTARING			FULL MORTARING		
	ULT.* LOAD (kN)	COV (%)	MEAN STRENGTH (MPa)	ULT.* LOAD (kN)	COV (%)	MEAN STRENGTH (MPa)
3	740.0	4.9	24.1	906.0	5.1	23.8
5	727.6	2.7	23.7	939.6	7.3	24.7
11	566.4	3.4	18.4	718.6	6.4	18.9
16	848.4	9.2	27.6	1072.4	7.3	28.2
17	733.6	5.5	23.9			
27	678.8	4.2	22.1	737.2	9.2	19.4
29	574.6	5.3	18.7			

* Average of 5 prisms
COV= Coefficient of Variation
Face-shell mortared prism strength was based on minimum face-shell area plus 23%.
Full mortared prism strength was based on unit minimum net area of 38028 mm . Strengths calculated based on net area instead, are around 6% lower depending on the individual block source.

face shell mortared prisms fine lines of cracking in the webs were also observed in some instances.

6.3.3 Strength Results

The compressive strengths for the various blocks were much higher than their specified 15 MPa strength. The average strength from the 29 block companies was 28.1 MPa and extremely high strength units (around 40 MPa) were found. Contacted companies indicated that blocks were shipped from their normal manufacturing runs and were not specially chosen for the test program. Unfortunately, the large range of strengths detracted from the ability to concentrate on the specified 15 MPa strength specification which would normally require that blocks have an average strength near 20 MPa.

Prism compressive strengths varied widely from one block company to another. The strength values ranged from 10.2 MPa to as high as 24.2 MPa. It is important to indicate that these extreme prism strength values did in fact correspond to the extreme units' compressive and tensile strength values.

For 2-course stack bond prisms, there was no difference in strength between face shell and fully mortared prisms where the average strength ratio of face shell to full bed was 1.01. This implies that a direct relationship exist between the mortar bedded area and the 2-course prism load capacity. For full mortaring of bed joints, the prism strength was calculated based on the unit minimum area (mortar bedded area), however the average net area of the units has often been used in test data[67]. If this latter area is used here, the strength of face shell mortared prisms would be on average 8% higher than that of prisms with fully mortared bed joints.

In comparison to the compressive strength of 4-course prisms built in running bond, the compressive strength of face shell mortared 2-course, stack bond prisms was on average 22.1% higher for the 7 different blocks used. This comparison was shown in Figure 6.1. This relationship is important if masonry strength is to be obtained from compression tests on 2-course stack bond prisms using the particular test set-up employed here which is also specified by ASTM-E447-84[7]. It is also worth noting that for 2-course prisms with face shell mortaring it was found in Chapter 3 that prism strength would be even higher if face shell hard capping had been used instead of the full capping.

6.3.4 Stress-Strain Relationships

Figure 6.2 contains the stress-strain relationships obtained for the 4-course prisms from the 29 block companies. The linear range of the stress-strain curve extended to between 30-40% of the ultimate strength for 15 block companies

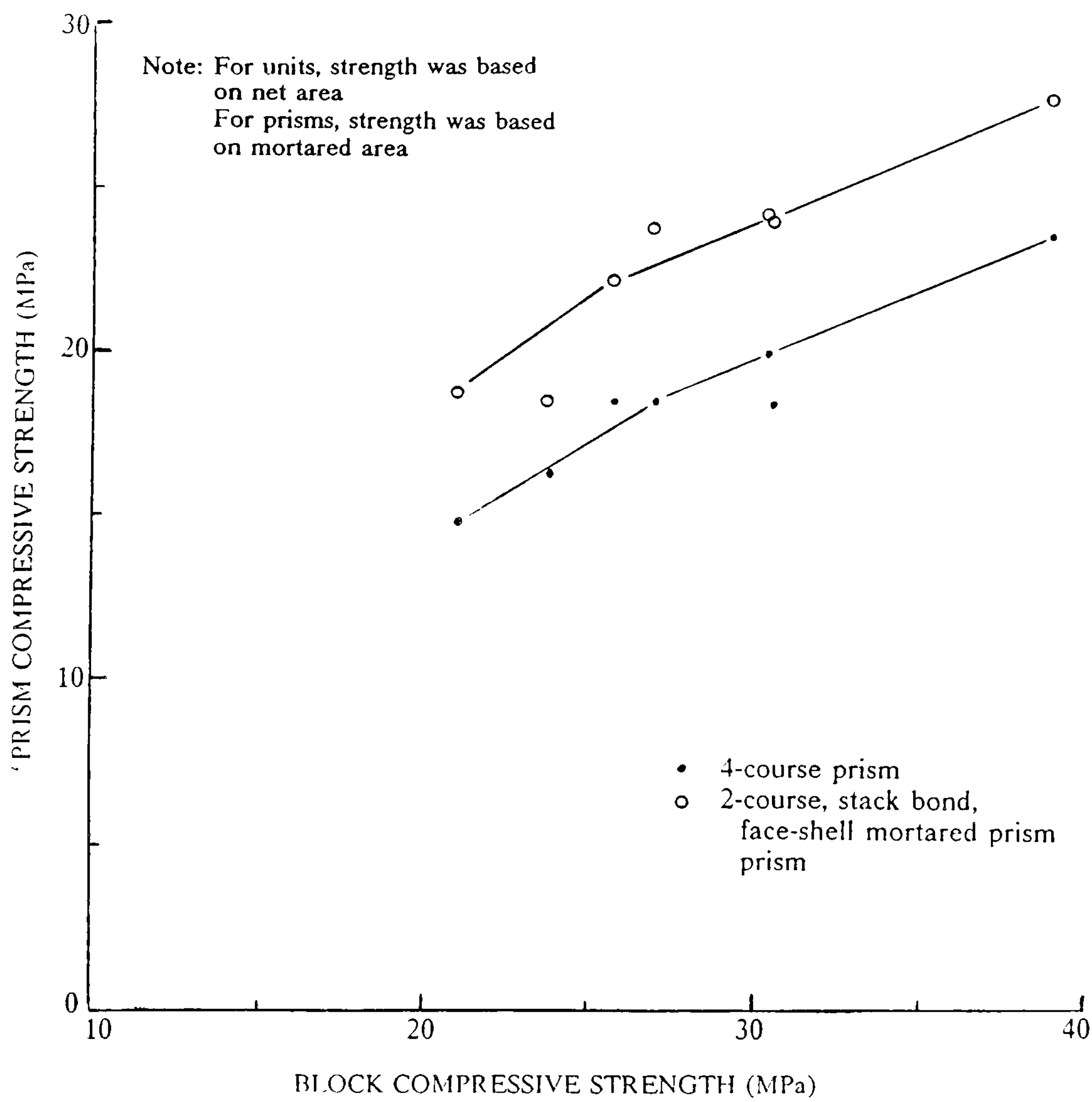

FIGURE 6.1 COMPARISON BETWEEN FACE SHELL MORTARED 2 AND 4 COURSE PRISMS

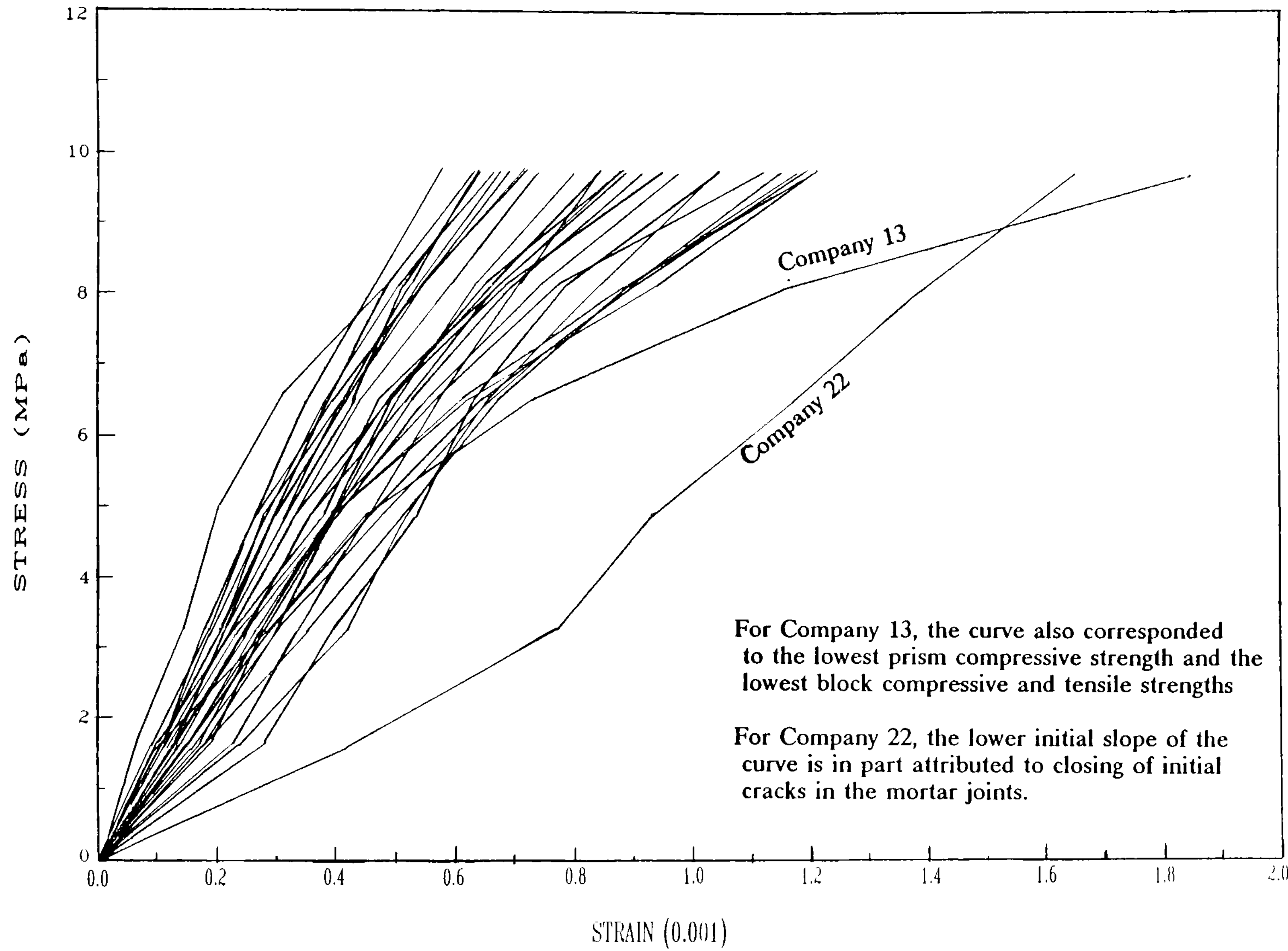

FIGURE 6.2 STRESS-STRAIN RELATIONSHIPS FOR 29 DIFFERENT SETS OF 4-COURSE PRISMS

and between 40-50% for 10 block companies. Three block companies showed almost no linear range in their stress-strain curves while for one block company only, the linear range extended to about 60% of the ultimate strength. Of a particular interest is the stress-strain curve for Company 13 prisms shown in Figure 6.2. Very large strains were obtained compared to the results for other companies. This in fact corresponded to the lowest prism compressive strength and also to the lowest block compressive and tensile strengths. The relatively low initial slope of the stress-strain curve for Company 22 can be attributed to closing of cracks in the mortar joints where a debonding between the units and the mortar occurred during handling of the prisms.

6.4 ANALYSIS AND INTERPRETATION OF RESULTS

6.4.1 Correlation of Block Compressive and Tensile Strengths with Prism Compressive Strengths

In Chapter 4 it was reported that increasing the block's compressive strength did not appear to affect the efficiency ratio (ratio of prism to block compressive strength). However by increasing the block's tensile strength, the efficiency ratio as well as the prism compressive strength were significantly improved. Given the nature of the web cracking failure initiation in face shell mortared blockwork, it seems that in addition to the block's compressive strength, it would be significant to relate the prism strength to the block's tensile properties.

In general, the efficiency ratio or prism to block strength ratio was around 0.63 with a minimum value of 0.48 and a maximum of 0.71. The variation in the prism strengths appears also to follow that of the unit tensile strength which suggests that while a strong relationship appears to exist between the prism and block compressive strengths, a relationship of at least equal significance also exists between the prism strength and the unit tensile strength. For example, for block companies 3, 9, 17 and 22 while the block compressive strengths are virtually equal, the prism compressive strength varied according to the blocks' tensile splitting strength.

A multiple linear regression analysis was employed to assess the relationship between prism strengths and the blocks' compressive and tensile strengths using the results from the 29 block companies. As shown in Figure 6.3(a) a relatively strong linear relationship appears to exist between the prism and the block compressive strengths. The correlation coefficient, r, is 0.885. A similar relationship also exists between the prism strengths and the blocks' tensile splitting strengths as shown in Figure 6.3(b). The correlation coefficient, r, is 0.869.

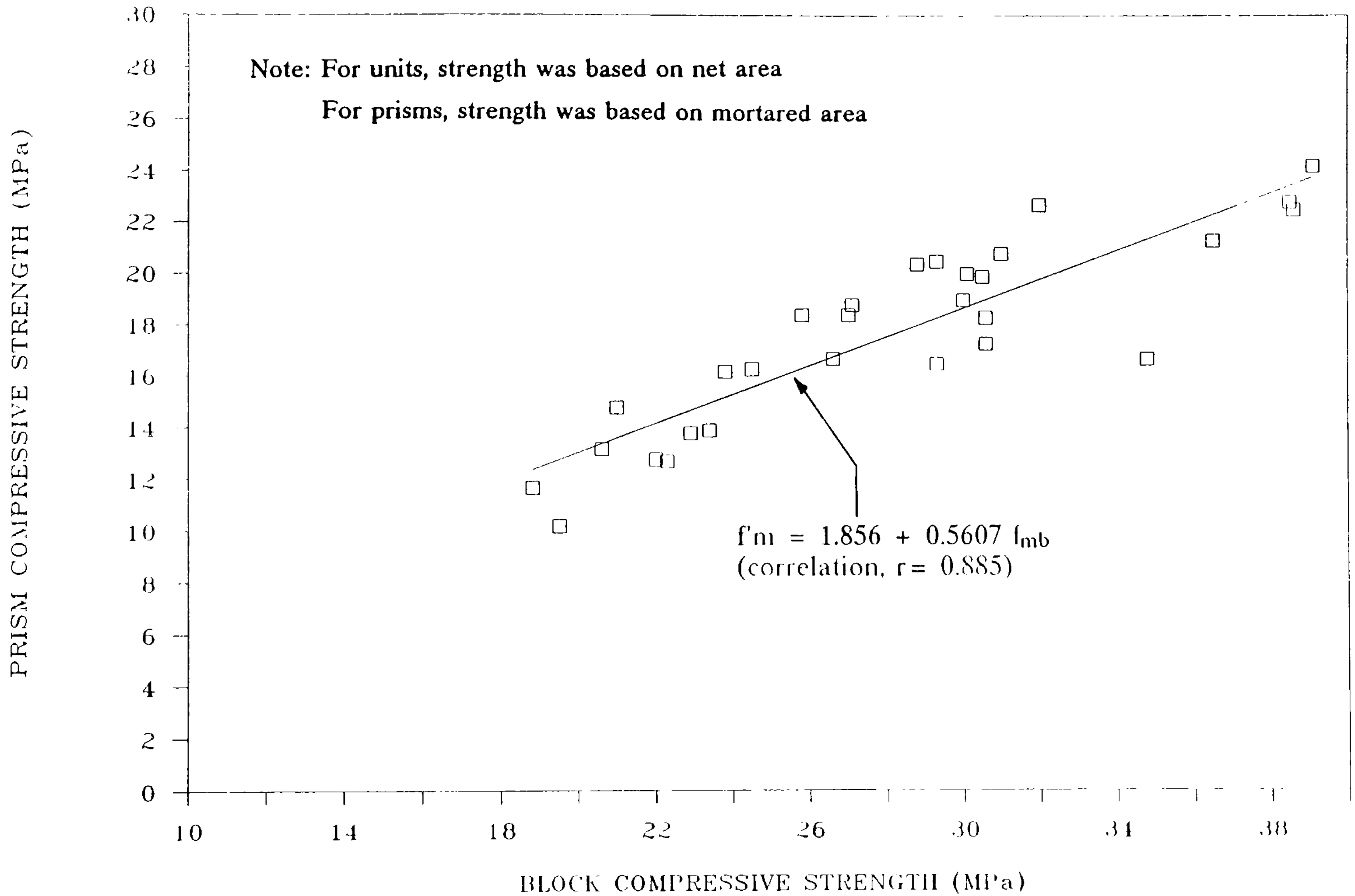

FIGURE 6.3 a) RELATIONSHIP BETWEEN 4-COURSE PRISM AND BLOCK COMPRESSIVE STRENGTHS

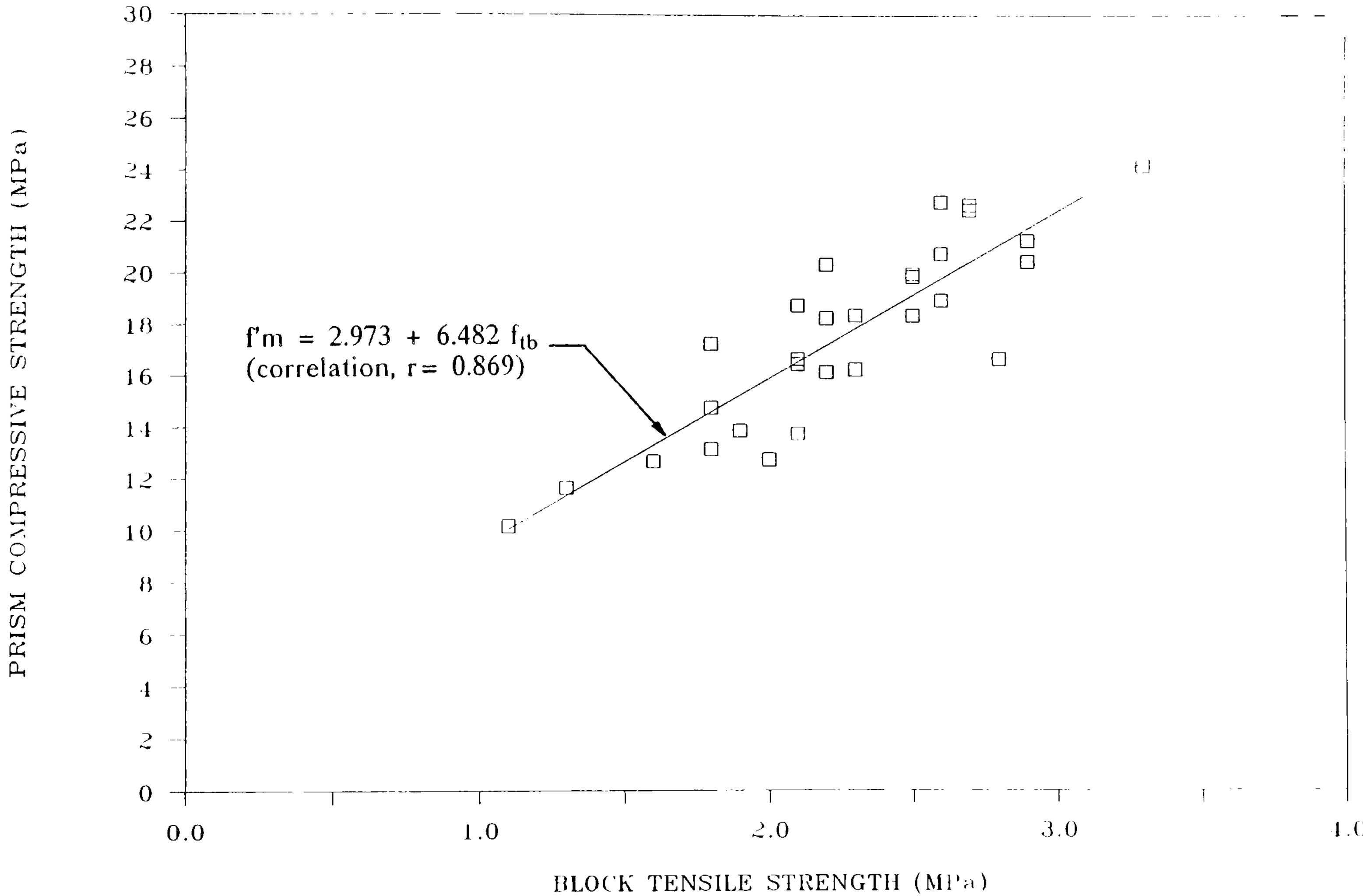

FIGURE 6.3 b) RELATIONSHIP BETWEEN 4-COURSE PRISM COMPRESSIVE STRENGTHS AND BLOCK TENSILE SPLITTING STRENGTHS

Incorporating the unit's two strength characteristics into the analysis would increase the correlation coefficient, r, to 0.918. The equation relating the prism compressive strength, f'_m, to the block's compressive and tensile strengths, f_{mb} and f_{tb} respectively, is:

$$f'_m = 0.931 + 0.334\ f_{mb} + 3.237\ f_{tb} \qquad \text{(Eq. 6.1)}$$

In Figure 6.4 the actual prism compressive strengths were compared to the predicted strengths using Equation 6.1. As can be seen, the compressive strength of face shell mortared prisms with Type S mortar can be predicted with an acceptable degree of accuracy. It is important to indicate that this relationship is not to be taken as a proposed formulation to determine the compressive strength of hollow concrete masonry. It simply reflects the importance of the unit's tensile strength on the prism compressive strength.

The observed influence of the block's tensile strength on the compressive strength of face shell mortared blockwork strongly suggests that the current approach of only relating the prism strength to the compressive strength of the block is questionable. Similar concerns were also raised regarding other types of masonry[17,55].

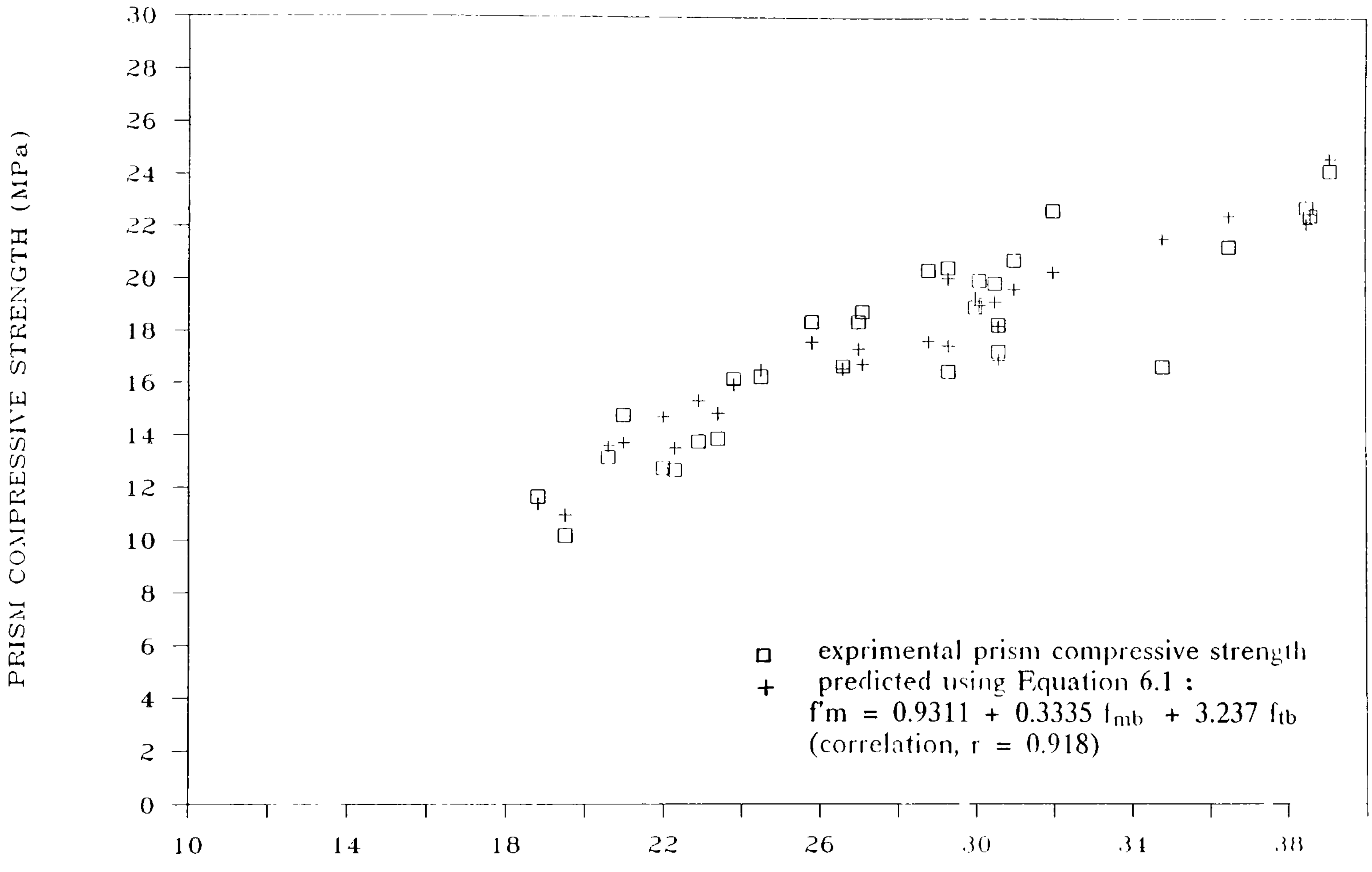

FIGURE 6.4 COMPARISON BETWEEN EXPERIMENTAL AND PREDICTED PRISM COMPRESSIVE STRENGTHS

6.4.2 Influence of Mortar Properties on Prism Compressive Strengths

The relationship between the mortar strength and the properties of the 19 different sands employed in this investigation was examined in Chapter 2. An attempt was made to incorporate the influence of the mortar strength in the statistical analysis carried out in the previous section. However, very little correlation ($r = 0.13$) between prism strength and mortar strength was found for the 29 block companies. This seems to confirm the Chapter 4 observation that for a normal strength mortar, the compressive strength of face shell mortared prisms is controlled by the tensile properties of the block and is relatively independent of the mortar properties.

Some researchers[43,72] have suggested that the assemblage compression capacity is affected by the mortar strength relative to that of the block and not the absolute value of the mortar strength. A review of the 29 block companies results showed that this suggestion is not necessarily true. For example, for the lowest mortar strength to block strength ratio of 0.20 (Company 26) the prism compressive strength of 16.7 MPa was 64% higher than the minimum prism strength. Nevertheless, a moderate correlation, $r = 0.49$, was found between the prism strength and the ratio of the mortar strength to the block compressive strength. Other relationships such as the efficiency ratio (ratio of prism strength to block strength) versus mortar strength [correlation r = 0.48] or versus the mortar strength to the block strength ratio [correlation r = 0.35] did not yield any better correlation.

It is worth noting that in studying the relationship between the mortar strength and the prism strength for the 29 block companies, the properties of the sand should be considered since Type S2 mortar was used throughout and sand was the only variable. Relating the Fineness Modulus of the sand to that of the prism strength showed a poor correlation, r = 0.41. An attempt to study the relationship between the efficiency ratio and the sand Fineness Modulus resulted in a poorer correlation of r = 0.29.

As a result of the above statistical analysis, it may be concluded that there appears to be a little influence of mortar strength (based on the range of the data examined here and for a normal strength mortar) on prism strength. The suggested[43,72] relationship between prism strength and the ratio of the mortar to the block strength were derived from observations of the behaviour of fully mortared blockwork and hence may not be entirely applicable to the face shell mortared case.

6.4.3 Relationship Between the Modulus of Elasticity and Compressive Strength of Prisms

The subject of modulus of elasticity was discussed in previous Chapters where it was indicated that a moderate relationship does exist between the modulus of elasticity and strength for prisms.

The secant moduli of elasticity taken at 0.3 of the ultimate strength were listed in Table 6.1 for the 29 block companies. While the highest prism compressive strength did correspond to a relatively high modulus of elasticity, this value was not the highest among the 29 block companies. With the exception of 4 companies the stiffness coefficients, K, relating modulus of elasticity to prism compressive strength ($K = E_m/f'_m$), are well below the 1000 value specified in the Canadian code[26].

For 2-course stack bond prisms with face shell mortared joints, the secant moduli of elasticity were on average 25% higher than those from prisms with fully mortared bed joints. This tends to agree with the findings in Chapter 4 and other data[63].

Figure 6.5 is a plot of elastic modulus versus compressive strength of 4-course prisms. The evident scatter of the data indicates a high degree of uncertainty in the estimation of the elastic modulus using a single linear equation. In addition, for most companies the elastic modulus was well below the code specified value.

A regression analysis was employed to examine the relationship between the prism modulus of elasticity and compressive strength. Linear and power relationships showed relatively poor correlation and as shown in Table 6.3, exponential relationship only slightly improved the correlation. Eventhough no strong correlation exists, the best fit of a linear equation passing through the origin is:

$$E_m = 735\ f'_m \qquad \text{(Eq. 6.2)}$$

Table 6.3: Relationship Between Modulus of Elasticity and Compressive Strength

RELATIONSHIP	CORRELATION, r
$E_m = 0.38182\ f'_m + 6.5170$	0.508
$E_m = 3.19335\ f'_m{}^{0.4976}$	0.510
$E_m = 6.6577e^{(0.0341f'm + 1)}$	0.552
$E_m = 3.3593e^{0.21677f'm} + 1.11177$	0.587
$E_m = Af'_m + B(f'_m)^2$	no good

While this is only an empirical relationship, it does conform to the observations in earlier Chapters and it is in line with some other reported relationships[47].

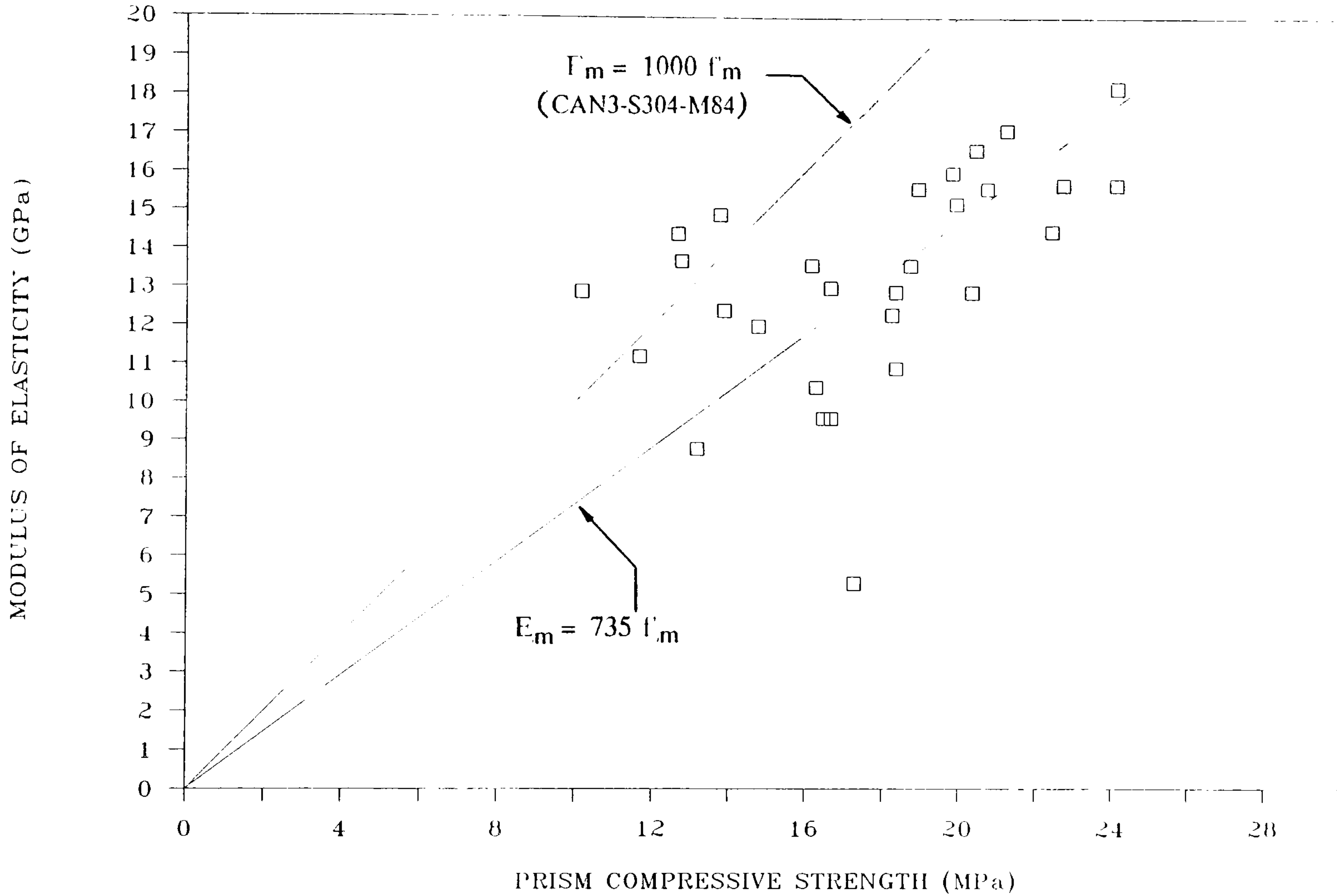

FIGURE 6.5 RELATIONSHIPS BETWEEN ASSEMBLAGE MODULUS OF ELASTICITY AND COMPRESSIVE STRENGTH

6.5 COMPRESSIVE STRENGTHS FOR HOLLOW CONCRETE MASONRY

Given the broad range of block strengths tested, it is possible to compare test and code compressive strengths values for hollow concrete blockwork with Type S mortar.

In Figure 6.6, the prism mean compressive strengths for the 4-course prisms for the 29 block companies were plotted against the code strengths for hollow block masonry. As can be seen, a fair number of points (10 prism strength values) fell below the code line. Furthermore, if the characteristic strengths (prism mean strength minus 1.5 standard deviation) as specified in Clause 5.3.2.2[26] were plotted instead, 15 strength values would fall below the code limiting line where no height correction has been applied.

If the current practice of not adjusting the prism strength to account for height to thickness is followed, then it is apparent that the prism strengths tend to be overestimated by the code in many cases. However as was demonstrated in Chapter 3, there is a significant effect of prism height. Therefore to satisfy the code, tests of 2 block high prisms would have to be used. Unfortunately, this would be counter-productive because, as was shown earlier, failure mechanisms for two course high hollow block prisms are quite different from higher prisms or walls. Therefore to encourage proper testing with more slender prisms, manufacturers should

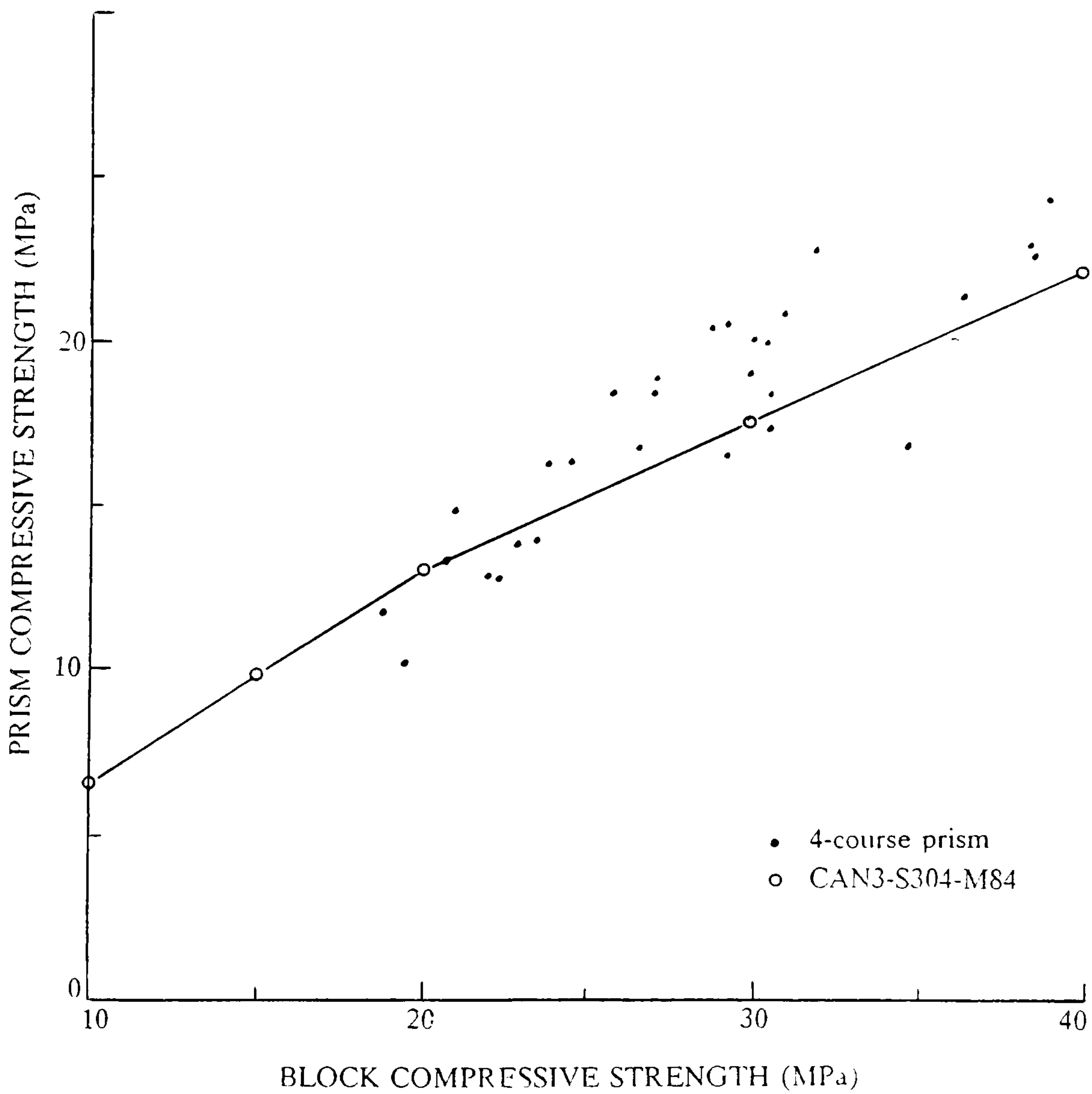

FIGURE 6.6 COMPARISON OF CODE AND 4-COURSE PRISM TEST VALUES FOR COMPRESSIVE STRENGTH OF HOLLOW BLOCK MASONRY

not be penalized.

Figure 6.7 is Figure 6.6 replotted but with the mean prism strengths modified for slenderness by multiplying by 1.22 which was the average ratio of 2 block high versus 4 block high compression strengths found in this research. It is also very close to the value of 1.25 previously used in the 1978 version of the Canadian code. As indicated earlier, the current code strength values were developed from test data which incorporated different testing techniques and sometimes undefined test conditions, some relatively old data and mostly 2 or 3 course prisms[67]. It is suggested that the best and most representative results are obtained from tests of 4-course prisms and therefore the code should not contain provisions which penalize these tests. Compressive strength based on more representative test data will lead to a greater confidence in the code specified strengths. Hence, it may be possible to appreciably reduce the level of uncertainty in the conversion of block strengths and mortar types to masonry compressive strength (Table 2 in CAN3-S304-M84[26]). Therefore it is recommended that the 29 strength values and various results developed in this chapter be considered for future development of specified strength values for hollow concrete masonry since these results are also based on a broad base of materials and an accurate and consistent test method.

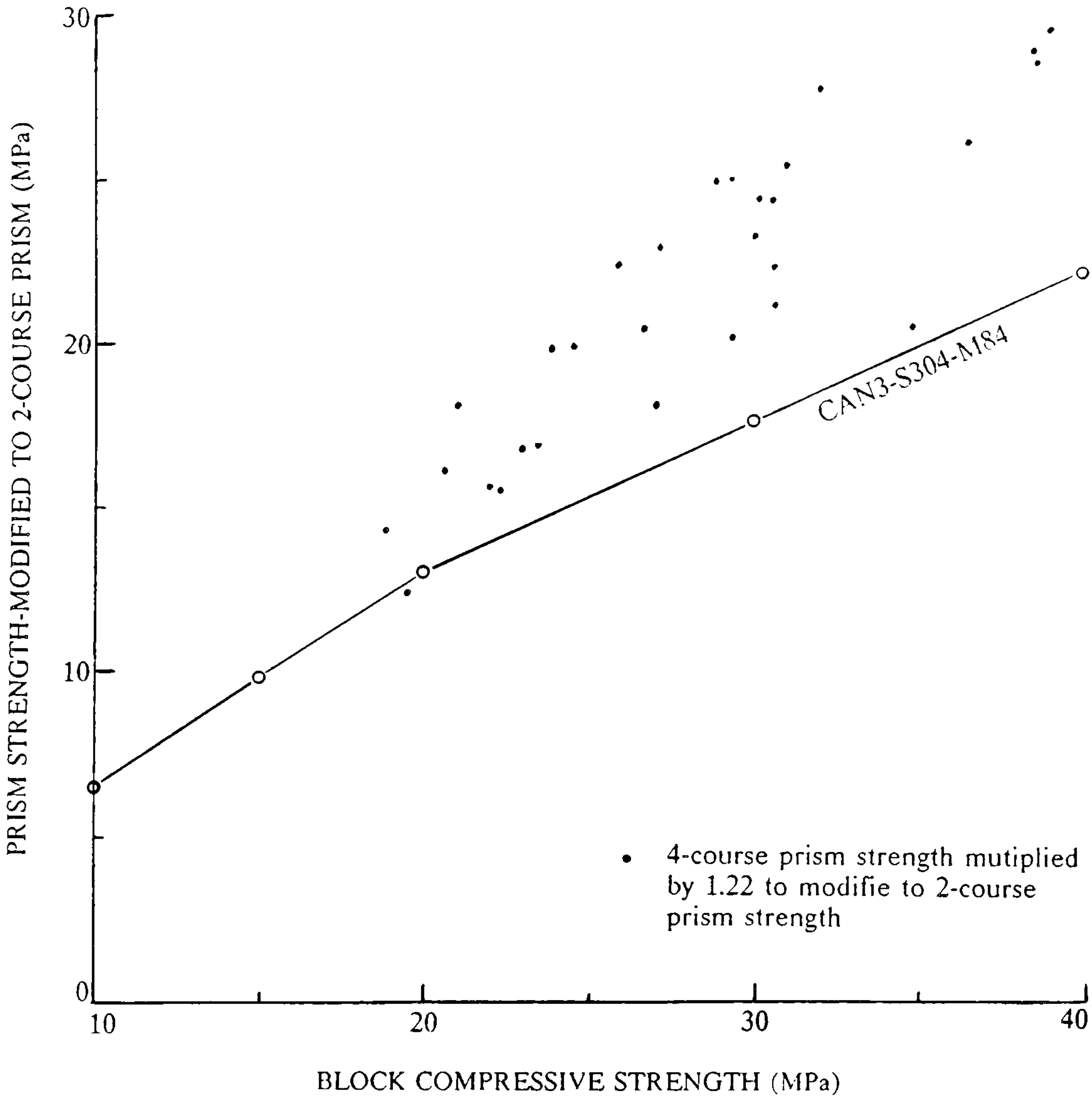

FIGURE 6.7 COMPARISON OF CODE AND 4-COURSE PRISM TEST VALUES (ADJUSTED FOR SLENDERNESS) FOR COMPRESSIVE STRENGTH OF HOLLOW BLOCK MASONRY

6.6 COMPRESSIVE STRENGTH FOR 15 MPa BLOCK MASONRY

Block manufacturing tolerances and the naturel of materials and testing do require supply of somewhat higher block strengths than specified to ensure compliance with the strength requirements. The margin usually used is about 20% where, for example, an 18 MPa or higher average strength of block would be supplied for a specified 15 MPa block. CAN3-S304-M84[26] requires that the masonry compressive strength, f'_m, be obtained by multiplying the average prism compressive strength by a reduction factor, ψ, which is the ratio of the block specified strength to the mean tested block strength. Therefore producing high strength units for a specified 15 MPa block strength may penalize the usable strength where only 15 MPa is guaranteed. Figure 6.8 is a plot of mean 4-block high prism strengths, f'_m, modified by the reduction factor, ψ , for a specified 15 MPa block. Over 50% of the plotted results fall below the code value where no correction for height is applied. However, if for comparison purposes the code value is adjusted by multiplying by 1/1.22 to correspond to 4-course prisms, only 2 Company's prisms fall below the code line. Nevertheless, the effect is very marked and is clearly a problem for high strength blocks such as Company 16 which had a block compressive strength of 39.1 MPa and a corresponding prism strength of 24.2 MPa. However the final reduced prism

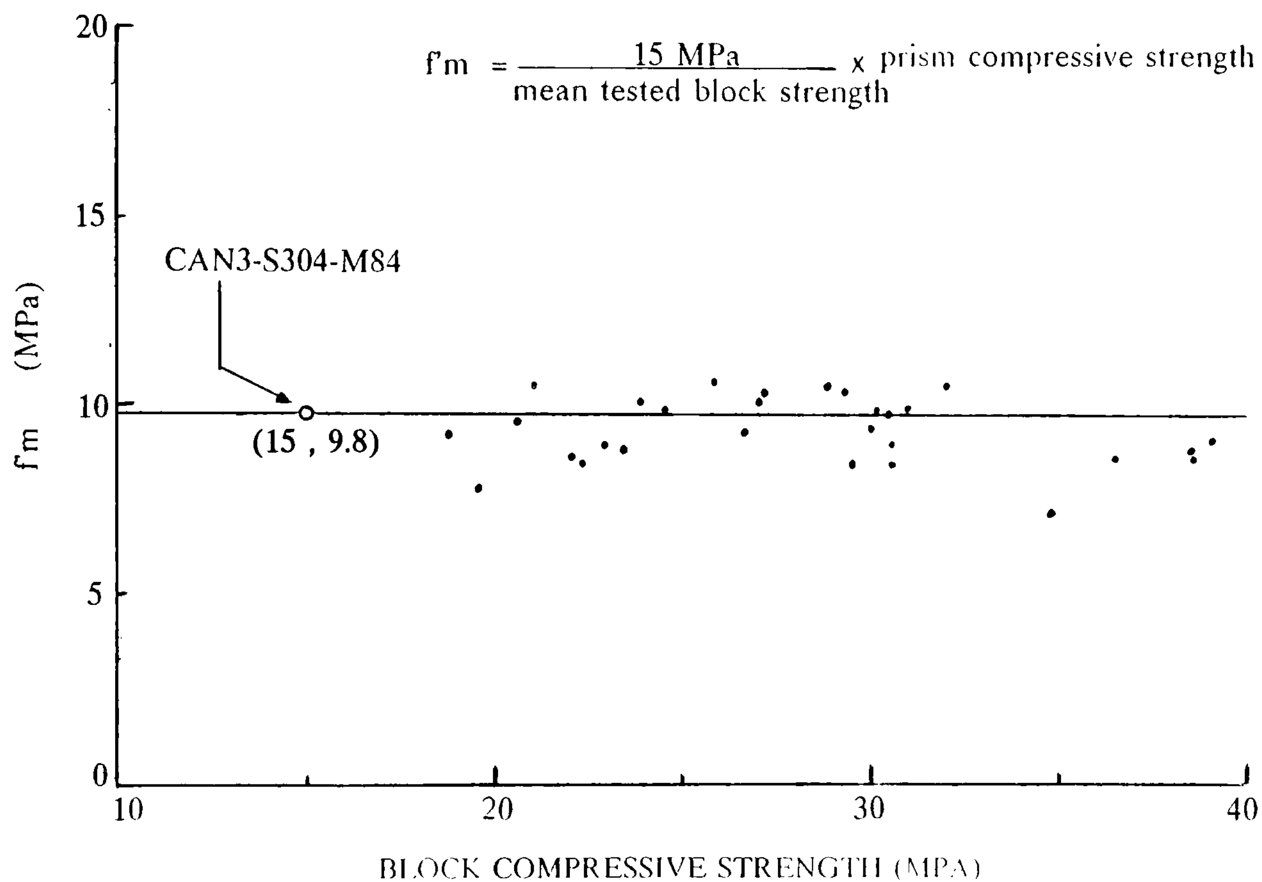

FIGURE 6.8 COMPRESSIVE STRENGTHS FOR 4-COURSE PRISMS REDUCED FOR SPECIFIED 15 MPa BLOCK STRENGTH

strength was only 9.3 MPa. A similar prism strength, f'_m, was obtained for Company 6 which had a block compressive strength of only 18.8 MPa. Since it appears that the code reduction factor penalize strong units, block producers should perhaps limit their manufacturing tolerance to within about 30%.

A more accurate comparison should then consider blocks with a manufactured strength with a tolerance of around 30%. For 15 MPa specified strength, Companies 6, 8 and 13 had block strengths around 20 MPa. For these block companies, the masonry strength, f'_m, (reduction factor, ψ , included) is below the code value of 9.8 MPa shown in Figure 6.8. In addition, if the variances of the experimental results were taken into account (as specified by Clause 5.3.2.2 in CAN3-S304[26]) the strength values would be even lower. However, when adjusted for height most of the test values are slightly higher than the code value.

6.7 CONCLUSIONS

1. Based on 29 different block manufacturers, for the same specified block strength of 15 MPa the actual block compressive strengths exceeded the normal tolerance limits by a large margin with some blocks having strengths as high as 40 MPa.

2. A strong relationship appears to exist between the prism and the block compressive strengths. However an equally

strong relationship also appears to relate the block splitting tensile strength to the prism strength.

3. The compressive strength of face shell mortared blockwork can be predicted more accurately based on the two strength characteristics of the block instead of the unit compressive strength only.

4. The average efficiency ratio of face shell prisms was around 0.63. It appears that this ratio may be improved by increasing the tensile strength of the blocks.

5. For the 29 sets of prisms, little correlation was obtained between the prism strength and the mortar cube compressive strength ($r = 0.13$). However a somewhat better relationship was obtained between prism strength and the ratio of mortar strength to block compressive strength ($r = 0.49$). An equivalent correlation ($r = 0.48$) was also obtained between the efficiency ratio and the mortar strength.

6. Based on a quantitative assessment, it is concluded that web cracking is the expected failure pattern in face shell mortared blockwork.

7. For 2-course stack bond prisms, no difference in compressive strength was observed between face shell and fully mortared joints with full capping being employed in both cases. [The findings in Chapter 3 indicated that employing face shell capping for face shell mortared 2-course prisms instead of full capping increased the prism strength by around

10%].

8. Based on results for 7 different block companies, the compressive strength of 2-course face shell mortared stack bond prisms was on average 22% higher than that of 4-course prisms built in running bond.

9. The linear range of the stress-strain relationships in face shell mortared blockwork was, on average, between 30% to 40% of the ultimate strength. Almost no linear range was observed for the weakest set of prisms in this investigation.

10. The relationship between the prism modulus of elasticity and compressive strength was not strong. An exponential relationship showed the best correlation but not significantly better than a linear relationship.

11. In most cases the code[26] equation, $E_m = 1000\ f'_m$ significantly overestimated the modulus of elasticity of face shell mortared blockwork.

12. For the 29 different sets of prisms, the compressive strengths (not including the reduction factor of specified to tested unit strength nor the influence of the variances of the results[26] nor any height correction) were higher than the code compressive strength value for 15 MPa block[26].

13. The code[26] reduction factor of specified to tested unit strength ratio severely penalizes the compressive strengths of prisms made with strong units unless the

specified strength is increased somewhat to reflect the actual strength.

14. In comparison to specified[26] strength values for hollow concrete blockwork, only 2 prism strength values (out of 29) fell below the code line when adjustment for height was considered. Not accounting for height raised the number of prism strength values to 10 falling below the code line.

6.8 RECOMMENDATIONS

1. Block manufacturers should consider limiting their manufactured block strength to within say 30% of the specified strength. Otherwise a strong penalty is imposed on the prism compressive strength. Producing extremely high strength units for 15 MPa block could result in rejection of the prism strength under the current code provisions[26]. An alternative solution is to increase the specified strength where tests show that over the longterm the actual strengths are quite consistent.

2. There appears to be a need for a stricter quality control in the manufacturing of concrete block. In some instances the dimensions' limits as set in CAN3-165.1-M85[24] were exceeded. The thicknesses of the two face shells in a single unit were occasionally observed to vary appreciably.

3. It is recommended that the modulus of elasticity of hollow concrete masonry be calculated using an equation of

a similar nature to the following: $E_m = 735\ f'_m$.

4. It is recommended that the results obtained in this research effort be considered for future development of compressive strength values for face shell mortared blockwork for the Canadian masonry design code[26]. To date this investigation presents the most comprehensive and broadly based Canadian research effort not only for face shell mortared but for concrete masonry in general.

CHAPTER 7

SUMMARY AND CONCLUSIONS

7.1 SUMMARY AND CONCLUSIONS

The behaviour characteristics of concrete blockwork with specific focus on face shell mortared blockwork under axial compression were investigated.

A total of 461 prisms using various block sources, sizes and shapes were built and tested under a variety of conditions. In addition, over 1400 associated tests on blocks and mortar were performed.

Although this dissertation contains the results of several investigations with each outlined in a separate chapter, along with its conclusions and recommendations, some general observations are summarized here to highlight the main findings for face shell mortared blockwork and block masonry in general.

1. The measured compressive strength of hollow concrete units is extremely sensitive to the test method but relatively independent of the direction of loading. Block strengths from tests of full bed hard capped single units appear to provide a reasonable measure for compressive strength.

2. The splitting tensile strength of hollow concrete blocks loaded across the webs is significantly lower than for loading across the face shells. This difference may be attributed to lesser degree of compaction of webs and possibly the indentation present at the bottom of the block webs. For face shell mortared blockwork, which fails by web cracking, defining the block tensile strength based on the web tensile capacity is of more significance. Splitting tension strengths appear to be relatively independent of the specimen geometry. While axial tension tests produced reasonable results they are relatively difficult to perform.

3. Most sands currently in use in making mortar do not meet the gradation limits set by CSA-A82.56[21]. New practical gradation limits based on 19 different sands were proposed for CSA specifications. Since increasing the Fineness Modulus of sand had little influence on the compressive strength of mortar use of finer sands is proposed. The compressive strength of masonry mortar was found to be significantly affected by curing conditions. Moist curing of low flow mortar resulted in as much as 90% increase in the mortar cube strength while only small increase in strength was achieved in the case of high flow mortar.

4. The prism strength characteristics are affected by the end conditions imposed by the test method/procedure:

.End effects do not only imply platen restraint and it was found that soft capping materials would introduce lateral expansion at the platen.

.Increasing the specimen height was found to reduce the influence of the end effects near the platen and provide a central zone relatively free of such effects.

.For soft capping materials, full capping resulted in premature prism failure regardless of the prism height while face shell capping resulted in larger web strains near the platen which in turn decreased the strength of the prism.

.Although hard capping materials introduce platen restraint, this was found to be relatively unimportant in sufficiently high specimens with either face shell or full capping.

.Use of thinner loading plates resulted in reduced prism strength which was attributed to plate bending.

.Pinned-end loading conditions produced a more uniform stress distribution over the loading surface than flat end loading.

5. Axial compression tests of 4-course prisms with line-loading, 75 mm thick bearing plates, Hydrostone capping material and full bed capping were found to yield the most reasonable and accurate results. Therefore this test set-up is recommended.

6. It was confirmed that 2-course prisms are not directly representative of behaviour of full scale block walls since the failure mode does not resemble that of walls. On average, 2-course prisms resulted in compressive strength 22% higher than 4-course prisms. This difference corresponds closely with the height correction factor used for solid masonry and applicable to hollow masonry in the 1978 Canadian code. Therefore it is recommended that this correction factor be re-introduced along with a standard test method.

7. While it is quite evident that the use of 4-course prisms is much more representative of actual wall behaviour than results from 2-course prisms, the meaning and use of prism defined compressive strengths require clarification. At present, where all strengths are converted to equivalent prisms with height to thickness ratios of 2.0, prism strength is analogous to cylinder strength for concrete and is a quality control parameter which provides a reference point for strength. Changing this benchmark to some other standard, say 4 block high prisms, would likely result in more realistic strengths and failure patterns, but would require other compensating adjustments in the design provisions.

8. Vertical cracking of the web is the expected failure pattern for face shell mortared blockwork regardless of the hollow block size. Much larger tensile strains developed in the webs than in the face shell and cracking was

observed to initiate at loads as low as 0.4 of the ultimate strength.

9. It was determined that failure theories developed for solid/fully mortared masonry were not applicable for face shell mortared blockwork since lateral stresses in both horizontal axes cannot be taken equal and the axial stress distribution along the prism height is highly non-uniform. The assumption of linear behaviour of block masonry is not justified with the modulus of elasticity showing decreasing values at loads as low as 30% of the ultimate strength. Models which predict cracking in face shell mortared blockwork should not be expected to predict ultimate strength since there is considerable reserve strength after initial cracking.

10. The results indicated that the block strengths (tensile and compressive) and mortar strength are the main variables affecting the strength characteristics of face shell mortared blockwork:

.Increasing the block compressive strength resulted in a significant increase in the prism strength while the efficiency ratio remained unchanged. However increasing the block tensile strength corresponded to an appreciable increase in the prism compressive strength and efficiency ratio.

.While the prism strength can be related to the unit compressive strength, a stronger relationship existed with the unit tensile strength.

.Codes should consider relating blockwork strength to the unit tensile strength or at least both compressive and tensile strength.

.Eventhough the initiation of failure in face shell mortared masonry is independent of mortar for normal range of mortars, the ultimate strength is not independent of the type or strength of mortar.

.Weak mortar resulted in a change of the failure mode and significant reduction in prism strength. For extremely weak mortar, the strength of face shell mortared prisms was found to be independent of the block strength.

11. Parameters of lesser significance on the strength characteristics of face shell mortared blockwork showed:

.Full mortaring of bed joints changed the mechanism causing the failure of hollow concrete blockwork.

.The combined effects of construction pattern and full mortaring increased the load capacity of running bond blockwork construction.

.Changing the unit geometry by adding an extra web improved the unmortared web area resistance to tensile stresses in face shell mortared blockwork.

12. The efficiency ratio of hollow block face shell mortared prisms appears to be reasonably consistent for different block sizes.

13. Initiation of failure in face shell mortared prisms under an eccentric loading of t/6 continued to be by web cracking. Previously reported high ratios of eccentric to axial stresses can be attributed to different methods used in calculating stresses under eccentric loading.

14. A study into an optimum geometry of the hollow concrete block could improve the strength characteristics of face shell mortared blockwork.

15. The code[26] approach of equating solid and grouted blockwork is questionable since not only were failure patterns different but also grouted prism strength were much lower than comparable solid blockwork. Determined strength values for grouted masonry based on the strength of hollow blockwork offers a more promising alternative.

16. Theories[32,54] developed for predicting strength of solid/grouted blockwork based on its constituents materials produce relatively high strength values since they consider the unit compressive strength (instead of the tensile strength) as the main parameter affecting the prism strength.

17. Since cracking in face shell mortared blockwork initiates at fairly low stress levels, placing much emphasis on the modulus of elasticity beyond such stress levels appears to be questionable. Nevertheless, it appears that most of the variables that affect the blockwork strength also affect the modulus of elasticity although the magnitude and direction of

such effects are not always the same. With the exception of grouted blockwork, the code[26] equation relating the modulus of elasticity, E_m, to the ultimate strength of concrete blockwork, f'_m, in general, by a 1000 value would overestimate the modulus. A representative relationship, $E = 735 f'_m$, is proposed.

APPENDICES

APPENDIX A

SUPPLEMENT TO CHAPTER 2

A1 UNIT COMPRESSIVE STRENGTH

A1.1 General

Detailed presentation of data from the block tests reported in Chapter 2 were provided in this Appendix.

For selected test series, mechanical strain reading (using a Huggenberger strain indicator and a 50 mm gauge length) were measured on the two face shells, as shown in Figure A1.1. The 0.001 mm resolution provided a precision of 20 micro-strains for the readings.

For full bed hard capping, the unit was set in liquid Hydrostone, which was poured on a levelled thick steel plate. At least 24 hours was allowed for setting even though half an hour was considered sufficient. For face shell hard capping, a similar procedure was followed except that the centre area of the block was covered by cardboard which was later removed. This resulted in a good quality control in capping only the desired area. [Eventhough this approach was time consuming it was deemed superior to capping the whole area and later on removing the Hydrostone from the centre webs.] The thickness

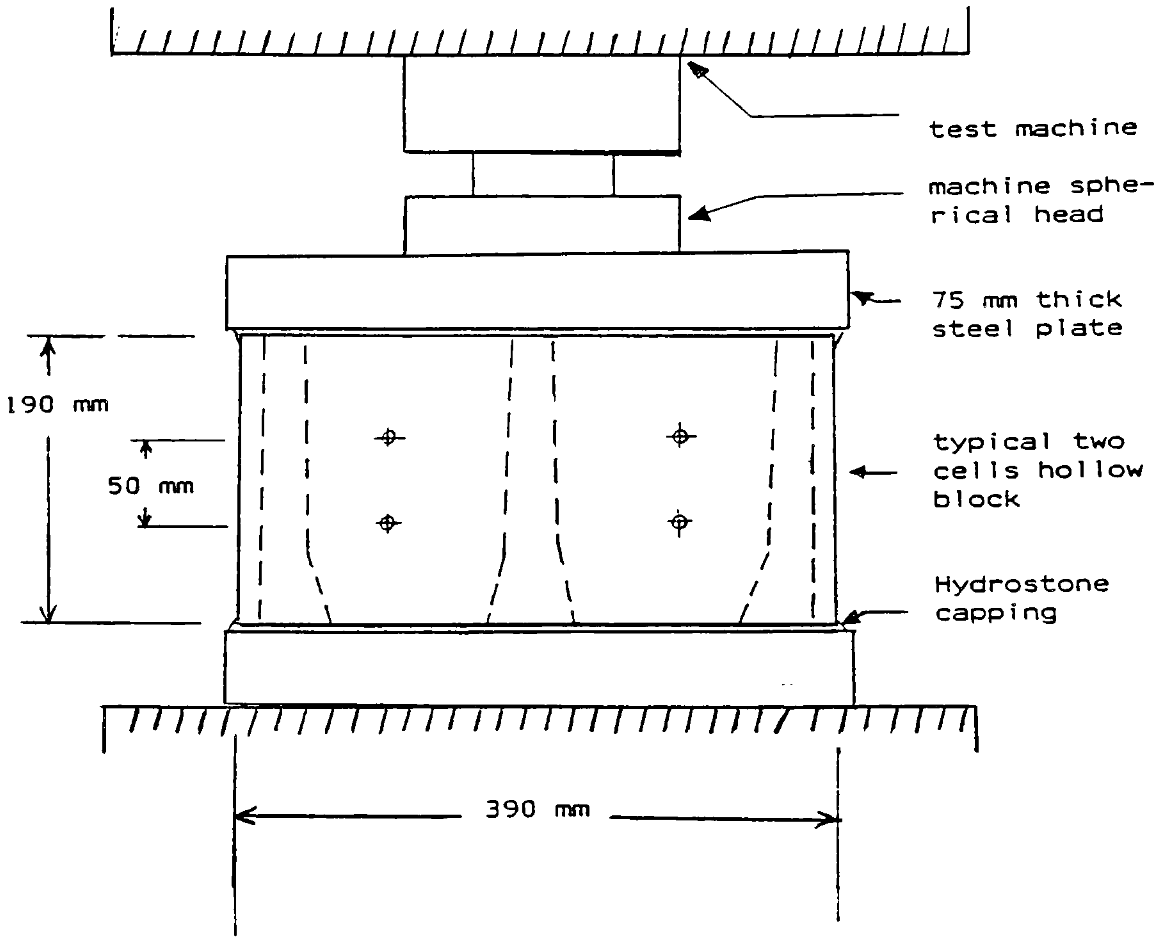

FIGURE A1.1: TEST SET-UP FOR SINGLE BLOCK WITH FULL HARD CAPPING
(SERIE C10-1)

of capping was less than or equal to 3 mm. It is worthwhile reporting that compression tests carried on 50 mm hardened Hydrostone cubes showed a compressive strength of 75 MPa.

When half blocks were used, they were saw cut, wet, from full splitter units. All the units used in the various tests were stored inside the laboratory and tested dry under the normal atmospheric conditions which existed inside the laboratory. For end loading of full units, Hydrostone capping was placed over the face shell ends only; two 32 mm wide strips of capping were employed. When soft capping was used, fibreboard was placed between the plates and the block and no Hydrystone capping was used. Full coverage of the desired area for loading was provided. Centrelines on the four sides of the unit were drawn to avoid any eccentric loading. The load was applied according to CSA-A369.1[25] and only when strain measurements were taken the time limit was exceeded.

A1.2 Various Compression Tests

Compression of Fully Hard Capped Blocks Tested Flatwise

(Series C10-1)

The loading was applied normal to bed joint. As discussed in Chapter 2, unit net area of 41500 mm^2 was used. The failure was mainly explosive and can be described as the typical conical shape. In one instance the block simply unloaded with some small spalling in the face shells. In addition the failure was not always symmetrically conical, i.e. one end only showed a conical failure.

The stress-strain results were shown in Figure A1.2 where at each load level, the average of the strains from both face shells were plotted for each specimen. Strains were plotted, using the mean strain of each specimen, at a stress level normalized in such a way that the failure load of each specimen equalled the mean failure load. The non-linear behaviour of the concrete block is quite evident under high axial compression. Regression analysis was employed to obtain the "best fit" of the data shown in Figure A1.2. In all cases, use of various non-linear polynomial models were tried and the model which resulted in the smallest "error sum of squares" was chosen.

The secant modulus of elasticity of the full concrete block, E_{mb}, in compression determined at 0.3 of the ultimate compressive strength was found to be 17430 MPa.

Compression of Half Block Fully Hard Capped (Series C10-7)

The net area used, based on calculated mid-height area, was 21815 mm^2. The mode of failure was the typical four sided conical failure. However in one instance the specimen simply unloaded. The stress-strain results were shown in Figure A1.3. The secant modulus was found to be 21940 MPa.

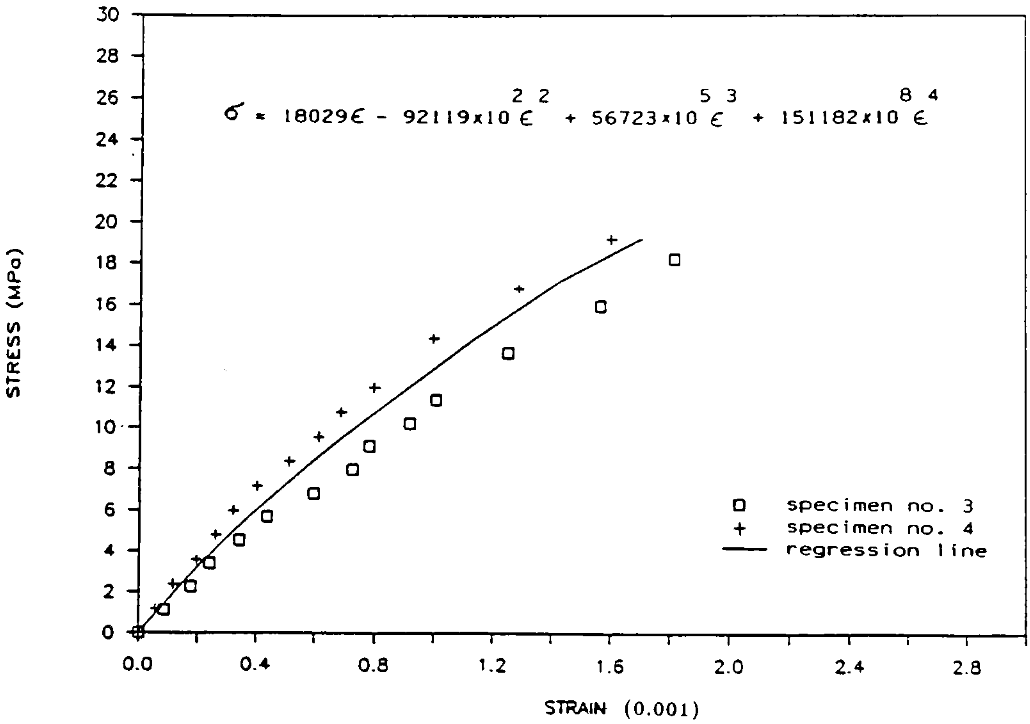

FIGURE A1.2 STRESS-STRAIN RELATIONSHIP FOR FULLY HARD CAPPED BLOCK (SERIES C10-1)

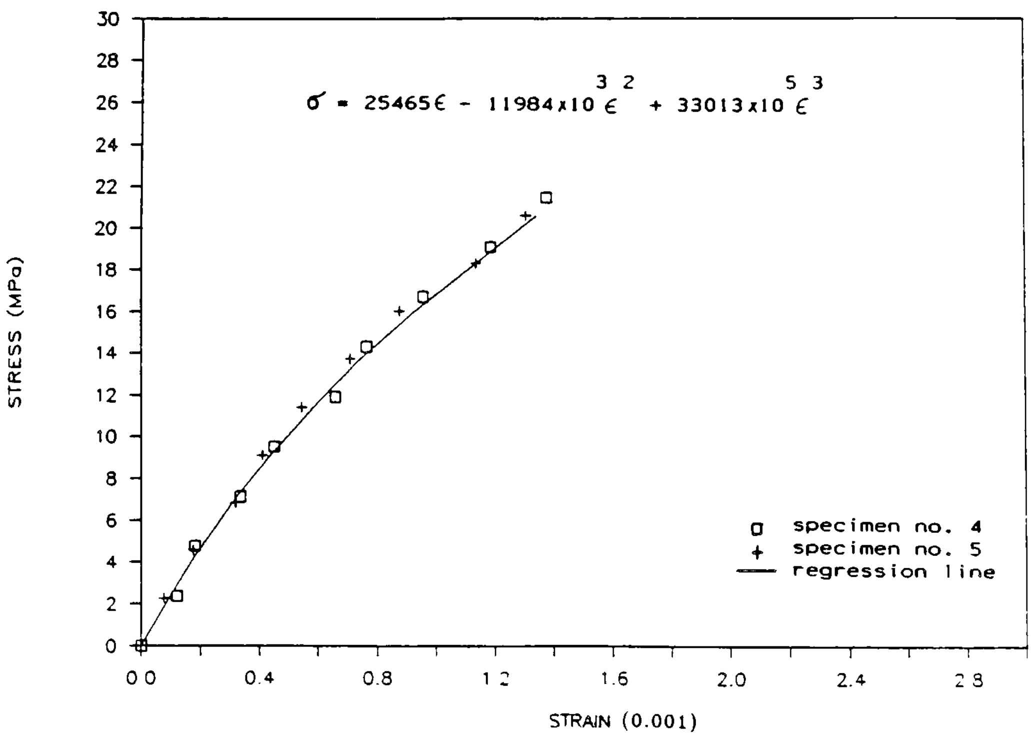

FIGURE A1.3 STRESS-STRAIN RELATIONSHIP FOR FULLY HARD CAPPED HALF BLOCK (SERIES C10-7)

Compression Tests of Face Shell Capped Full Units, Loaded Normal to Head Joint (Series C10-8)

The net area used for calculating the compressive strength was based on the average mid-height face shell thickness of 34 mm; this came out to be 12920 mm^2. The mode of failure was characterized by the diagonal failure plane joining the two opposite corners, as shown in Figure A1.4(a). However another mode of failure as indicated in Figure A1.4(b) was observed. The diagonal failure lines initiated at the two corners and continued to propagate at approximately a 45° angle, then joined at about a third of the unit height. This failure resembled that of a concrete prism or cylinder in compression. The four different strain measurements were taken on each face shell at the location shown in Figure A1.4. An important observation was that the section of the face shell at the hollow core experienced less deformation than that of the cross-web. This behaviour, shown in Figure A1.5, was observed on both sides. The complication introduced by the cross-webs is quite evident and suggests a large stress concentration at the interface of the face shell and the web. The overall stress-stain relationship, for the 200 mm gauge length, was presented in Figure A1.6.

Three different secant moduli of elasticity were determined:

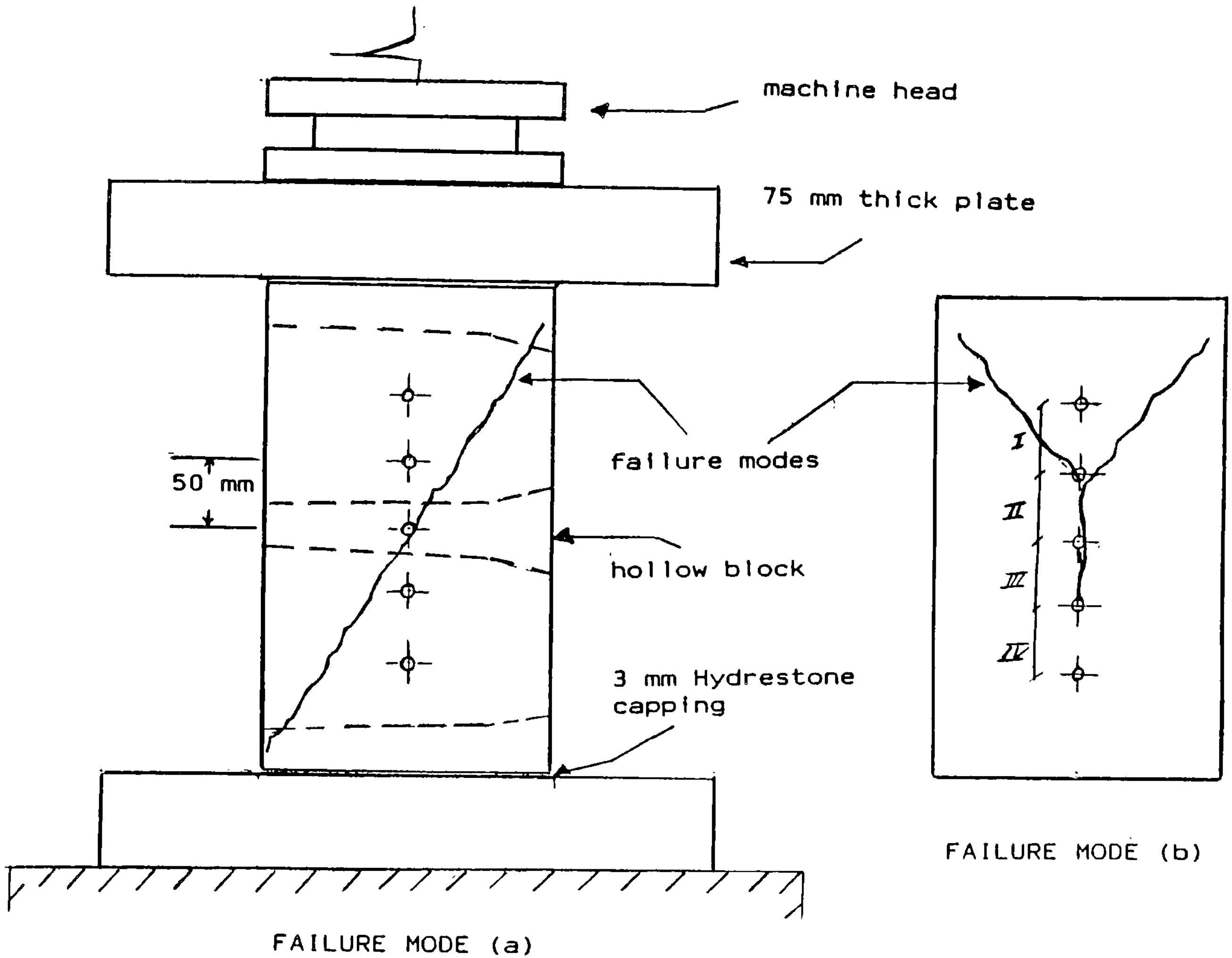

FIGURE A1.4: COMPRESSION TEST SET-UP AND FAILURE MODES OF FULL UNIT LOADED ENDWISE (SERIESC10-8)

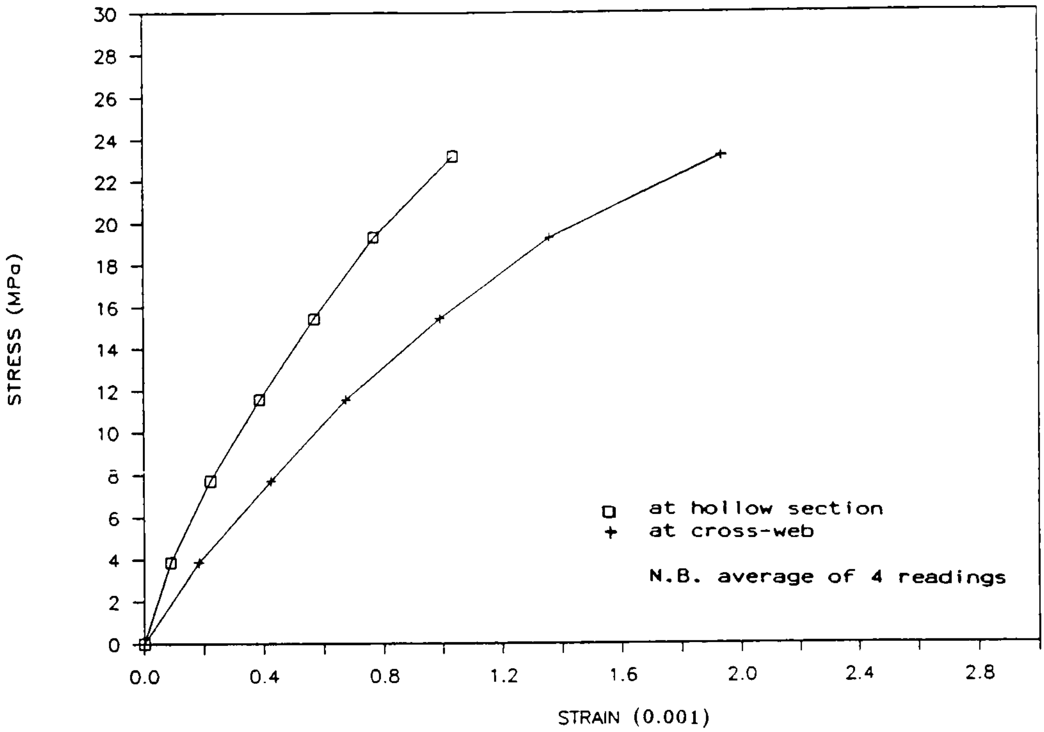

FIGURE A1.5 STRESS-STRAIN RELATIONSHIP FOR END LOADED COMPRESSION TEST, INFLUENCE OF GEOMETRY (SERIES C10-8)

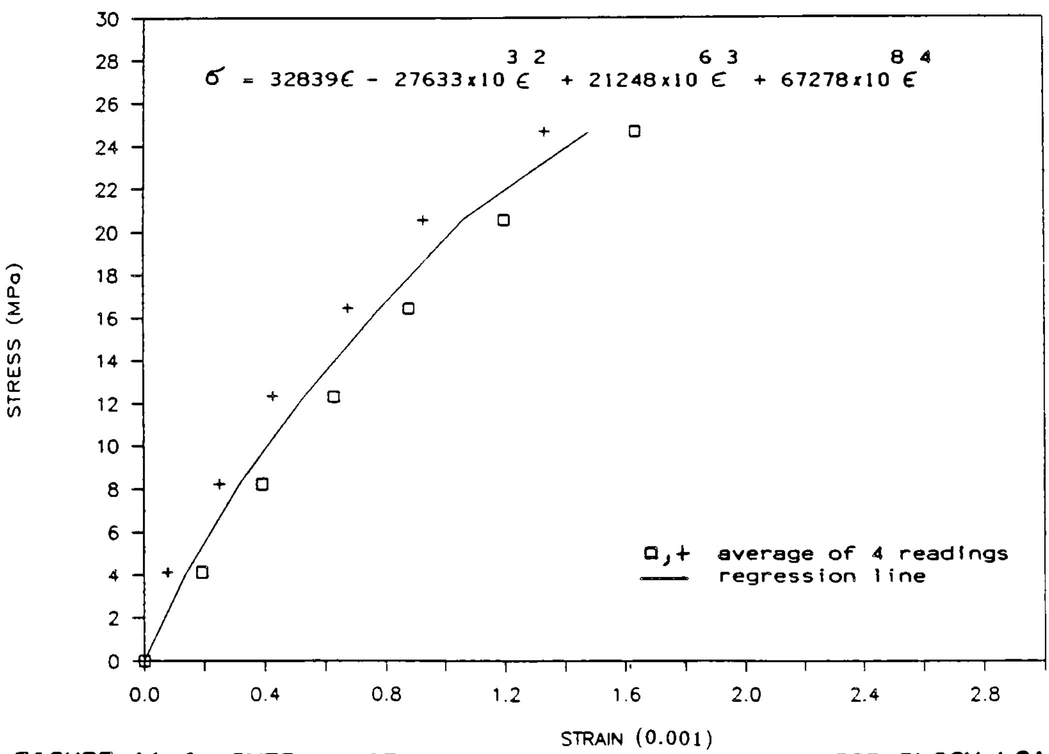

FIGURE A1.6 OVERALL STRESS-STRAIN RELATIONSHIP FOR BLOCK LOADED ENDWISE (SERIES C10-8)

E_{mb1}: for face shell section near hollow core = 35100 MPa

E_{mb2}: for face shell section at cross-web = 18280 MPa

E_{mb3}: overall modulus of elasticity = 24080 MPa

<u>Compression Tests of Full Units with Face Shell Hard Capping; 32 mm and 50 mm Widths</u> (Series C10-2 and C10-3)

For Series C10-2 the minimum face shell net area of 2 x 32 x 390 = 24960 mm^2 and for Series C10-3 an equivalent to the mortar bedded area in running bond masonry concrete wall, were used. Determination of the latter area was discussed in Chapter 3 and was determined to be 30700.8 mm^2 which translates into a 39.4 mm equivalent face shell thickness. In the block compression test this was achieved by capping over a width of 50 mm. For the 32 mm width of hard capping (Series C10-2) no conical failure was observed; only some evidence of spalling in the face shells. This was the only sign of failure in this series. For the 50 mm width of hard capping (Series C10-3), units failed by extensive spalling of the face shells. In some instances in-plane splitting of a face shell was observed.

<u>Compression tests of Full Units with Full Bed Soft Fibreboard Capping</u> (Series C10-4)

The capping board did cover the whole surface of the block, top and bottom. After failure, examination of the board showed that the thickness was reduced to about half (from 11.0 mm to 5.5 mm). The rough surface of the unit was seen printed on the board. The effect of using only fibreboard was examined in this series. Two distinct modes of failure were observed as shown in Figure A1.7. Units tended to fail by either 1) Crushing of the unit which was characterized by spalling in the face shells as well as the webs. Horizontal spalling lines in the face shell as well as the web were observed and tended to form a plane at mid-height parallel to the surface of the unit. 2)Wedge failure of the unit which was characterized by shearing of a corner of the block. What is of importance is that the shearing action extended well into the middle of the web. No vertical splitting was observed. Both modes of failure were shown in Figure A1.7.

Compression Tests of Full Units with Face Shell Soft Capping (Series C10-5 and C10-6)

Similarly to the case of face shells hard capping, the widths of the soft capping for face shells were 32 mm and 50 mm (effective 39.4 mm) for Series C10-5 and C10-6, respectively. For the 32 mm soft capping strips, the failure was mainly restricted to the loaded face shells. Shearing of

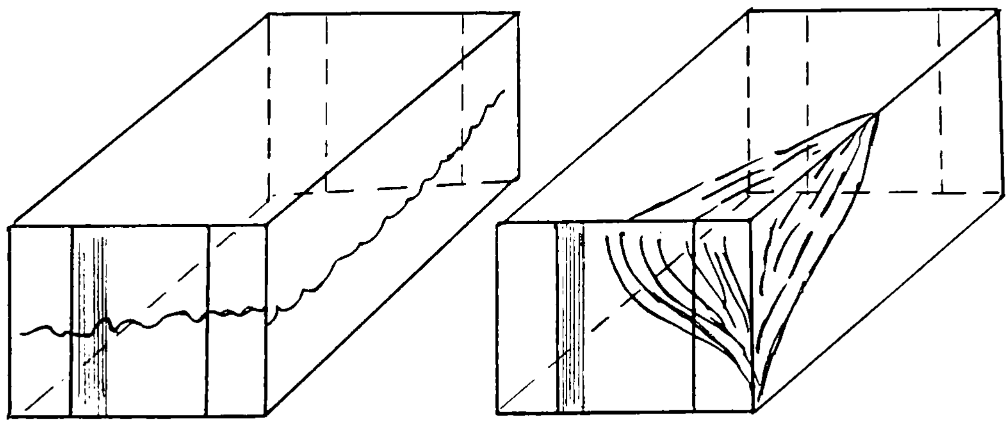

FAILURE MODE (1) FAILURE MODE (2)

FIGURE A1.7 MODES OF FAILURES OF BLOCKS WITH FULL BLOCK SOFT CAPPING (SERIES C10-4) the face shells was predominant. Vertical face shell splitting was also observed. Only in one instance was a vertical splitting line observed in the web. For Series C10-6, various failure patterns were observed. Fine lines of spalling were observed in two blocks. One block showed a conical failure on one side and another block exhibited extensive cracks in the web and shearing of one face shell.

Compression Tests of Full Units with Full Bed Hard Capping Using 50 mm and 75 mm Thick Plates (Series C13-9 and C13-10)

Concrete blocks used in these two series came from a different source (Company No. 13, identified as C13) because no more blocks were available from C10. No strain measurements were recorded since the effect of platen restraint would affect significantly the actual stress-strain relationship. Table A1.1 contains a listing of the results from these two series.

The unit failure mode in these two series was similar. This was characterized by simply unloading. No conical failure was observed but in some instances a fine line of face shell spalling was observed.

TABLE A1.1: RESULTS OF SERIES C13-9 AND C13-10

TEST SERIES	DESCRIPTION OF TEST	ULTIMATE LOAD- KN	MEAN STRENGTH (MPa)	C.O.V. (%)
C13-9	75 mm thick steel bearing plates (ful hard capping)	983 884 1021 1017 1064 922 966 841 866 942	22.9	7.7
C13-9	50 mm thick steel bearing plates (ful hard capping)	933 973 862 839 825	21.2	5.9

A1.3 Statistical Analysis of Compression Test Results

In order for any statement/observation to be conclusive a statistical assessment is needed. A statistical analysis has been performed on the results from the various series. Variances were tested for equality as well as mean strengths. Before attempting any analysis some assumptions and limits need to be stated:

1. There are two samples of data randomly selected from the same population. In this case the samples are termed "paired samples".
2. Standard deviations are not known and are assumed unequal. These are estimated from the samples. The F test (one-sided test) was employed to test the variances of two samples.
3. The paired-data t-test was used to test for means equality where applicable.
4. Tests were conducted at the 5% significance level. This significance level has been used by some masonry researchers [95,104] and tends to compare well with the level of coefficient of variation obtained throughout the test series.

A summary of the statistical analysis results was listed in Table A1.2.

TABLE A1.2: STATISTICAL ANALYSIS OF COMPRESSION TEST RESULTS.

COMPARED PARAMETER	VARIANCES TEST	STRENGTH TEST
Full capping: hard VS soft	Sim*	Diff
Face shell capping: hard VS soft (32mm)	Sim	Diff**
Face shell capping: hard VS soft (50mm)	Sim	Diff
Hard capping: full VS face shell (32mm)	Sim	Diff
Soft capping: full VS face shell (32mm)	Sim	Diff
Full unit VS half unit	Sim	Sim
Flatwise VS endwise loading	Sim	Sim
Half unit flatwise VS full unit endwise	Sim	Sim
Bearing plate thickness: 75mm VS 50mm (1)	Sim	Sim
(2)	Sim	Diff

Sim = similar, Diff = different
* also at 1 % significance level
** also at 2 % significance level
(1) if 5 values of Series C13-9 with smallest difference are considered
(2) if 5 values of Series C13-9 with largest difference are considered

A2 UNIT TENSILE STRENGTH

A2.1 General

Because the tension investigation used units obtained at different time periods than the blocks used in the investigation described in later chapters, it was necessary to determine the characteristics of these units. Table A2.1 contains this information. Compression tests were carried out on full units with full bed hard capping. The compression tests and the various tension tests were carried out on the blocks at an age between one and two and a half months.

Tension splitting tests on half stretches as well as half splitters were carried in accordance with ASTM-C1006-84[6]. Ten half hollow 190mm blocks were saw cut and tested dry. They were loaded under a compressive line loads across the face shells as shown in Figure A2.1. The load was applied over the thin part of the face shells to achieve the lowest possible result. The wooden strips (plywood) were changed after each test. The same test was repeated for ten half blocks loaded across the webs. Most currently manufactured hollow units have an indentation in the webs. This defect extends as much as 15 mm in some units. To provide a levelled surface where the load was to be applied, Hydrostone capping was used to fill these indentations.

TABLE A2.1: CHARACTERISTICS OF HOLLOW CONCRETE BLOCKS

	COMPANY 10	COMPANY 21
Ultimate compressive load (KN)	874 986 963 905 1054	864 889 1054 1001 912
Mean strength (MPa) Coefficient of varation (%)	23.1 7.4	22.8 8.5
Dry weight (Kg) Curing process	16.81 Bubble curing	15.59 Autoclave

Six square 165 x 165 mm specimens, cut from the face shells of the units with tapers removed to provide uniform thickness along the height, were tested in a similar set-up to that shown in Figure A2.1 by applying a line load perpendicular to shell plane. Similar tests were also carried on specimens cut from webs. These specimens were cut down to the 165 x 165 mm size so that the web indentation could be removed.

The rate of loading during the splitting test was kept fairly constant at 0.2 in/min (5 mm/min). Thomas and O'Leary[102] and Brochelt and Brown[17] have reported that the rate of loading is of a little significance in such tests. But a change in packing material could considerably affect the

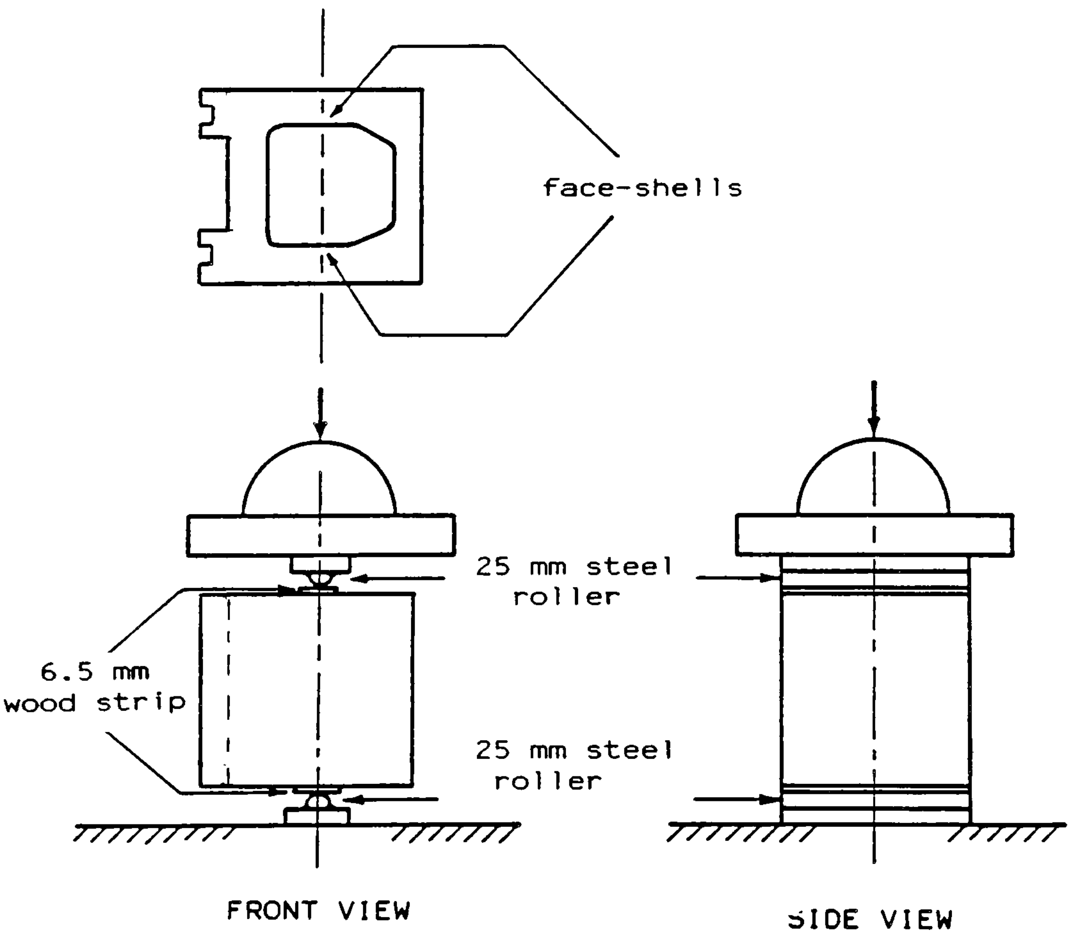

FIGURE A2.1: SPLITTING TENSION TEST SET-UP ultimate load[112]. In this investigation, the same packing material (plywood) was used throughout the various tests.

Specimens tested under direct tension were attached to a loading mechanism to both ends as shown in Figure 2.2, in Chapter 2. High modulus 2-components epoxy-resin system, SIKADUR 31 HI-Mod Gel, was used to bond the masonry specimen at the ends to the steel plates. Steel angles were also epoxied to both faces, at both ends, of the specimen and the steel plate to prevent the possibility of premature failure at either end of the specimen. The epoxy was allowed to cure for 24 hours before testing. To minimize eccentricity of the applied load, the apparatus was designed so that the mechanical connection, connecting the steel plate to the bar, would allow movement in a plane perpendicular to the plane of the specimen. Also, the steel rollers at the top and the bottom machine plates permitted movement in the plane of the specimen. Having this flexibility in the two orthogonal directions helped ensure proper alignment of the specimen. A rate of loading of 0.02 in/min. (0.5 mm/min) was used during the axial tension tests. The loading rate of 0.2 in/min employed in the splitting tension tests was considered to be too fast since the ultimate load for the axial tension test was expected to be much smaller.

A2.2 Various Tension Tests

Splitting Tests of Half units, Loaded Across Face Shells and Webs (Series T10-1, T10-2, T21-1 and T21-2)

The results of the splitting tests on half stretcher units were listed in Table A2.2 for loading across the face shells and across the webs. The splitting tensile strength was calculated using the following formula adapted by Self[97], Brochelt and Brown[17], and Hamid[43].

$$f_t = \frac{2P}{\pi A_n} \qquad \text{(A2.1)}$$

where P = ultimate load

A_n = sectional area of splitting plane (net sectional area) [For loading across the face shells of a half stretcher unit, the splitting plane was taken as the thickness of the face shells at mid-height of the blocks, 34 mm, times the height of the unit multiplied by 2 because both face shells are loaded. For loading across the webs, A_n is the sum of the mid-height thickness of the outside and inside webs times the height of the block].

Splitting Tests of Square Pieces of Concrete Masonry from Face Shells and Webs (Series T10-3, T10-4, T21-3 and T21-4)

The square pieces of concrete masonry had a nominal dimension of 165 x 165 mm. In cutting the specimens, consistency in dimensions could not be maintained. Hence measurements of each specimen height and thickness were made

TABLE A2.2: SPLITTING OF HALF STRETCHER UNIT TEST RESULTS
(SERIES T10-1, T10-2, T21-1 AND T21-2)

SERIES	T10-1		T10-2		T21-1		T21-2	
n	LOAD (KN)	TENSILE STRESS (MPa)	LOAD (KN)	TENSILE STRESS (MPa)	LOAD (KN)	TENSILE STRESS (MPa)	LOAD (KN)	TENSILE STRESS (MPa)
1	41.9	2.03	27.2	1.57	43.2	2.10	21.8	1.26
2	32.3	1.57	22.5	1.30	42.6	2.07	22.9	1.32
3	39.8	1.92	29.2	1.69	41.9	2.04	23.9	1.38
4	37.9	1.84	22.3	1.29	38.5	1.87	20.8	1.20
5	41.3	1.99	31.1	1.80	40.5	1.97	25.2	1.45
6	41.1	2.00	27.4	1.58	41.3	2.01	18.7	1.08
7	34.1	1.65	25.5	1.47	37.9	1.84	22.2	1.31
8	39.9	1.94	28.1	1.62	38.9	1.89	21.6	1.25
9	42.6	2.06	23.3	1.35	41.0	1.99	25.4	1.46
10	-	-	24.5	1.42	36.1	1.75	17.9	1.03
Mean		1.89		1.51		1.95		1.28
C.O.V.		9.1		11.4		5.6		12.3

and the stresses were determined accordingly. The thickness for the face shell specimens ranged from 32 mm to 36 mm and the thickness for the web specimens ranged from 24 mm to 26 mm. Equation A2.1 was used to determine the tensile strength and the splitting plane was the average height times the average thickness. The individual results for both Companies were listed in Table A2.3.

<u>Direct Tension Tests of Square Pieces of Concrete from Face Shells and Webs</u> (Series T10-5, T10-6, T21-5 and T21-6)

Table A2.4 contains the results of the direct tension tests for face shell and web specimens for Companies 10 and 21 where the areas were calculated from measurements of individual specimens. The failure was brittle with cracking running more or less horizontally across the specimen.

<u>Direct Tension Tests of Web Square Specimens Including Effect of Indentation</u> (Series T10-7 and T21-7)

Table A2.5 lists the results from these two series.

<u>Splitting Tension Tests of Half Splitter Units</u>

(Series T21-8 and T21-9)

TABLE A2.3: SPLITTING OF SQUARE SPECIMEN TEST RESULTS (SERIES T10-3, T10-4, T21-3 AND T21-4)

SERIES	T10-3		T10-4		T21-3		T21-4	
n	LOAD (KN)	TENSILE STRESS (MPa)	LOAD (KN)	TENSILE STRESS (MPa)	LOAD (KN)	TENSILE STRESS (MPa)	LOAD (KN)	TENSILE STRESS (MPa)
1	16.3	1.99	14.2	1.97	14.6	1.82	11.0	1.65
2	19.2	2.30	14.2	2.09	16.2	1.81	12.5	1.86
3	17.3	2.13	13.0	1.92	15.4	1.83	12.2	1.90
4	17.9	2.02	11.8	1.79	14.4	1.66	12.2	1.74
5	19.6	2.30	13.2	2.14	15.7	1.74	9.4	1.55
6	17.5	2.15	13.8	2.05	13.8	1.66	11.1	1.65
Mean		2.15		1.99		1.75		1.73
C.O.V.		6.2		6.5		4.5		8.0

TABLE A2.4: DIRECT TENSION TEST RESULTS (SERIES T10-5, T10-6, T21-5 AND T21-6)

SERIES	T10-5		T10-6		T21-5		T21-6	
n	LOAD (KN)	TENSILE STRESS (MPa)	LOAD (KN)	TENSILE STRESS (MPa)	LOAD (KN)	TENSILE STRESS (MPa)	LOAD (KN)	TENSILE STRESS (MPa)
1	7.7	1.53	7.8	1.88	11.5	2.07	7.2	1.74
2	10.6	2.02	6.4	1.66	10.9	2.15	7.5	1.88
3	9.1	1.70	5.6	1.40	10.9	2.10	7.4	1.69
4	10.3	1.95	6.8	1.61	8.8	1.56	7.6	1.88
5	10.0	1.98	7.9	1.73	10.0	1.86	6.9	1.50
6	9.6	1.89	-	-	-	-	-	-
Mean		1.85		1.66		1.94		1.74
C.O.V.		10.3		10.6		12.5		9.1

Indirect splitting tests were also carried on half splitter units with the load being applied across the face shells then again across the webs. The interest from these two series was to compare hollow stretcher units to splitter units and to investigate if there is any difference of strength by applying the load across the face shells vs. across the webs. The results for these two series were listed in Table A2.6.

Splitting Tension Tests of Half Splitter Units to Investigate the Influence of Packing Material (Series ST1 and ST2)

Hollow units from a different source were employed in these series. The half units were tested with the load applied across the face shells. Only a small number was used however the difference can be easily detected. Table A2.7 lists the results from these series.

A2.3 Statistical Analysis of Tension Test Results

A statistical assessment was carried out before any conclusions were drawn. It followed the description given in Section A1.3. The statistical tests were carried at the 5% significance level. A summary of the statistical analysis was listed in Table A2.8.

A3 MORTAR PROPERTIES

TABLE A2.5: RESULTS OF SERIES T10-7 AND T21-7

SERIES	T10-7				T21-7			
n	LOAD (KN)	TENSILE STRESS (MPa)	MEAN STRESS (MPa)	C.O.V. (%)	LOAD (KN)	TENSILE STRESS (MPa)	MEAN STRESS (MPa)	C.O.V (%)
1	5.7	1.42			9.1	2.08		
2	6.0	1.45			8.2	2.09		
3	7.1	1.64	1.56	8.4	8.8	2.03	1.88	13.8
4	6.4	1.55			6.2	1.60		
5	7.5	1.73			6.6	1.60		

TABLE A2.6: RESULTS OF SERIES T21-8 AND T21-9

SERIES	T21-8				T21-9			
n	LOAD (KN)	TENSILE STRESS (MPa)	MEAN STRESS (MPa)	C.O.V. (%)	LOAD (KN)	TENSILE STRESS (MPa)	MEAN STRESS (MPa)	C.O.V (%)
1	42.6	2.10			24.6	1.47		
2	46.6	2.30	1.98	19.7	19.3	1.16	1.24	16.5
3	31.3	1.50			18.2	1.10		

TABLE A2.7: RESULTS OF SPECIAL SERIES ST1 AND ST2

SERIES	ST1 (NO PACKING)				ST2 (PACKING)			
n	LOAD (KN)	TENSILE STRESS (MPa)	MEAN STRESS (MPa)	C.O.V. (%)	LOAD (KN)	TENSILE STRESS (MPa)	MEAN STRESS (MPa)	C.O.V (%)
1	37.5	1.85			53.0	2.61		
2	35.7	1.76	1.85	4.9	56.5	2.30		
3	39.4	1.94			49.0	2.41		
4					46.0	2.27	2.38	5.0
5					49.2	2.42		
6					46.2	2.28		
7					47.7	2.35		

TABLE A2.8: STATISTICAL ANALYSIS OF TENSILE STRENGTH RESULTS.

COMPARED PARAMETER	COMPANY 10	COMPANY 21
STRENGTH OF FACE SHELLS versus WEBS		
1- splitting half units	Diff	Diff
2- splitting square peices	Sim	Sim
3- direct tension test	Sim	Sim
SPLITTING STRENGTH OF HALF UNITS versus SQUARE PIECES		
1- face shells	Diff	Diff
2- webs	Diff	Diff
SQUARE PIECES SPLITTING STRENGTH versus DIRECT TENSION STRENGTH		
1- face shells	Diff	Sim
2- webs	Diff	Sim
EFFECT OF INDENTATION		
1- web pieces	Sim	Sim

Sim = similar, Diff = different

A3.1 General

This section applies to mortar related laboratory activities throughout this research work. Type S2 mortar (Portland Cement-Masonry Cement) was used throughout unless otherwise noted. Type 10 Normal Portland Cement and Type H Masonry Cement were used. When lime was used, type N hydrated lime was employed. The mortar mixes were batched by weight instead of by volume to ensure better quality control.

Mortar was prepared in small batches (40 - 50 kg approximately) so that they could be mixed by hand and would not last longer than a half hour. An experienced technician and the author did the mixing. No retempering of the mortar was allowed. Flow, air content and water retentivity tests were done according to CSA-A8[9]. The mason was satisfied with the workability of the mortar since he is accustomed to use fine masonry and masonry cement. Three 50.8 mm (2 in.) mortar cubes were made from each mortar batch. The cubes were removed from the non-absorbent steel molds after one day and air cured in the laboratory, unless noted otherwise.

A3.2 Experimental Data

Mortar data included here were only those related to the areas investigated in Chapter 2. Mortar data related to the various prism series were reported in the appropriate chapters.

Series BM1: Different Types of Sand

Results of the individual sieve analysis of the 19 samples of sand and the McMaster masonry sand were listed in Table A3.1. Individual mortar cube compressive load, strength and coefficient of variation for every block company were listed in Appendix E, Tables E2.1 to E2.29.

Series BM2: Curing of Masonry Mortar

The individual cube compressive strength for 11 different mortar batches cured in 100% moist environment, in saturated lime-water and in air were listed in Table A3.2. The mean strengths and the coefficients of variation were also listed along with the properties of the fresh mortar. Compression tests were carried out at 28 days of age. Mortar cubes were cured in the identified method until the time of testing.

TABLE A3.1: SEIVE ANALYSIS OF SANDS USED IN SERIES BM1

SAND SAMPLE NO.	PERCENT PASSING (%) SEIVE SIZE (mm) 5	2.5	1.25	.63	.315	.16	<.16	FIN. MODULUS
1	100.0	98.4	95.2	88.8	54.8	4.8	.0	1.58
2	100.0	99.9	99.6	95.7	54.4	16.5	0.0	1.34
4	99.9	99.4	97.8	91.8	59.2	16.8	.0	1.35
5	100.0	99.7	98.1	91.4	59.6	16.7	.0	1.34
6	100.0	100.0	99.9	98.3	78.5	23.9	.0	0.99
11	100.0	99.9	99.4	97.4	72.8	22.3	.0	1.08
12	100.0	99.7	99.2	97.7	72.3	13.6	-0.3	1.18
13	99.8	99.5	98.9	97.3	92.6	17.7	.0	0.94
14	100.0	99.6	97.6	89.6	60.1	15.9	.0	1.37
15	100.0	99.9	98.8	80.3	26.2	7.7	.0	1.87
18	100.0	99.3	94.0	80.7	58.5	22.6	.0	1.45
19	100.0	99.6	95.8	83.5	46.6	7.3	0.1	1.67
20	100.0	99.9	98.3	89.7	53.5	10.3	0.1	1.48
22	99.9	99.3	98.2	93.5	51.3	12.5	.0	1.45
23	100.0	94.8	82.6	63.0	33.8	8.4	.0	2.17
24	100.0	99.7	98.3	85.7	39.0	7.6	.0	1.70
25	100.0	99.6	96.6	82.0	34.3	3.5	.0	1.84
26	100.0	100.0	100.0	92.0	34.3	6.4	.0	1.67
28	99.9	99.8	98.2	86.6	45.9	9.6	0.3	1.60
M.M.S.	100.0	99.7	99.1	97.8	68.3	15.9	.0	1.19

M.M.S.= McMaster Masonry Sand

TABLE A3.2: SERIES BM2: EFFECTS OF CURING ON MORTAR COMPRESSIVE STRENGTH

Batch no. :	M1*	1	15	20	25	5	4	26	18	M2*	M3*
Initial Flow	111.5	120.0	118.0	118.5	119.0	120.0	120.0	117.5	115.5	129.0	129.0
Air content (%)	13.0	11.5	15.0	14.5	17.0	15.0	14.5	15.5		14.5	14.5
Flow After	96.0	109.8	96.0	96.0	91.0	102.0	92.5	98.0	89.0	96.0	96.0
W.Retention (%)	86.1	91.5	81.4	81.0	76.5	85.0	77.1	80.9	77.1	74.4	74.4
Moist cured	19.8	15.0	15.6	11.7	13.4	14.5	15.1	15.8	16.2	15.7	17.6
Comp.Str.(MPa)	19.6	15.4	14.9	10.9	13.0	13.5	13.8	15.5	16.4	14.7	17.7
	18.9	16.8	15.0	11.7	13.1	13.8	15.3	15.6	16.4	15.0	16.3
Mean Strength	19.4	16.1	15.2	11.4	13.2	13.9	14.7	15.6	16.3	15.1	17.2
C.O.V. (%)	2.4	4.4	2.3	3.7	1.7	3.7	5.3	0.9	0.5	3.6	2.2
Lime-water	15.7	13.2	14.7	11.1	14.4	15.2	14.3	15.0	14.8	14.6	14.1
Comp.Str.(MPa)	15.8	13.8	15.3	10.0	13.9	14.2	15.2	12.0	17.5	13.1	15.7
	14.6	13.7	16.5	10.9	14.1	13.4	15.3	12.6	15.9	13.9	14.8
	15.1	13.3	17.0	11.2	13.8	12.7	14.3	12.7	116.2	13.1	14.9
	14.9	13.1	15.1	11.3	14.3	13.0	14.3	13.4	16.3	14.1	15.5
	15.5	13.6	14.8	11.0	13.9	14.4	14.6	12.1	16.2	14.3	15.2
Mean Strength	15.3	13.5	15.6	10.9	14.1	13.8	14.7	13.1	16.2	13.8	15.0
C.O.V. (%)	3.1	2.2	6.1	4.4	1.9	6.8	3.1	8.8	5.4	4.5	3.7
Air Cured	10.0	9.7	17.8	10.9	13.7	10.3	13.1	10.3	15.5	13.7	14.5
Comp.Str.(MPa)	10.1	9.5	13.0	9.7	13.7	9.7	13.9	12.6	14.9	13.2	14.9
	10.5	9.1	13.4	10.2	12.3	9.0	11.7	10.9	14.1	13.2	14.3
			13.1	10.4				9.4			
Mean Strength	10.2	9.5	13.3	10.3	12.9	9.6	12.9	10.8	14.8	13.3	14.5
C.O.V. (%)	2.7	3.2	2.6	5.0	5.7	7.0	8.5	12.3	4.8	2.2	2.3

* Mortar used McMaster masonry sand and for Batch M3 the mortar was placed on the face-shells of the block for 2 minutes prior to being cast into cube molds.

APPENDIX B

SUPPLEMENT TO CHAPTER 3

B1 STRAIN INDICATORS AND DATA

B1.1 Comparison of Mechanical Strain Indicator Results

To accommodate the various gauge lengths within the prism, two mechanical strain indicators were employed. A "DEMEC" strain indicator with a 200 mm gauge length and a "Huggenberger" strain indicator with a 50 mm gauge length were used. The DEMEC provided a 10 micro-strain precision for the strain reading while the Huggenberger yielded a 20 micro-strain precision. Note that the Huggenberger gives deformation reading in millimeters while the DEMEC indicates strain reading directly.

It was necessary to examine the accuracy of these two strain indicators against each other since strain data generated by each indicator will be often compared and used to complement one another. Mechanical gauge points were placed at 50 mm intervals along the face shell longitudinal centerline of a hollow concrete unit. The unit was loaded endwise in axial compression as shown in Figure A1.7 in Appendix A. At 50 KN load increments, deformation readings were taken by the Huggenberger indicator for the four gauge lengths of 50 mm each while an overall strain reading for the 200 mm gauge length was taken with the DEMEC indicator.

As shown in Figure B1.1, the stress-strain curves generated by each strain indicators over a 200 mm gauge length confirmed that the two strain indicators yielded very comparable results. A similar curve was also obtained from strain measurements on the other side. The overall difference between strain readings was 5.6%. However this difference maybe attributed to the complex geometry of the specimen employed (See Figure A1.7). In this research work, the DEMEC and Huggenberger strain indicators were assumed to produce similar strain readings.

B1.2 Summary of Prism Strain Data

A summary of the strain measurements obtained from 2-course and 4-course prisms, tested in axial compression under various testing procedures as described in Chapter 3 were listed in Tables B1.1 and B1.2. Each strain is the average of four readings. For vertical compressive strain, positive value indicates shortening of length while for lateral strain positive value indicates expansion. The whole 14 different strains were only monitored for some specific loading

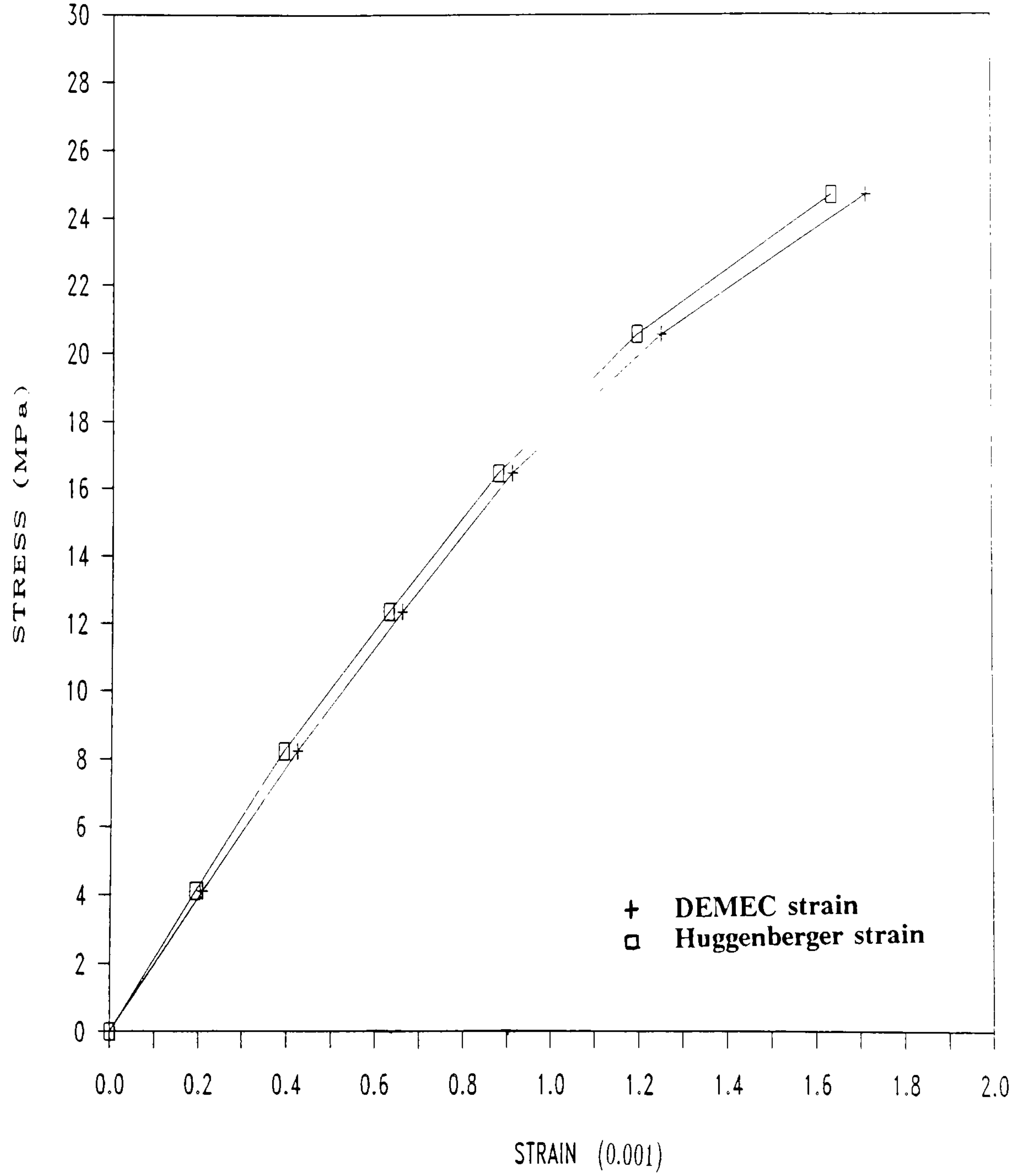

FIGURE B1.1 COMPARISON OF MECHANICAL STRAIN INDICATOR READINGS

TABLE B1.1: SUMMARY OF 2-COURSE PRISM STRAIN READINGS

STRAIN (0.00001)

TESTING PROCEDURE (Series)

Strain no.	Load (kN)	Pinned (PH2-1)	FSHC (PH2-4)	Flat (PH2-2)	50mm pl. (PH2-3)	FBSC (PH2-5)	FSSC (PH2-6)	sta.FSSC (PH2-7)
	0.0				0.0			
	50.0				5.5			
	100.0				12.4			
	150.0				20.9			
	200.0				30.5			
	250.0				40.9			
1	300.0				49.4			
	350.0				53.7			
	400.0				69.2			
	450.0				80.4			
	500.0				96.2			
	550.0				117.3			
	600.0							

Strain no.	Load (kN)	Pinned (PH2-1)	FSHC (PH2-4)	Flat (PH2-2)	50mm pl. (PH2-3)	FBSC (PH2-5)	FSSC (PH2-6)	sta.FSSC (PH2-7)
	0.0	0.0	0.0	0.0	0.0	0.0	0.0	0.0
	50.0	10.1	9.8	9.9	9.2	10.5	9.1	10.3
	100.0	19.4	18.0	20.3	18.5	20.0	18.7	19.6
	150.0	29.6	28.4	31.4	27.4	30.7	30.1	31.4
	200.0	43.1	41.1	44.0	39.4	43.7	46.1	52.2
	250.0	57.3	54.7	56.9	51.4	58.5	67.2	72.7
2	300.0	72.8	69.9	72.1	59.4	-16.7	86.4	101.2
	350.0	86.5	89.1	88.3	69.6	-39.1	118.9	132.3
	400.0	107.3	108.6	103.4	88.9	-81.4	149.1	167.3
	450.0	129.5	128.8	124.8	103.2		178.2	201.3
	500.0	150.5	150.3	149.3	122.3		203.1	240.1
	550.0		178.9		146.7			
	600.0		207.4					

Strain no.	Load (kN)	Pinned (PH2-1)	FSHC (PH2-4)	Flat (PH2-2)	50mm pl. (PH2-3)	FBSC (PH2-5)	FSSC (PH2-6)	sta.FSSC (PH2-7)
	0.0				0.0			
	50.0				12.9			
	100.0				23.0			
	150.0				35.1			
	200.0				48.3			
	250.0				61.5			
3	300.0				69.6			
	350.0				81.4			
	400.0				105.2			
	450.0				121.6			
	500.0				143.7			
	550.0				167.7			
	600.0							

TABLE B1.1 continued

STRAIN (0.00001)

TESTING PROCEDURE (Series)

Strain no.	Load (kN)	Pinned (PH2-1)	FSHC (PH2-4)	Flat (PH2-2)	50mm pl. (PH2-3)	FBSC (PH2-5)	FSSC (PH2-6)	sta.FSSC (PH2-7)
	0.0	0.0	0.0	0.0	0.0	0.0	0.0	0.0
	50.0	3.9	2.2	2.7	3.3	1.0	2.2	1.4
	100.0	4.3	4.9	6.4	6.9	2.5	2.9	3.6
	150.0	7.3	6.1	9.0	12.5	3.7	2.8	4.7
	200.0	8.0	9.6	12.1	20.3	3.9	4.3	6.2
	250.0	13.6	13.2	16.0	29.4	-2.1	8.6	8.7
4	300.0	16.4	16.1	20.3	40.9	0.9	11.9	12.0
	350.0	19.9	18.9	25.4	50.1	3.2	16.7	16.3
	400.0	26.3	23.2	31.6	63.0	11.1	21.5	20.3
	450.0	32.5	26.1	35.8	71.3		26.7	25.3
	500.0	35.9	32.2	42.6	86.9		30.4	34.5
	550.0		38.5					
	600.0		44.7					

Strain no.	Load (kN)	Pinned (PH2-1)	FSHC (PH2-4)	Flat (PH2-2)	50mm pl. (PH2-3)	FBSC (PH2-5)	FSSC (PH2-6)	sta.FSSC (PH2-7)
	0.0	0.0	0.0	0.0	0.0	0.0	0.0	0.0
	50.0	1.9	1.8	2.1	1.1	-0.6	-0.1	0.7
	100.0	3.4	3.7	2.9	3.6	1.0	4.4	1.7
	150.0	4.6	5.4	4.6	7.1	2.6	11.1	2.3
	200.0	5.1	8.2	8.0	10.3	5.4	26.0	2.2
	250.0	9.5	9.8	10.1	14.6	11.4	46.7	2.5
6	300.0	10.0	12.2	11.5	18.9	28.5	70.6	4.1
	350.0	12.9	15.9	13.5	22.3	36.9	93.3	4.9
	400.0	15.5	17.3	15.9	26.6	62.4	115.6	6.5
	450.0	23.8	19.3	21.7	30.0		130.3	6.9
	500.0	18.9	23.3	22.9	32.7		143.1	9.5
	550.0		26.1					
	600.0		28.8					

Strain no.	Load (kN)	Pinned (PH2-1)	FSHC (PH2-4)	Flat (PH2-2)	50mm pl. (PH2-3)	FBSC (PH2-5)	FSSC (PH2-6)	sta.FSSC (PH2-7)
	0.0	0.0	0.0	0.0	0.0	0.0	0.0	0.0
	50.0	-2.8	-4.0	-0.8	4.0	-3.3	-0.8	6.3
	100.0	-0.6	-2.3	0.3	8.3	-2.0	4.8	12.0
	150.0	-2.8	0.3	2.0	10.0	-2.0	7.8	39.5
	200.0	-6.5	1.0	-0.8	12.0	-6.5	16.0	84.0
	250.0	-5.0	3.5	4.8	11.3	41.3	38.3	169.0
10	300.0	1.5	2.8	2.5	22.0	439.5	81.5	228.8
	350.0	6.0	4.0	4.5	36.3	677.3	97.3	308.8
	400.0	16.8	5.4	15.5	55.3	902.0	139.8	344.5
	450.0	23.5	6.0	22.3	66.3		162.8	399.5
	500.0	30.0	7.5	32.0	76.8		192.8	456.8
	550.0		6.7					
	600.0		5.8					

TABLE B1.1 continued

STRAIN (0.00001)

TESTING PROCEDURE (Series)

Strain no.	Load (kN)	Pinned (PH2-1)	FSHC (PH2-4)	Flat (PH2-2)	50mm pl. (PH2-3)	FBSC (PH2-5)	FSSC (PH2-6)	sta.FSSC (PH2-7)
	0.0	0.0	0.0	0.0	0.0	0.0	0.0	0.0
	50.0	0.0	0.9	0.5	2.8	-3.3	-0.9	-0.5
	100.0	10.5	4.8	7.3	6.0	1.0	1.9	1.8
	150.0	16.7	10.3	16.5	8.3	20.0	5.3	1.8
	200.0	43.0	23.3	33.0	11.0	55.0	16.4	1.8
	250.0	119.5	43.0	65.3	28.0	714.3	27.9	2.3
11	300.0	299.5	62.8	107.8	231.8	2782.8	29.9	4.3
	350.0	509.5	89.3	221.0	436.0	2894.0	33.6	9.3
	400.0	675.5	130.5	358.5	559.0	3000.0	38.9	12.0
	450.0	822.5	161.0	460.0	817.8		41.6	10.8
	500.0	994.0	307.0	600.8	827.8		49.9	15.5
	550.0		314.3					
	600.0		321.5					

Strain no.	Load (kN)	Pinned (PH2-1)	FSHC (PH2-4)	Flat (PH2-2)	50mm pl. (PH2-3)	FBSC (PH2-5)	FSSC (PH2-6)	sta.FSSC (PH2-7)
	0.0	0.0	0.0	0.0	0.0	0.0	0.0	0.0
	50.0	2.5	4.5	5.8	1.8	3.9	6.5	8.0
	100.0	6.3	8.3	3.8	1.3	8.0	15.3	20.3
	150.0	9.0	14.5	5.0	0.3	12.0	22.5	33.8
	200.0	12.0	19.8	7.3	3.0	18.5	33.3	43.5
	250.0	18.5	23.8	11.3	3.4	24.0	42.5	57.5
12	300.0	30.5	31.3	16.3	11.5	26.0	51.8	70.0
	350.0	40.3	39.8	21.8	19.5	30.8	64.8	82.8
	400.0	49.5	46.0	30.0	27.5	44.0	73.0	98.5
	450.0	61.0	52.8	37.8	33.0		82.3	113.8
	500.0	69.3	65.3	43.3	42.0		93.3	131.8
	550.0		76.6					
	600.0		87.8					

Strain no.	Load (kN)	Pinned (PH2-1)	FSHC (PH2-4)	Flat (PH2-2)	50mm pl. (PH2-3)	FBSC (PH2-5)	FSSC (PH2-6)	sta.FSSC (PH2-7)
	0.0	0.0	0.0	0.0	0.0	0.0	0.0	0.0
	50.0	4.0	1.5	5.8	3.0	-0.5	2.0	0.8
	100.0	5.8	1.9	3.5	3.3	2.8	-0.5	1.0
	150.0	9.8	5.0	4.3	3.0	5.5	-1.8	-1.3
	200.0	7.0	2.8	6.5	4.7	7.5	-0.8	-2.5
	250.0	9.8	4.3	8.5	4.8	14.0	-3.3	-5.5
13	300.0	11.5	5.0	11.0	-2.3	13.6	-4.0	-4.0
	350.0	4.9	3.3	8.0	-7.3	13.3	-6.3	-4.0
	400.0	4.3	2.3	6.0	-7.5	13.5	-6.5	-5.3
	450.0	2.8	2.6	4.0	-8.0		-6.3	-1.5
	500.0	1.8	3.3	-1.3	-7.5		-7.5	-1.3
	550.0		1.9					
	600.0		0.5					

TABLE B1.1: **continued**

		STRAIN (0.00001)						
		TESTING PROCEDURE (Series)						
Strain no.	Load (kN)	Pinned (PH2-1)	FSHC (PH2-4)	Flat (PH2-2)	50mm pl. (PH2-3)	FBSC (PH2-5)	FSSC (PH2-6)	sta.FSSC (PH2-7)
	0.0				0.0			
	50.0				8.0			
	100.0				15.2			
	150.0				25.5			
	200.0				35.4			
	250.0				48.2			
14	300.0				53.4			
	350.0				61.2			
	400.0				79.6			
	450.0				92.1			
	500.0				105.5			
	550.0				129.6			
	600.0							

Pinned (Series PH2-1) - Pin-Ended Conditions; (full hard capping & 75mm thick bearing plates)
FSHC (Series PH2-4) Face Shell Hard Cap; (pin-ended conditions & 75mm thick bearing plates)
Flat (Series PH2-2) = Flat-Ended Conditions; (full hard capping & 75mm thick bearing plates)
50mm pl. (Series PH2-3) 50mm Thick Bearing Plates; (pin-ended conditions & full hard capping)
FBSC (Series PH2-5) Full Bed Soft Capping; (pin-ended conditions & 75mm thick bearing plates)
FSSC (Series PH2-6) Face Shell Soft Cap; (pin-ended conditions & 75mm thick bearing plates)
sta.FSSC (Series PH2-7) Stack Bond Face Shell Soft Capping; (pin-ended conditions & 75mm thick bearing plates)

TABLE B1.2: SUMMARY OF 4-COURSE PRISM STRAIN READINGS

		STRAIN (0.00001)					
		TESTING PROCEDURE (Series)					
Strain no.	Load (kN)	Pinned (PH4-1)	FSHC (PH4-4)	Flat (PH4-2)	50mm pl. (PH4-3)	FBSC (PH4-5)	FSSC (PH4-6)
	0.0	0.0		0.0	0.0	0.0	0.0
	50.0	12.6		6.6	17.4	7.5	7.4
	100.0	19.8		18.7	29.2	15.6	15.9
	150.0	30.8		27.4	41.2	25.0	25.9
	200.0	41.8		39.2	52.7	34.1	37.3
1	250.0	55.5		52.9	69.8	49.6	50.9
	300.0	71.7		67.3	87.6	66.7	65.4
	350.0	93.6		85.8	110.2	98.7	83.2
	400.0	120.7		109.9	136.0		108.3
	450.0	145.2		137.6	160.6		121.9
	500.0						142.5
Strain no.	Load (kN)	Pinned (PH4-1)	FSHC (PH4-4)	Flat (PH4-2)	50mm pl. (PH4-3)	FBSC (PH4-5)	FSSC (PH4-6)
	0.0	0.0	0.0	0.0	0.0	0.0	0.0
	50.0	13.3	9.8	6.3	19.7	9.0	7.9
	100.0	21.0	19.1	19.3	30.4	19.2	17.5
	150.0	33.3	28.8	28.8	40.7	29.4	27.3
	200.0	46.1	43.2	43.0	56.7	41.8	39.4
2	250.0	61.5	59.8	58.4	73.8	56.2	53.4
	300.0	77.3	79.1	74.9	94.5	75.9	69.5
	350.0	104.7	99.8	97.5	120.2	107.5	87.6
	400.0	122.2	133.4	119.1	150.4		115.4
	450.0	162.4	159.5	153.5	191.5		130.8
	500.0						155.7
Strain no.	Load (kN)	Pinned (PH4-1)	FSHC (PH4-4)	Flat (PH4-2)	50mm pl. (PH4-3)	FBSC (PH4-5)	FSSC (PH4-6)
	0.0	0.0		0.0	0.0	0.0	
	50.0	12.0		7.9	13.9	7.2	
	100.0	20.1		20.0	28.4	15.4	
	150.0	33.6		30.4	41.6	27.1	
	200.0	45.8		44.8	56.9	40.1	
3	250.0	64.6		60.0	74.4	55.3	
	300.0	82.8		79.2	99.0	77.1	
	350.0	111.4		98.0	125.0	113.9	
	400.0	154.6		133.8	162.3		
	450.0	182.1		170.1	227.7		
	500.0						

TABLE B1.2: continued

		STRAIN (0.00001)					
		TESTING PROCEDURE (Series)					
Strain no.	Load (kN)	Pinned (PH4-1)	FSHC (PH4-4)	Flat (PH4-2)	50mm pl. (PH4-3)	FBSC (PH4-5)	FSSC (PH4-6)
	0.0	0.0	0.0	0.0	0.0	0.0	0.0
	50.0	2.0	0.5	1.5	1.4	0.6	0.9
	100.0	2.8	4.6	2.8	8.1	1.8	2.5
	150.0	6.5	11.1	5.7	9.9	4.8	5.9
	200.0	9.0	12.6	18.6	20.1	7.1	9.7
4	250.0	14.0	29.4	21.0	20.0	12.5	10.6
	300.0	19.0	28.2	30.4	27.7	15.2	17.9
	350.0	29.4	35.9	24.4	30.8	20.1	24.1
	400.0	42.3	49.0	32.7	42.7		34.8
	450.0	57.3	61.9	45.7	84.8		39.3
	500.0						51.4
Strain no.	Load (kN)	Pinned (PH4-1)	FSHC (PH4-4)	Flat (PH4-2)	50mm pl. (PH4-3)	FBSC (PH4-5)	FSSC (PH4-6)
	0.0	0.0					
	50.0	0.8					
	100.0	2.3					
	150.0	3.3					
	200.0	7.6					
5	250.0	11.4					
	300.0	14.6					
	350.0	20.4					
	400.0	36.4					
	450.0	45.3					
	500.0						
Strain no.	Load (kN)	Pinned (PH4-1)	FSHC (PH4-4)	Flat (PH4-2)	50mm pl. (PH4-3)	FBSC (PH4-5)	FSSC (PH4-6)
	0.0	0.0	0.0	0.0	0.0	0.0	0.0
	50.0	-0.4	0.5	5.4	1.9	-2.4	2.1
	100.0	2.3	2.6	7.4	5.6	-0.6	4.3
	150.0	2.2	11.4	9.9	9.2	1.2	9.9
	200.0	5.4	14.7	13.4	13.7	4.6	24.4
6	250.0	4.0	18.4	12.9	15.0	10.0	47.5
	300.0	7.4	18.9	16.8	17.3	18.4	60.3
	350.0	11.7	27.8	16.6	20.1	28.6	78.3
	400.0	8.1	17.9	19.6	24.2		95.6
	450.0	15.7	17.8	21.8	32.2		108.6
	500.0						120.0

TABLE B1.2: continued

STRAIN (0.00001)

TESTING PROCEDURE (Series)

Strain no.	Load (kN)	Pinned (PH4-1)	FSHC (PH4-4)	Flat (PH4-2)	50mm pl. (PH4-3)	FBSC (PH4-5)	FSSC (PH4-6)
	0.0	0.0					
	50.0	8.3					
	100.0	9.3					
	150.0	20.7					
	200.0	31.8					
7	250.0	37.1					
	300.0	49.6					
	350.0	64.3					
	400.0	80.7					
	450.0	95.7					
	500.0						

Strain no.	Load (kN)	Pinned (PH4-1)	FSHC (PH4-4)	Flat (PH4-2)	50mm pl. (PH4-3)	FBSC (PH4-5)	FSSC (PH4-6)
	0.0	0.0				0.0	
	50.0	3.8				5.5	
	100.0	5.8				7.5	
	150.0	5.5				14.8	
	200.0	12.4				21.5	
8	250.0	18.0				21.3	
	300.0	25.8				28.0	
	350.0	34.5				33.8	
	400.0	44.6					
	450.0	59.3					
	500.0						

Strain no.	Load (kN)	Pinned (PH4-1)	FSHC (PH4-4)	Flat (PH4-2)	50mm pl. (PH4-3)	FBSC (PH4-5)	FSSC (PH4-6)
	0.0	0.0				0.0	
	50.0	-0.3				5.5	
	100.0	4.6				10.0	
	150.0	10.8				14.5	
	200.0	15.3				15.8	
9	250.0	27.8				23.0	
	300.0	33.2				32.0	
	350.0	47.0				38.5	
	400.0	54.7					
	450.0	75.3					
	500.0						

TABLE B1.2: continued

		STRAIN (0.00001)					
		TESTING PROCEDURE (Series)					
Strain no.	Load (kN)	Pinned (PH4-1)	FSHC (PH4-4)	Flat (PH4-2)	50mm pl. (PH4-3)	FBSC (PH4-5)	FSSC (PH4-6)
	0.0	0.0	0.0	0.0	0.0	0.0	0.0
	50.0	3.8	4.0	6.3	-1.8	0.5	4.0
	100.0	3.4	2.0	10.0	-1.0	2.5	6.7
	150.0	4.0	3.7	7.7	4.0	11.0	16.8
	200.0	2.5	5.7	9.5	6.5	9.3	25.7
10	250.0	5.5	4.5	13.7	9.5	12.0	32.0
	300.0	3.0	5.8	12.4	9.3	8.0	39.9
	350.0	9.3	4.8	9.5	14.8	113.3	67.2
	400.0	16.9	3.6	10.5	22.8		76.0
	450.0	24.3	5.0	22.0	55.0		88.9
	500.0						102.1

Strain no.	Load (kN)	Pinned (PH4-1)	FSHC (PH4-4)	Flat (PH4-2)	50mm pl. (PH4-3)	FBSC (PH4-5)	FSSC (PH4-6)
	0.0	0.0	0.0	0.0	0.0	0.0	0.0
	50.0	2.0	1.2	1.0	-3.0	-2.3	-1.5
	100.0	-0.8	3.5	2.5	-5.5	-2.3	-0.8
	150.0	1.0	1.5	-8.0	-3.9	0.1	0.5
	200.0	-0.7	1.4	1.5	0.5	3.5	5.8
11	250.0	3.5	3.6	3.0	1.5	7.5	3.3
	300.0	12.6	3.9	7.5	5.0	42.3	6.0
	350.0	51.0	18.2	22.6	25.8	210.9	5.5
	400.0	152.5	127.1	69.0	86.0		14.3
	450.0	234.5	174.3	148.0	174.5		91.3
	500.0						188.5

Strain no.	Load (kN)	Pinned (PH4-1)	FSHC (PH4-4)	Flat (PH4-2)	50mm pl. (PH4-3)	FBSC (PH4-5)	FSSC (PH4-6)
	0.0	0.0	0.0			0.0	0.0
	50.0	-0.5	6.0			4.8	5.3
	100.0	2.0	9.8			6.5	14.1
	150.0	4.5	15.3			11.7	23.8
	200.0	9.5	24.8			14.3	27.3
12	250.0	11.5	26.5			23.0	47.3
	300.0	16.3	35.0			28.5	56.3
	350.0	18.5	43.5			34.0	66.0
	400.0	25.0	46.0				77.3
	450.0	35.0	55.0				89.0
	500.0						97.5

TABLE B1.2: continued

		STRAIN (0.00001)					
		TESTING PROCEDURE (Series)					
Strain no.	Load (kN)	Pinned (PH4-1)	FSHC (PH4-4)	Flat (PH4-2)	50mm pl. (PH4-3)	FBSC (PH4-5)	FSSC (PH4-6)
	0.0	0.0	0.0			0.0	0.0
	50.0	-2.0	1.0			0.3	-4.8
	100.0	-6.3	0.8			1.0	-4.1
	150.0	5.0	-1.9			5.0	-2.8
	200.0	7.0	1.8			3.8	2.2
13	250.0	9.5	1.5			8.0	-5.9
	300.0	11.2	0.5			13.0	-6.8
	350.0	16.0	3.0			19.0	-6.8
	400.0	12.7	-1.5				-8.8
	450.0	20.0	-3.2				-9.3
	500.0						-10.8
Strain no.	Load (kN)	Pinned (PH4-1)	FSHC (PH4-4)	Flat (PH4-2)	50mm pl. (PH4-3)	FBSC (PH4-5)	FSSC (PH4-6)
	0.0				0.0		
	50.0				13.8		
	100.0				22.3		
	150.0				35.5		
	200.0				48.6		
14	250.0				60.6		
	300.0				83.0		
	350.0				106.0		
	400.0				130.2		
	450.0				158.8		
	500.0						

Pinned (Series PH4-1) - Pin-Ended Conditions; (full hard capping & 75mm thick bearing plates)
FSHC (Series PH4-4) Face Shell Hard Cap; (pin-ended conditions & 75mm thick bearing plates)
Flat (Series PH4-2) - Flat-Ended Conditions; (full hard capping & 75mm thick bearing plates)
50mm pl. (Series PH4-3) - 50mm Thick Bearing Plates; (pin-ended conditions & full hard cap)
FBSC (Series PH4-5) - Face Bed Soft Cap; (pin-ended conditions & 75mm thick bearing plates)
FSSC (Series PH4-6) Face Shell Soft Cap; (pin-ended conditions & 75mm thick bearing plates)

conditions. The number shown in the left hand side of the Table indicate the gauge length location on the prism as shown in Figures 3.2 and 3.3. For every gauge location number, the strain readings from the 7 different test series were listed together. A brief description of each series was included at the bottom of each of the two tables.

B2 MORTAR AND UNIT STRENGTH DATA

B2.1 Mortar

The individual mortar cube ultimate compressive loads, mean strengths and the coefficients of variation for mortar (Type S2 mortar, see mix proportion in Table 2.4) used in the tests reported in Chapter 3 were listed in Table B2.1.

B2.2 Splitting Tensile Strength of Blocks

The concrete block splitting tensile strength was determined in a similar manner to Series T1 in Section 2.2.4. (For more details refer also to Section A2.2 and Figure A2.1 in Appendix A). The tensile strength results were listed in Table B2.2.

TABLE B2.1: CUBE COMPRESSIVE STRENGTHS OF TYPE S2 MORTAR

BATCH NO.	PRISM SERIES	COMPRESSIVE LOAD (KN)	MEAN LOAD (KN)	MEAN STRENGTH (MPa)	COEFF. OF VARIATION (%)
2	PH2-2 & PH4-2	25.1 25.8 23.9	24.9	9.7	3.9
3	PH2-3 & PH4-3	21.7 22.2 20.8	21.6	8.4	3.2
4	PH2-4 & PH4-4	22.7 22.4 20.9	22.0	8.5	4.5
5	PH2-1 & PH4-1	22.6 20.8 22.7	22.0	8.5	4.9
6	PH2-5 & PH4-5	19.6 18.3 19.4	19.1	7.4	3.7
7	PH2-6, PH4-6 & PH2-7	19.9 21.0 19.4	20.1	7.8	4.1

TABLE B2.2: SPLITTING TENSILE STRENGTHS OF HOLLOW CONCRETE BLOCKS

UNIT NO.	ULTIMATE LOAD (KN)	TENSILE STRENGTH (MPa)	MEAN STRENGTH (MPa)	C.O.V. (%)
1	52.7	2.60		
2	45.8	2.26		
3	38.9	1.92	2.28	10.9
4	48.3	2.38		
5	45.5	2.24		

APPENDIX C

SUPPLEMENT TO CHAPTER 4

C1 BLOCK COMPRESSION AND TENSION TEST RESULTS, COMPANIES 10 AND 21

The individual block compressive ultimate load, individual ultimate splitting load, mean strengths and coefficients of variation were listed in Table C1.1 for Companies 10 and 21.

These units were used in the investigation included in Chapter 4. Details of the preparation and test procedures were indicated in Section 4.2.3.

TABLE C1.1: RESULTS OF UNIT COMPRESSION AND TENSION TESTS; COMPANIES 10 & 21

COMPANY NO.	UNIT COMPRESSION TEST				UNIT TENSION TEST			
	ULT. LOAD (kN)	MEAN LOAD (KN)	MEAN STRENGTH (MPa)	C.O.V. (%)	ULT. LOAD (kN)	MEAN LOAD (KN)	MEAN STRENGTH (MPa)	C.O.V. (%)
	1417				50.5			
	1430				45.1			
	1294				41.2			
	1296				55.8			
10	1226	1288.5	31.0	6.5	61.9	53.5	2.6	14.1
	1184				65.0			
	1309				56.3			
	1235				48.3			
	1298				59.3			
	1196				51.2			
	1054				45.1			
	1036				49.1			
	1032				55.3			
	980				50.3			
21	1101	1018.4	24.5	5.2	48.2	48.3	2.3	7.3
	915				45.0			
	1010				48.5			
	964				49.2			
	1044				42.4			
	1048				49.9			

APPENDIX D

SUPPLEMENT TO CHAPTER 5

D1 GROUT

The medium strength grout had a mix proportion of 1:0.1:3.0 by volume or 1:0.44 : 3.55 by weight of Portland-Cement to Lime to sand. The grout was mixed by weight using a mechanical mixer. The same type of sand as employed in the mortar was used. A 247 mm slump was obtained using a water to cement ratio of 0.64. The grout in the masonry prism as well as the control specimens was compacted with a poker vibrator at the time of mixing.

The 75 mm x 75 mm x 150 mm control specimens were cast in block molds using paper towel as a bond breaker as specified by CSA-179A-76[23]. Dry blocks were used in making the block molds. The grout molds as with as the masonry prisms were covered with an impermeable plastic sheeting for the first 48 hours. After that, the prisms as well as the control specimens were air cured until testing. The control specimens were capped with a 5 to 6 mm thick sulphur layer prior to testing which was carried out at the time of prism testing and one month exactly from the day of grouting. The grout control specimens had a compressive strength of 36.7 MPa with a 7.6% coefficient of variation.

D2 EVALUATION OF PROPOSED FORMULATIONS FOR PREDICTING THE COMPRESSIVE STRENGTH OF CONCRETE MASONRY PRISMS

The only available analytical approach[32] for predicting the compressive strength of block masonry was evaluated by comparing the predicted strengths against the results in this investigations. Grouted and solid fully mortared block prisms were compared. In addition, the results from Series S7 in Chapter 4, hollow block stacked pattern prisms with full mortaring, were included in this comparison.

D2.1 Grouted Masonry

Two formulas were proposed for predicting the strength of grouted prisms. One was for the case where the shell (blocks) reaches its unconfined compressive strength first (Case I) and the second was for the case where the grouted core reaches its unconfined compressive strength first (Case II). In this comparison, Case I formulation was employed since the grout had a higher compressive strength than the blocks of Companies 10 and 21:

$$f'_{mg} = \frac{4.1\,\sigma_{tb} + 1.14\,\alpha\,\sigma_{cm} + \beta\,\sigma_{cg}}{4.1\,\sigma_{tb} + (1.14\,\alpha + c\beta/n)\,\sigma_{cb}} \cdot \frac{\sigma_{cb}}{n\gamma k} \qquad \text{(D2.1)}$$

where f'_{mg} = compressive strength of grouted masonry

σ_{cg} = unconfined compressive strength of grout

σ_{tb} = tensile splitting strength of block

σ_{cm} = mortar compressive strength from standard cube test

σ_{cb} = compressive strength of block unit

α = joint thickness to block height ratio, t_m/t_b

n = modular ratio, E_{bs}/E_g

E_g = modulus of elasticity of grout

E_{bs} = modulus of elasticity of block

γ = $1/(1 + (n-1)\eta)$

c = ratio of maximum to minimum cross-sectional area of the grouted core

= 1.27

η = minimum net to gross area ratio of the block An/Ag

k = coefficient intended to account the for redistribution of the vertical stress between the shell and the grouted core at failure and given by:

= $1.08 + 0.21\,(E_g/E_{bs})$

$$\beta = \frac{1 - \eta}{1 - \sqrt{1 - \eta}}$$

in predicting the strength the following values were used:

σ_{cb}, σ_{tb}, σ_m = compressive and tensile block strengths and mortar strength, respectively were taken from Tables 5.3 and 5.4

σ_{cg} = 36.7 MPa

n = 0.83 and 0.77 for Companies 10 and 21 respectively

η = 0.513 for standard hollow 190 mm block

t_m = thickness of mortar joint = 11.0 mm.

For the grouted prisms, the predicted strengths using Equation D2.1 were 20.1 MPa and 18.1 MPa for Companies 10 and 21, respectively. These predicted strengths corresponded to experimental values of 13.6 MPa and 10.7 MPa, respectively. The formulation resulted in 48% and 69% higher values than the experimental results.

D2.2 Solid and Fully Mortared Masonry

Equation D2.2 was used to predict the strength of plain blockwork with any percent solid, on the basis of the net area[43]. In this equation the k value is now 1.08.

$$f'_{mu} = \frac{3.5\,\sigma_{tb} + \alpha\sigma_{cm}}{3.6\,\sigma_{tb} + \alpha\sigma_{cb}} \cdot \frac{\sigma_{cb}}{k} \qquad \text{(D2.2)}$$

For 100% solid prisms, the predicted strength was 23.9 MPa in comparison to an experimental value of 17.5 MPa. For 75% solid prisms the predicted strength was 31.6 MPa versus an experimental value of 23.4 MPa. For both types of solid prisms the predicted strengths using Equation D2.2 were 36% and 35% higher than the experimental values.

In addition, the strengths of hollow prisms with full mortaring (Series S7-10 and S7-21 in Chapter 4) were 26.8 MPa and 21.8 MPa in comparison to experimental values of 20.8 and 16.5 MPa for Companies 10 and 21, respectively.

D3 ELASTIC AND PLASTIC ANALYSES FOR ECCENTRIC LOADING

D3.1 Elastic Analysis

For hollow face shell mortared blockwork, the Kern eccentricity is nearly at t/3 (one side of the two face shells at zero stress). Since only eccentricity of e=t/6 was considered here, stress for uncracked section was calculated only:

$$f'_{me} = \frac{P_e}{2bt_m} \left\{ 1 + \frac{6\ e}{3t - 6t_m + 4\ (t_m^2/t)} \right\} \qquad \text{(D3.1)}$$

where P_e = load at eccentricity e

f'_{me} = compressive stress at the most compressed side

b = length of section

t = width of block

t_m = equivalent thickness of mortar bedded face shell

= 1.23 x minimum face shell thickness

D3.2 Plastic Analysis

The formulation for a plastic analysis was taken from Maurenbrecher[69] where a rectangular stress block, no tensile strength and a failure stress equals the failure stress of axially loaded prism were assumed. The equations for uncracked section are:

For $0 \leqslant e/t \leqslant 0.5\,(1-\alpha)$

$$x/t = [\,\alpha(1 - \alpha - 2e/t) + (0.5 - \alpha + e/t)^2\,]^{1/2} + (0.5 - e/t)$$

$$P_e/P_o = (x/t + 2\alpha - 1)/2\alpha$$

where $\alpha = t_m/t$

x = width of rectangular stress block

P_o = load at e=0

APPENDIX E

SUPPLEMENT TO CHAPTER 6

E1 PHYSICAL CHARACTERISTICS OF CONCRETE BLOCKS

Table E1.1 contains a listing of some of the important characterises for hollow stretcher blocks from 29 different block plants. Blocks from 18 companies had flared tops all around, whereas 2 companies produced blocks with flares in the middle web only. For 9 companies, their blocks did not have flares. The block areas were based on the net average area and not the minimum. Discussion regarding how these values are obtained can be found in Chapter 2. As shown in Table E1.1, three different types of curing processes were used. The block weight was the laboratory dry weight after a sufficient period of inside storage.

E2 INDIVIDUAL BLOCK COMPANY TEST RESULTS

For the 29 block companies, the individual test results were listed in TAbles E2.1 to E2.29. In each table the prism compression, block compression and tensile splitting and mortar cube test results were all listed along with the mean values and corresponding coefficients of variation. Prism compressive strengths were based on the

TABLE E1.1: PHISYCAL CHARACTERISTICS OF 29 DIFFERENT BLOCKS

COMPANY NO.	BLOCK DESCRIPTION	BLOCK NET AREA (mm^2)	CURING PROCESS	WEIGTH (Kg)
1	Cores with flared tops	41500	Autoclave	17.02
2	Cores with flared tops	41500	Low steam	17.45
3	No flares	39860	Low steam	17.01
4	Cores with flared tops	41500	N/A	17.23
5	Cores with flared tops	41500	N/A	17.08
6	Cores with flared tops	41500	Autoclave	17.66
7	Cores with flared tops	41500	Low steam	16.88
8	Cores with flared tops	41500	Autoclave	16.12
9	Cores with flared tops	41500	Low steam	17.16
10	Cores with flared tops	41500	Bubble	17.30
11	No flares	39860	Low steam	17.60
12	Cores with flared tops	41500	Autoclave	17.65
13	Cores with flared tops	41500	Autoclave	17.50
14	Cores with flared tops	41500	Low steam	17.64
15	Flares at middle web only	39860	Autoclave	17.69
16	Cores with flared tops	41500	Low steam	17.72
17	No flares	39860	Low steam	16.86
18	Flares at middle web only	39860	Low steam	17.20
19	No flares	39860	Low steam	17.00
20	Cores with flared tops	41500	Autoclave	16.88
21	Cores with flared tops	41500	Autoclave	17.08
22	Cores with flared tops	41500	Autoclave	17.23
23	Cores with flared tops	41500	Low steam	17.24
24	No flares	39860	Low steam	17.22
25	Cores with flared tops	41500	Low steam	N/A
26	No flares	39860	Low steam	17.02
27	No flares	39860	Low steam	N/A
28	No flares	39860	Low steam	16.98
29	No flares	39860	Low steam	N/A

effective mortar bedded area of 30700 mm^2. For blocks, the compressive strengths were calculated using the corresponding area shown in Table E1.1. At the top of each table, opposite SAND, Y indicates that the block company's own sand was used. N indicated that McMaster sand was used. Properties of the individual sand and discussion of the corresponding mortar can be found in Chapter 2 and Appendix A.

Related testing procedures and basis for strength calculations can also be found in Section 6.2.

TABLE E2.1: BLOCK COMPANY 1 TEST RESULTS

COMPANY NUMBER = 1

BLOCK MANUF. = N/A
SAND (Y OR N) = Y

PRISM COMPRESSION TESTS — PRISM MANUF. = 1/29/87

PRISM CODE	TEST DATE	FAILURE LOAD (kN)	STRENGTH (MPa)
P - 1		628.5	20.5
P - 2		647.8	21.1
P - 3	2/24/87	642.6	20.9
P - 4		610.0	19.9
P - 5		597.2	19.5
MEAN		625.2	20.4
COV (%)		3.4	3.4

BLOCK TESTS

COMPRESSION DATE: 2/24/87 — TENSION DATE: 2/24/87

CODE	LOAD (kN)	STRENGTH (MPa)	CODE	LOAD (kN)	STRENGTH (MPa)
1	1262.5	30.4	1	37.5	1.8
2	1192.0	28.7	2	35.7	1.7
3	1220.0	29.4	3	39.4	1.9
4	1133.0	27.3	4	53.0	2.6
5	1201.0	28.9	5	46.5	2.3
6	1259.0	30.3	6	49.0	2.4
7	1173.0	28.3	7	46.0	2.2
8	1187.0	28.6	8	49.2	2.4
9	1211.0	29.2	9	46.2	2.2
10	1130.0	27.2	10	47.7	2.3
MEAN	1196.9	28.8	MEAN	45.0	2.2
COV (%)	3.8	3.8	COV (%)	12.5	12.5

MORTAR CUBE COMPRESSION RESULTS

DATE: 2/24/87 — FLOW: 120%

CODE	LOAD (kN)	STRENGTH (MPa)
1	19.4	7.5
2	18.7	7.2
3	19.2	7.4
MEAN	19.1	7.4
COV (%)	1.9	1.9

TABLE E2.2: BLOCK COMPANY 2 TEST RESULTS

COMPANY NUMBER = 2

BLOCK MANUF. = 11/24/86
SAND (Y OR N) = Y

PRISM COMPRESSION TESTS — PRISM MANUF. = 1/29/87

PRISM CODE	TEST DATE	FAILURE LOAD (kN)	STRENGTH (MPa)
P - 1		640.8	20.9
P - 2		633.6	20.6
P - 3	2/25/87	590.6	19.2
P - 4		686.0	22.3
P - 5		602.8	20.5
MEAN		630.8	20.5
COV (%)		5.9	5.9

BLOCK TESTS

COMPRESSION DATE: 2/25/87 — TENSION DATE: 2/26/87

CODE	LOAD (kN)	STRENGTH (MPa)	CODE	LOAD (kN)	STRENGTH (MPa)
1	1259.0	30.3	1	63.8	3.1
2	1292.0	31.1	2	61.6	3.0
3	1178.0	28.4	3	50.2	2.4
4	1226.0	29.5	4	59.6	2.9
5	1197.0	28.8	5	60.7	2.9
6	1230.0	29.6	6	67.3	3.3
7	1243.0	30.0	7	57.1	2.8
8	1149.0	27.7	8	58.4	2.8
9	1215.0	29.3	9	56.7	2.8
10	1190.0	28.7	10	61.9	3.0
MEAN	1217.9	29.3	MEAN	59.7	2.9
COV (%)	3.4	3.4	COV (%)	7.7	7.7

MORTAR CUBE COMPRESSION RESULTS

DATE: 2/25/87 — FLOW: 120%

CODE	LOAD (kN)	STRENGTH (MPa)
1	20.0	7.8
2	20.8	8.1
3	19.0	7.4
MEAN	19.9	7.7
COV (%)	4.6	4.6

TABLE E2.3: BLOCK COMPANY 3 TEST RESULTS

COMPANY NUMBER = 3 | BLOCK MANUF. = 11/19/86 | SAND (Y OR N) = N

PRISM COMPRESSION TESTS | PRISM MANUF. = 1/30/87

PRISM CODE	TEST DATE	FAILURE LOAD (kN)	STRENGTH (MPa)
P-1		590.0	19.2
P-2		655.0	21.3
P-3	2/17/87	611.0	19.9
P-4		525.0	17.1
P-5		674.0	22.0
MEAN		611.0	19.9
COV (%)		9.6	9.6

BLOCK TESTS

COMPRESSION DATE: 3/17/87 — TENSION DATE: 3/24/87

CODE	LOAD (kN)	STRENGTH (MPa)	CODE	LOAD (kN)	STRENGTH (MPa)
1	1226.0	30.7	1	58.0	2.8
2	1176.0	29.5	2	55.7	2.7
3	1220.0	30.6	3	53.0	2.6
4	1210.0	30.4	4	58.8	2.9
5	1226.0	30.7	5	50.5	2.5
6	1170.0	29.4	6	52.5	2.5
7	1288.0	32.3	7	52.7	2.6
8	1145.0	28.7	8	53.5	2.6
9	1174.0	29.5	9	42.7	2.1
10	1301.0	32.8	10	43.3	2.1
MEAN	1213.6	30.5	MEAN	52.1	2.5
COV (%)	4.2	4.2	COV (%)	10.4	10.4

MORTAR CUBE COMPRESSION RESULTS

DATE: 2/17/87 — FLOW: 119%

CODE	LOAD (kN)	STRENGTH (MPa)
1	34.4	13.3
2	31.1	12.1
3	32.0	12.4
MEAN	32.5	12.6
COV (%)	5.2	5.2

TABLE E2.4: BLOCK COMPANY 4 TEST RESULTS

COMPANY NUMBER = 4 | BLOCK MANUF. = N/A | SAND (Y OR N) = Y

PRISM COMPRESSION TESTS | PRISM MANUF. = 1/30/87

PRISM CODE	TEST DATE	FAILURE LOAD (kN)	STRENGTH (MPa)
P-1		529.0	17.2
P-2		588.0	19.2
P-3	3/27/87	559.0	18.2
P-4		578.0	18.8
P-5		631.8	20.6
MEAN		577.2	18.8
COV (%)		6.6	6.6

BLOCK TESTS

COMPRESSION DATE: 4/03/87 — TENSION DATE: 4/10/87

CODE	LOAD (kN)	STRENGTH (MPa)	CODE	LOAD (kN)	STRENGTH (MPa)
1	1139.0	27.4	1	42.1	2.0
2	1074.0	25.9	2	41.9	2.0
3	1170.0	28.2	3	36.7	1.8
4	1047.0	25.2	4	45.1	2.2
5	1067.0	25.7	5	40.0	1.9
6	1069.0	25.8	6	52.9	2.6
7	1142.0	27.5	7	45.6	2.2
8	1176.0	28.3	8	44.3	2.2
9	1163.0	28.0	9	40.5	2.0
10	1181.0	28.5	10	51.2	2.5
MEAN	1122.8	27.1	MEAN	44.0	2.1
COV (%)	4.7	4.7	COV (%)	11.3	11.3

MORTAR CUBE COMPRESSION RESULTS

DATE: 3/27/87 — FLOW: 120%

CODE	LOAD (kN)	STRENGTH (MPa)
1	30.0	11.6
2	29.1	11.3
3	31.1	12.1
MEAN	30.1	11.7
COV (%)	3.3	3.3

TABLE E2.5: BLOCK COMPANY 5 TEST RESULTS

COMPANY NUMBER = 5	BLOCK MANUF. = N/A SAND (Y OR N) = Y

PRISM COMPRESSION TESTS		PRISM MANUF. = 1/30/87	
PRISM CODE	TEST DATE	FAILURE LOAD (kN)	STRENGTH (MPa)
P-1		575.0	18.7
P-2		611.0	19 9
P-3	3/27/87	536.4	17.5
P-4		548.0	17.8
P-5		559.0	18.2
MEAN		565.9	18.4
COV (%)		5.1	5.1

BLOCK TESTS

COMPRESSION DATE: 4/6/87			TENSION DATE: 4/15/87		
CODE	LOAD (kN)	STRENGTH (MPa)	CODE	LOAD (kN)	STRENGTH (MPa)
1	1204.0	29.0	1	41.5	2.0
2	1104.0	26.6	2	39.5	1.9
3	1152.0	27.8	3	42.1	2.0
4	1076.0	25.9	4	45.6	2.2
5	1073.0	25.9	5	49.4	2.4
6	1097.0	26.4	6	42.7	2.1
7	1110.0	26.7	7	51.2	2.5
8	1115.0	26.9	8	49.1	2.4
9	1188.0	28.6	9	55.5	2.7
10	1106.0	26.7	10	47.9	2.3
MEAN	1122.5	27.0	MEAN	46.5	2.3
COV (%)	4.0	4.0	COV (%)	10.9	10.9

MORTAR CUBE COMPRESSION RESULTS

DATE: 3/27/87		FLOW: 120%
CODE	LOAD (kN)	STRENGTH (MPa)
1	35.4	13.7
2	31.8	12.3
3	28.7	11.1
MEAN	32.0	12.4
COV (%)	10.5	10.5

TABLE E2.6: BLOCK COMPANY 6 TEST RESULTS

COMPANY NUMBER = 6	BLOCK MANUF. = N/A SAND (Y OR N) = Y

PRISM COMPRESSION TESTS		PRISM MANUF. = 1/30/87	
PRISM CODE	TEST DATE	FAILURE LOAD (kN)	STRENGTH (MPa)
P-1		347.0	11 3
P-2		330 0	10.7
P-3	4/08/87	386.0	12.6
P-4		357.0	11.6
P-5		370.0	12.1
MEAN		358.0	11.7
COV (%)		6.0	6.0

BLOCK TESTS

COMPRESSION DATE: 4/6/87			TENSION DATE: 4/15/87		
CODE	LOAD (kN)	STRENGTH (MPa)	CODE	LOAD (kN)	STRENGTH (MPa)
1	734.0	17.7	1	26.7	1.3
2	824.0	19 9	2	29.4	1.4
3	803.0	19.3	3	33.8	1 6
4	795.0	19.2	4	27.2	1 3
5	805.0	19.4	5	26.9	1.3
6	738.0	17 8	6	24.8	1 2
7	794.0	19.1	7	28.5	1 4
8	804.0	19.4	8	23 9	1.2
9	720.0	17.3	9	28.8	1.4
10	802.0	19.3	10	25.6	1.2
MEAN	781.9	18.8	MEAN	27.6	1.3
COV (%)	4.7	4.7	COV (%)	10.2	10.2

MORTAR CUBE COMPRESSION RESULTS

DATE: 4/08/87		FLOW: 118%
CODE	LOAD (kN)	STRENGTH (MPa)
1	29.7	11.5
2	29.8	11.5
3	28.1	10.9
MEAN	29.2	11.3
COV (%)	3.3	3.3

TABLE E2.7: BLOCK COMPANY 7 TEST RESULTS

COMPANY NUMBER = 7 | BLOCK MANUF. = 12/03/86 | SAND (Y OR N) = N

PRISM COMPRESSION TESTS | PRISM MANUF. = 2/02/87

PRISM CODE	TEST DATE	FAILURE LOAD (kN)	STRENGTH (MPa)
P-1		444.0	14.5
P-2		444.0	14.5
P-3	4/09/87	446.0	14.5
P-4		421.0	13.7
P-5		367.0	12.0
MEAN		424.4	13.8
COV (%)		7.9	7.9

BLOCK TESTS

COMPRESSION DATE: 4/7/87 — TENSION DATE: 4/15/87

CODE	LOAD (kN)	STRENGTH (MPa)	CODE	LOAD (kN)	STRENGTH (MPa)
1	968.0	23.3	1	41.1	2.0
2	970.0	23.4	2	40.8	2.0
3	890.0	21.4	3	46.3	2.2
4	965.0	23.3	4	40.8	2.0
5	962.0	23.2	5	39.9	1 9
6	969.0	23.3	6	43.2	2.1
7	943.0	22.7	7	44.7	2.2
8	961.0	23.2	8	41.9	2.0
9	974.0	23.5	9	46.1	2.2
10	898.0	21.6	10	44.9	2.2
MEAN	950.0	22.9	MEAN	43.0	2.1
COV (%)	3.2	3.2	COV (%)	5.5	5.5

MORTAR CUBE COMPRESSION RESULTS

DATE: 4/09/87 — FLOW: 116%

CODE	LOAD (kN)	STRENGTH (MPa)
1	25.9	10.0
2	30.5	11.8
3	22.8	8.8
MEAN	26.4	10.2
COV (%)	14.7	14.7

TABLE E2.8: BLOCK COMPANY 8 TEST RESULTS

COMPANY NUMBER = 8 | BLOCK MANUF. = 12/17/86 | SAND (Y OR N) = N

PRISM COMPRESSION TESTS | PRISM MANUF. = 2/02/87

PRISM CODE	TEST DATE	FAILURE LOAD (kN)	STRENGTH (MPa)
P-1		384.0	12 5
P-2		406.0	13.2
P-3	4/10/87	413.0	13.5
P-4		387 0	12.6
P-5		437.0	14.2
MEAN		405.4	13.2
COV (%)		5.3	5.3

BLOCK TESTS

COMPRESSION DATE: 4/8/87 — TENSION DATE: 4/16/87

CODE	LOAD (kN)	STRENGTH (MPa)	CODE	LOAD (kN)	STRENGTH (MPa)
1	853.0	20.0	1	41 7	2.0
2	833.0	20.1	2	35.4	1.7
3	825.0	19.9	3	35.4	1.7
4	807 0	19.4	4	39.0	1.9
5	858.0	20.7	5	37.3	1.8
6	864.0	20.8	6	34.7	1.7
7	870.0	21.0	7	40 5	2 0
8	928.0	22.4	8	31.8	1.5
9	827.0	19.9	9	37.5	1.8
10	875.0	21.1	10	35.2	1.7
MEAN	854.0	20.6	MEAN	36.9	1.8
COV (%)	4.0	4.0	COV (%)	8.0	8.0

MORTAR CUBE COMPRESSION RESULTS

DATE: 4/10/87 — FLOW: 120%

CODE	LOAD (kN)	STRENGTH (MPa)
1	42.4	16.4
2	42.1	16.3
3	39.7	15.4
MEAN	41.4	16.0
COV (%)	3.6	3.6

TABLE E2.9: BLOCK COMPANY 9 TEST RESULTS

COMPANY NUMBER = 9 | BLOCK MANUF. = 12/01/86 | SAND (Y OR N) = N

PRISM COMPRESSION TESTS | PRISM MANUF. = 2/02/87

PRISM CODE	TEST DATE	FAILURE LOAD (kN)	STRENGTH (MPa)
P-1		578.0	18.8
P-2		624.5	20.3
P-3	4/13/87	622.0	20.3
P-4		605.0	19.7
P-5		634.0	20.7
MEAN		612.7	20.0
COV (%)		3.6	3.6

BLOCK TESTS

COMPRESSION DATE: 4/15/87 | TENSION DATE: 4/16/87

CODE	LOAD (kN)	STRENGTH (MPa)	CODE	LOAD (kN)	STRENGTH (MPa)
1	1254.0	30.2	1	48.8	2.4
2	1252.0	30.2	2	56.1	2.7
3	1226.0	29.5	3	45.5	2.2
4	1207.0	29.1	4	53.3	2.6
5	1257 0	30.3	5	50.2	2.4
6	1245.0	30.0	6	52.2	2.5
7	1265.0	30.5	7	46.7	2.3
8	1253.0	30.2	8	56.3	2.7
9	1256.0	30.3	9	54.5	2.6
10	1261.0	30.4	10	51.1	2.5
MEAN	1247.6	30.1	MEAN	51.5	2.5
COV (%)	1.4	1.4	COV (%)	7.2	7.2

MORTAR CUBE COMPRESSION RESULTS

DATE: 4/13/87 | FLOW: 120%

CODE	LOAD (kN)	STRENGTH (MPa)
1	34.5	13.4
2	32.8	12.7
3	33.7	13.1
MEAN	33.7	13.0
COV (%)	2.5	2.5

TABLE E2.10: BLOCK COMPANY 10 TEST RESULTS

COMPANY NUMBER = 10 | BLOCK MANUF. = 12/10/86 | SAND (Y OR N) = N

PRISM COMPRESSION TESTS | PRISM MANUF. = 2/02/87

PRISM CODE	TEST DATE	FAILURE LOAD (kN)	STRENGTH (MPa)
P-1		615.3	21.4
P-2		657.3	21.4
P-3	03/04/87	651.6	21.2
P-4		671.1	21 9
P-5		592.4	19 3
MEAN		637.5	20.8
COV (%)		5.1	5.1

BLOCK TESTS

COMPRESSION DATE: 3/6/87 | TENSION DATE: 3/6/87

CODE	LOAD (kN)	STRENGTH (MPa)	CODE	LOAD (kN)	STRENGTH (MPa)
1	1417.0	34.1	1	50.5	2.5
2	1430.0	34.5	2	45.1	2 2
3	1294.0	31.2	3	41.2	2.0
4	1296.0	31 2	4	55.8	2.7
5	1226.0	29.5	5	61 9	3.0
6	1184.0	28 5	6	65.0	3.2
7	1309.0	31.5	7	56.3	2.7
8	1235.0	29.8	8	48 3	2.3
9	1298.0	31.3	9	59 3	2.9
10	1196.0	28.8	10	51.2	2.5
MEAN	1288.5	31.0	MEAN	53.5	2.6
COV (%)	6.5	6.5	COV (%)	14.1	14.1

MORTAR CUBE COMPRESSION RESULTS

DATE: 03/04/87 | FLOW: 125%

CODE	LOAD (kN)	STRENGTH (MPa)
1	30.6	11.9
2	27.4	10.6
3	34.1	13.2
MEAN	30.7	11.9
COV (%)	10.9	10.9

TABLE E2.11: BLOCK COMPANY 11 TEST RESULTS

COMPANY NUMBER = 11

BLOCK MANUF. = 12/16/86
SAND (Y OR N) = Y

PRISM COMPRESSION TESTS — PRISM MANUF. = 2/02/87

PRISM CODE	TEST DATE	FAILURE LOAD (kN)	STRENGTH (MPa)
P-1		538.0	17.5
P-2		568.0	18.5
P-3	4/15/87	461.0	15.0
P-4		485.0	15.8
P-5		441.0	14.4
MEAN		498.6	16.2
COV (%)		10.7	10.7

BLOCK TESTS

COMPRESSION DATE: 4/20/87 — TENSION DATE: 5/05/87

CODE	LOAD (kN)	STRENGTH (MPa)	CODE	LOAD (kN)	STRENGTH (MPa)
1	981.0	24.6	1	54.3	2.6
2	921.0	23.1	2	45.5	2.2
3	965.0	24.3	3	42.1	2.0
4	918.0	23.0	4	40.0	1.9
5	933.0	24.4	5	41.1	2.0
6	958.0	24.1	6	44.0	2.1
7	986.0	23.4	7	50.6	2.5
8	935.0	24.8	8	43.0	2.1
9	891.0	22.4	9	39.6	1.9
10	955.0	24.0	10	53.1	2.6
MEAN	944.3	23.8	MEAN	45.3	2.2
COV (%)	3.2	3.2	COV (%)	12.0	12.0

MORTAR CUBE COMPRESSION RESULTS

DATE: 4/15/87 — FLOW: 120%

CODE	LOAD (kN)	STRENGTH (MPa)
1	25.5	9.9
2	23.4	9.1
3	28.2	10.9
MEAN	25.7	10.0
COV (%)	9.5	9.5

TABLE E2.12: BLOCK COMPANY 12 TEST RESULTS

COMPANY NUMBER = 12

BLOCK MANUF. = 12/18/86
SAND (Y OR N) = Y

PRISM COMPRESSION TESTS — PRISM MANUF. = 2/03/87

PRISM CODE	TEST DATE	FAILURE LOAD (kN)	STRENGTH (MPa)
P-1		390.0	12.7
P-2		393.0	12.8
P-3	4/22/87	391.0	12.7
P-4		394.0	12.8
P-5		396.0	12.9
MEAN		392.8	12.8
COV (%)		0.6	0.6

BLOCK TESTS

COMPRESSION DATE: 4/23/87 — TENSION DATE: 5/06/87

CODE	LOAD (kN)	STRENGTH (MPa)	CODE	LOAD (kN)	STRENGTH (MPa)
1	930.0	22.4	1	37.0	1.8
2	878.0	21.2	2	40.6	2.0
3	931.0	22.4	3	42.9	2.1
4	915.0	21.1	4	40.6	2.0
5	877.0	20.4	5	39.9	1.9
6	848.0	22.0	6	40.3	2.0
7	955.0	23.0	7	41.7	2.0
8	900.0	21.7	8	39.4	1.9
9	929.0	22.4	9	41.6	2.0
10	962.0	22.9	10	41.7	2.0
MEAN	911.5	22.0	MEAN	40.6	2.0
COV (%)	3.8	3.8	COV (%)	4.0	4.0

MORTAR CUBE COMPRESSION RESULTS

DATE: 4/22/87 — FLOW: 116%

CODE	LOAD (kN)	STRENGTH (MPa)
1	25.0	9.7
2	24.7	9.6
3	26.3	10.2
MEAN	25.3	9.8
COV (%)	3.4	3.4

TABLE E2.13: BLOCK COMPANY 13 TEST RESULTS

COMPANY NUMBER = 13 BLOCK MANUF. = 12/21/86
SAND (Y OR N) = Y

PRISM COMPRESSION TESTS PRISM MANUF. = 2/03/87

PRISM CODE	TEST DATE	FAILURE LOAD (kN)	STRENGTH (MPa)
P-1		309.0	10.1
P-2		306.0	10.0
P-3	4/22/87	310.0	10.1
P-4		318.0	10.4
P-5		316.0	10.3
MEAN		311.8	10.2
COV (%)		1.6	1.6

BLOCK TESTS

COMPRESSION DATE: 4/22/87 — TENSION DATE: 5/08/87

CODE	LOAD (kN)	STRENGTH (MPa)	CODE	LOAD (kN)	STRENGTH (MPa)
1	758.0	18.3	1	21.8	1.1
2	798.0	19.2	2	27.1	1.3
3	791.0	19.1	3	16.2	0.8
4	838.0	20.2	4	27.7	1.3
5	799.0	19.3	5	27.0	1.3
6	805.0	19.4	6	30.9	1.5
7	834.0	20.1	7	15.0	0.7
8	805.0	19.4	8	17.7	0.9
9	822.0	19.8	9	24.3	1.2
10	829.0	20.0	10	20.0	1.0
MEAN	807.9	19.5	MEAN	22.8	1.1
COV (%)	3.0	3.0	COV (%)	23.9	23.9

MORTAR CUBE COMPRESSION RESULTS

DATE: 4/22/87 FLOW: 124%

CODE	LOAD (kN)	STRENGTH (MPa)
1	24.2	9.4
2	26.8	10.4
3	26.4	10.2
MEAN	25.8	10.0
COV (%)	5.5	5.5

TABLE E2.14: BLOCK COMPANY 14 TEST RESULTS

COMPANY NUMBER = 14 BLOCK MANUF. = 12/17/86
SAND (Y OR N) = Y

PRISM COMPRESSION TESTS PRISM MANUF. = 2/02/87

PRISM CODE	TEST DATE	FAILURE LOAD (kN)	STRENGTH (MPa)
P-1		485.0	15.8
P-2		546.0	17.8
P-3	4/22/87	523.0	17.0
P-4		505.0	16.4
P-5		501.0	16.3
MEAN		512.0	16.7
COV (%)		4.6	4.6

BLOCK TESTS

COMPRESSION DATE: 5/21/87 — TENSION DATE: 5/20/87

CODE	LOAD (kN)	STRENGTH (MPa)	CODE	LOAD (kN)	STRENGTH (MPa)
1	1110.0	26.7	1	51.3	2.5
2	1124.0	27.1	2	41.8	2.0
3	1135.0	27.3	3	35.2	1.7
4	1098.0	26.5	4	51.1	2.5
5	1137.0	27.4	5	44.5	2.2
6	1086.0	26.2	6	43.7	2.1
7	1140.0	27.5	7	41.1	2.0
8	1163.0	28.0	8	40.7	2.0
9	1037.0	25.0	9	40.4	2.0
10	1020.0	24.6	10	42.5	2.1
MEAN	1105.0	26.6	MEAN	43.2	2.1
COV (%)	4.2	4.2	COV (%)	11.3	11.3

MORTAR CUBE COMPRESSION RESULTS

DATE: 4/22/87 FLOW: 120%

CODE	LOAD (kN)	STRENGTH (MPa)
1	21.3	8.2
2	22.2	8.6
3	20.5	7.9
MEAN	21.3	8.3
COV (%)	4.1	4.1

TABLE E2.15: BLOCK COMPANY 15 TEST RESULTS

COMPANY NUMBER = 15 — BLOCK MANUF. = 12/14/86 — SAND (Y OR N) = Y

PRISM COMPRESSION TESTS — PRISM MANUF. = 2/02/87

PRISM CODE	TEST DATE	FAILURE LOAD (kN)	STRENGTH (MPa)
P-1		663.0	21.6
P-2		560.0	18.2
P-3	4/27/87	668.0	21.8
P-4		686.0	22.3
P-5		686.0	22.3
MEAN		652.6	21.3
COV (%)		8.1	8.1

BLOCK TESTS

COMPRESSION DATE: 5/27/87 — TENSION DATE: 5/04/87

CODE	LOAD (kN)	STRENGTH (MPa)	CODE	LOAD (kN)	STRENGTH (MPa)
1	1555.0	37.5	1	62.6	3.0
2	1557.0	37.5	2	57.9	2.8
3	1559.0	37.6	3	51.6	2.5
4	1512.0	36.4	4	54.7	2.7
5	1464.0	35.3	5	60.6	2.9
6	1393.0	33.6	6	61.6	3.0
7	1552.0	37.4	7	55.5	2.7
8	1528.0	36.8	8	61.9	3.0
9	1569.0	37.8	9	64.3	3.1
10	1448.0	34.9	10	58.9	2.9
MEAN	1513.7	36.5	MEAN	59.0	2.9
COV (%)	3.9	3.9	COV (%)	6.8	6.8

MORTAR CUBE COMPRESSION RESULTS

DATE: 4/27/87 — FLOW: 121%

CODE	LOAD (kN)	STRENGTH (MPa)
1	26.3	10.2
2	28.0	10.8
3	26.5	10.2
MEAN	26.9	10.4
COV (%)	3.4	3.4

TABLE E2.16: BLOCK COMPANY 16 TEST RESULTS

COMPANY NUMBER = 16 — BLOCK MANUF. = N/A — SAND (Y OR N) = N

PRISM COMPRESSION TESTS — PRISM MANUF. = 2/02/87

PRISM CODE	TEST DATE	FAILURE LOAD (kN)	STRENGTH (MPa)
P-1		763.0	24.9
P-2		734.0	23.9
P-3	4/28/87	799.0	26.0
P-4		772.0	25.1
P-5		652.8	21.3
MEAN		744.2	24.2
COV (%)		7.5	7.5

BLOCK TESTS

COMPRESSION DATE: 5/01/87 — TENSION DATE: 5/05/87

CODE	LOAD (kN)	STRENGTH (MPa)	CODE	LOAD (kN)	STRENGTH (MPa)
1	1605.0	38.7	1	61.3	3.0
2	1708.0	41.2	2	69.2	3.4
3	1600.0	38.6	3	69.0	3.4
4	1636.0	39.4	4	74.7	3.6
5	1705.0	41.1	5	74.3	3.6
6	1620.0	39.0	6	70.2	3.4
7	1590.0	38.3	7	68.3	3.3
8	1585.0	38.2	8	70.4	3.4
9	1580.0	38.1	9	67.5	3.3
10	1595.0	38.4	10	54.4	2.6
MEAN	1622.4	39.1	MEAN	67.9	3.3
COV (%)	2.9	2.9	COV (%)	8.9	8.9

MORTAR CUBE COMPRESSION RESULTS

DATE: 4/28/87 — FLOW: 120%

CODE	LOAD (kN)	STRENGTH (MPa)
1	30.5	11.8
2	31.2	12.1
3	35.4	13.7
MEAN	32.4	12.5
COV (%)	8.2	8.2

TABLE E2.17: BLOCK COMPANY 17 TEST RESULTS

COMPANY NUMBER = 17 | BLOCK MANUF. = N/A | SAND (Y OR N) = N

PRISM COMPRESSION TESTS | PRISM MANUF. = 2/03/87

PRISM CODE	TEST DATE	FAILURE LOAD (kN)	STRENGTH (MPa)
P-1		653.0	21.3
P-2		592.0	19.3
P-3	5/5/87	536.0	17.5
P-4		557.2	18.1
P-5		476.9	15.5
MEAN		563.0	18.3
COV (%)		11.6	11.6

BLOCK TESTS

COMPRESSION DATE: 5/07/87 | TENSION DATE: 5/05/87

CODE	LOAD (kN)	STRENGTH (MPa)	CODE	LOAD (kN)	STRENGTH (MPa)
1	1192.0	29.9	1	48.0	2.3
2	1198.0	30.1	2	49.8	2.4
3	1315.0	33.0	3	49.5	2.4
4	1212.0	30.4	4	47.9	2.3
5	1166.0	29.3	5	46.8	2.3
6	1323.0	33.2	6	50.9	2.5
7	1318.0	33.1	7	30.1	1.5
8	1163.0	29.2	8	37.8	1.8
9	1138.0	28.5	9	43.9	2.1
10	1170.0	29.4	10	40.5	2.0
MEAN	1219.5	30.6	MEAN	44.5	2.2
COV (%)	5.9	5.9	COV (%)	14.8	14.8

MORTAR CUBE COMPRESSION RESULTS

DATE: 5/5/87 | FLOW: 121%

CODE	LOAD (kN)	STRENGTH (MPa)
1	30.8	11.9
2	29.3	11.4
3	31.0	12.0
MEAN	30.4	11.8
COV (%)	2.9	2.9

TABLE E2.18: BLOCK COMPANY 18 TEST RESULTS

COMPANY NUMBER = 18 | BLOCK MANUF. = N/A | SAND (Y OR N) = Y

PRISM COMPRESSION TESTS | PRISM MANUF. = 2/03/87

PRISM CODE	TEST DATE	FAILURE LOAD (kN)	STRENGTH (MPa)
P-1		767.0	25.0
P-2		759.0	24.7
P-3	5/6/87	695.0	22.6
P-4		625.0	20.4
P-5		638.0	20.8
MEAN		696.8	22.7
COV (%)		9.5	9.5

BLOCK TESTS

COMPRESSION DATE: 5/07/87 | TENSION DATE: 5/05/87

CODE	LOAD (kN)	STRENGTH (MPa)	CODE	LOAD (kN)	STRENGTH (MPa)
1	1361.0	32.8	1	53.2	2.6
2	1350.0	32.5	2	50.9	2.5
3	1360.0	32.8	3	66.0	3.2
4	1258.0	30.3	4	55.8	2.7
5	1443.0	34.8	5	60.6	2.9
6	1296.0	31.2	6	51.2	2.5
7	1287.0	31.0	7	49.8	2.4
8	1335.0	32.2	8	52.4	2.5
9	1266.0	30.5	9	58.1	2.8
10	1315.0	31.7	10	56.0	2.7
MEAN	1327.1	32.0	MEAN	55.4	2.7
COV (%)	4.2	4.2	COV (%)	9.1	9.1

MORTAR CUBE COMPRESSION RESULTS

DATE: 5/6/87 | FLOW: 120%

CODE	LOAD (kN)	STRENGTH (MPa)
1	32.1	12.4
2	32.9	12.7
3	35.1	13.6
MEAN	33.4	12.9
COV (%)	4.7	4.7

TABLE E2.19: BLOCK COMPANY 19 TEST RESULTS

COMPANY NUMBER = 19 | BLOCK MANUF. = 12/17/86 | SAND (Y OR N) = Y

PRISM COMPRESSION TESTS | PRISM MANUF. = 2/03/87

PRISM CODE	TEST DATE	FAILURE LOAD (kN)	STRENGTH (MPa)
P-1		545.0	17.8
P-2		536.0	17.5
P-3	5/8/87	458.0	14.9
P-4		504.0	16.4
P-5		493.0	16.1
MEAN		507.2	16.5
COV (%)		6.9	6.9

BLOCK TESTS

COMPRESSION DATE: 5/12/87 | TENSION DATE: 5/20/87

CODE	LOAD (kN)	STRENGTH (MPa)	CODE	LOAD (kN)	STRENGTH (MPa)
1	1268.0	31.9	1	41.1	2.0
2	1214.0	30.5	2	41.2	2.0
3	1154.0	28.9	3	44.8	2.2
4	1120.0	28.1	4	32.1	1.6
5	1235.0	31.0	5	45.1	2.2
6	1169.0	29.4	6	41.0	2.0
7	1158.0	29.1	7	42.1	2.0
8	1140.0	28.6	8	49.9	2.4
9	1115.0	28.0	9	48.0	2.3
10	1105.0	27.7	10	46.3	2.2
MEAN	1167.8	29.3	MEAN	43.2	2.1
COV (%)	4.7	4.7	COV (%)	11.5	11.5

MORTAR CUBE COMPRESSION RESULTS

DATE: 5/8/87 | FLOW: 118%

CODE	LOAD (kN)	STRENGTH (MPa)
1	18.3	7.1
2	21.8	8.5
3	23.6	9.1
MEAN	21.2	8.2
COV (%)	12.6	12.6

TABLE E2.20: BLOCK COMPANY 20 TEST RESULTS

COMPANY NUMBER = 20 | BLOCK MANUF. = 11/28/86 | SAND (Y OR N) = Y

PRISM COMPRESSION TESTS | PRISM MANUF. = 2/03/87

PRISM CODE	TEST DATE	FAILURE LOAD (kN)	STRENGTH (MPa)
P-1		378.0	12.3
P-2		387.0	12.9
P-3	5/11/87	365.0	11.9
P-4		440.0	14.3
P-5		362.0	11.8
MEAN		388.4	12.7
COV (%)		8.2	8.2

BLOCK TESTS

COMPRESSION DATE: 5/12/87 | TENSION DATE: 5/20/87

CODE	LOAD (kN)	STRENGTH (MPa)	CODE	LOAD (kN)	STRENGTH (MPa)
1	960.0	23.1	1	31.7	1.5
2	917.0	22.1	2	30.8	1.5
3	935.0	22.5	3	35.5	1.7
4	946.0	22.8	4	28.2	1.4
5	900.0	21.7	5	25.2	1.2
6	929.0	22.4	6	29.3	1.4
7	923.0	22.2	7	33.1	1.6
8	925.0	22.3	8	38.5	1.9
9	902.0	21.7	9	34.8	1.7
10	912.0	22.0	10	33.6	1.6
MEAN	924.9	22.3	MEAN	32.1	1.6
COV (%)	2.0	2.0	COV (%)	12.1	12.1

MORTAR CUBE COMPRESSION RESULTS

DATE: 5/11/87 | FLOW: 118%

CODE	LOAD (kN)	STRENGTH (MPa)
1	15.9	6.2
2	13.3	5.1
3	17.1	6.6
MEAN	15.4	6.0
COV (%)	12.7	12.7

TABLE E2.21: BLOCK COMPANY 21 TEST RESULTS

COMPANY NUMBER = 21 | BLOCK MANUF. = 1/05/87 | SAND (Y OR N) = N

PRISM COMPRESSION TESTS — PRISM MANUF. = 2/03/87

PRISM CODE	TEST DATE	FAILURE LOAD (kN)	STRENGTH (MPa)
P-1		480.5	15.7
P-2		442.3	14.4
P-3	3/05/87	555.7	18.1
P-4		485.6	15.8
P-5		533.7	17.4
MEAN		499.6	16.3
COV (%)		9.0	9.0

BLOCK TESTS

COMPRESSION DATE: 3/05/87 — TENSION DATE: 3/05/87

CODE	LOAD (kN)	STRENGTH (MPa)	CODE	LOAD (kN)	STRENGTH (MPa)
1	1054.0	25.4	1	45.1	2.2
2	1036.0	25.0	2	49.1	2.4
3	1032.0	24.9	3	55.3	2.7
4	980 0	23.6	4	50.3	2.4
5	1101.0	26.5	5	48.2	2.3
6	915.0	22.0	6	45.0	2.2
7	1010.0	24.3	7	48.5	2.4
8	964.0	23.2	8	49.2	2.4
9	1044.0	25.2	9	42.4	2.1
10	1048.0	25.3	10	49.9	2.4
MEAN	1018.4	24.5	MEAN	48.3	2.3
COV (%)	5.2	5.2	COV (%)	7.3	7.3

MORTAR CUBE COMPRESSION RESULTS

DATE: 3/05/87 — FLOW: 121%

CODE	LOAD (kN)	STRENGTH (MPa)
1	31.8	12.3
2	27.6	10.7
3	28.4	11.0
MEAN	29.3	11.3
COV (%)	7.6	7.6

TABLE E2.22: BLOCK COMPANY 22 TEST RESULTS

COMPANY NUMBER = 22 | BLOCK MANUF. = 1/13/87 (R) | SAND (Y OR N) = Y

PRISM COMPRESSION TESTS — PRISM MANUF. = 2/04/87

PRISM CODE	TEST DATE	FAILURE LOAD (kN)	STRENGTH (MPa)
P-1		557.0	18.1
P-2		554.0	18.0
P-3	5/13/87	520.0	16 9
P-4		561.0	18.3
P-5		461.0	15.0
MEAN		530.6	17.3
COV (%)		8.0	8 0

BLOCK TESTS

COMPRESSION DATE: 5/15/87 — TENSION DATE: 5/20/87

CODE	LOAD (kN)	STRENGTH (MPa)	CODE	LOAD (kN)	STRENGTH (MPa)
1	1202.0	29.0	1	37.2	1 8
2	1158.0	27.9	2	32.6	1.6
3	1116.0	26.9	3	37.9	1 8
4	1306.0	31.5	4	35.2	1.7
5	1179.0	28.4	5	41.1	2.0
6	1365.0	32 9	6	40.8	2.0
7	1358.0	32.7	7	32.3	1.6
8	1377.0	33.2	8	37.2	1.8
9	1285.0	31.0	9	44.4	2.2
10	1356.0	32.7	10	34.4	1.7
MEAN	1270.2	30 6	MEAN	37.3	1.8
COV (%)	7.7	7.7	COV (%)	10.5	10.5

MORTAR CUBE COMPRESSION RESULTS

DATE: 5/13/87 — FLOW: 118%

CODE	LOAD (kN)	STRENGTH (MPa)
1	19.2	7.4
2	18.2	7.0
3	20.4	7.9
MEAN	19.2	7.5
COV (%)	5.8	5.8

TABLE E2.23: BLOCK COMPANY 23 TEST RESULTS

COMPANY NUMBER = 23 — BLOCK MANUF. = 1/13/87 (R) — SAND (Y OR N) = Y

PRISM COMPRESSION TESTS — PRISM MANUF. = 2/04/87

PRISM CODE	TEST DATE	FAILURE LOAD (kN)	STRENGTH (MPa)
P-1		723.0	23.5
P-2		682.0	22.2
P-3	5/14/87	694.0	22.6
P-4		707.0	23.0
P-5		698.0	22.7
MEAN		700.8	22.8
COV (%)		2.2	2.2

BLOCK TESTS

COMPRESSION DATE: 5/15/87 — TENSION DATE: 5/20/87

CODE	LOAD (kN)	STRENGTH (MPa)	CODE	LOAD (kN)	STRENGTH (MPa)
1	1700.0	41.0	1	54.8	2.7
2	1568.0	37.8	2	48.3	2.3
3	1682.0	40.5	3	58.3	2.8
4	1590.0	38.3	4	55.2	2.7
5	1544.0	37.2	5	57.5	2.8
6	1535.0	37.0	6	57.8	2.8
7	1659.0	40.0	7	52.4	2.5
8	1548.0	37.3	8	52.8	2.6
9	1532.0	36.9	9	51.6	2.5
10	1630.0	39.3	10	50.3	2.4
MEAN	1598.8	38.5	MEAN	53.9	2.6
COV (%)	4.0	4.0	COV (%)	6.3	6.3

MORTAR CUBE COMPRESSION RESULTS

DATE: 5/14/87 — FLOW: 120%

CODE	LOAD (kN)	STRENGTH (MPa)
1	25.8	10.0
2	27.8	10.8
3	27.7	10.7
MEAN	27.1	10.5
COV (%)	4.2	4.2

TABLE E2.24: BLOCK COMPANY 24 TEST RESULTS

COMPANY NUMBER = 24 — BLOCK MANUF. = 1/13/87 (R) — SAND (Y OR N) = Y

PRISM COMPRESSION TESTS — PRISM MANUF. = 2/04/87

PRISM CODE	TEST DATE	FAILURE LOAD (kN)	STRENGTH (MPa)
P-1		659.0	21.5
P-2		683.0	22.2
P-3	5/19/87	747.0	24.3
P-4		678.0	22.1
P-5		694.0	22.6
MEAN		692.2	22.5
COV (%)		4.8	4.8

BLOCK TESTS

COMPRESSION DATE: 5/21/87 — TENSION DATE: 5/20/87

CODE	LOAD (kN)	STRENGTH (MPa)	CODE	LOAD (kN)	STRENGTH (MPa)
1	1634.0	41.0	1	56.5	2.7
2	1604.0	40.3	2	54.8	2.7
3	1521.0	38.2	3	60.4	2.9
4	1489.0	37.4	4	47.5	2.3
5	1513.0	38.0	5	57.4	2.8
6	1541.0	38.6	6	49.4	2.4
7	1509.0	37.9	7	54.8	2.7
8	1581.0	39.7	8	60.4	2.9
9	1497.0	37.6	9	60.4	2.9
10	1474.0	37.0	10	57.3	2.8
MEAN	1536.3	38.6	MEAN	55.9	2.7
COV (%)	3.5	3.5	COV (%)	8.0	8.0

MORTAR CUBE COMPRESSION RESULTS

DATE: 5/19/87 — FLOW: 120%

CODE	LOAD (kN)	STRENGTH (MPa)
1	19.8	7.7
2	22.3	8.7
3	24.8	9.6
MEAN	22.3	8.6
COV (%)	11.4	11.4

TABLE E2.25: BLOCK COMPANY 25 TEST RESULTS

COMPANY NUMBER = 25

BLOCK MANUF. = 1/13/87 (R)
SAND (Y OR N) = Y

PRISM COMPRESSION TESTS — PRISM MANUF. = 2/04/87

PRISM CODE	TEST DATE	FAILURE LOAD (kN)	STRENGTH (MPa)
P-1		408.0	13.3
P-2		428.0	13.9
P-3	5/19/87	433.0	14.1
P-4		412.0	13.4
P-5		447.0	14.6
MEAN		425.6	13.9
COV (%)		3.7	3.7

BLOCK TESTS

COMPRESSION DATE: 5/21/87			TENSION DATE: 5/20/87		
CODE	LOAD (kN)	STRENGTH (MPa)	CODE	LOAD (kN)	STRENGTH (MPa)
1	948.0	22.8	1	39.0	1.9
2	993.0	23.9	2	37.8	1.8
3	1047.0	25.2	3	43.2	2.1
4	958.0	23.1	4	40.0	1.9
5	939.0	22.6	5	37.8	1.8
6	914.0	22.0	6	34.7	1.7
7	927.0	22.3	7	44.0	2.1
8	980.0	23.6	8	41.9	2.0
9	955.0	23.0	9	34.7	1.7
10	1058.0	25.5	10	36.4	1.8
MEAN	971.9	23.4	MEAN	39.0	1.9
COV (%)	5.0	5.0	COV (%)	8.5	8.5

MORTAR CUBE COMPRESSION RESULTS

DATE: 5/19/87 — FLOW: 122%

CODE	LOAD (kN)	STRENGTH (MPa)
1	19.2	7.4
2	20.5	7.9
3	19.7	7.6
MEAN	19.8	7.7
COV (%)	3.2	3.2

TABLE E2.26: BLOCK COMPANY 26 TEST RESULTS

COMPANY NUMBER = 26

BLOCK MANUF. = 1/13/87 (R)
SAND (Y OR N) = Y

PRISM COMPRESSION TESTS — PRISM MANUF. = 2/03/87

PRISM CODE	TEST DATE	FAILURE LOAD (kN)	STRENGTH (MPa)
P-1		561.0	18.3
P-2		458.0	14.9
P-3	5/20/87	487.0	15.9
P-4		524.0	17.1
P-5		541.0	17.6
MEAN		514.2	16.7
COV (%)		8.1	8.1

BLOCK TESTS

COMPRESSION DATE: 5/21/87			TENSION DATE: 5/20/87		
CODE	LOAD (kN)	STRENGTH (MPa)	CODE	LOAD (kN)	STRENGTH (MPa)
1	1412.0	35.4	1	55.8	2.7
2	1335.0	33.5	2	55.6	2.7
3	1443.0	36.2	3	54.4	2.6
4	1397.0	35.1	4	52.6	2.6
5	1363.0	34.2	5	59.3	2.9
6	1350.0	33.8	6	59.7	2.9
7	1296.0	32.5	7	58.8	2.9
8	1425.0	35.7	8	56.7	2.8
9	1472.0	37.0	9	62.3	3.0
10	1367.0	34.3	10	53.7	2.6
MEAN	1386.0	34.8	MEAN	56.9	2.8
COV (%)	3.9	3.9	COV (%)	5.4	5.4

MORTAR CUBE COMPRESSION RESULTS

DATE: 5/20/87 — FLOW: 121%

CODE	LOAD (kN)	STRENGTH (MPa)
1	19.4	7.5
2	16.9	6.5
3	18.9	7.3
MEAN	18.4	7.1
COV (%)	7.2	7.2

TABLE E2.27: BLOCK COMPANY 27 TEST RESULTS

COMPANY NUMBER	= 27	BLOCK MANUF. = 11/28/86	
		SAND (Y OR N) = Y	

PRISM COMPRESSION TESTS — PRISM MANUF. = 1/30/87

PRISM CODE	TEST DATE	FAILURE LOAD (kN)	STRENGTH (MPa)
P-1		529.9	17.3
P-2		578.7	18.8
P-3	3/03/87	555.3	18.1
P-4		588.4	19.2
P-5		570.5	18.6
MEAN		564.6	18.4
COV (%)		4.0	4.0

BLOCK TESTS

COMPRESSION DATE: 3/02/87 — TENSION DATE: 2/02/87

CODE	LOAD (kN)	STRENGTH (MPa)	CODE	LOAD (kN)	STRENGTH (MPa)
1	863.0	21.7	1	55.1	2.7
2	1144.0	28.7	2	47.0	2.3
3	1102.0	27.7	3	55.4	2.7
4	1017.0	25.5	4	51.1	2.5
5	825.0	20.7	5	49.6	2.4
6	1030.0	25.8	6	59.1	2.9
7	1176.0	29.5	7	49.9	2.4
8	1093.0	27.4	8	44.6	2.2
9	995.0	25.0	9	49.5	2.4
10	1067.0	26.8	10	54.1	2.6
MEAN	1031.2	25.9	MEAN	51.5	2.5
COV (%)	11.0	11.0	COV (%)	8.5	8.5

MORTAR CUBE COMPRESSION RESULTS

DATE: 3/03/87 — FLOW: 120%

CODE	LOAD (kN)	STRENGTH (MPa)
1	32.6	12.6
2	33.1	12.8
3	27.4	10.6
MEAN	31.0	12.0
COV (%)	10.2	10.2

TABLE E2.28: BLOCK COMPANY 28 TEST RESULTS

COMPANY NUMBER	= 28	BLOCK MANUF. = 11/17/86	
		SAND (Y OR N) = Y	

PRISM COMPRESSION TESTS — PRISM MANUF. = 1/30/87

PRISM CODE	TEST DATE	FAILURE LOAD (kN)	STRENGTH (MPa)
P-1		578.0	18.8
P-2		533.0	17.4
P-3	2/27/87	583.7	19.0
P-4		650.3	21.2
P-5		576.7	18.8
MEAN		584.3	19.0
COV (%)		7.2	7.2

BLOCK TESTS

COMPRESSION DATE: 3/02/87 — TENSION DATE: 2/27/87

CODE	LOAD (kN)	STRENGTH (MPa)	CODE	LOAD (kN)	STRENGTH (MPa)
1	1186.0	29.8	1	53.7	2.6
2	1170.0	29.4	2	58.1	2.8
3	1183.0	29.7	3	48.5	2.4
4	1289.0	32.4	4	49.4	2.4
5	1164.0	29.2	5	48.7	2.4
6	1244.0	31.2	6	51.9	2.5
7	1279.0	32.1	7	44.0	2.1
8	1143.0	28.6	8	55.0	2.7
9	1124.0	28.2	9	62.8	3.0
10	1159.0	29.1	10	53.1	2.6
MEAN	1194.1	30.0	MEAN	52.5	2.6
COV (%)	4.8	4.8	COV (%)	10.2	10.2

MORTAR CUBE COMPRESSION RESULTS

DATE: 2/27/87 — FLOW: 124%

CODE	LOAD (kN)	STRENGTH (MPa)
1	31.0	12.0
2	24.7	9.6
3	25.9	10.0
MEAN	27.2	10.5
COV (%)	12.3	12.3

TABLE E2.29: BLOCK COMPANY 29 TEST RESULTS

COMPANY NUMBER	= 29	BLOCK MANUF. =	N/A
		SAND (Y OR N) =	N

PRISM COMPRESSION TESTS		PRISM MANUF. = 1/30/87	
PRISM CODE	TEST DATE	FAILURE LOAD (kN)	STRENGTH (MPa)
P-1		427.3	13.9
P-2		503.2	16.4
P-3	2/26/87	484.9	15.8
P-4		433.5	14.1
P-5		417.0	13.6
MEAN		453.2	14.8
COV (%)		8.5	8.5

BLOCK TESTS

COMPRESSION DATE: 2/26/87			TENSION DATE: 2/27/87		
CODE	LOAD (kN)	STRENGTH (MPa)	CODE	LOAD (kN)	STRENGTH (MPa)
1	765.0	19.2	1	30.4	1.5
2	733.0	18.4	2	36.0	1.7
3	816.0	20.5	3	38.6	1.9
4	856.0	21.5	4	31.4	1.5
5	873.0	21.9	5	40.6	2.0
6	883.0	22.2	6	31.3	1.5
7	875.0	22.0	7	37.2	1.8
8	917.0	23.0	8	37.2	1.8
9	795.0	20.0	9	40.3	2.0
10	834.0	20.9	10	40.0	1.9
MEAN	834.7	21.0	MEAN	36.3	1.8
COV (%)	6.9	6.9	COV (%)	10.8	10.8

MORTAR CUBE COMPRESSION RESULTS

DATE: 2/27/87		FLOW: 118%
CODE	LOAD (kN)	STRENGTH (MPa)
1	34.0	13.2
2	33.8	13.1
3	38.4	14.9
MEAN	35.4	13.7
COV (%)	7.3	7.3

REFERENCES

1. A.C.I. Committee 531, Building Code Requirements for Concrete Masonry Structures, ACI 531-79, Detroit, MI, 1978.

2. A.S.C.E.,Committee 530, Building Code Requirements for Masonry Structures and specifications for Masonry Structures, The American Soceity for Civil Engineers, New York, New York.

3. A.S.T.M., Standard Methods of SAMPLING OF CONCRETE MASONRY UNITS, C140-75, 1984.

4. A.S.T.M., Standard Specification for AGGREGATE FOR MASONRY MORTAR, C144-81, 1984.

5. A.S.T.M., Standard Specification for MORTAR FOR UNIT MASONRY, C270-82 & C780, 1984.

6. A.S.T.M., Standard Test Method for SPLITTING TENSILE STRENGTH OF MASONRY UNITS, C1006-84, 1984.

7. A.S.T.M., Standard Test Methods for COMPRESSIVE STRENGTH OF MASONRY PRISMS, E447-84, 1984.

8. Anderson, G.W., "Stack-Bonded Small Specimens as Design and Construction Criteria", SIBMAC Proceedings, British Ceramic Research Association, Stoke-on-Trent, England, 1971,pp. 38-43.

9. Arya, S.K., Hegemier, G.A., "On Non-Linear Response Prediction of Concrete Masonry Assemblage", Proc. of the North American Masonry Confernene, The Masonry Soceity, Boulder, Colorado, 1978, Paper 19.

10. Atkinson, R.H., Noland, J.L.," A Proposed Failure Theory for Brick Masonry in Compression", Proc. Third Canadian Masonry Symposium, Edmomton, Canada, 1983.

11. Atkinson, R.H., Noland, J.L., Abrams, D.P. and Mcmary, S., " A Deformation Failure Theory for Stack-Bond Brick Masonry Prisms in Compression", Proc. Third North American Masonry Conference, Boulder, Colorado, 1985, pap. 18.

12. Beccia, I.J., "Behavior of Hollow Concrete Masonry Prisms under Axial and Bending Loads and its Implications on Ultimate Strength Design of Masonry Structures", M.S. Thesis, Drexel University, Philadelphia, Pennsylvania, June, 1980.

13. Blank, L., Statistical Procedures for Engineering, Management and Science, McGrow-Hill Inc., N.Y., 1980.

14. Boult, B.F., "Concrete Masonry Prism Testing", ACI Journal, vol. 76, April 1979, pp. 513-535.

15. British Standards Institution, Code of Practice for Structural Masonry, Part 1, Unreinforced Masonry, BS5628: Part 1:1978, London, 1978.

16. Brochelet, J.G., "Use and Interpretation of Mortar Specifications and Test Methods", Proc. Fourth North American Masonry Conference, Los Angelos, California, August, 1987, pap.59.

17. Brochelet, J.G., Brown, R.H., "An Indirect Tensile Test for Masonry Units", Journal of Testing and Evaluation, JTEVA, vol. 6, no. 2, March, 1978, pp.134-143.

18. Brown, R.H., "Effect of Mortar on Water Permeance of Masonry" Proc. of the North American Conference, The Masonry Soceity, Boulder, Colorado, 1978, pap.115.

19. Canadian Standards Association (CSA), Standard A8-1970, Masonry Cement, Rexdale, Ontario, 1970.

20. Canadian Standards Associiation, Standard A82.43.

21. Canadian Standards Association, Standard A82.56, Agreggate for Masonry Mortar, Rexdale, Ontario, 1976.

22. Canadian Standards Association, Standard A247, Insulation

23. Canadian Standards Association, Standard A179M-1976, Mortar and Grout for Unit Masonry, Rexdale, Ontario, 1976.

24. Canadian Standards Association, CAN3-A165 Series-M85, CSA Standards on Concrete Masonry Units, Rexdale, Ontario, 1985.

25. Canadian Standards Association, CAN3-A369.1-M84, Method of Test for Compression Strength of Masonry Prisms (Masonry), Rexdale, Ontario, June, 1984.

26. Canadian Standards Association, CAN3-S304-M84, Masonry Design for Buildings, Rexdale, Ontario, 1984.

27. Copeland, R.E., Timms, A.G.,"Effect of Mortar Strength and Strength of Unit on the Strength of Concrete Walls", ACI Journal, vol. 28, 1932, pp. 551-562.

28. Copeland, R.E., Saxer, 1., "Tests of Structural Bond of Masonry Mortars to Concrete Block", ACI Journal, vol. 61, Nov., 1964, pp. 1411-1451.

29. Cranston, W.B., Roberts, J.J., "The Structural Behaviour of Concrete Masonry- Reinforced and Unreinforced", The Structural Engineer, vol. 54, no. 11, Nov. 1976, pp. 423-436.

30. Davison, J.I., "Developement of ASTM Specification for Mortar for Unit Masonry (C 270)", Masonry: Past and Present, ASTM STP 589, A.S.T.M., Philadelphia, PA., 1975, pp. 10-24.

31. Davison, J.I., "Mortar Technology", Proc. First Canadian Masonry Symposium, Calgary, Canada, 1976.

32. Drysdale, R.G., Hamid, A.A., "Suggested Failure Criteria for Grouted Concrete Masonry under Axial Compression", ACI Journal, October 1979, pp. 1047-1061.

33. Drysdale, R.G., Hamid, A.A., "Capacity of Concrete Block Masonry Prisms under Eccentric Compressive Loading", ACI Journal, March-April 1983, pp. 102-108.

34. Drysdale, R.G., Suter, G.T., Modern Engineering Masonry, Canadian Soceity for Civil Engineering, Nov. 1981.

35. Drysdale, R.G., Hamid, A.A., Toneff, J.D., "Comments on Block Masonry Design Code Provision for Allowable Stresses", Proc. 3rd Canadian masonry Symposium, Edmonton, Canada, 1983, pap. 7.

36. Essawy, A.S., "Strength of Hollow Concrete Block Masonry Walls Subject to Lateral (Out-of-Plane) Loading", Ph.D. Thesis, McMaster University, Ontario, 1986.

37. Fattal, S.G., Cattaneo, L.E., "Structural Performance of Masonry Walls under Compression and Flexure", National Bureau of Standards, Building Sciences Series 73, Washington, June 1976, 57 pages.

38. Francis, A.J., Horman, C.B. and Jerrems, L.E., "The Effect of Joint Thickness and other Factors on the Compressive

Strength of Brickwork, Proc. SIBMAC, Stoke-on-Trent, 1971.

39. Froerer, D.D., "The Benefit of High Strength Masonry", Proceedings of the North American Masonry Conference, The Masonry Soceity, Boulder, Colorado, 1978, pap. 92.

40. Gazzola, E.A., Bagnorial, D., Toneff, J. and Drysdale, R.G., Influence of Mortar Materials on the Flexural Tensile Bond Strength of Block and Brick Masonry", Masonry: Research, Application and problems, ASTM STP A.S.T.M., Philadelphia, PA, 1985, pp. 15-26.

41. Gazzola, E.A., "Macroscopic and Microscopic Failure Criteria for Concrete Block Masonry Subject to General Biaxial Bending", M.Eng. Thesis, McMaster University, Hamilton, Ontario, 1986.

42. Gremely, D.G., "Study of the Effect of Certain Modified Mortar on Compressive and Flexure Strength of Masonry", Designing, Engineering and Construction with Masonry Products, Johanson F.B., Gulf Publishing Co., Texas, May 1969.

43. Hamid, A.A., "Behaviour Characteristics of Concrete Masonry", Ph.D. Thesis, McMaster University, Ontario, Sept. 1978.

44. Hamid, A.A., Abboud, B.E., "Effect of Block Geometry on the Compressive Strength of Block Masonry", Proc. 4th Canadian Masonry Symposium, Fredericton, N.B., 1986, p. 290.

45. Hamid, A.A., Chukwunenye, A.O., Effect of Type of Mortar Bedding on the Behaviour of Axially Loaded Hollow Block Masonry Prisms", Proc. Third North American Masonry Conference, The Masonry Soceity, Texas, 1985, pap. 16.

46. Hamid, A.A., Drysdale, R.G. and Heidebrecht, A.C., "Effect of the Grouting on the Strength Charactheristics of Concrete Block Masonry", Proc. of the North American Masonry Conference, Boulder, Colorado, August 1978, pap. 11.

47. Hamid, A., Ziab, G., El Nawaway, O., "Modulus of Elasticity of Concrete Block Masonry", Proc. Fourth North American Masonry Conference, Los Angelos, California, August, 1987, pap. 7.

48. Hatzinikolas, M., Longworth, J. and Warwaruk, J., "Failure Modes of Eccentrically Loaded Concrete Block Masonry Walls", ACI Journal, 1980, pp. 258-263. (Also Discussion

by Shrive-ACI Journal, 1981, pp. 230-240).

49. Hedstrom, R.O., "Load Tests of Patterned Concrete Masonry Walls", Journal of the American Concrete Institue (ACI), Vol. 57, No. 10, April 1961, pp. 1265-1286.

50. Hegemier, G.A., Arya, S.K. et al., "On the Behaviour of Joints in Concrete Masonry", Proc. of the North American Masonry Conference, The Masonry Soceity, Boulder, Colorado, 1978, pap. 4.

51. Hegemier, G.A., Krishnamoorthy, G., et al., "Prisms Tests for The Compressive Strength of Concrete Masonry", Proc. of The North American Masonry Conference, The Masonry Soceity, Boulder, Colorado, 1978, pap. 18.

52. Hendry, A.W., "Testing Methods in Engineering Masonry", Proc. Fourth North American Masonry Conference, Los Angelos, California, August, 1987, pap. 49.

53. Hendry, A.W., Khoo, C.L., "Strength Tests on Brick and Mortar under Complex Stresses for the Development of a Failure Criterion for Brickwork in Compresion", Proc. of the British Ceramic Soceity, No. 21, April 1973, p. 51.

54. Hilsdorf, H.K., "Investigation into the Failure Mechanism of British Masonry Loaded in Axial Compression", Designing, Engineering and Construction with Masonry Products, Johanson, F.B., Gulf Publishing Co., Texas, May 1969, pp. 34-41.

55. Holm, T.A., "Structural Properties of Block Concrete", Proc. of the North American Masonry Conference, Boulder, Colorado, August 1978, pap. 5.

56. Huizer, A., Ward, M.A. and Morstead, H., "Field and Laboratory Study Using Current and Proposed Procedures for Testing Masonry Mortar", Masonry: Past and Present, ASTM STP 589, A.S.T.M., Philadelphia, PA., 1975, pp. 107-122.

57. Huizer, A., Jessop, E.L. et al, "Measuring the Consistency of Mortar in the Laboratory and on the Job Site", Proc. First Canadian Masonry Symposium, Calgary, 1976, pp. 39.

58. Isberner, A.W., "Properties of Masonry Cement Mortars", Designing, Engineering and Construction with Masonry Products, Johanson, F.B., Gulf Publishing Co., Houston, Texas, May, 1969, pp. 51-57.

59. Jessob, E.L., Langan, B.W., "Test Methods for Masonry

Mortar", Proc. of The North American Masonry Conference, The Masonry Soceity, Boulder, Colorado, 1978, pap. 72.

60. Jessob, E.L., Proposed Provisions to CSA Standards: A82.56M-76, Agreggate for Masonry Mortar & A179M-76, Mortar and Grout for Masonry, January, 1984.

61. Johanson, F.B., Thompson, J.N., "Development of Diametric Testing Procedures to Provide a Measure of Strength Characteristics of Masonry Assemblages", Designing, Engineering and Construction with Masonry Products, Johanson F.B., Gulf Publishing Co., Houston, Texas, May 1969, pp. 51-57.

62. Jones, R.S., Mechanics of Composite Materials, McGraw-Hill Book Co. Inc., First Edition, Washington, DC, 1975.

63. Kingsley, L.E., Atkinson, R.H., "Comparison on the Behaviour of Clay and Concrete Masonry in Construction", Proc. Fourth Canadian Masonry Symposium, Fredericton, N.B., 1986.

64. Kupfer, H., Hilsdorf, H.K., Rusch, H., "Behaviour of Concrete under Biaxial Stresses", ACI Journal, Proceedings Vol. 66, No. 8, August 1969, pp. 656-665.

65. Langan, B.W., Jessop, E.L., "Test Methods for Masonry Mortar, Proc. of the North Americam Masonry Conference, The Masonry Soceity, Boulder, Colorado, 1978, pap. 72.

66. Maurenbrecher, A.H.P., "Proposed Amendements to CAN3-S304-M84 Masonry Design for Buildings", National Research Council, Division of Building Research, Ottawa, Canada, March, 1986.

67. Maurenbrecher, A.H.P., "Compressive Strength of Hollow Concrete Masonry", Proc. Fourth Canadian Masonry Symposium, Fredericton, N.B., 1986, p. 997.

68. Maurenbrecher, A.H.P., "Axial Compression Tests on Masonry Walls and Prisms", Proc. Third North American Masonry Conference, The Masonry Soceity, Texas, 1985, pap. 19.

69. Maurenbrecher, A.H.P.,"Compressive Strength of Eccentrically Loaded Masonry Prisms", Proc. Third Canadian Masonry Symposium, Edmonton, Alberta, 1983, pap. 10.

70. Maurenbrecher, A.H.P., "Effect of Test Procedure on Compressive Strength of Masonry Prisms", Proc. Second Canadian Masonry Symposium, Ottawa, Ontario, 1980, pp. 119-132.

71. Maurenbrecher, A.H.P., "Use of the Prism Test to Determine Compressive Strength of Masonry", Proc. of the North American Conference, The Masonry Soceity, Boulder, Colorado, 1978, pap. 91.

72. Mayes, R.L., Clough, R.W., "A Literature survey: Compressive, Tensile, Bond and Shear Strength of Masonry", Report No. EERC-75-15, College of Engineering, University of California, Berkely, California, 1975.

73. Meyer, S.L., Data Analysis for Scientists and Engineers, John Wiley and Sons, 1975.

74. Miller, M.E., Hegemier, G.A. et al, "The Influence of Flaws Compaction and Admixture on the Strength and Elastic Moduli of Concrete Masonry", Proc. of the North American Masonry Conference, The Masonry Soceity, Boulder, Colorado, 1978, pap. 18.

75. Monk, C.B., "A Historical Survey and Analysis of the Compressive Strength of Brick Masonry, Structural Clay Products Research Foundation, Research Report No. 12, 1967.

76. Motteu, H., "Research on Load-Bearing Masonry in Belgium since 1963", Designing, Engineering and Construction in Masonry Products. Johanson, F.B., Gulf Publishing Co., Texas, May 1969, pp. 171-184.

77. Nacos, C.J.,"Comparison of Fully-Bedded and Face-Shell Bedded Concrete Block", Colorado State University, USA, CE-495,1980.

78. National Bureau of Standards, "Building Code Requirements for Reinforced Masonry", NBS Handbook 74, ASA41.2-1960.

79. National Concrete Masonry Association, Specification for the Design and Construstion of Load-Bearing Concrete Masonry, NCMA, Arlington, VA., 1970.

80. National Concrete Masonry Association, "Prism Testing for Engineered Concrete Masonry", NCMA, Tek 22, Arlington, VA. 1970.

81. National Concrete Masonry Association, "Compressive Strength of Concrete Masonry", NCMA, USA, Tek 15, 1969.

82. Neville, A.M., Properties of Concrete, Pitman and Sons Ltd., London, England, 1963, chp. 8.

83. New Zealand Concrete Masonry Association, "Concrete Masonry Prism Testing", Special Lab. Report No. 1, Porirura, New Zealand, 1975.

84. Noland, J.L., Hanada, K.T. and Feng, C.C., "The Effect of Slenderness and End Conditions on the Strength of Clay Unit Prisms", Proc. of The North American Masonry Conference, The Masonry Soceity, Boulder, Colorado, 1978, pap. 14.

85. O.C.B.A., Concrete Block- Metric Technical Manual, Ontario Concrete Block Association, Downsview, Ontario, 1985.

86. Page, A.W., "A Model for The In-Plane Deformation and Failure of Brickwork", Engineering Bulletin CE8, Australia, 1978.

87. Page, A.W., Shrive, N.G., "Failure of Hollow Masonry Subjected to Concentrated Loads", Proceeds. 8th International Brick Masonry Conference, Dublin, In Press, 1988.

88. Page, A.W., Shrive, N.G., "A Critical Assessement of Compression Tests for Hollow Block Masonry", Masonry International, Journal of the British Masonry Soceity, The British Masonry Soceity, England, vol. 2, no. 2, September 1988, pp. 64-70.

89. Plewes, W.G., Suter, G.T., "Canadian Masonry: Yesterday and Today", Proc. Second Canadian Masonry Symposium, Ottawa, Canada, 1980.

90. Preistly, M.J.N., Elder, D.M., "Stress-Strain Curves for Unconfined and Confined Concrete Masonry", ACI Journal, vol. 80, May-June 1983, pp. 192-201.

91. Read, J.B., Clements, S.W., "The Strength of Concrete Block Walls, Phase II: Under Uniaxial Loading", Cement and Concrete Association, Technical Report 42.473, London, 1972.

92. Read, J.B., Clements, S.W., "The Strength of Concrete Block Walls, Phase III: Effect of Workmanship, Mortar Strength and Bond Pattern", Cement and Concrete Association, Technical Report 42.518, London, 1977.

93. Richart F.E., Moorman, R.B.B. et al, "Strength and Stability of Concrete Masonry Walls", University of Illinois, Bulletin 251, 1932.

94. Ridigner, W., Noland, J. et al, "On the Effect of the

Interface Condition and Capping Configuration on the Results of Hollow Clay Masonry Unit Compressive Tests", Proceeds. Second Canadian Masonry Symposium, Ottawa, Canada, 1980.

95. Roberts, J.J., "The Effect upon the Indicated Strength of Concrete Blocks in Compression of Replacing Mortar with Board Capping", Proceeds. First Canadian Masonry Symposium, Galgary, Canada, 1976, pp. 22-38.

96. Sahlin, S., Structural Masonry, Prentice-Hall Inc., Englewood, Cliffs, New Jersey, U.S.A., 1971.

97. Self, M.W., "Structural Properties of Loadbearing Concrete Masonry", Masonry; Past and Present, A.S.T.M. STP 589, Philadelphia, PA, 1975.

98. Shrive, N.G., Jessop, E.L., "An Examination of The Failure Mechanism of Masonry Piers, Prisms and Walls Subjected to Compression", Proceeds. of The British Ceramic Soceity, London, England, 1982, pp. 110-117.

99. Shrive, N.G., Review of: "Failures modes for Eccentrically Loaded Masonry Walls", by Hatzinikolas, M. (Reference 48).

100. Shrive, N.G., "The Prism Test as a Measure of Masonry Strength", Proc. of The British Masonry Soceity, 1986, pp. 117-121.

101. Shrive, N.G., "Compressive Strength and Strength Testing of Masonry", Proc. 7th International Brick Masonry Conference, Melbourne, Australia, 1985, pp. 699-710.

102. Shrive, N.G., "A Fundemental Approach to the Fracture of Masonry", Proc. 3rd Canadian Masonry Symposium, Edmonton, Canada, 1983, pap. 4.

103. Shrive, N.G., "Compressive Testing and The Crack of Plain Concrete", Magazine of Concrete Research, vol 35, no.122, 1983, pp. 27-39.

104. Shrive, N.G., "The failure Mechanics of Ungrouted Face-shell Bedded Masonry", International Journal of Masonry Construction, vol. 2, no. 3, 1982, pp. 115-129.

105. Simbeya, K.W., McMullin, A.E., Jessob, E.L., Shrive, N.G., "Concentrated Loading on Face-Shell Bedded Hollow Masonry", Proc. 4th Canadian Masonry Symposium, 1986, pp.251-262.

106. Sneck, T., "Dependance of the Masonry Properties on the

Interaction between Masonry Units and Mortar", Proc. of The North American Masonry Conference, Boulder, Colorado, 1978, pap. 21.

107. Standards Association of Australia, S.A.A. Blockwork Code, Part 1-Unreinforced Blockwork, AS1475, Part 1-1977, North Sydney, Australia, 1977, 32 pages.

108. Standards Association of New Zeland, The Design of Masonry Structures, NZS 4230P:1985, New Zealand, 1985.

109. Stafford-Smith, B., Carter, C., "Distribution of Stresses in Masonry Walls Subjected to Vertical Loading", Proc. Second International Brick Masonry Conference, Stoke-on-Trent, April 1970, pp. 119-124.

110. Suwalski, P.D., "Capacity of Eccentrically Loaded Slender Concrete Block Walls", M.Eng. Thesis, McMaster University, Hamilton, Ontario, 1986.

111. Thimoshenko, S.P., Goodier, J.N., Theory of Elasticity, McGraw-Hill Book Co., 3rd. Edition, New York, 1970, chp. 4.

112. Thomas, K., O'Leary, D.C., "Tesnile Strength Tests on Two Types of Bricks", Proc. Second International Brick Masonry Conference, Stoke-on Trent, April 1970, pp. 69-74.

113. Turkstra, C.J., Thomas, G.R., "Strain Gradient Effect in Masonry", Proc. of the First North American Masonry Conference, Colorado, August 1978, pap. 22.

114. Vanderkeyl, R., "Behaviour Characteristics of Brick Masonry ", M.Eng. Thesis, McMaster University, Hamilton, Ontario, 1979.

115. Whelan, M.L., "Hollow Concrete Masonry Unit Shape Modification to Improve Productivity of Placement: Results of the Preliminary Research Effort", Proc. of the Third North American Masonry Conference, The Masonry Soceity, Texas, 1985, pap. 8.

116. Wong, H.E., "Compression Characteristics of Concrete Block Masonry Prisms", Unpublished M.Eng. Thesis, McMaster University, Hamilton, Ontario, 1985.

117. Wong. H.E., Drysdale, R.G., "Compression Characteristics of Concrete Block Masonry Prisms", Masonry: Research, Applications and Problems, ASTM STP 871, 1985, pp. 167-177.

118. Yokel, F.Y., Mathey, R.D., "Compressive Strength of Slender Concrete Masonry Walls", National Bureau of Standards, BSS 33, 1970.